DEVELOPMENT OF CEMENTITIOUS COMPOSITE USING RECYCLED PULP FROM BEVERAGE CARTONS AND VIRGIN BAMBOO, AND EUCALYPTUS FIBERS AS REINFORCEMENT

PHOUTHANOUTHONG XAYSOMBATH

DOCTOR OF PHILOSOPHY
IN
MATERIALS INNOVATION

SCHOOL OF SCIENCE
MAE FAH LUANG UNIVERSITY
2024

DEVELOPMENT OF CEMENTITIOUS COMPOSITE USIN RECYCLED PULP FROM BEVERAGE CARTONS AND VIRGIN BAMBOO, AND EUCALYPTUS FIBERS AS REINFORCEMENT

PHOUTHANOUTHONG XAYSOMBATH

THIS DISSERTATION IS A PARTIAL FULFILLMENT OF
THE REQUIREMENTS FOR THE DEGREE OF
DOCTOR OF PHILOSOPHY
IN
MATERIALS INNOVATION

SCHOOL OF SCIENCE
MAE FAH LUANG UNIVERSITY
2024

DEVELOPMENT OF CEMENTITIOUS COMPOSITE USING RECYCLED PULP FROM BEVERAGE CARTONS AND VIRGIN BAMBOO, AND EUCALYPTUS FIBERS AS REINFORCEMENT

PHOUTHANOUTHONG XAYSOMBATH

THIS DISSERTATION HAS BEEN APPROVED
TO BE A PARTIAL FULFILLMENT OF THE REQUIREMENTS
FOR THE DEGREE OF DOCTOR OF PHILOSOPHY
IN
MATERIALS INNOVATION
2024

EXAMINATION COMMITTEE

.....CHAIRPERSON
(Prof. Prinya Chindaprasirt, Ph. D.)

.....ADVISOR
(Asst. Prof. Suthee Wattanasiriwech, Ph. D.)

.....CO-ADVISOR
(Assoc. Prof. Darunee Wattanasiriwech, Ph. D.)

.....CO-ADVISOR
(Assoc. Prof. Nattakan Soykeabkaew, Ph. D.)

.....EXAMINER
(Asst. Prof. Uraiwan Intatha, Ph. D.)

ACKNOWLEDGEMENTS

I would like to express my sincere gratitude to Assistant Professor Dr. Suthee Wattanasiriwech, my advisor, Associate Professor Dr. Darunee Wattanasiriwech, and Associate Professor Dr. Nattakan Soykeabkaew, my co-advisors at the Center of Innovative Materials for Sustainability, School of Science, Mae Fah Luang University. They provided me with diligent supervision, proofread my manuscripts and dissertation, and showed great enthusiasm throughout my study. I am grateful for the Material Innovation for Sustainability Program as it has offered me a valuable opportunity to enhance my profession and expand my knowledge.

I wish to express my gratitude to Assistant Professor Dr. Uraiwan Intatha, the Dean of the School of Science at Mea Fah Luang University, for graciously accepting the invitation to take on as the external examiner. Special gratitude is expressed to Professor Dr. Pinya Chindaprasirt, Director of the Sustainable Infrastructure Research and Development Center, Department of Civil Engineering, Khon Kaen University, for his honorable chair of the examination committee.

Thanks are also extended to all staff members of the School of Science, in particular the technical staff of the technical workshop, the center of innovative materials for sustainability, and the center for scientific analysis of MFU for their help in manufacturing all my mold and samples and for their advice and support in the laboratory throughout this research project.

I would also like to thank Fiber Pattana Ltd., Thailand, for supplying the recycled pulp from beverage cartons used in this study. My warmest thanks to Mea Fah Luang University for financial support.

I would like to acknowledge the Office of Postgraduate Studies, Library, teachers, and staff of Mae Fah Luang University (MFU) for all their help and assistance during my study.

I would like to express my gratitude to Mae Fah Luang University for their financial assistance. They awarded me a scholarship for my Ph.D. studies in the Material Innovation program from 2019 to 2022, as well as supplied research funding.

Last but not least, deep gratitude is expressed to my wife and children for their unlimited patience and encouragement. My sincere gratitude also goes to my organization for giving me a great opportunity to upgrade my knowledge and research experiences.

Phouthanouthong Xaysombath

Dissertation Title	Development of Cementitious Composite Using Recycled Pulp from Beverage Cartons and Virgin Bamboo, and Eucalyptus Fibers as Reinforcement
Author	Phouthanouthong Xaysombath
Degree	Doctor of Philosophy (Materials Innovation)
Advisor	Asst. Prof. Suthee Wattanasiriwech, Ph. D.
Co-Advisor	Assoc. Prof. Darunee Wattanasiriwech, Ph. D.
	Assoc. Prof. Nattakan Soykeabkaew, Ph. D.

ABSTRACT

Concern about environmental degradation, climate change, and sustainability development is increasing internationally. The production of building materials is a major contributor to greenhouse gas emissions. Several research groups are making an effort to reduce the carbon footprint in the construction materials sector by encouraging innovative methods and materials. The steady increase in innovative construction materials could help reduce energy consumption and lower CO_2 emissions, leading to reduced climate change-related impacts from CO_2 emissions.

There has been an increased effort to promote a circular bio-economy by using recycled pulp in developing new composite materials. This dissertation sought to develop an environmentally friendly, commercially competitive natural cellulose fiber-reinforced cement composite by using recycled pulp from beverage cartons (RPBC). The properties of recycled pulp-reinforced cementitious composites were assessed in comparison to those of other natural fiber-reinforced cementitious composites.

The research process involved several steps: Firstly, the recycled pulp from beverage cartons and natural fibers (bamboo and eucalyptus fibers) were prepared. The properties of reinforcement fiber were characterized. As a result, the RPBC has different freeness levels of 650, 600, 550, 500, and 400 mL CSF after mechanical treatment. The minimum fiber length ranged from 0.14 to 0.33 mm and the maximum fiber length ranged from 4 to 5.1 mm. The average fiber length for 650, 600, 550, 500, and 400 mL CSF was 1.91, 1.76, 1.58, 1.45, and 1.36 mm, respectively. The minimum width of RPBC ranged from 5 to 9 µm. The maximum width fluctuated from 60 to 90 µm. The average fiber width for 650, 600, 550, 500, and 400 mL CSF was 31, 31, 32, 32, and 34 µm, respectively. The fiber length and width of virgin bamboo after the treatment with 10% NaOH-catalyzed hydrothermal have an average value of 2.07 mm and 20 µm, respectively. Virgin eucalyptus fiber has an average length of 2.65 mm and an average width of 41 µm. The fiber strength was determined by measuring the zero-span tensile index of the RPBC, BF, and EF handsheets. RPBC, BF, and EF had tensile indexes of 29 N.m/g, 20 N.m/g, and 24 N.m/g, respectively. It was found that RPBC has a short fiber length but shows a high tensile index, while BF and EF exhibit a long fiber but have a lower tensile index. The high fibrillation of RPBC (550 mL CSF) contributed to its high tensile index, whereas BF and EF have a freeness of 730 and 710 mL CSF, respectively. RPBC fibrillation improves fiber interfacial bonding, resulting in high tensile strength.

The next experiments involved the formation of cementitious composites reinforced with RPBC, BF, and EF. The properties of the composites were evaluated, and the fracture surfaces of the corresponding composites were analyzed. The results showed that the flexural strength of composites reinforced with RPBC increased with an increase in fiber content and reached a maximum value of 12 MPa at a fiber content of 14 wt%, while composites reinforced with BF and EF achieved maximum flexural strengths of 9 and 10 MPa at a fiber content of 8 wt%. In contrast to the flexural strength, BF and EF-reinforced composites demonstrated fracture toughness of 1.35

kJ/m^2 and 3.6 kJ/m^2. These values were higher than those of the RPBC-reinforced composite by 114% and 457%, respectively, at the same fiber content.

The last part of the experiment was focused on the improvement of the properties of the RPBC-reinforced cementitious composite, particularly the fracture toughness. The fracture toughness of the RPBC-reinforced composite was very low (about 0.6 kJ/m^2). To improve the fracture toughness of the RPBC-reinforced composite, the RPBC was partially substituted with virgin cellulose fiber. Eucalyptus fiber was selected as virgin cellulose to mix with RPBC in different ratios. As a result, the fracture toughness of the hybrid fiber-reinforced composite increased by 370% at a fraction ratio of 1:1 (RPBC:EF) compared to the pure RPBC-reinforced composite. It had a flexural strength of 11 MPa.

In conclusion, using RPBC as a reinforcement to produce a cementitious composite is flexible. The flexural strength and the fracture toughness achieved 12 MPa and 1.6 kJ/m^2 at a fiber content of 14 wt%. When combining the RPBC and virgin EF with a ratio of 1:1, the fracture toughness increased by a third-fold, and the flexural strength was 11 MPa at a fiber content of 8%. This value meets the requirements of grade II according to the standard specification ASTM C-1186-02 (2002).

Keywords: Recycle Pulp, Beverage Cartons, Bamboo, Eucalyptus, Cement Composite, Fracture Toughness, Flexural Strength, Hybrid Fiber, Bioeconomy

TABLE OF CONTENTS

TABLE OF CONTENTS (continued)

TABLE OF CONTENTS (continued)

TABLE OF CONTENTS (continued)

LIST OF TABLES

LIST OF TABLES (continued)

LIST OF FIGURES

LIST OF FIGURES (continued)

LIST OF FIGURES (continued)

Figure **Page**

LIST OF FIGURES (continued)

ABBREVIATIONS AND SYMBOLS

ACE	alliance for beverage cartons and the environment
APTS	aminopropyltri ethoxysilane
ASTM	American Society for Testing and Materials
a_θ	proportion of fiber oriented at an angle θ
b	width of the specimen
BF	bamboo fiber
cm	centimeter
CO_2	carbon dioxide
CSF	Canadian Standard Freeness tester
CSH-gel	calcium silicate hydrate gel
CTMP	chemithermo-mechanical pulping
d	diameter
d	average thickness of the specimen
D	dry weight of specimen
DEVA	diatomaceous earth and volcanic ash
e.g.	for example
et al.	and others
Equ.	equation
EF	eucalyptus fiber
EU	European Union
FRC	fiber-reinforced cement composite
g	gram
GPa	giga pascal
g/cm^3	gram per cubic centimeter

ABBREVIATIONS AND SYMBOLS (continued)

H_2O	water
hrs	hours
i.e.	that is
kGy	kilogray
kJ/m^2	kilo joule per square meter
l	length
l_c	critical length
L	length of span
m	meter
mg	milligram
ml	milliliter
mm	millimeter
mm/min	millimeter per minute
MOE	modulus of elasticity
MOE	modulus of elasticity
MOR	modulus of rapture
MPa	maga pascal
MPTS	methacryloxypropyltri-methoxysilane
NaOH	sodium hydroxide
n.d	no date
NF	natural fiber
N/m	newton per meter
Nm/g	newton meter per gram
No.	number
O_2	oxygen
OCC	old corrugated container

ABBREVIATIONS AND SYMBOLS (continued)

OM	optical microscopy
OPC	ordinary portland cement
P	maximum load
P_0	porosity of composite
P_1	load at the point 1
P_2	load at the point 2
PBS	polybutylene succinate
Quo.	quotient
r	radius
Ref.	reference
RMT	roller mill technique
RPBC	recycled pulp from beverage cartons
rpm	revolutions per minute
SEM	scanning electron microscope
S	suspended weight of the specimen
TAPPI	Technical Association of the Pulp and Paper Industry
TS_{index}	tensile strength index
TS	Tensile strength of the fiber
UTM	universal test machine
V_m	volume fraction of matrix
V_f	volume fraction of fiber
wt%	percentage by weight
W	saturated weight
XDXRF	energy-dispersive X-ray fluorescence method
y_1	deflection of the specimen at point 1
y_2	deflection of the specimen at point 2

ABBREVIATIONS AND SYMBOLS (continued)

α	alpha
β	beta
η_l	length efficiency factor of fibers
η_θ	orientation efficiency factor of fibers
θ	angle between fiber and the load direction
μm	micrometer
μl	microliter
$\sum$	sum
σ_{fu}	ultimate tensile strength of fiber
σ'_f	tensile strength of fiber at the first crack strain
σ'_{mo}	tensile strength of void-free matrix at fiber failure
σ_c	first crack stress of composite
τ_{fu}	ultimate interfacial bond of fiber and matrix
°C	degree centigrade
%	percent

CHAPTER 1

GENERAL INTRODUCTION

1.1 Background

A fiber-reinforced cementitious composite is an important building material that consists of hydraulic cement and silica sand as a matrix, fiber reinforcement, and other additives. Fiber-reinforced cement composite (FRC) has been used in construction for a long time. It can be applied in both interior and exterior conditions of residential and non-residential buildings and manufactured in various forms of products such as board, panel, and others that are applied in cladding, roofing, flooring, ceilings, fencing, partitioning, and decorative applications. Due to remarkable advantages such as high resistance to deterioration by decay fungi, insects, and vermin, good acoustic insulation, fire resistance, low thermal conductivity, and affordable strengths (Ranachowski & Schabowicz, 2018; Nicole & Cai, 2021), FRC, with its extraordinary properties, could serve as a substitute for massive wood and wood-based products such as middle-density fiber-board (MDF), oriented strand board (OSB), wood particleboard, and plywood.

It is reported that the market value of fiber cement products was USD 16.4 billion in 2020, and it is projected to be worth USD 24.87 billion by 2028 (Market Research Future, 2021). The compound annual growth rate was estimated at 5.59% from 2012 to 2028. Due to rapid urbanization and industrialization in developing countries, the demand for FRC products such as board, planks, flat sheets, corrugated roofing sheets, and panels is increasing year over year.

As reinforcements, different fiber types have been used to improve some properties of cementitious composites because the cement mortar or concrete is brittle and has low tensile strength and strain (Bentur & Mindess, 2005).

Fibers that have been used with hydraulic cement include asbestos, steel, glass, carbon, polypropylene, nylon, and natural cellulose fiber, as reported by Bentur and Mindess (2005). Those fibers can be applied in different forms, such as discrete, discontinued fiber, or long, continued fiber. In this study, fiber reinforcement was referred to as discrete and discontinuous fiber.

Due to the high brittleness of the cementitious matrix and the addition of fiber to the cementitious matrix, some mechanical properties of the composite are enhanced, such as flexural strength, fracture toughness, ductility, and crack resistance, compared to the cement slabs. The fiber reinforcement can reduce the shrinkage within the structure, prevent cracks, decrease the thermal conductivity, and improve acoustic insulation and fire resistance (Ranachowski & Schabowicz, 2018).

At the beginning of the production of fiber cement materials in 1900, asbestos fibers were used as reinforcement (Bentur & Mindess, 2005). Asbestos cement sheets were very durable (26 years) due to their excellent properties as asbestos cement composites (MOR = 60 MPa at a fiber content of 15 wt%) (Akers & Garrett, 1986). However, the asbestos fibrils were split up in the air during the mining, manufacture, and disposal of old asbestos-contained products.

In the early 1970s, it was realized that it needed to legislate to control the use of asbestos fiber because it causes dangerous diseases, e.g., lung cancer (asbestosis) (Ranachowski & Schabowicz, 2018; Coutts, 2005). Later, awareness of the harm of asbestos fiber on human health was growing (Campbell & Coutts, 1980). Therefore, some developed countries have banned the application of asbestos fiber in construction materials (Bassani et al., 2007) and replaced it with wood pulp fibers combined with synthetic fiber. Asbestos fiber was replaced partially by softwood pulp fiber in Australia in the early 1960s (Coutts & Michell, 1983). In 1972, Krenchel proposed that wood pulp fibers might replace asbestos fibers in fiber-cement sheets cited by Coutts and Michell (1983). Sweden, Norway, and Denmark had prohibited the use of asbestos by 1987 (Coutts, 2005). While Singapore has banned the application of asbestos fiber, Lao PDR currently uses this fiber to produce construction materials.

Since the initial global effort to search for alternative fibers to substitute asbestos fiber 50 years ago, natural cellulose fibers have become the central interest of researchers to find the most suitable, sustainable, no harmful, and economical fiber

sources used in fiber cement composites. Among the natural plant fibers, kraft wood pulp was the best solution for fiber cement products in commercial production, and it was chosen to replace the asbestos fiber because it is suitable and compatible with the Hatschek process, as stated by Coutts (2005). It is low-cost, renewable, and not hazardous to health (Coutts & Michell, 1983). Consequently, the demand for wood kraft pulp for fiber cement production is growing worldwide. In addition, kraft wood pulp is the main raw material for papermaking. The global consumption of pulp and paper amounted to an estimated 399 million metric tons in 2020. It is expected that demand will increase steadily over the next decade, reaching approximately 461 million metric tons in 2030, as reported on the STATISTA website (Tiseo, 2021).

With the growth of demand for wood pulp and wood fiber cement products, as mentioned above, more trees were cut down and the forest was destroyed. Moreover, a large amount of land was needed for industrial wood plantations. Large monoculture plantations and deforestation lead to a loss of biodiversity, particularly in developing countries (Amenu, 2017). As a consequence, it causes climate change, the loss of natural habitat, and impacts the environment significantly. However, the natural forest plays a crucial role in biodiversity conservation, the capture of carbon dioxide, and the habitation of wild-life.

With the increase in environmental and sustainable concerns, many studies have been conducted on the utilization of non-wood fiber, agricultural waste fiber, and recycled pulp as alternative sources for fiber reinforcement, such as bamboo, flax, hemp, jute, banana, rice straw, wheat straw, sisal, pineapple, coconut (coir), waste paper, and cardboard (Coutts, 2005; Ardanuy et al., 2015). These raw materials are characterized as widely available, renewable, biodegradable, sustainable, and low-cost. While the flexural strength of pine wood and eucalyptus pulp cement composites was 25 MPa and 23 MPa (Savastano et al., 2000), the flexural strengths of bamboo, banana, and recycled pulp cement were 21 MPa (Coutts et al., 1994), 20 MPa (Savastano et al., 2000), and 18 MPa (Coutts, 1989), respectively.

Waste paper fiber is an alternative sustainable potential source of fiber for fiber cementitious composites, as stated by Coutts (2005). It is a valuable raw material for recycling paper because the re-pulping of wastepaper requires less energy than the pulping of wood-based pulp (Oriyomi et al., 2015). However, about 58.6% of total

global pulp and paper consumption was recycled in 2020, according to the European Paper Recycling Council (European Paper Recycling Council, 2020). The rest has gone into incineration and landfills, particularly in some developing and least developed countries where there is no facility for recycling wastepaper available.

Nevertheless, in the last few decades, a range of research has demonstrated that recycled pulp from waste paper and beverage cartons can be used as reinforcement in building materials (Oriyomi et al., 2015; Bentchikou et al., 2012). Coutts (1989) reported that the maximum flexural strength and toughness of recycled pulp cement were 18.2 MPa and 1 kJ/m^2 at a fiber content of 12 wt% using only cement as a matrix after 28 days of curing, while Khalilitabas et al. (2009) presented the maximum flexural strength of 8 MPa at an 8 wt% fiber content. Teixeira et al. (2012) stated that the flexural strength of a recycled pulp cement composite was 10.95 MPa at 9 wt% fiber fractions using a matrix consisting of cement, kaolin, and sand.

Since recycled pulp from wastepaper was produced through the re-pulping process, the fiber contains a high proportion of short fiber, which is less effective as reinforcement in the cementitious matrix. The average length of recycled fiber from old containers was about 1.56 mm, and the number of fine particles was about 32.1%, as reported by Teixeira et al. (2012). Reinforcement with high fines acted very less effectively in the strengthening of composites but as filler instead. Therefore, it leads to low flexural strength (around 8 MPa) (Khalilitabas et al., 2009). Soroushian et al. (1995) proposed a combination of recycled pulp and virgin pulp to improve the efficiency of fiber contribution. However, the fiber mass fraction, substitution level of a virgin with recycled pulp, and other influent parameters need to be optimized to achieve desirable properties.

The application of recycled pulp from beverage cartons (RPBC) in the production of construction materials was studied by several researchers to promote a circular economy and environmental sustainability (Ayrilmis, 2008; Rhamin, 2013; Platnieks, 2020; Martinez-Barrera, 2015). Nevertheless, the use of RPBC as reinforcement in cementitious composites has not yet been widely explored.

Another drawback of recycled pulp cement composites is the short-term durability of the fiber in the cementitious matrix (Soroushian et al., 1994), because cellulose fiber degrades under the alkaline attack. To overcome this problem, several

researchers proposed the use of supplementary cementitious materials for the mitigation of fiber degradation, such as silica fume, fly ash, ground granulated blast furnace slag, and metakaolin, by reducing the calcium hydroxide products in the cementitious matrix.

Additionally, an interest in scientific studies of bamboo fiber as a reinforcing material for cementitious matrix composites has been growing (Coutts & Ni, 1995; Correia et al., 2014; Ban et al., 2020). Due to its fast growth, bamboo could be harvested for construction within 4-5 years. Individual bamboo fibers have a cylinder form. The average fiber length and diameter range are 2–3 mm and 10–40 μm, respectively (Mwaikambo, 2006). Due to these unique attributes, bamboo fiber also has a high potential to be used in cement-based materials as a substitute for wood fiber (Ban et al., 2020).

The addition of inorganic admixtures such as silica fume, fly ash, metakaolin, and wollastonite to the cementitious composite could improve the physical and mechanical properties and performance of fiber cement composites (Ardanuy et al., 2015; Mohr et al., 2007; Tichi et al., 2016). By adding metakaolin, the strengths and performance of fiber cement composites were improved after aging because the alkaline degree was reduced in a cementitious matrix (Mohr et al., 2007). It mitigates the degradation of cellulose fiber and improves the durability of fiber-cement composites. The porosity and water absorption were also reduced using silica fume, metakaolin, or wollastonite (Mohr et al., 2007; He et al., 2020). de Gutirrez et al. (2005) stated that by adding 15% silica fume or metakaolin, the strengths of fiber cement mortar were improved up to 20 to 68%, respectively. Courard et al. (2003) reported that the flexural and compressive strengths of mortar were increased to 4% and 20% at 15% metakaolin replacement after 28 days' cure and reduced the chloride diffusion and sulfate attack in the composite.

In summary, recycled pulp and bamboo fiber are shown as potential alternative sustainable sources for replacing asbestos fiber in fiber cementitious composite production. It can promote circular economic and sustainable development. By adding inorganic materials, the properties of a matrix can be improved. This study focuses on a demonstration of the utilization of recycled pulp and bamboo fiber as reinforcement for the replacement of asbestos fiber in cementitious building materials.

1.2 Justification

There has been an increased effort to promote a circular bio-economy by using recycled pulp in developing new composite materials (Oriyomi et al., 2015; Soroushian et al., 1994; Amiandamhen & Osadolor, 2020). Although several types of research demonstrated that the recycled pulp from waste paper was a potential and suitable source for fiber-reinforced cement composites, there is very limited information about the study on the application of recycled pulp from beverage cartons (RPBC) in the public literature. In addition, the properties of recycled pulp cement projected a variation of results because the recycled pulp consisted of different sources of pulp types (mechanical and chemical pulps) and was reused several times. These could lead to the decay of the pulp fiber properties. Therefore, a recycled pulp-reinforced cement composite exhibited average properties and short-term performance (Soroushian et al., 1995). To get a better idea of how well a cementitious composite reinforced with RPBC works, its properties will be studied as a result of different factors, such as its freeness, fiber content, and the pressure used to form it.

Due to the high amount of fine short fiber in RPBC, which could be a disadvantage, an addition of virgin long cellulose fiber is proposed to improve the efficiency of fiber reinforcement. Two candidates, bamboo fiber (BF) and eucalyptus fiber (EF), were selected to be mixed with RPBC in a suitable proportion. However, a result of a preliminary experiment demonstrated that a reinforced cement composite having only bamboo fiber at 8 wt% content gave a fair flexural strength of 8.45 MPa, but it exhibited high water absorption (36.72%) and high porosity (46.61%). The cause of the high porosity and water absorption of such composites could lie in the inhomogeneous dispersion of bamboo fiber in the cementitious composite and the high interaction between fibers during the mixing process caused by long bamboo fiber (1–3.5 mm) (Amiandamhen & Osadolor, 2020). Thus, in this study, RPBC fiber will be partially replaced with one of the long fibers to find the optimized mix proportion to improve the properties and performance of reinforced cement composite.

1.3 Research Objectives

The study aims to evaluate the effect of fiber characteristics on the physical and mechanical performance of cementitious composites reinforced with RPBC, BF, and EF in comparison with non-fiber-reinforced specimens and to find out the possibility of improving their properties and performances using a mixture of RPBC, BF, and EF. According desirable properties should meet a flexural strength greater than 10 MPa with a desirable fracture toughness under equilibrium condition testing, according to ASTM C 1186-08, the standard specification for flat non-asbestos fiber-cement sheets (ASTM C 1186, 2002).

The specific objectives are the following:

1. Assessment of the appropriate freeness of RPBC for desirable properties of RPBC cement composite;
2. Obtain an appropriate pressure for the fiber-reinforced cement composite;
3. Obtain a suitable fiber content of each fiber type for the fiber-reinforced cement composite;
4. Achievement of an optimum mass fraction between recycled pulp from beverage cartons and virgin cellulose fiber for the improvement of cementitious composites.
5. Obtain an economic analysis of the production of hybrid fiber-reinforced cement composites.

1.4 Overall Research Scopes

The study began with the characterization of fiber reinforcement, which includes recycled pulp from beverage cartons, virgin bamboo fiber, and virgin eucalyptus fiber. The research was conducted in several steps, as follows:

Firstly, the RPBC, BF, and EF were prepared, and their properties, such as morphologies and physical and mechanical properties, were characterized. RPBC was made from old beverage cartons supplied by Pattana Fiber Company, Thailand. The received RPBC was treated using a lab-scale blender to disintegrate the clump and fibrillate the recycled pulp. The effects of the blending process on the properties and morphologies of recycled pulp, as well as the properties of cementitious composites reinforced with sheared recycled pulp, were investigated.

After determining the appropriate level of flexibility of the RPBC, the impact of fiber characteristics (RPBC, BF, and EF) was investigated by varying the fiber content from 2 to 14 wt% of the total solid weight. The specimens were made and their qualities were evaluated according to the ASTM C 1186-09 (2002) standard.

The next step was to identify the optimum mass fraction for the mixture between RPBC and EF. The mixing of fibers was aimed at improving the efficiency of fiber reinforcement. The optimized fractions between RPBC and EF are the fractions that lead to the maximum flexural strength of the composite. In addition, the properties of the mixed fiber-reinforced cement composites were evaluated to compare with those of the composites reinforced with un-mixed fiber composites. The specimens were formed using a similar procedure as the previous experiments. Furthermore, the fracture surfaces of specimens were analysed by SEM photographs to understand the failure behaviour of fiber-reinforced cementitious composites.

CHAPTER 2

LITERATURE REVIEW

2.1 Fiber-reinforced Cementitious Composites

Fiber-reinforced cementitious composite (FRC) is a composite that is mostly made up of cement, silica sand, and other materials mixed together to form a matrix, along with reinforced fibers and other additives (Ranachowski & Schabowicz, 2018). The properties of FRC depend on different factors such as the fiber types, morphologies, aspect ratio, fiber distribution, the structure of the fiber-matrix interface, and the properties of the matrix and processing parameters (Bentur & Mindess, 2005).

2.1.1 Reinforcement Fibers

As reinforcements, different fiber types have been used to improve some properties of composites because the cement mortar or concrete is brittle and its tensile strength and strain are low (Bentur & Mindess, 2005). The main objective of adding fiber to the cementitious composite is to reduce cracking and crack propagation. Fibers that have been used with hydraulic cement include asbestos, steel, glass, carbon, polypropylene, nylon, and natural cellulose fiber, as shown in Table 2.1. Table 2.1 presents the properties of asbestos fiber in comparison to other alternative fibers, according to Bentur & Mindess (2005).

Asbestos is a mineral crystal fiber with small diameters, but higher specific gravity and tensile strengths compared to synthetic and wood fibers. Therefore, this kind of fiber was widely used to produce fiber cement boards in the Hatschek process. Glass and carbon are the most common man-made fibers to reinforce cementitious composites with great mechanical properties. Nevertheless, they are non-renewable materials, and their production requires high energy consumption.

Table 2.1 Properties of reinforcement fibers

Fibers	Diameter (μm)	Specific gravity	MOE (GPa)	Tensile strength (GPa)	Elongation at break (%)
Asbestos					
Crocidolite	0.02 - 0.4	3.4	196	3.5	2.0 - 3.0
Chrysotile	0.02 - 0.4	2.6	164	3.1	2.0 - 3.0
Steel	5 - 500	7.84	200	0.5 - 2.0	0.5 - 3.5
Glass	9 - 15	2.60	70 - 80	2 - 4	2 - 3.5
Polypropylene Aramid	10	1.45	65 - 133	3.6	2.1- 4.0
Carbon	9	1.90	230	2.6	1.0
Nylon	23	1.1	4.0	0.9	13.0 - 15.0
Acrylic	18	1.18	14 - 19.5	0.4 - 1.0	3
Polyethylene	20	0.95	0.3	0.7×10^{-3}	10
Wood fiber	10 - 45[a]	1.5	71	0.9	

Sources Bentur and Mindess (2005) and [a]Coutts and Michell (1983)

Since the 1960s, natural fiber has centered interest in research due to the health harm of asbestos fiber. The attempt to use natural fibers (NF) is due to their wide availability and high strength. Moreover, natural fiber was compatible with the existing production process for making fiber cement composites of various shapes. Therefore, they are potentially suitable for low-cost housing applications, as stated by Bentur and Mindess (2005). Natural cellulose fibers are classified into wood fiber and non-wood fiber or plant fibers, according to Biagiotti et al., (2004). The fiber can be classified into four classes based on its morphology: stem (or blast), leaf, surface, and wood (Biagiotti et al., 2004; Jawaid & Khali, 2011).

The physical and mechanical properties of some natural fibers are presented in Table 2.2. As shown in Table 2.2, natural fibers have a high variation in their properties, leading to inaccurate predictions of composite properties. For example, the tensile strength decreases with an increase in fiber length. Some natural fibers have high tensile strength but low elongation, such as hemp and kenaf. On the other hand, coir and oil palm, for example, have high elongation. The properties of natural fiber, such as fiber length, diameter, aspect ratio, strength, stiffness, elongation, and texture of the fibers, have a significant influence on the mechanical behavior of fiber-reinforced cementitious composites (Coutts, 2005).

Table 2.2 Physical and mechanical properties of natural fibers

Fibers	Length of fiber (mm)	Diameter of fiber (µm)	Density (g/cm^3)	Tensile strength (MPa)	Elongation at break (%)	Young's modulus (GPa)	Ref.
Abaca	4.6-5.2	17-21.4	1.5	400	3-10	12	Mwaikambo (2006)
Bagasse	0.8-2.8	10-34	1.25	290	-	17	Jawaid and Khali (2011), Faruk et al. (2012)
Bamboo	2.7	14	0.6-1.1	140 - 230	-	11-17	Jawaid and Khali (2011), Faruk et al. (2012)
Banana	0.17	13.16	1.35	355	5.3	33.8	Jawaid and Khali (2011)
Flax	10-65	5-38	1.5	345 – 1,035	2.7-3.2	27.6	Jawaid and Khali (2011), Faruk et al. (2012)
Hemp	5-55	10-51	1.48	690	1.6	70	Jawaid and Khali, (2011), Faruk et al. (2012)

Table 2.2 (continued)

Fibers	Length of fiber (mm)	Diameter of fiber (μm)	Density (g/cm^3)	Tensile strength (MPa)	Elongation at break (%)	Young's modulus (GPa)	Ref.
Jute	0.8-6	5-25	1.3	393 - 773	1.5-1.8	26.5	Jawaid and Khali (2011), Faruk et al. (2012)
Kenaf (bast)	1.4-11	12-36		930	1.6	53	Jawaid and Khali (2011), Faruk et al. (2012)
Sisal	0.8-8	7-47	1.5	511 - 635	2.0-2.5	9.4-22	Jawaid and Khali (2011), Faruk et al. (2012)
Ramie	40-250	18-80	1.5	560	2.5	24.5	Jawaid and Khali (2011), Faruk et al. (2012)
Oil palm	0.89-099	19.1-25	0.7-1.55	248	25	3.2	Jawaid and Khali (2011), Faruk et al. (2012)
Pineapple	3-9	20-80	0.8-1.6	400 - 627	14.5	1.44	Jawaid and Khali (2011), Faruk et al. (2012)

Table 2.2 (continued)

Fibers	Length of fiber (mm)	Diameter of fiber (µm)	Density (g/cm^3)	Tensile strength (MPa)	Elongation at break (%)	Young's modulus (GPa)	Ref.
Coir	0.3-1.0	100-450	1.2	175	30	4-6	Jawaid and Khali (2011), Faruk et al. (2012)
Cotton	15-56	12-35	1.51	400	3-10	12	Jawaid and Khali (2011)
Henequen		8-33	1.4	430-580	1-3	-	Jawaid and Khali (2011)
Softwood	2-6	13-45	1.5	500-900	-	7-28	Bentur and Mindess (2005), Coutts and Michell (1983)
Hardwood	1.0	20	-	-	-	-	Bentur and Mindess (2005)

2.1.2 Influence of Fiber Characteristics

The mechanical performance of the FRC depends on several parameters, including the matrix, fiber characteristics, interfacial bonding between reinforced fibers and matrix, and processing technique. The fiber length and morphologies are the main influences on the toughness properties of the fiber-reinforced cement composites due to their fiber-matrix bonding behavior.

In considering the effects of fiber length, its orientation, and void volume, the rule of mixtures can be used to predict the first crack stress of the cementitious composite, σ_c, in tension by following the equation 2.1 according to Bentur and Mindess (2005):

$$\boldsymbol{\sigma_c} = (1 - p)\boldsymbol{\sigma'_{mo}}\boldsymbol{V_m} + \boldsymbol{\eta_l}\boldsymbol{\eta_\theta}\boldsymbol{\sigma'_f}\boldsymbol{V_f} \qquad \text{Equation 2.1}$$

Where σ_c is the first crack stress of composite in MPa, σ'_{mo} is the tensile strength of void-free matrix at fiber failure (MPa), V_m is the volume fraction of matrix, σ'_f is the tensile strength of fiber at the first crack strain, V_f is the volume fraction of fiber, η_l is the length efficiency factor of fibers, η_θ is the orientation efficiency factor of fibers, p is the porosity of composite in %.

2.1.2.1 Fiber reinforcement efficiency

Equation 2.1 demonstrates how the fiber length efficiency factor (η_l) and orientation efficiency factor (η_θ) affect the strength of the composite. The efficiency of fiber reinforcement can be described by the effective improvement in strength and toughness of the composite compared with the brittle matrix (Bentur & Mindess, 2005). These factors are related to the critical fiber length (see equations 2.3 and 2.4) and its orientations. The critical fiber length is the minimum length necessary to bear the stress from matrix to fiber effectively. It is also associated with the interfacial bonds, diameter, and tensile strength of fiber (see Equ. 2.2). It is possible to reduce the critical length by improving the interfacial bonds between fiber and matrix or reducing the fiber diameter (Coutts & Ni, 1995). Equation 2.2 can be used to determine the critical length.

$$l_c = \frac{\sigma_{fu} d}{2\tau_{fu}} \qquad \text{Equation 2.2}$$

Where l_c is a critical length, d is the diameter of the fiber, σ_{fu} is the ultimate tensile strength of the fiber, and τ_{fu} is the ultimate interfacial bond of fiber and matrix.

Fibers shorter than the critical length will not carry their maximum load and are unable to function effectively. For a fiber length less than the critical length ($l<l_c$), an unsatisfactory embedded length occurs and it leads to the generated stress unequal to the tensile strength of reinforced fiber, consequently the fiber is not applied efficiently (see Equ. 2.3). For the fiber length longer than the critical length (l_c), the stress along the fiber reaches its maximum tensile strength (see Equ. 2.4), therefore, the maximum potential strength of the fiber reinforcement is applied fully, as shown in Figure 2.1. Figure 2.1 illustrates the fiber profile in a cement matrix associated with fiber length before and after a fracture. If the length of the fiber is greater than the critical length, the fiber is broken at the increase of tensile load. In contrast, when the fiber length is less than the critical length, it is pulled out.

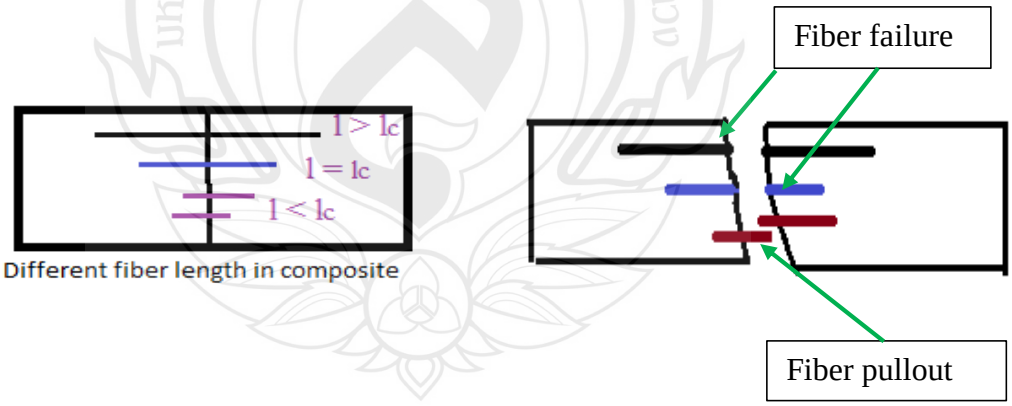

Figure 2.1 Stress profile of fiber in a matrix as a function of fiber length

The fiber length efficiency factor for $l < l_c$ and $l > l_c$ can be determined by Equations 3 and 4 according to Bentur and Mindess (2005).

For $l < l_c$; $$\eta_l = \frac{\tau_{fu}}{2r\sigma_{fu}} = \frac{\tau_{fu}}{d\sigma_{fu}} = \frac{l}{2l_c}$$ Equation 2.3

For $l > l_c$; $$\eta_l = 1 - \frac{l_c}{2l}$$ Equation 2.4

Van den Oever and Bos (1998) stated that the critical length of fiber decreased with an increase in the aspect ratio of fiber. Therefore, the fiber length must be 5 to 10 times longer than its critical length, to achieve 90% strength efficiency as stated by Bentur and Mindess (2005). The aspect ratio of cellulose fiber used for reinforcement in the cementitious composite is between 50 and 75 as reported by Coutts (1983, 1984).

2.1.2.2 Fiber orientation

The orientation of fiber reinforcement is categorized into one-dimensional aligned, two-dimensional random, and three-dimensional random forms according to Krenchel and Cox cited by Bentur and Mindess (2005) as shown in Figure 2.2.

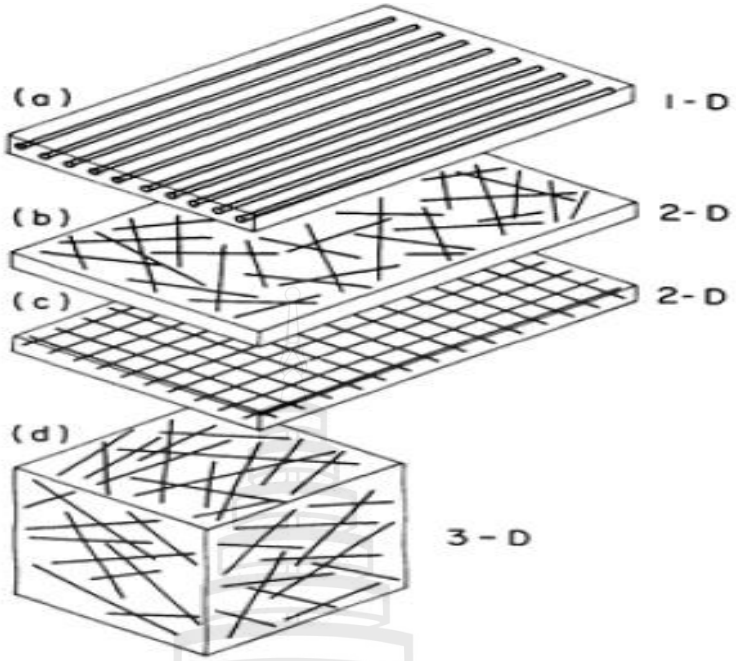

Source Alien use as cited in by Bentur and Midess (2005)

Figure 2.2 Fiber arrangements in 1-D, 2-D, and 3-D dimensions and (a) and (c) continuous, (b) and (d) discrete, short fiber

The efficiency factor of fiber orientation can be determined by the equation 2.5 below:

$$\eta_\theta = \Sigma a_\theta cos^4\theta \qquad \text{Equation 2.5}$$

Where, a_θ – a proportion of fiber oriented at an angle θ. θ is the angle between the fiber and the load direction.

The orientation efficiency factor according to the three types of composite structure summaries in Table 2.3 according to Krenchel and Cox cited by Bentur and Mindess (2005).

Table 2.3 Orientation factors derived for constrained composites

Fiber orientation	Orientation efficiency factor (η_θ)
Aligned, 1-D	1
Random, 2-D	3/8
Random, 3-D	1/5

Source Bentur and Mindess (2005)

As shown in Table 2.3, the best efficiency is achieved when the fibers are aligned in one dimension. However, the specimens for this study were formed by the slurry vacuum dewatering method at a laboratory scale, and the orientation of the fiber was assumed randomly in a 2-dimensional distribution.

2.1.2.3 Fiber content

Fiber content is a crucial factor in the final properties of the composite. It is associated directly with the workability of the mixture. Generally, adding fiber tends to increase the strength and fracture toughness of the fiber-cement composites. However, the strengthening effect of fiber appears, as do optimum fiber contents, at which maximum improvement is achieved, as stated by Coutts and Ni (1995). The authors also stated that the fiber content affects the physical properties of composites, such as bulk density, porosity, and water absorption.

Correia et al. (2014) evaluated the performance of a cementitious composite reinforced with bamboo organosolv pulp associated with the fiber content from 2 to 14 wt%. The flexural strength increased with an increase in fiber content to 8 wt% and decreased after that. The authors reported that the reduction in flexural strength when the fiber content is above 8 wt% is caused by an increase in void volume and low interfacial bonding. However, the fracture toughness of the composite increased steadily until it reached a maximum value of 1.2 kJ/m^2 at 14 wt% fiber content. Xie et al. (2019) also reported a similar tendency. The author evaluated the flexural strength and impact resistance of the composites with bamboo kraft pulp weight fractions ranging from 4% to 16%, as shown in Figure 2.3. In this study, the maximum flexural strength was 11.5 MPa at 12 wt% fiber content, and the impact was 2.2 kJ/m^2. The

author found that at a fiber content of 2-4 wt%, the fiber couldn't be distributed uniformly in the composite. It leads to microcracks in the composite; thus, the strength was decreased.

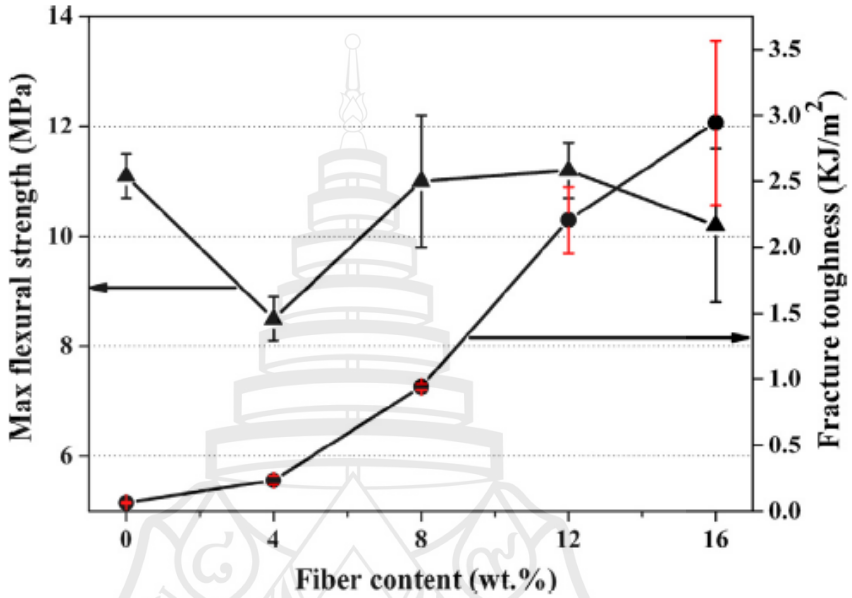

Source Xie et al. (2019)

Figure 2.3 The effect of fiber fraction on the flexural strength and fracture toughness of bamboo kraft pulp cementitious composites

The information from literature studies shows that the effect of natural cellulose fiber content in cementitious composites was maximum in a range of 8–12 wt%. When the fiber content was higher than 8 wt%, fiber was agglomerated, the compaction of fiber was less efficient, the porosity increased, and the reinforcing function of the added fiber was decreased.

2.1.2.4 Freeness

The freeness measures the amount of water that indicates the ability of pulp fiber to allow diluted pulp fiber suspension drainage. It is a parameter used to control the refining or beating process of pulp (Coutts, 1984) and is related to the fiber surface

condition and small particle content. Freeness has a significant impact on the properties of fiber cement composites manufactured by the slurry vacuum dewatering technique. Coutts (1984) studied the effect of beaten wood pulp on the mechanical properties of the composite. The kraft pulp was treated in a Valley beater, and the freeness of the pulp was determined using a Canadian Standard Freeness Tester (CSF). The result indicated that the beaten fiber pulp with a freeness of about 550 CSF improved the flexural strength of the composite, while a higher or lower freeness led to reduced strength, as shown in Figure 2.4. Figure 2.4 illustrates the effect of the freeness level of the fiber on the flexural strength of the fiber cementitious composite.

Therefore, in this work, the suitable freeness of fiber for fiber cement composite should be between 500 and 550 CSF.

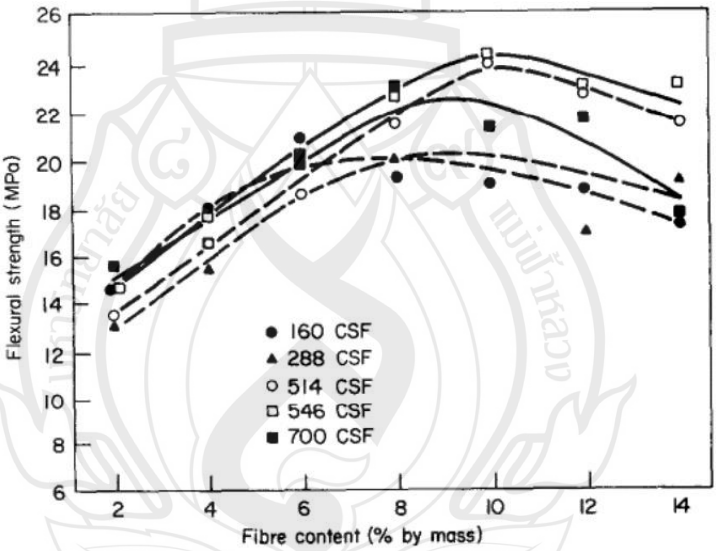

Source Coutts (1984)

Figure 2.4 Effect of P. *radiata* fiber freeness on flexural strength of the composite at various fiber contents

2.1.3 Recycled Pulp

Wastepaper is the paper that is already used, including newspapers, office paper, old corrugated containers, and packaging, which are collected from offices, households, public facilities, commercial activities, and industries (Oriyomi et al., 2015).

Recycled pulp from waste paper has been used as a reinforcement in cementitious composites with satisfactory flexural strength (Coutts, 1989). The use of old corrugated containers (OCCs) as recycled pulp for fiber cement composites can be economical as well as environmentally attractive (Teixeira et al., 2012). However, OCC consisted of two outer liners and a corrugated middle sheet, which were produced from different sources of fibers (kraft pulp and semi-chemical pulp). They are formed as layer sheets with adhesive material. Teixeira et al. (2018) studied the properties of cement sheets reinforced with OCC pulp in comparison with the kraft pulp of Douglas fir. The author reported that the OCC pulp cement sheet had a flexural strength of 11.7 MPa at 10 wt% fiber content, which was classified as grade II according to ASTM C-1186-08, while the flexural strength of the cement sheet reinforced with kraft pulp from Douglas fir was 18.6 MPa, which can be classified as grade III. The author used a matrix consisting of Portland cement, silica sand, and kaolin clay. The cement, silica, and clay ratio was 0.7:1:0.1. Khalilitabas et al. (2009) reported that the maximum flexural strength of the recycled pulp cement paste composite was 8 MPa at 8 wt% fiber content.

To improve the reinforcement efficiency of recycled pulp, a combination with other fibers can be considered, such as polypropylene, acrylic (Khorami et al., 2016), virgin cellulose pulp (Soroushian et al., 1994), and kenaf fiber (Amiandamhen et al., 2020). Soroushian et al. (1994) reported that the best fraction of recycled pulp and virgin pulp was 50:50. As a result, the maximum flexural strength was 14 MPa and the fracture toughness was 98 N.mm at 8 wt% fiber content. The cement mortar with a sand-cement ratio of 1:1 was used in this study.

One problem in the recycling of the old corrugated containers is the hot melt adhesive that was used to bind the liner board and corrugated medium, forming a corrugated sheet. In the recycling of the old corrugated containers, the hot melt adhesives bind the recycled pulp together, and when it has passed through the pulper, the hot melt adhesives are broken down into small particles known as stickies. Blazey et al., (n.d) suggested that the hot melt stickies in the old corrugated container pulp can

be illuminated by using a modified smectite clay in conjunction with a cationic polymer in recycling papermaking.

The pulp from the beverage carton could be recovered by the conventional pulping process using a hydra-pulper to separate the pulp fiber from polyethylene and aluminum (Robertson, 2021). According to the Alliance for Beverage Cartons and the Environment (ACE), only half of 900,000 tons of beverage cartons placed on the EU market in 2019 were recycled (Lahme et al., 2020). Several researchers have attempted to utilize recycled pulp from beverage cartons (RPBC) in the production of construction materials to promote a circular economy and environmental sustainability (Ayrilmis, 2008; Rhamin, 2013; Platnieks, 2020; Martinez-Barrera, 2015). A cardboard panel that was produced by recycled beverage cartons overlaid with veneers could be considered as an alternative raw material for furniture production (Ayrilmis, 2008). The RPBC could also be used to produce a carton board with acceptable properties without the addition of resin and veneer layer (Rhamin, 2013). Adding 50 wt% of RPBC into the polybutylene succinate (PBS) matrix led to an improvement in the hardness of the composites (Platnieks, 2020). The compressive strength and modulus of elasticity values of recycled cellulose-reinforced cement concrete increased by 45% and 47%, respectively, when adding 3 wt% of RPBC and applying gamma ray at 300 kGy (Martinez-Barrera, 2015). Nevertheless, the use of RPBC as reinforcement in cementitious composites has not yet been widely explored.

Therefore, the recycled pulp needs to be treated by a mechanical process to minimize the tufts without damaging the fiber excessively. A combination of recycled pulp and other cellulose fiber in a suitable ratio can contribute to improving the enforcement of fiber.

2.1.4 Bamboo Fiber

Bamboo fiber is a potential substitute for wood pulp (Correia et al., 2014). Tables 2.4 and 2.5 list the physical and mechanical characteristics of bamboo fiber obtained using various extraction techniques. Bamboo fibers are natural cellulose fibers characterized by their cylinder form. The fibers are located around the vessels, phloem, and protoxylem as sheaths and as isolated stands (see Figure 4.5). It stretches along with the height of the culm. The fiber length varies remarkably between bamboo species

(Liese & Koehl, 2015). It ranges from 1to 3 mm, and the fiber width varies from 10 to 30 µm, as shown in Table 2.4. The tensile strength of bamboo fiber ranges between 300 and 800 MPa, and the modulus of elasticity lies between 20 and 40 GPa. In comparison to other natural fibers, bamboo fiber exhibits low elongation (see Table 2.4).

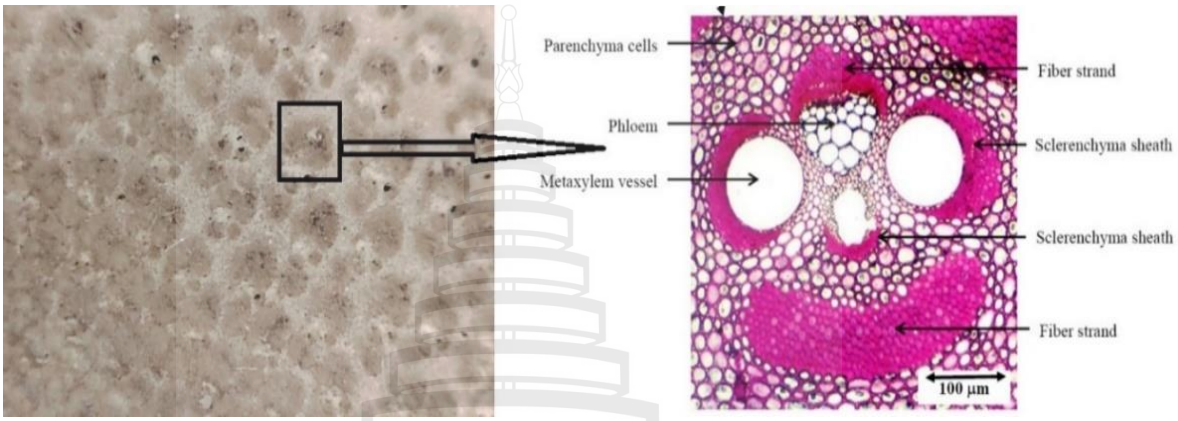

Source Chaowana (2013)

Figure 2.5 Cross-section of bamboo culm

Table 2.6 presents the mechanical properties of bamboo fiber cement in comparison to wood pulp fiber-reinforced cement composites. Coutts et al. (1994) investigated the properties of bamboo fiber-reinforced cement using unbeaten and beaten unbleached bamboo pulp (*Sinocalamus affinis* species) in an air-cured environment. The flexural strength of the unbeaten, unbleached bamboo pulp cement composite increased from 10 MPa to 22 MPa, and the fracture toughness also increased as the fiber content increased from 2% to 14% by mass. The study shows that the fracture toughness of unbeaten fiber cement composite was ~ 0.7 kJ/m^2, while that of beaten fiber was 1.0 kJ/m^2 at 14 wt% fiber content.

Table 2.4 Physical properties of bamboo fiber prepared by different extraction processes

Bamboo species	Extraction Process	Length (mm)	Width (μm)	Aspect ratio	Ref.
Sinocalamus affinis	Unbleached kraft pulp	1.3	-	-	Coutts and Ni (1995)
Guadua angustifilia	Organosolv pulp	0.6 – 1.3	12-23	40.4	Correia et al. (2014)
Guadua angustifolia Kunth	Alkaline pulping	1.02-3.5	<20	-	Sanchez-Echeverri (2021)
Gigantochloa Scortechinii	-	1.45-3.2	20-30		Ashaari et al. (2010)
Bamboo	Commercial pulp	2.5 ± 0.4	13.1	-	Xie et al. (2019)

Table 2.5 Mechanical properties of bamboo fiber prepared by different extraction methods

Bamboo species	Extraction methods	Mechanical properties			Ref.
		Tensile strength (MPa)	Young's modulus (GPa)	Strain (%)	
Guadua angustifolia	Mechanical	860 ± 119	46 ± 1.2		Osorio et al. (2011)
Phyllostachys edulis	Mechanical	420 ± 170	38.2 ± 16.0	9.8±2.5	Phong et al. (2012)
Phyllostachys edulis	Chemical (1% NaOH)	395±155	26.1±14.5	2.82±1.3	Phong et al. (2012)
Phyllostachys edulis	Steam-explosion	308 ± 185	25.7 ± 14	2.51±1.2	Phong et al. (2012)
Bamboo	Mechanical	503	35.91	1.4	Rao and Rao (2007)
Bamboo	Mechanical	717.53	43.34	2.03	Huang and Young (2019)

Table 2.5 (continued)

Bamboo species	Extraction methods	Mechanical properties			Ref.
		Tensile strength (MPa)	Young's modulus (GPa)	Strain (%)	
Phyllostachys edulis	Steam explosion	383	28	2.82	Kim et al. (2013)
Phyllostachys edulis	Alkali extraction	419	30	2.67	Kim et al. (2013)
Phyllostachys edulis	Chemical extraction	329	22	2.35	Kim et al. (2013)
Bamboo	Steam-explosion	441 ± 220	35.9 ± 13.1		Okubo et al. (2004)
Bamboo	Chemical-CMT	644.8 ± 145.5	-	-	Deshpande et al. (2000)
Bamboo	Chemical-RMT	370.1 ± 71.8	-	-	Deshpande et al. (2000)

Table 2.6 Properties of bamboo fiber reinforced cement composites compared with wood fiber

Fiber sources	**Fiber form**	**Fiber length (mm)**	**Fiber diameter (µm)**	**Aspect ratio**	**Fiber contents (wt%)**	**MOR (MPa)**	**Toughness (kJ/m^2)**	**Ref.**
Eucalyptus regnans	Kraft pulp	1	14	71	8	20.3	1.37	Coutts (1987)
Pinus radiate	Kraft pulp	3	30	100	8	30	2	Coutts (1987)
Sinocalamus affinis	Kraft pulp	1.7	-	-	14	21.3	1	Coutts et al. (1994)
Guadua angustifolia	Organosolv pulp	0.8	19.8	40.4	8	7.5	1.2	Correia et al. (2014)
Guadua angustifolia	Refined Kraft pulp	1.02-3.5	20	-	5	11	6.3	Sanchez-Echeverri et al. (2021)
Bambusa vulgaris	Flakes	14-17.1	390 - 610	-	36.3	9.25	-	Sudin and Swamy (2006)
Commercial bamboo fiber	Kraft pulp	2.5	13.1	190	12	11.2	2.2	Xie et al. (2019)

Correia et al. (2014) evaluated the performance of a cementitious composite reinforced with bamboo organosolv pulp. The maximum flexural strength reached 7.5 MPa at 8% fiber content by mass. The fracture toughness of bamboo organosolv pulp cement composite was 1.2 kJ/m^2, which is greater than that of cement composite reinforced with bamboo kraft pulp (0.32 kJ/m^2) at 8% fiber content.

The most common bamboo fiber used to reinforce the cementitious matrix reported in the literature is pulping fiber (Coutts et al., 1994; Coutts & Ni, 1995). Bamboo pulp is mostly obtained from chemical pulping processes (kraft pulp). However, the use of bamboo fiber isolated by alkaline-catalyzed hydrothermal pretreatment as a reinforcement in the cementitious matrix was not yet reported in the previous study. Moreover, the hybridization of bamboo fiber with recycled pulp in cement composites has not yet been deeply studied.

Therefore, the use of bamboo fiber extracted by the hydrothermal process at a temperature of 170 °C for 1 hour is the target of the study, and sodium hydroxide is employed as a catalyst agent. The blending of bamboo fiber with recycled pulp aims to improve the reinforcement efficiency of the fiber and, consequently, the properties of the composite.

2.2 Cementitious Matrix

A cementitious matrix used in fiber-reinforced cement composite mostly is usually the Ordinary Portland Cement (OPC). The main ingredients of OPC are Calcium Oxide (CaO), silicon dioxide or silica (SiO_2), aluminum oxide (Al_2O_3), iron dioxide (Fe_2O_3), and others.

The main chemical compositions of Portland Cement are tricalcium silicate ($3CaO.SiO_2$ in short C_3S), and dicalcium silicate ($2CaO.SiO_2$ in short C_2S), tricalcium aluminate ($3CaO.Al_2O_3$ in short C_3A), and tetracalcium aluminoferrite ($4CaO.Al_2O_3.Fe_2O_3$ in short C_4AF) (Illston & Domone, 2001).

The hydration process of cement starts when it reacts with water. Figure 2.5 shows the hydration stages of Portland cement, according to Nelson (2006). The initial stage takes about 15 minutes. The cement and water form a calcium silicate hydrate gel (CSH-gel). The second stage takes between 15 minutes and 4 hours. The cement grains

reached maximum solubility. CSH-gel starts to set up slowly, and it tends to solidify. At this time, it is called the initial set time. The third stage is the acceleration stage. This stage, also called the final set time, takes about 4 to 8 hours.

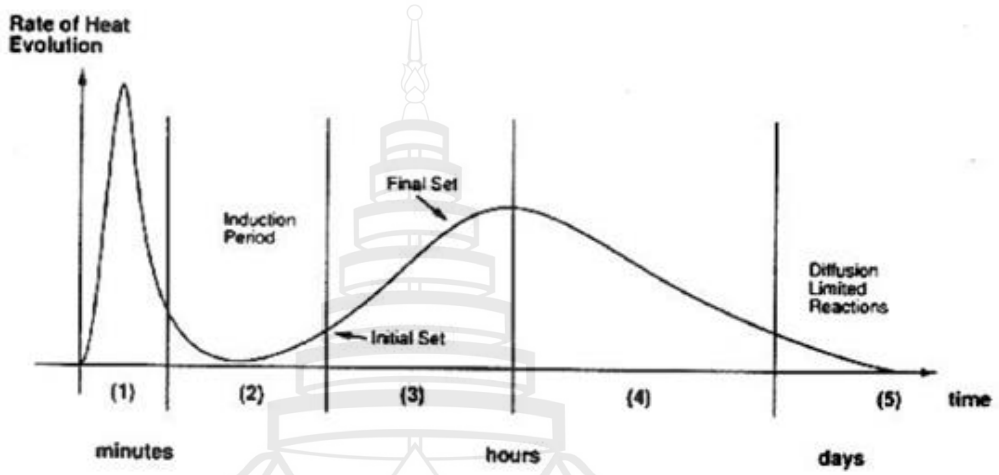

Source Nelson (2006)

Figure 2.6 Hydration stages of Portland Cement

Coutts (1987) stated that the flexural strength of wood fiber-reinforced cement mortars was lower than that of wood fiber-reinforced cement paste under air curing; however, the fracture toughness was the opposite.

Adding metakaolin to cement composites influenced properties such as water demand and setting time, as reported by Badogiannis et al. (2005). The water demand and setting time increased with an increase in metakaolin content. Therefore, the preparation time for fiber cement specimens by the slurry vacuum dewatering method should not be longer than 1 hour per specimen.

Matrix modification aims to reduce the alkalinity degree of the cementitious matrix by adding pozzolanic by-products to Portland cement, such as rice husk ash, fly ashes, silica fume, blast furnace slag, or metakaolin (Ardanuy et al., 2015; Mohr et al.,

2007; Filho et al., 2003; Marikunte et al., 1997), by the fast carbonation curing process (Filho et al., 2003; Almeida et al., 2013).

Filho et al. (2003) investigated the effect of silica fume and blast-furnace slag substitution of OPC in the matrix. The authors reported that by adding silica fume and blast furnace slag, the properties of the composite were not changed after 46 wet-dry cycles. Mohr et al. (2007) studied the performance of softwood wood fiber composites, which contain a variety of supplementary cementitious materials such as silica fume, ground granulated blast furnace slag, class F fly ash, class C fly ash, metakaolin, and a mix of raw and calcined diatomaceous earth and volcanic ash (DEVA). The authors found that the binary composites with 30% SF, 50% silica fume, 90% furnace slag, and 30% metakaolin replacement of OPC are the most effective compositions to prevent degradation of kraft pulp fiber after 25 wet-dry cycles.

Therefore, by modifying the matrix, the durability of the fiber cementitious composite was improved, but it depends on the fraction of supplementary materials.

2.3 Fiber Matrix Interface

The mechanical performance of the FRC depends not only on the matrix and fiber characteristics but also on the interface properties. In addition to fiber length, fiber-matrix bonding is the primary factor influencing composite toughness.

The fiber-matrix interface has a significant effect on the performance of composites (Coutts & Campbell, 1979). It plays an important role in controlling the strength and fracture toughness of the composite. When a load is applied, the stress will be transferred from the matrix to the fibers. The fibers have a role in preventing and reducing the propagation of cracks to avoid catastrophic failure (Bentur & Mindess, 2005). Two types of fiber failure mechanisms occur during tensile load, namely a fiber fracture and a fiber pullout. Silva et al. (2011) studied the interfacial bond of sisal fiber in different cross-section shapes with cement matrices. The authors reported that the adhesive bond between sisal fiber and cement matrix ranged from 0.48 to 0.92 MPa for 28 days of curing.

Tonoli et al. (2009) studied the influence of chemical modification on the surface of eucalyptus fibers with silanes on the durability of fiber-cement composites. The silane agents were methacryloxypropyltri-methoxysilane (MPTS) and aminopropyltri-ethoxysilane (APTS). The researchers found that non-mineralized filaments in composites with MPTS-modified fibers after 200 aging cycles led to less damage to toughness than composites with APTS-treated fibers.

The shape and surface of the reinforced fiber had an impact on the interfacial bond between fiber and matrix. The interfacial surface of fiber can also be improved by mechanical or chemical treatment. Both methods will be considered in this study.

2.4 Porosity

Porosity is a measure of the volume of voids in fiber cement composites. According to ASTM C 20-00 (2010), the apparent porosity is defined as a percentage of the relationship of the volume of the open pores in the specimen to its exterior volume. The porosity in the composite was mostly obtained by the experimental testing stated by Bentur and Mindess (2005). Figure 2.6 shows a drawing of porosity in the cross-section of the cementitious composite. When the fibers overlap or closely contact each other and the fibers are not compacted efficiently, water is filled into the spaces between the fibers, which then turn into voids upon curing, as shown in Figure 2.6.

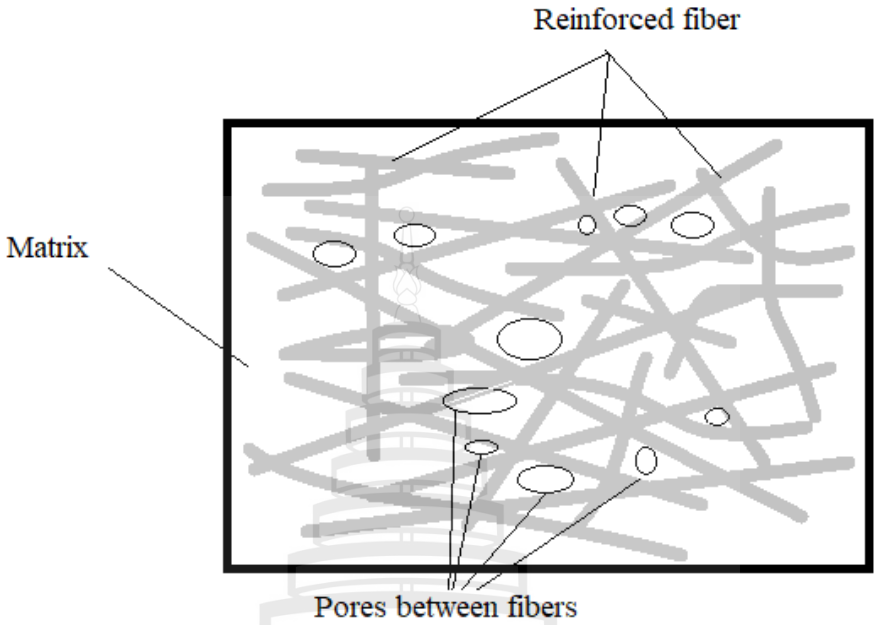

Figure 2.7 Schematic of porosity in the cross-section of the cement mortar matrix

Xie et al. (2015) reported that the porosity of the fiber cement composite was related to the fiber content, as shown in Figure 2.7. He also found that porosity influences predominantly the water absorption and density of composites.

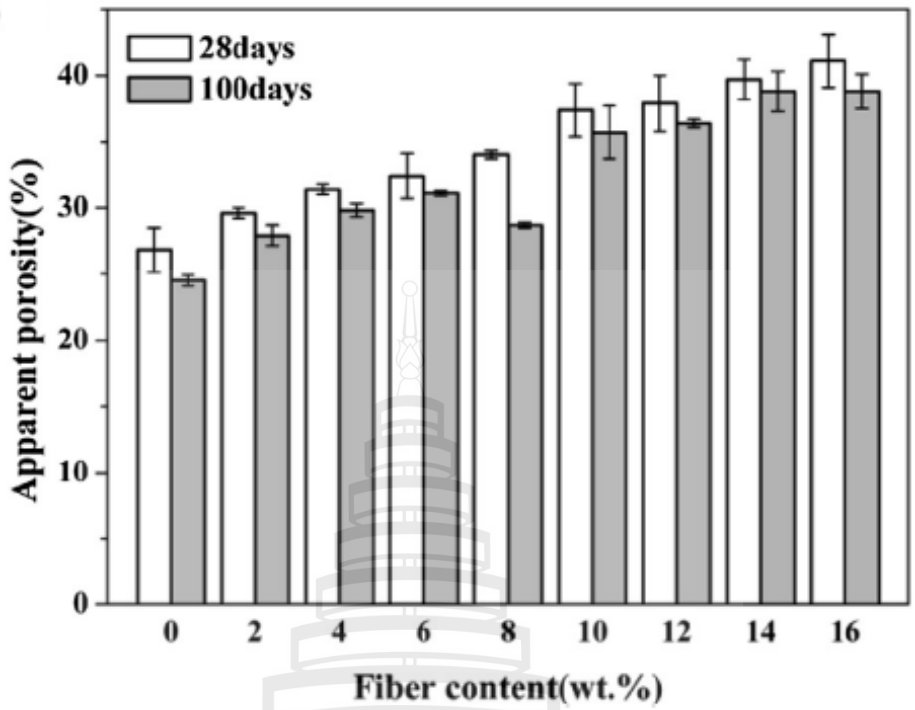

Source Xie et al. (2015)

Figure 2.8 Apparent porosity of rice straw fiber cement composite associated with fiber content

Habibi et al. (2017) studied the relationship between the surface density of composites, fiber length, and pore size distribution. The author stated that higher surface density increases the number of fibers per unit area and decreases the free space between the fibers, which gives a denser fibrous network with a low porosity rate. Bredy et al. (1988) stated that by adding metakaolin between 10% and 20% of the replacement of Portland cement, the porosity decreases compared with plain cement, as shown in Figure 2.8. Figure 2.8 presents a relationship between the porosity property of metakaolin-blend cement and the fraction of metakaolin replacement.

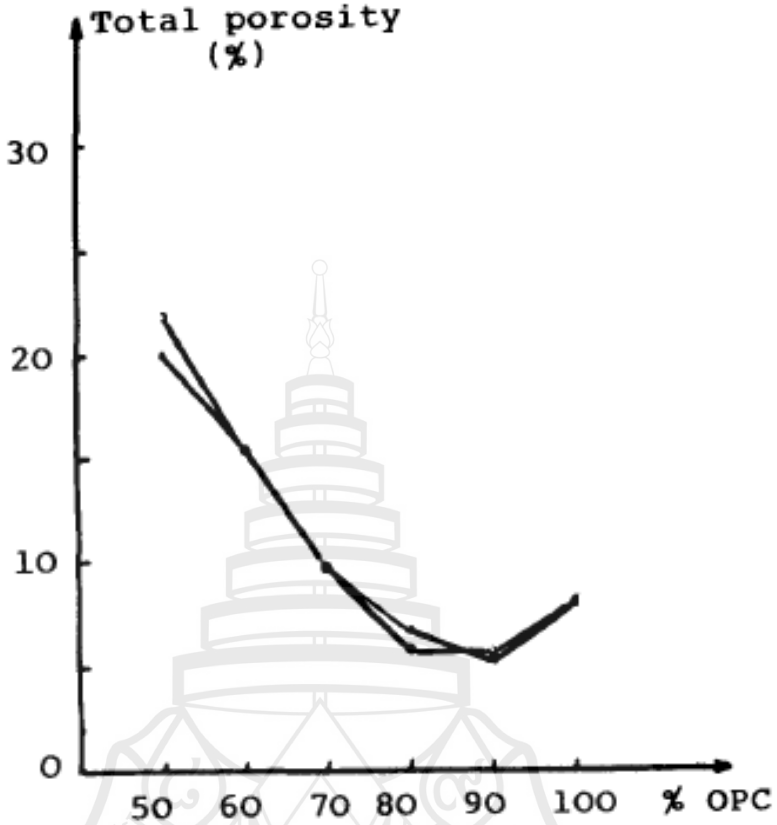

Source Bredy et al. (1988)

Figure 2.9 Porosity of metakaolin blended cement after 28 days

To reduce the void volume in the fiber cement composite, an addition of metakaolin as an admixture in this work will be considered, which ranges from 5–20 wt%.

2.5 Production Processes of FRC

2.5.1 Hatschek Process

The industrial manufacturing process for cementitious composites reinforced with natural cellulose pulp is based on the Hatschek process, invented by Ludwik Hatschek in 1900 (Ardanuy et al., 2015). Figure 2.9 shows the schema of the manufacturing process of fiber cement sheets.

The process begins with the preparation of slurry, which is a mixture of cement, sand, fiber, and additives. A dilute slurry is contained in the vat and drains through a rotating porous sieve cylinder. The solid materials are forming as a layer on the surface of the sieve when the sieve cylinder rotates in the slurry vat. The water drains through the sieve surface of the cylinder and flows back to the vat. A felt runs in a loop continuously and bridges between the sieve cylinder and the accumulation roll. Due to the surface tension forces, the green sheet is transferred from the top of the sieve cylinder to the felt underside. The movement of the felt transfers the green sheet from the sieve to the accumulation roll, and, on the way, at this point, water is drained out by vacuum. The layers are accumulated until the desired sheet thickness is obtained. One layer is usually a 0.25–0.4 mm tick. The final sheet consists of approximately 20–30 or more thin films (Ranachowski & Schabowicz, 2018). Then the green sheets are pressed in flat or corrugated form with a pressure of 3.2 MPa. Finally, the formed products are cured. There are two curing methods used, namely low temperature or air cure and autoclaved cure. Figure 2.9 shows the diagram of the Hatschek process.

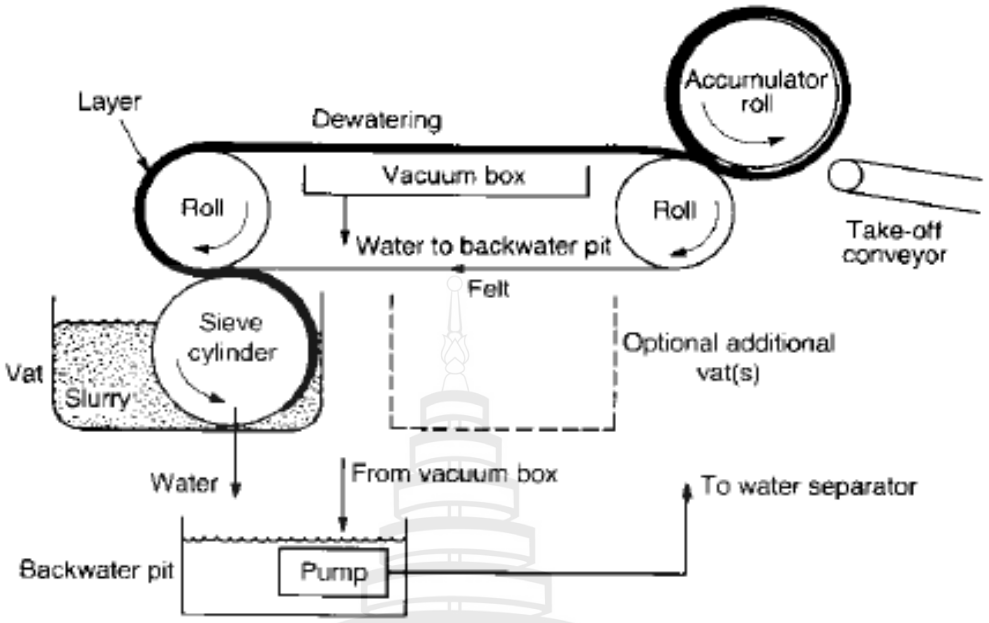

Source Illston and Domone (2001)

Figure 2.10 Schematic of Hatschek manufacturing process for asbestos fiber cement sheet

2.5.2 Slurry Vacuum De-watering Technique

A slurry vacuum de-watering technique is developed from the Hatschek principle. It is used for producing fiber-reinforced cement composites at the laboratory level. First, a mixture of fiber and water is prepared by a mixer and stirred at 1000–1500 rpm for 2.5–5 minutes to disintegrate the fiber thoroughly. Other solid ingredients are added after that, and the slurry is stirred continuously for 5–10 minutes. The solid content in the slurry should range from 20–30% by mass. After that, the slurry is transferred to a casting box connected to a vacuum. The overwater is sucked at a pressure of about 60–80 kPa. The plastic fiber cement sheet is pressed with a pressure of 3.2–4 MPa for 5 minutes. Finally, the sample is contained in sealed plastic bags for 24 hours before curing in an open-air environment.

Several researchers used the slurry vacuum de-watering technique for the production of samples (Coutts & Michell, 1983; Savastano et al., 2000; Coutts et al.,

1994; Savastano et al., 2005; Tonoli et al., 2011). Therefore, the specimens for this study will be formed according to the principle of the slurry vacuum dewatering methods because this technique facilitates the excellent dispersion of fiber in the cement.

2.5.3 Influent of Pressure

The green fiber cement sheet is subjected to pressing immediately after dewatering so that the excess water is released and the structure of the composite is compacted and densified. The pressure has a significant effect on the properties of the fiber cement composite, e.g., strength, density, maximum fiber content, water-cement ratio, and other properties (Akers & Garrett, 1986).

Coutts and Warden (1990) studied the effect of compaction on the properties of air-cured wood fiber reinforced cement. The authors reported that as the pressure was increased from 0.14 MPa to 3.17 MPa, there was a continuous increase in the flexural strength of composites greater than 50%. They also reported that the density increased and the water absorption decreased due to the porosity being reduced. However, the fracture toughness was slightly affected by the increase in pressure. It remained unchanged. The reason lay in the helical character of the wood fiber itself, as stated by Coutts and Warden (1990). Figure 2.10 shows that the flexural strength increased as the pressure increased.

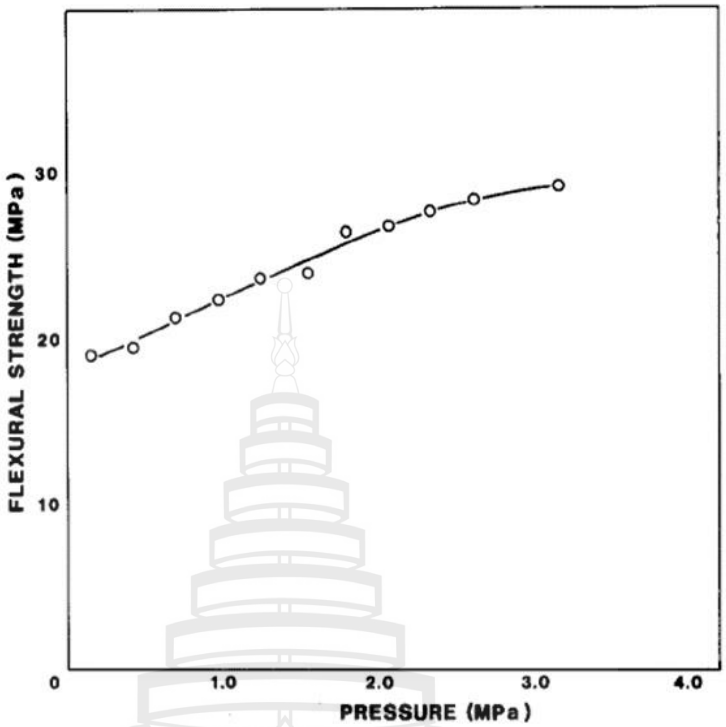

Source Coutts and Warden (1990)

Figure 2.11 Relationship between the pressure and the flexural strength of wood fiber cement composite

2.6 Summary

Researchers have extensively studied the use of several natural cellulose fibers, including recycled cellulose pulp, as reinforcement in cementitious composites to replace asbestos and synthetic fibers in construction materials and create an environmentally friendly material in the last few decades. Different fiber characteristics lead to a variety of properties and performances in fiber-reinforced cementitious composites. However, to get a deeper understanding of the properties of some potential fibers, it is necessary to thoroughly investigate their properties and performance and the significant impact of fiber characteristics on the properties of fiber-reinforced cementitious composite materials. Therefore, understanding the relationship between fiber characteristics and the properties of newly developed products is a crucial process.

The several influent factors, such as fibrillation level, fiber morphologies, fiber content, and compaction pressures, needed to be investigated more in detail.

CHAPTER 3

MATERIALS AND GENERAL METHODOLOGIES

The recycled pulp from beverage cartons, bamboo fiber, and eucalyptus fiber were the reinforced fibers used in this study. Ordinary Portland cement and ground silica sand were the ingredients for the matrix of the composites. These ingredient materials were characterized then by different techniques to understand their morphologies, dimensions, chemical composition, physical, and mechanical properties.

3.1 Materials

3.1.1 Recycled Pulp from Beverage Cartons

Recycled pulp was supplied by the Fiber Pattana Company in Thailand. It was obtained mainly from used beverage cartons. The beverage carton is a type of packaging material used for containing long-life liquid products such as milk, juices, drinking water, and pharmaceuticals. The beverage cartons are multi-layer coated paperboards, which consist of 75% paperboard, 20% low-density polyethylene, and 5% aluminum foil compacted in multilayer-coated phases (Robertson, 2021; Jacob et al., 2021). The paperboard used for beverage carton production was produced from a variety of pulp types, such as bleached and unbleached sulfate pulp and chemo-thermomechanical pulp, which depended on the type of drinking product (Abreu, 2000).

The repulping process was conducted in the factory by using a hydro pulper machine. The beverage cartons were submerged in water and converted into the hydro pulper machine. The waste cartons were agitated by a rotating stirrer at the bottom and broken up into small pieces. The layers of the carton were separated due to the centrifugal forces inside the pulper.

The slurry was washed in a perforated rotating cylinder, through which the polyethylene, aluminum residual, and recycled pulp were isolated (Robertson, 2021).

The as-received recycled pulp exhibits a clumped form and a moisture content of about 250 %. To avoid degradation of fiber and for long-period storage, the pulp was dried at 70 °C for 24 hours and kept in a plastic bag for further experimentation. Figure 3.1 shows the RPBC before and after soaking in water.

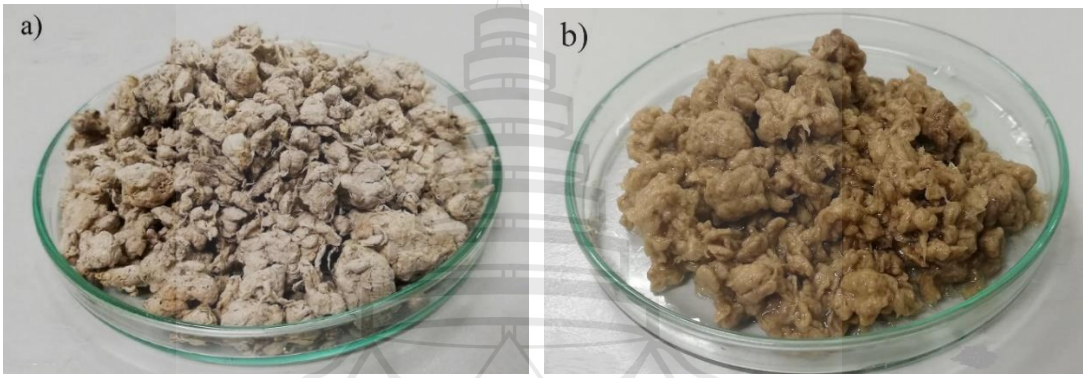

Figure 3.1 The RPBC in different stages: (a) dried RPBC and (b) wet RPBC

3.1.2 Virgin Bamboo Fiber

The bamboo source is an increasingly important economic source that can contribute significantly to poverty eradication and economic and environmental development. It has played a crucial economic and cultural role across Asia. It is used today for a wide variety of purposes, namely making chopsticks, furniture, food, construction materials (laminate, veneer, flooring), pulp, paper, textiles, and other instruments. Moreover, bamboo plantations are lauded for their ability to sequester carbon dioxide (CO_2) and emit oxygen (O_2). Seethalakshmi et al. (2016) stated that one hectare of bamboo plantation absorbs about 17 tons of carbon per year. Bamboo has contributed scientifically to conserving a sustainable ecological system due to its rapid growth and adaptability in carbon sequestration.

Recently, the attempt at bamboo fiber application has been growing in construction materials because of their advantages such as availability, low cost,

renewability, biodegradability, and acceptable properties (Seethalakshmi et al., 2016; Xie et al., 2019).

The bamboo species *Dendrocalamus membranaceous*, the local name Pai Saang Nuan, was selected for the research. A bamboo culm approximately 3–4 years old was obtained from the bamboo plantation located in Chiang Rai, Thailand. This bamboo species grows mostly in the northern part of Thailand and is easy to access.

Bamboo culms were cut into short rods with a length of 15–20 cm. Then the bamboo tubes were stripped into small pieces with 2–5 mm in the radial direction, and the bamboo strips were sliced and divided into thin strips. The strips were cut into small chips with dimensions of approximately 10–30 mm in length, 2–5 mm in width, and 0.5 mm in thickness with a sharp knife. Figure 3.2 shows bamboo chips for the extraction and bamboo fiber.

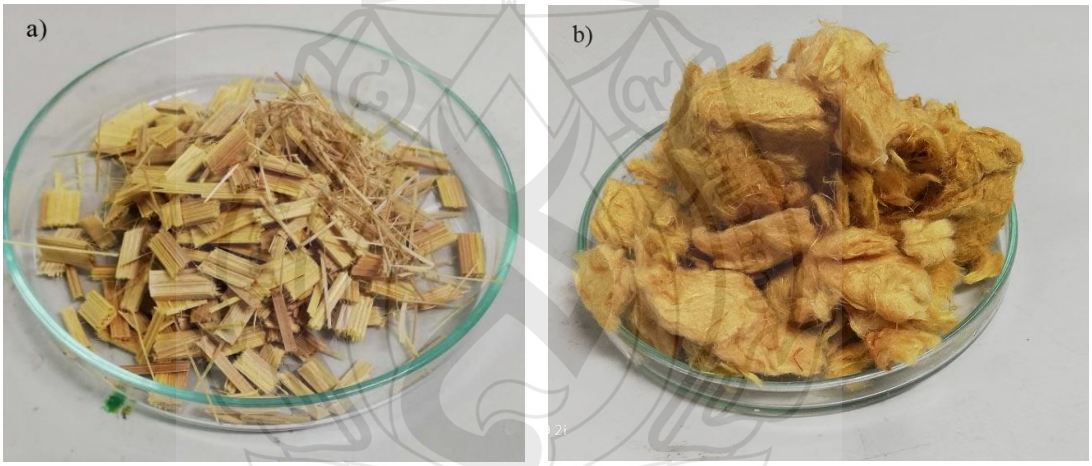

Figure 3.2 Bamboo: a) raw bamboo chips, and b) extracted dry bamboo fiber

3.1.3 Virgin Eucalyptus Fiber

Unbeaten, unbleached virgin EF was obtained by a commercial supplier. Before virgin EF was mixed with the cementitious matrix, it was weighted at a selected mass and immersed in water for 24 hours. After that, it was disintegrated by a mechanical stirrer at a speed of 1,500 rpm for 10 minutes. The dried and wet EFs are shown in Figure 3.3.

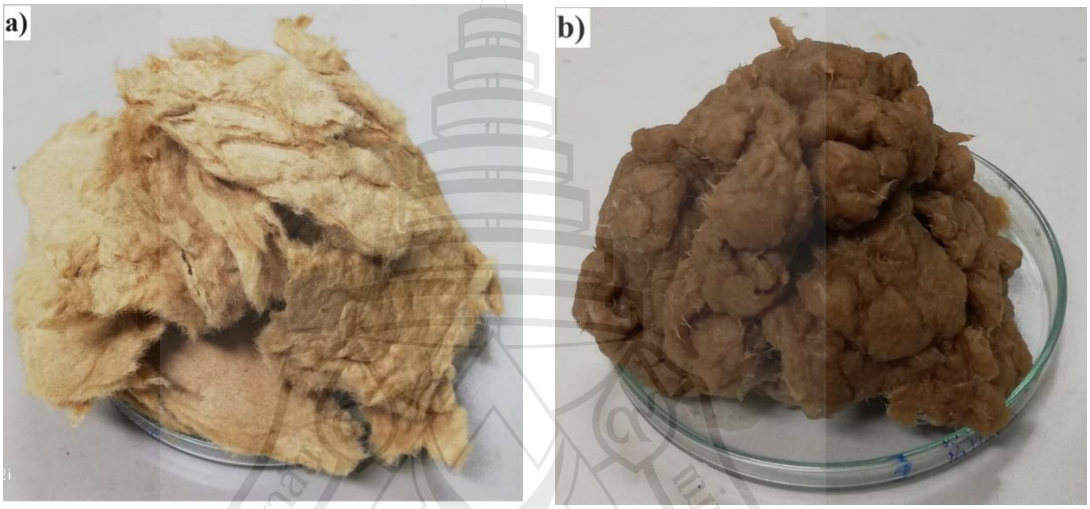

Figure 3.3 Virgin eucalyptus fiber: a) dried and b) wet condition

3.1.4 Matrix Ingredients

Ordinary Portland cement (OPC) Type I and ground silica sand were used as the ingredients for the cementitious matrix. PC was produced in accordance with the ASTM 150 standard reported by the producer. Both ingredient materials were supplied by a local commercial company and subjected to analysis before being used in the experiments.

3.2 General Methodologies

3.2.1 Fiber Reinforcement Characterization

3.2.1.1 Fibrillation and freeness determination of RPBC

To separate it into a single fiber and archive different freeness levels, RPBC was subjected to mechanical treatment. The blending process was used to treat the recycled pulp to disperse and generate fibrillation in RPBC with desirable freeness levels. Figure 3.4 shows the blending process of RPBC using a fruit blender.

Figure 3.4 Shearing process of RPBC with a fruit blender

To determine the freeness level of RPBC, firstly, 7.2 g of dried RPBC was soaked in water overnight (Figure 3.1b) to make it soften. The immersed recycled pulp was then subjected to disintegration and dispersion in 1 L of water using a fruit blender with a power of 1,500 W and a rotational speed of 25,000 rpm. The blended period ranged from 20 to 460 seconds, with an interval of 20 seconds. At the end of each period, 416 mL of the slurry sample was taken out for the freeness determination. The freeness of fiber, measured according to TAPPI T 227 om-99 (1999), was recorded until the value reached 400 mL CSF. The procedure was repeated five times. Figure 3.5 shows an example of the refined RPBC (500 mL CSF).

Figure 3.5 Refined RPBC with 500 mL CSF

Freeness has a significant impact on the properties of fiber cement composites manufactured by the slurry vacuum dewatering technique. The freeness level of fiber is measured according to TAPPI T 227 om-99 (1999), freeness of pulp (Canadian Standard Method). To determine the freeness of recycled pulp from beverage cartons used for the study of the influence of freeness on the properties of RPBC-reinforced composites, the following experiment was conducted:

Firstly, 7.2 g of dried recycled pulp (8 wt% of the solid weight of a specimen) was soaked in water overnight to make it soften. The immersed recycled pulp was then subjected to disintegration and dispersion in 1 L of water using a fruit blender with a power of 1,500 W and a rotational speed of 25,000 rpm. The blending period ranged from 20 to 460 seconds, with an interval of 20 seconds. At the end of each period, 416 mL of the slurry sample was taken out for the freeness determination, which is equivalent to 3 g of dried pulp according to TAPPI T 227 om-99 (1999). After the blending process, the slurry sample was added with 584 mL of water to an archive of 1,000 mL of recycled pulp solution. After that, the blended recycled pulp solution was poured into the drainage chamber of the tester, as shown in Figure 3.8, and the chamber was closed tightly. Then the bottom cover was opened, and the volume of

water drained through the side discharge orifice was measured and recorded as the level of CSF freeness of the sheared RPBC.

The value of experimented freeness for each blending period was recorded until the value reached 400 mL CSF. The procedure for each blending condition was repeated 5 times. Figure 3.6 shows a picture of the Canadian Standard Freeness Tester (CSF Tester).

Figure 3.6 CSF freeness tester

3.2.1.2 Determination of BF and EF

For the determination of bamboo and eucalyptus fiber freeness, 3 g of each fiber was immersed in water for 24 hours and disintegrated in 1000 ml of water using a homogenizer with a speed of 1,500 rpm for 10 minutes until there were no fiber bundles presented. After disintegration, the sample is poured into the drainage chamber of the tester. The volume of drained waste at the discharge orifice was measured and

recorded as the freeness level of BF and EF. Five samples were prepared for different fiber types.

3.2.1.3 Virgin bamboo fiber extraction

The hydrothermal method is a chemical reaction in water in a sealed pressure vessel, high temperature, and pressure. It can be considered an environmentally friendly fractionation process (Qien et al., 2015). A chemical reaction occurs in water in a sealed vessel. The reaction operates at both high temperature and pressure. Water is used as a solvent, reactant, and catalyst during the hydrothermal processing of biomass. During the treatment, water itself acts as a hydrolytic catalyst, especially at a higher temperature. Moreover, the organic acid liberated from hemicelluloses would promote the cleavage of carbohydrates (Qien et al., 2015). In the case of non-catalyzed hydrothermal degradation of cellulose, the cellulose hydrolysis rate is much lower than that of acid hydrolysis (Ma et al., 2013).

The virgin bamboo fiber was extracted by the hydrothermal process at a temperature of 170 °C for 1 hour in a hot air dryer using sodium hydroxide as the catalyzer. The hydrothermal method was conducted using a hydrothermal autoclave reactor and a Teflon chamber synthesis vessel. Figure 3.7 shows the components of a hydrothermal reactor with a synthesis vessel. Pelletized sodium hydroxide (NaOH) 99% AR grade Type QRëC, New Zealand, was used for catalysis, as shown in Figure 3.8. The alkaline concentration was optimized to obtain the best bamboo fiber properties for use as a reinforcement in the cementitious composite. Table 3.1 demonstrates the treatment conditions for bamboo chips. After the extraction, bamboo fiber will be dried in an oven at 105 °C for 24 hours and then kept in plastic bags for characterization and further experimentation. The extraction was repeated several times until a sufficient amount of fiber was used for the experiments. The extracted bamboo fiber is shown in Figure 3.1b.

Figure 3.7 Hydrothermal autoclave reactor and Teflon chamber

Figure 3.8 Catalyzer (Sodium hydroxide pullets)

Table 3.1 Condition for hydrothermal treatment

Conditions	**Data**
Temperature	170 °C
Operating time	1 hour
Fiber-water ratio	1:10
Bamboo fiber (D. *menbranaceus*)	10 g
Water	100 ml
NaOH concentration	2, 4, 6, 8, 10%

The yield of extracted bamboo fiber with different alkaline concentrations will be determined based on the initial weight of bamboo chips that were subjected to treatment with an alkaline hydrothermal method and the dry mass of the obtained fiber.

The yield efficiency was estimated by equation 3.1 below:

$$Yield\ efficiency\ (\%) = \frac{M_2}{M_1}\ x\ 100 \qquad \text{Equation 3.1}$$

Where M_1 is the initial weight of the bamboo chip in grams, M_2 is the weight of the oven-dry bamboo fiber after extraction.

3.2.1.4 Fiber dimension determination

The dimensions of all fiber types were determined using optical microscopy (MOTIC type BA310E), a portable digital microscope camera, and imageJ digital microscope software (see Figure 3.9). The images of fibers were taken with optical microscopy (OM) for the measurement of diameter and with a portable digital microscope camera for length measurement (see Figure 3.10). A total of 200 fibers were measured per sample using ImageJ software. The average value with standard deviations was calculated using an Excel sheet.

Figure 3.9 Optical microscope attached to a digital camera

Figure 3.10 Portable digital microscope camera

3.2.1.5 Morphology of fiber and fracture surface analysis

The surface and cross-section morphologies of RPBC, BF, and EF and the fracture surface of composites were examined using scanning electronic microscopy (SEM), model MIRA of TESCAN Company, Czech Republic (see Figure 3.11). Before the examination, the samples were gold-coated at 30 mA under a pressure of 1 mbar for 2 min using an SC7620 Sputter Coater to make them conductive. The analysis was

performed at a 10-kV electron acceleration voltage for bamboo fiber and recycled pulp surfaces and 5 kV for the fracture surface of composites using the secondary electron signal detector. The micrographs of the fiber surface and fracture surface of the composites were taken in resolution mode.

Figure 3.11 Scanning electronic microscope, model MIRA of TESCAN company, Czech Republic

3.2.1.6 Mechanical properties of fibers

To characterize the mechanical properties of RPBC, BF, and EF, the zero-span tensile strengths of the handsheet of RPBC, BF, and EF were assessed. Then the zero-span tensile index was estimated based on the grammage of the sample. The zero-span tensile strength has explained the quality of pulp and fiber, including fiber strength and bonding between fibers. The tensile strength and tensile index tests of RPBC, EF, and BF handsheets followed the TAPPI T 231 cm-96 (1996), *zero-span breaking strength of pulp* (dry zero-span tensile). The handsheets were prepared according to TAPPI T 205 cp-02 (2006), *forming handsheets for physical tests of pulp*. The sheets were produced with a weight of 150 g/m^2, referring to Annex B of TAPPI T 231 cm-96 (1996), and a dimension of 20 cm x 20 cm at a laboratory scale (see Figure 3.12). A 6 g-dry reinforced fiber was soaked in water for 24 hours, then disintegrated using an overhead homogenizer at a speed of 1600 rpm for 20 min. After that, the disintegrated pulp was transferred to a bucket. Then add 3 liters of water into the bucket to make the

solution with 0.2% consistency. The solution was stirred with a wooden stick until the mixture was well dispersed. The solution was poured into the quarter mold with a steel sieve at the bottom, which was in a 20-liter bucket. After pouring, the sieve was slowly taken out of the bucket without releasing the pulp from the mold, and the pulp was dispersed uniformly on the sieve. The pulp sheet was pressed at a pressure of about 345 kPa at room temperature for 5 minutes to drain water. Then continue with the hot press at a temperature of 110 °C for 5 minutes. Figure 3.12 shows the pulp sheet in wet and dry conditions.

The handsheets of each fiber type were cut into rectangular sheets having dimensions of 25 mm in width and 50 mm in length, as shown in Figure 3.13. The thickness of the test samples was around 0.4 mm. A set of 10 specimens for each fiber type was used for the zero-span tensile test. The test was conducted with the universal test machine (UTM) Instron Type 5632 (see Figure 3.14).

Figure 3.12 Handsheets of RPBC: a) after sieving and b) after pressing and drying

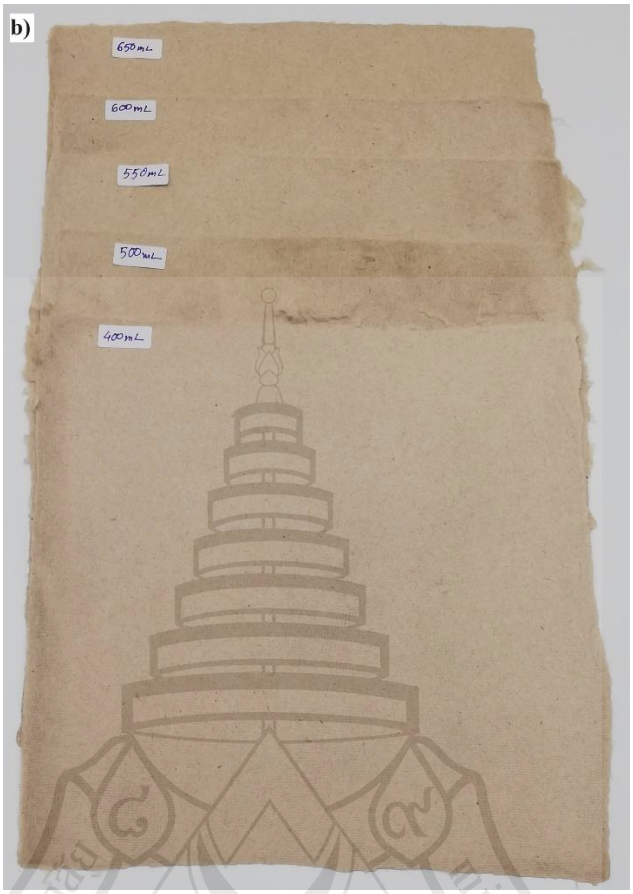

Figure 3.12 (continued)

Figure 3.13 Samples for the zero-span tensile test (Bamboo fiber)

Figure 3.14 Universal testing machine (Instron type 5632)

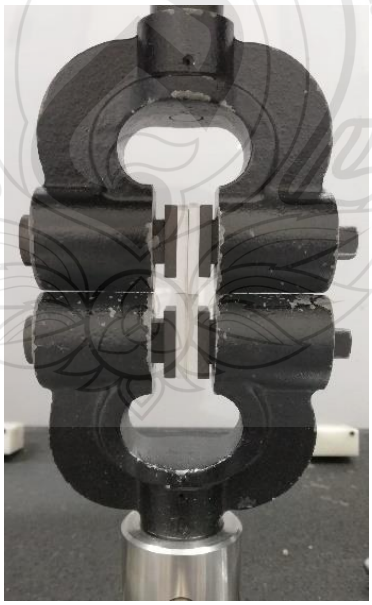

Figure 3.15 Cramping jaw for the zero-span test of handsheet paper

The test speed of 25 mm/min was employed and the 10 kN load cell was used. The specimens were kept in a control cabinet at 50 ± 2 % relative humidity and 23 ± 1°C for 48 hours. Figure 3.13 shows the clamping jaw for the zero-span test of the handsheet samples.

The tensile index of RPBC, BF, and EF was estimated by equation 3.2 below:

$$TS_{index} = \frac{TS}{g} \qquad \text{Equation 3.2}$$

Where TS_{index} is the tensile strength index in Nm/g, TS is the tensile strength of the fiber based on the width of the sample in N/m, and g is the grammage of the sample in g/m^2.

3.2.2 Characterization of Matrix Ingredients

Due to the many different types of Portland cement and siliceous materials, the analysis of the chemical composition of each ingredient is important in helping to understand the chemical reactions, setting, and strength development of hard composite. It affects significantly the properties and performance of fiber-reinforced cement composite. The chemical compositions of the OPC and ground silica sand were analyzed using an energy-dispersive X-ray fluorescence method (EDXRF), as shown in Figure 3.16. The particle sizes were analyzed using a laser scattering particle size distribution analyzer (LA-960), as shown in Figure 3.17.

Figure 3.16 Energy-dispersive X-ray fluorescence method (EDXRF)

Figure 3.17 Laser scattering particle size distribution analyzer (LA-960)

3.2.3 Specimen Forming Process

The fiber-reinforced cement composites were produced by a slurry vacuum dewatering technique. All specimens were formed using the same procedure. Firstly, the reinforced fiber was dispersed in water using a homogenizer and stirred at 1000 rpm for 2–5 minutes, depending on the fiber content, thoroughly before mixing with the matrix. Then the mixture of cement and ground silica sand was added to the fiber-contained bleaker. The slurry was stirred continuously for an additional 2 to 5 minutes to facilitate the homogenous dispersion of matrix and fiber. The fraction of solid materials in the slurry was maintained between 20 and 30% of the total solution, depending on the fiber type and fiber content. The obtained slurry was poured into the steel frame, which was placed on the well-sealed steel box. The #400 filter mesh was placed between the steel frame and the steel box to retain the solid particles and form a wet fiber cement sheet. The box was connected to a vacuum system to facilitate the drainage of water from the slurry. After thorough pouring, the excess water was drained out using a vacuum pump at a pressure of 90 kPa until the surface of the specimen was formed softly. The specimen was pressed at a pressure of 3.5 to 5 MPa for 5 minutes, depending on the objective of the assessment. The specimen was kept in a sealed plastic bag overnight to avoid the fast evaporation of water and then stored in a plastic box with a humidity of 99% at room temperature for 28 days. Five specimens were formed for each fiber type and percentage of fiber content. The specimen has a width of 40 mm, a length of 200 mm, and a thickness between 8 and 10 mm, depending on the fiber contents (see Figure 3.18).

Two days before bending testing, the specimens were placed in an ambient atmosphere according to ASTM C 1186-09 (2002), *the standard specification for flat non-asbestos fiber-cement sheets*. Figure 3.18 shows the components for specimen formation.

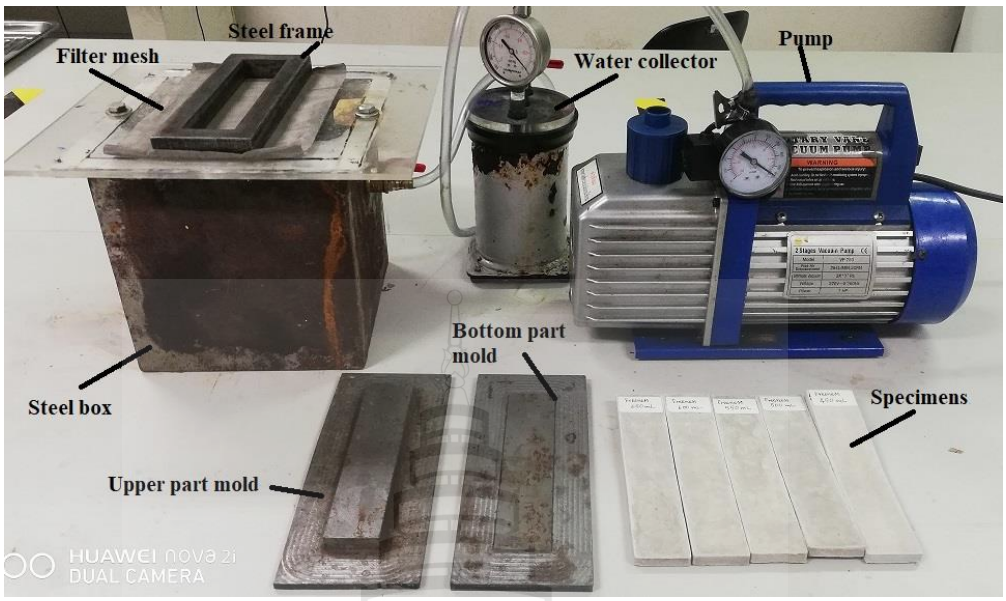

Figure 3.18 Steel mold for RPBC, BF, and EF reinforced cementitious specimen formations using slurry dewatering method

3.3 Assessment of Properties of Composites

3.3.1 Physical Properties Testing

The physical properties such as density, water absorption, and porosity of fiber-reinforced cement specimens were determined following ASTM C1185-08 (2016), *standard test methods for sampling and testing non-asbestos fiber-cement flat sheets, roofing and siding shingles, and clapboards* using the water displacement method. The Mettler Toledo balance of the Jewelry JS 2002G model, with an accuracy of 0.01 g, is used for specimen weighing.

After the flexural test, the specimen was used for density, water absorption, and porosity determination. The bulk density of the specimen can be calculated using equation 3.3 below.

$$B = \frac{D}{W-S} \times \rho_w \qquad \text{Equation 3.3}$$

Where B is the bulk density (g/cm^3), D is the dry weight of specimen (g), W is the saturated weight (g), S is the suspended weight (g), and ρ_w is the density of water (g/cm^3).

The water absorption of the specimen can be estimated using equation 3.4.

$$WA = \frac{W-D}{D} \times 100 \qquad \text{Equation 3.4}$$

Where WA is the water absorption (%), W is the saturated weight (g), and D is the dry weight (g).

The dry weight of specimen (D) was determined after drying in an oven at 90 ± 2 °C until the altering of weight was less than 0.1% at 2 h intervals. Then the specimen was immersed in water contained in a 1000-mL beaker for 24 hours and boiled for 2 hours. After boiling, the specimen was cooled to room temperature. It was taken at least 12 hours before weighing. After that, the suspended weight (S) of the specimen was determined by using a halter with a copper wire, which is placed on a balance. The specimen was hung on the halter with the copper wire and immersed in water (see Figure 3.19). After measuring a suspended weight, the specimen was removed from the water and wiped with a soft cloth to remove water from the surface. Then the weight of the specimen was measured as saturated weight (W).

We determined the apparent porosity using the ASTM C20-00 (2010) *standard test methods for apparent porosity, water absorption, apparent specific gravity, and bulk density of burned refractory brick and shapes by boiling water*. It is calculated as a percentage of the volume of the open pores in the specimen divided by the exterior volume. Porosity (P_O) in percentage can be calculated as follows:

$$P_O = \frac{(W-D)}{(W-S)} \text{x}100 \qquad \text{Equation 3.5}$$

Where W is the saturated weight (g), D is the dry weight (g), and S is the suspended weight (g). Figure 3.19 shows the equipment for the measurement of the physical properties of the composites.

Figure 3.19 Measurement of physical properties of the composites

3.2.3 Mechanical Properties Testing

3.3.2.1 Flexural strength and modulus of elasticity

The mechanical tests were conducted after specimens were cured for 7 and 28 days in air-cured conditions. The modulus of rupture (MOR) was determined in the three-point bending mode with a 10-kN load cell and 1.5 mm/min load speed. The test was conducted using a Universal Test Machine (UTM) Instron Type 5632, according to ASTM C1185-08 (2016), *standard test methods for sampling and testing non-asbestos fiber-cement flat sheet, roofing and siding shingles, and clapboards*. The support span was 160 mm. The span-length to thickness ratio is about 20, which is greater than the requirement in ASTM C 1185-08 (the recommended span-length to thickness ratio should be greater than 18).

Equations 3.6 and 3.7 below are used to estimate the flexural strength and strain:

$$\mathrm{MOR} = \frac{3\mathrm{PL}}{2\mathrm{bd}^2} \qquad \text{Equation 3.6}$$

$$\mathrm{Strain} = \frac{6*\mathrm{d}}{\mathrm{L}^2} * \mathrm{deflection} \qquad \text{Equation 3.7}$$

Where MOR is flexural strength (MPa), P is the maximum load (N), L is the length of span (mm), b is the width of the specimen (mm), and d is the average thickness (mm).

The modulus of elasticity was calculated by equation 3.8:

$$\mathrm{MOE} = \frac{(\mathrm{P}_2 - \mathrm{P}_1)\mathrm{L}^3}{(\mathrm{y}_2 - \mathrm{y}_1)\,4\mathrm{bd}^3} \qquad \text{Equation 3.8}$$

Where MOE is the modulus of elasticity (GPa), P_2 and P_1 are load (N), taken from two points within the linear section of the plot, y_2 and y_1 are the deflections (mm) corresponding to the loads selected, b is the width of the specimen (mm), d is the thickness of specimen (mm), and L is the length of span (mm).

3.3.2.2 Fracture toughness

The absorbed energy of the specimen is defined as the area under the load-deflection curve as described by Savastano et al. (2000). The corresponding point is defined at the point where the load reduces to 50% of the maximum load as shown in Figure 3.20. The fracture toughness is calculated as the division of fracture energy to the cross-section area of the specimen as equation 3.9.

$$\mathrm{Fracture\ toughness} = \frac{\mathrm{Fracture\ Energy}}{\mathrm{b}*\mathrm{d}} \quad (\mathrm{J/m^2}) \qquad \text{Equation 3.9}$$

Where b is the width of the specimen (mm), and d is the average thickness (mm). The fracture energy is defined as the area under the load-deflection curve (see Figure 3.20)

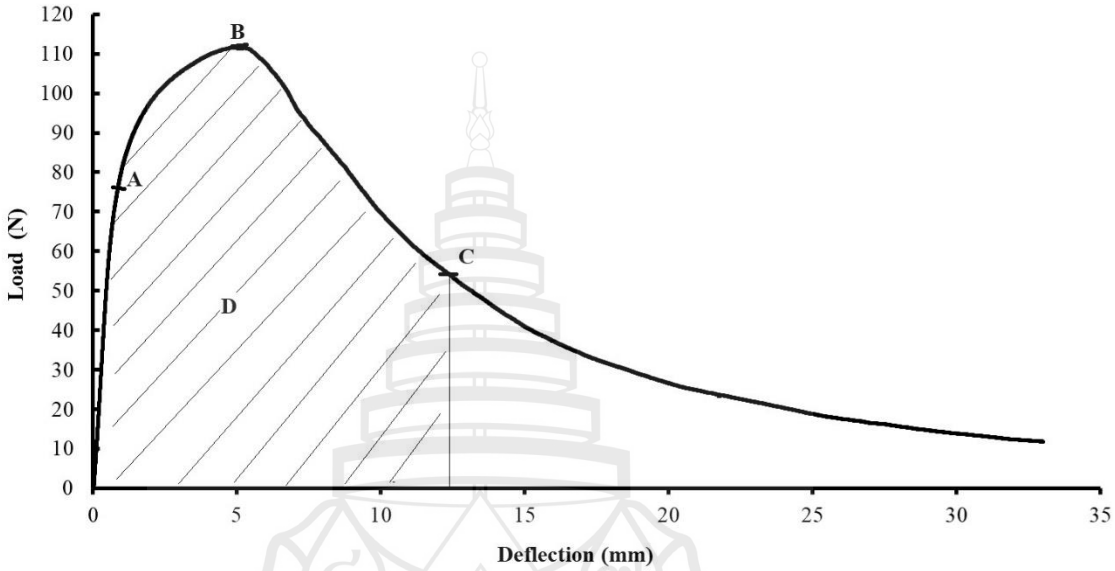

Figure 3.20 Definition of fracture toughness of composite

Figure 3.20 presents the typical load-deflection cure of fiber cement composite. A is the point of linear proportion, B is the maximum load, and C is the correspondent point at 50% of the maximum load. D is the area under the curve which is defined as the fracture energy.

3.4 Fracture Surface Analysis

The fracture surface analysis data can provide valuable information in the understanding of the failure mechanisms related to the mechanical behaviors of fiber-reinforced cementitious composites. These include interfacial bonding between fiber and matrix, fiber failure, fiber pullout, and porosity appearance. Figure 3.21 shows the fracture behavior of the fiber reinforcement in the cementitious composite. The reinforced fiber plays a role in crack bridging and hinders crack propagation. In addition, under a continuous load, the fiber carries the load transferred by the matrix.

Tow fiber failure modes (fiber pull-out and fiber fracture) will occur, depending on the fiber characteristics. The fracture surface of fiber cement composites was analyzed using a scanning electron microscope as described in 3.2.1.4.

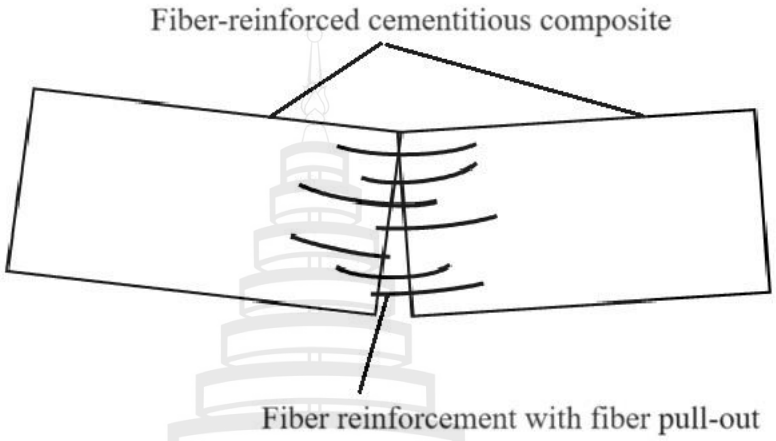

Figure 3.21 Fiber-reinforced toughening mechanism

CHAPTER 4

FIBER PREPARATION AND CHARACTERISATION

4.1 Introduction

The performance of the natural cellulose fiber application depends on the source of fiber and the method employed to extract the fiber. Each fiber type has a different characteristic. To understand how to utilize natural cellulose with high benefits, it needs knowledge of the microstructure, properties, and chemical composition of the natural cellulose fiber. To advance the application of natural cellulose fibers for different materials, continued investigation into the fiber characteristics, properties, and methods of extracting the fibers is essential. Therefore, it needs to characterize the raw fibers for the development of new products and production methods.

4.2 Materials and Methods

4.2.1 Materials

The recycled pulp from beverage cartons, bamboo fiber, and eucalyptus fiber was subjected to characterization before being used as reinforcement in cementitious composites. In addition to that, OPC and ground silica sand that were used as matrix ingredients were also analyzed.

4.2.2 Methods

4.2.2.1 Freeness measurement

The measurements of the freeness levels of treated RPBC, BF, and EF followed the description 3.2.1.1 and 3.2.1.2, respectively.

4.2.2.2 Dimension determination

The length and width of all reinforced fibers were determined according to the explanation in 3.2.1.4.

4.2.2.3 Surface feature analysis

The feature surfaces of sheared RPBC, extracted BF, and EF were investigated following the methods described in Chapter 3 (3.2.1.5).

4.2.2.4 Tensile strength index

The tensile strength indexes of fiber reinforcements followed the method as explained in 3.2.1.6.

4.3 Results and Discussions

4.3.1 Effect of Shearing Process on RPBC Characteristics

4.3.1.1 Freeness

Figure 4.1 demonstrates the relationship between the freeness levels of RPBC and shearing periods. The initial freeness of untreated RPBC after immersion for 25 hrs in water was 870 mL CSF. The low freeness values indicate a high refining level (Tonoli et al., 2013). The freeness of RPBC decreased from 800 mL to 370 mL CSF as the shearing period increased from 20 to 460 seconds. With the gradually increasing shearing period up to 200 seconds, the freeness level of RPBC sharply decreased in this early stage of the refining from around 870 mL to 540 mL CSF.

However, when the shearing period reached 460 seconds, the freeness decrease to 370 mL CSF with a lower rate. The slow fibrillation of the sheared RPBC may be caused by an increase in short fiber content during shearing treatment. This phenomenon was also reported by the previous study (Tonoli et al., 2013). However, the alteration of fiber continued gradually after a long shearing period.

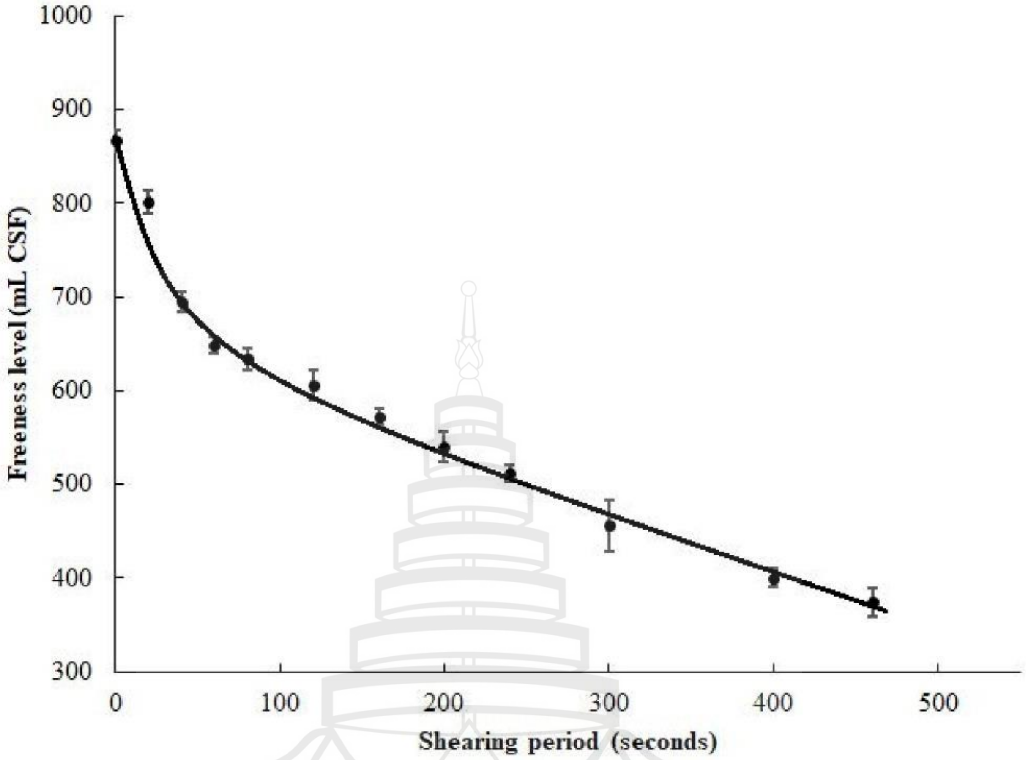

Figure 4.1 Relation between the freeness level of RPBC and the shearing period

4.3.1.2 RPBC Fiber Dimensions

From the above-mentioned results, the freeness levels of 650, 600, 550, 500, and 400 mL CSF of RPBC were selected for the study. The corresponding shearing periods for those freeness levels were 60, 140, 200, 320, and 460 seconds, respectively. For the measurement of the RPBC dimension after the refining process, several optical microscope photos were used, as described in section 3.2.1.1.

Appendix A summarizes some optical microscope photographs of the RPCB used for fiber length and width measurements. In addition to this, the histogram of fiber length and width distribution for shared RPBC was also presented in this appendix.

Table 4.1 presents the properties of sheared RPBC depending on the shearing period, which varied from 60 to 460 seconds. The dimensions of RPBC fibers were changed according to the respective shearing times. As shown in Table 4.1, the maximum length of sheared RPBC ranged from 5.10 mm to 4 mm, while the minimum

length ranged from 0.33 to 0.14 mm when the freeness decreased from 650 to 400 mL CSF. It was noted that the average fiber length of RPBC decreased by 28% as the freeness decreased from 650 to 400 mL CSF. The reduction in fiber length of sheared RPBC was due to the pulp fiber being cut during the long shearing treatment. The shortening of refined pulp length was also reported in the literature (Gharehkhani et al., 2015).

In contrast to the shortening of the length, the average fiber width of blended RPBC slightly increased (~11.6% from 650 to 400 CSF) with an increase in refining levels. The increase in the width of the sheared RPBC was caused by the swelling of outer cell wall and the internal fibrillation of the RPBC after the shearing process. Tonoli et al. (2009) and Uetani and Yano (2011) also reported this effect. The fibrillation of RPBC resulted in an increase in specific surface area (Lu et al., 2018).

Table 4.1 Effect of shearing period on the freeness and dimensions of RPBC

Parameters	**Recycled pulp from beverage cartons**				
Blending period (seconds)	60	140	200	320	460
Freeness (mL CSF)	650 ± 7.6	600 ± 12	550 ± 10	500 ± 15	400 ± 12
length (mm)	0.33-5.10	0.21- 4.98	0.27- 4.88	0.19 - 4.20	0.14 - 4.00
Average length (mm)	1.91 ± 1.0	1.76 ± 1.0	1.58 ± 0.8	1.45 ± 0.8	1.36 ± 0.7
Width (µm)	7 - 75	9 - 60	9 – 90	5 - 70	8 – 71
Average width (µm)	31 ± 11	31 ± 11	32 ± 13	32 ± 12	34 ±12

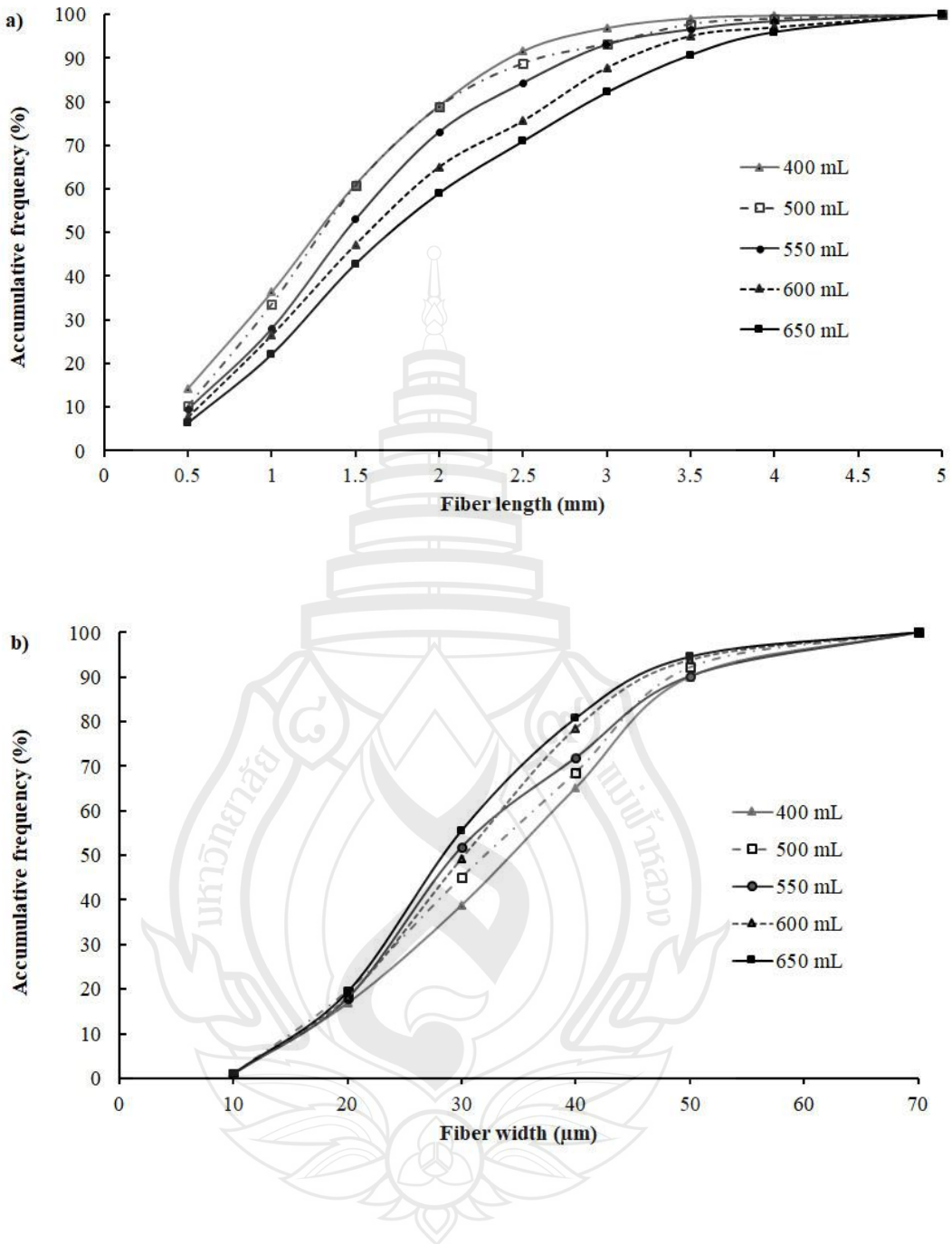

Figure 4.2 Accumulative fiber length (a) and fiber width (b) distribution of RPBC with various freeness levels

The accumulative fiber length and width distributions of the sheared RPBC are presented in Figure 4.2. A fiber that is longer than 2.5 mm was defined as a long fiber; otherwise, it was regarded as short. The result indicated that the percentage of

long fiber (> 2.5 mm) in sheared RPBC decreased as the freeness decreased because the fiber was shortened during blending treatment (see Figure 4.2a). The graphs in Figure 4.2b indicated that the width of sheared RPBC increased when the freeness decreased as the fibrillation of recycled pulp increased. The finding is in accordance with the previous studies (Savastano et al., 2000; Tonoli et al., 2009). The reason for the increase in the fiber width could properly be related to the increase in the specific surface area of sheared RPBC (Lu et al., 2018).

4.3.1.3 Surface feature

Figure 4.3 shows the surface morphologies of RPBC at different refining levels. An overall observation states that the external surfaces of recycled pulp were peeled and parts of the pulp were shortened after refining. The outer surface of 650 mL CSF RPBC shows a smooth and rough feature (see Figure 4.3a), while other sheared RPBCs were opened with thin microfibrils, resulting in a rougher surface (see Figure 4.3b-e). This was caused by the shearing process of the RPBC (Fardim & Durán, 2003). The fibrillation of the RPBC led to an enhancement of the frictional force between fiber-to-fiber and fiber-to-cementitious matrix (Coutts & Ridikas, 1982), reflecting directly on the performance of the composite materials (Uetani & Yano, 2011). The evidence of improvement in fiber-to-fiber bonding was in well agreement with the tensile strength index test result of the corresponding handsheet specimens of treated RPBC as shown in Figure 4.4, which indicates the progressive increase in the degree of fibrillation with decrease in freeness levels.

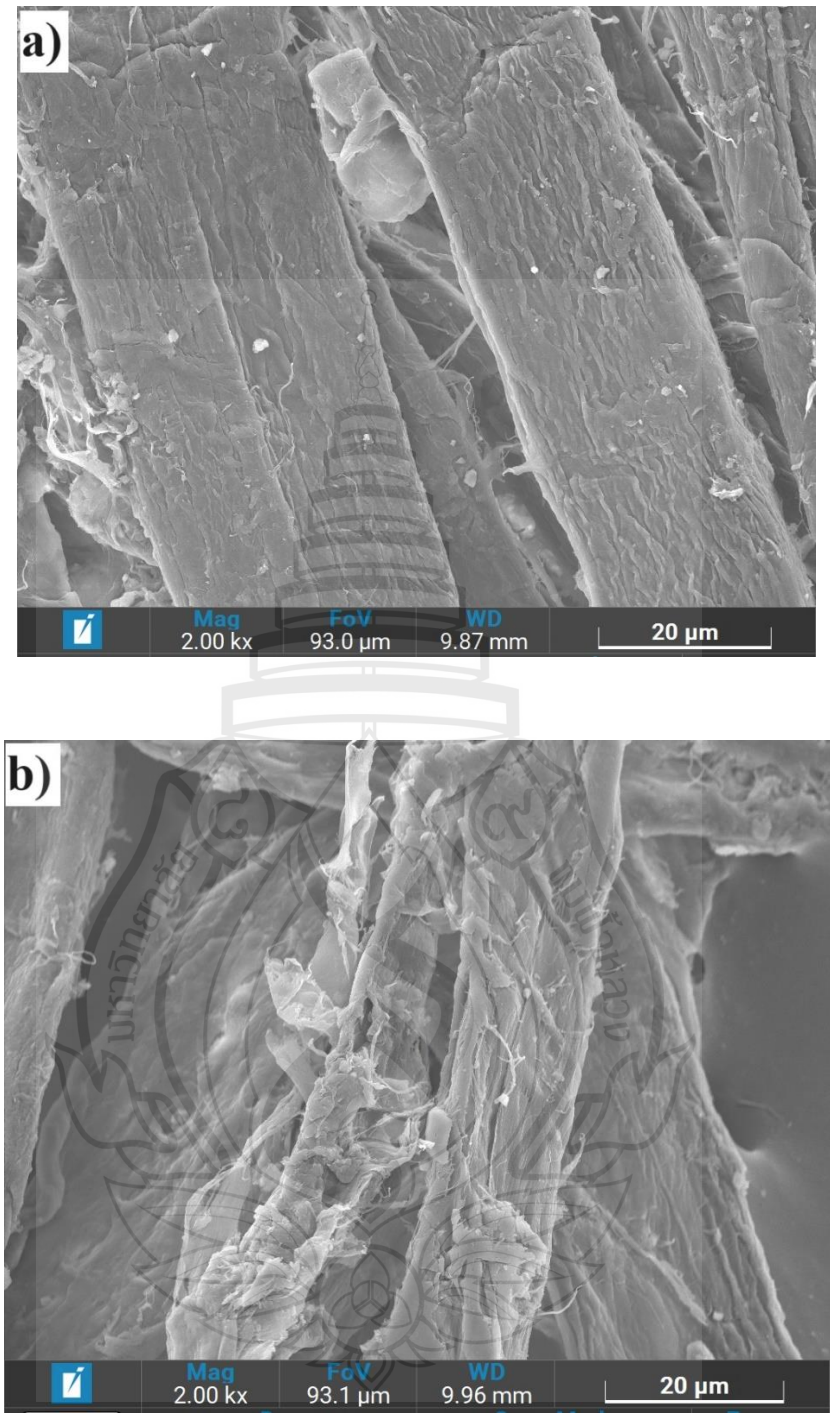

Figure 4.3 SEM photographs of RPBC at different freeness level: a) 650 mL CSF, b) 600 mL CSF, c) 550 mL CSF, d) 500 mL CSF, and e) 400 mL CSF

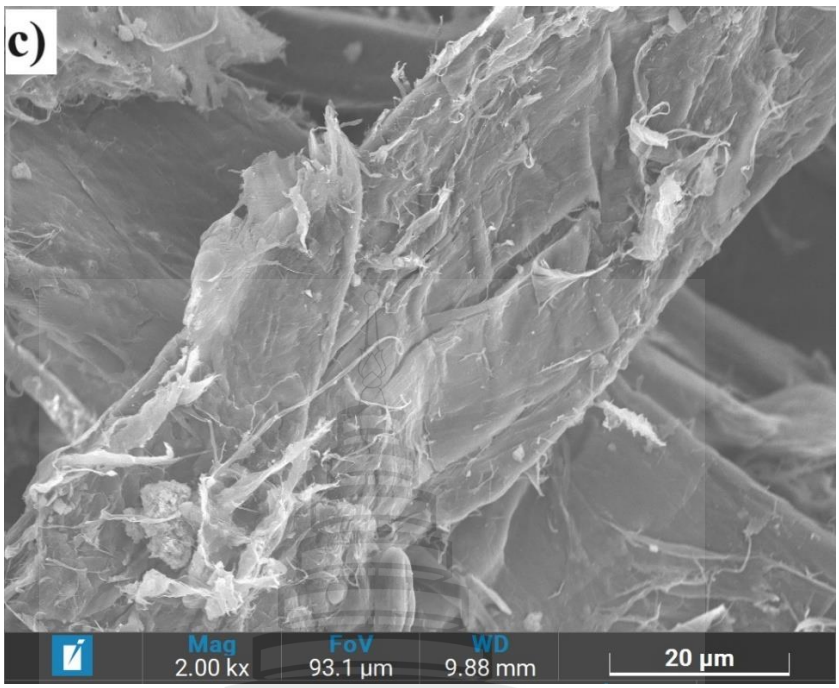

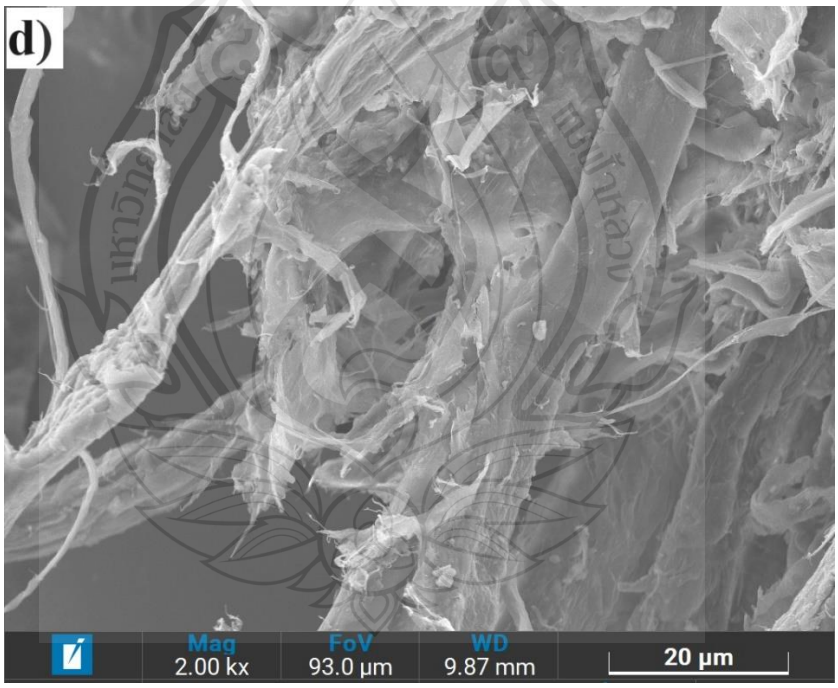

Figure 4.3 (continued)

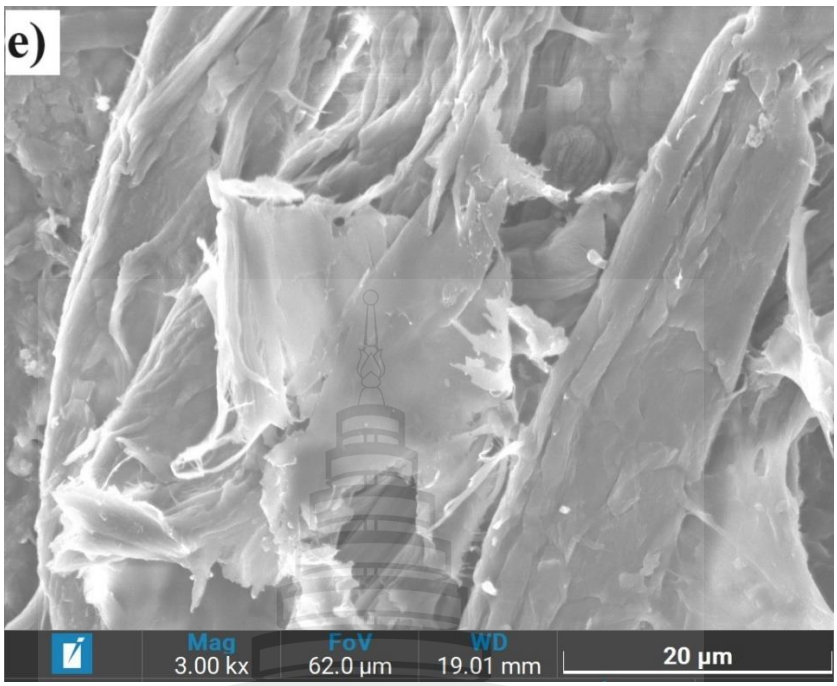

Figure 4.3 (continued)

4.3.1.4 Tensile strength index

Figure 4.4 illustrates the tensile strength index of the refined RPBC handsheets. Reducing the freeness of RPBC increased the tensile strength index. The increase in the tensile strength index of the RPBC handsheets was caused by an increase in specific surface area of refined RPBC and, consequently, the enhancement of the strength of the interfacial bonding of fibrillated RPBC (Savastano, 2000; Tonoli, 2007).

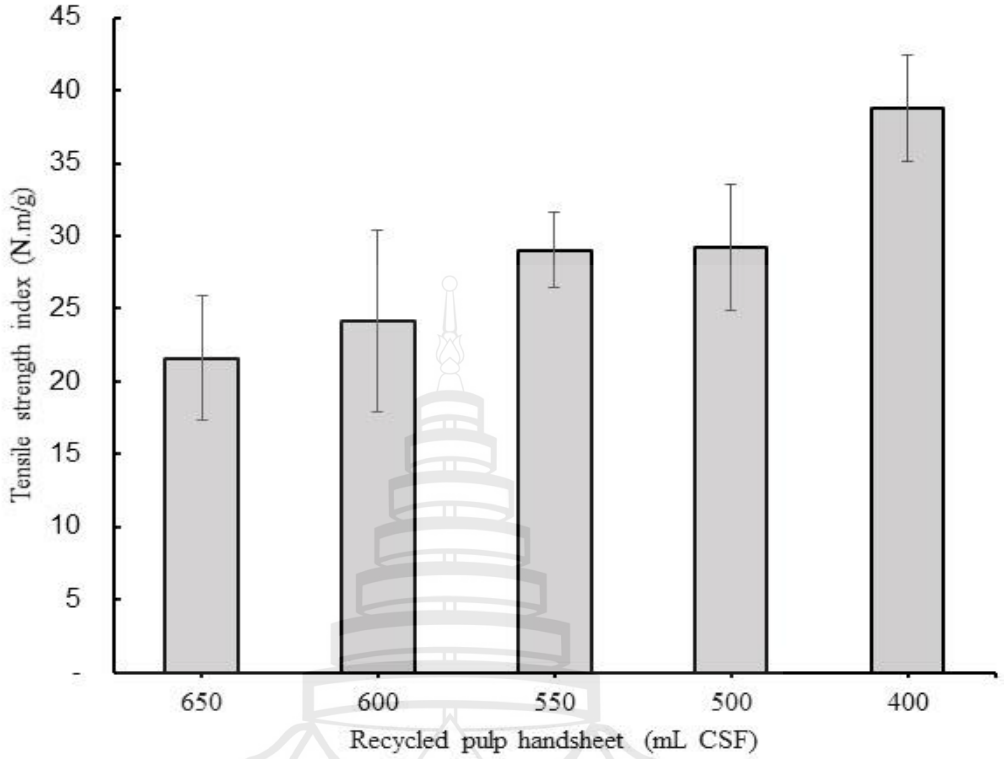

Figure 4.4 Tensile strength index related to the refining levels

4.3.2 Effect of Hydrothermal Treatment on Virgin Bamboo Fiber Characteristics

4.3.2.1 Recovery yields

Table 4.2 summarizes the physical and mechanical properties of virgin bamboo fiber, which was extracted using hydrothermal treatment with different concentrations of catalyst. The production yield of BF ranged from 41.3 to 43.8%. The higher the concentration of the NaOH catalyst, the lower the production yield of fiber. Kamthai et al. (2005) also suggested that the bamboo fiber yield by the kraft pulping process lied between 41.10 and 46.32%. The result shows that the hydrothermal pretreatment provides a high level of delignification.

4.3.2.2 Freeness

The freeness of the extracted BF ranged between 735 and 750 mL CSF. All types of extracted bamboo fiber exhibit a similar freeness level, about 740 mL CSF.

The results indicated that the extraction by hydrothermal process affects slightly the freeness of BF (see Table 4.2).

4.3.2.3 Dimension

The average fiber length and width of BF ranged from 2.07 to 5.76 mm and 20.68 to 55.01 μm, respectively. The histograms of the length and width distribution of the extracted BF are presented in Appendix B. It can be observed that both the average fiber length and width of BF decreased gradually with an increase in the concentration of NaOH catalyst at the fixed temperature and heating period. The reduction in the fiber dimension is caused by the increase in the solubility of hemicellulose and lignin in the cell wall, resulting in more flexible fiber. The delignification influenced heavily the morphology of bamboo fiber. The levels of cellulose increased with a reduction of lignin and hemicellulose in the bamboo fiber. This result was also correlated to the result of the recovery yield in 4.3.2.1. It can be seen that the reduction of length and width was correlated together, resulting in a similar aspect ratio, as shown in Table 4.2.

Table 4.2 Physical and mechanical properties of extracted bamboo fiber

Parameters	NaOH concentration in %				
	2	**4**	**6**	**8**	**10**
Yield (%)	43.8	43.5	42.6	41.5	41.3
Minimum width (µm)	14	15	14	14	6
Maximum width (µm)	245	95	65	69	78
Average width (µm)	55 ± 28	42 ±13	33 ± 9	29 ± 10	21 ± 9
Minimum length (mm)	2.30	0.67	0.60	0.991	0.45
Maximum length (mm)	9.64	7.59	6.87	6.57	5.70
Average length (mm)	5.76 ± 2.75	3.93 ± 1.13	3.16 ± 1.03	2.62 ± 1.09	2.07 ± 0.86
Aspect ratio	104 ± 74	93 ± 39	93 ± 39	90 ± 50	100 ± 50
Freeness (CSF)	746 ± 5.4	740 ± 0.0	738 ± 8.36	738 ± 8.36	738 ± 8.36
Zero-span strength index (Nm/g)	10 ± 2	12 ± 3	17 ± 3	18 ± 4	20 ± 4

4.3.2.4 Surface feature

The SEM photographs of extracted BF with different concentrations of NaOH catalyst are presented in Figure 4.5. As described in 2.1.4, the structure of a bamboo culm in a transverse section is characterized by numerous vascular bundles embedded in the parenchymatous ground tissue. Since the removal of lignin and hemicelluloses becomes more effective under higher concentrations of the alkaline catalyst with hydrothermal treatment, there has been an increase in the levels of cellulose. The higher the alkaline concentration, the more fibers are isolated from the bundles (see Figures 4.5a–e). With a higher concentration of alkaline, the outer surface of bamboo fiber became smoother than the lower. The diameters of fiber are smaller, but the lengths are longer. The lower NaOH concentration reveals a significant number of fiber bundles and some lignin on the fiber surface (see Figures 4.5 a–c). The average diameter of the bamboo fiber extracted with the 2% NaOH solvent was 55 µm. It reduced to 20.6 µm as the concentration increased to 10% by mass. The fiber bundle disappeared at the 10% NaOH BF (see Figure 4.5e).

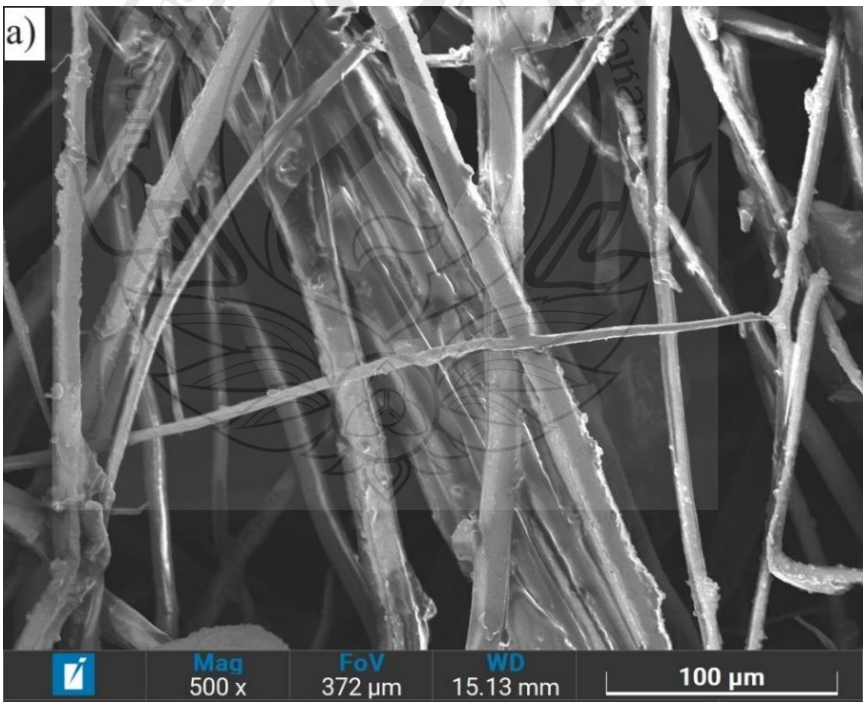

Figure 4.5 SEM photographs of bamboo fiber extracted by different concentrations: a) 2%NaOH, b) 4%NaOH, c) 6%NaOH, d) 8%NaOH, and e) 10%NaOH

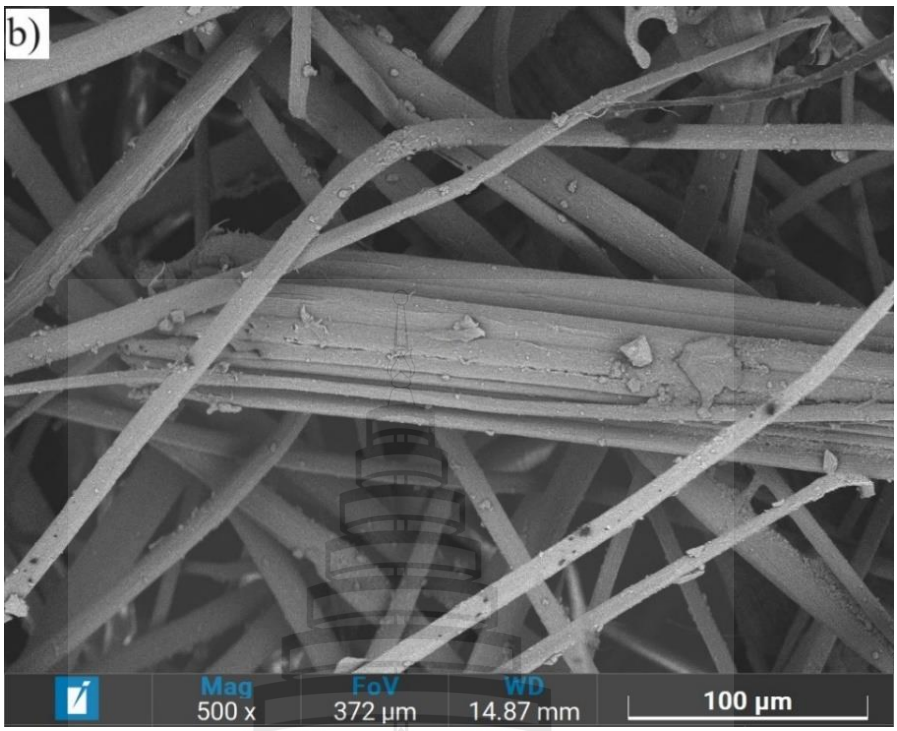

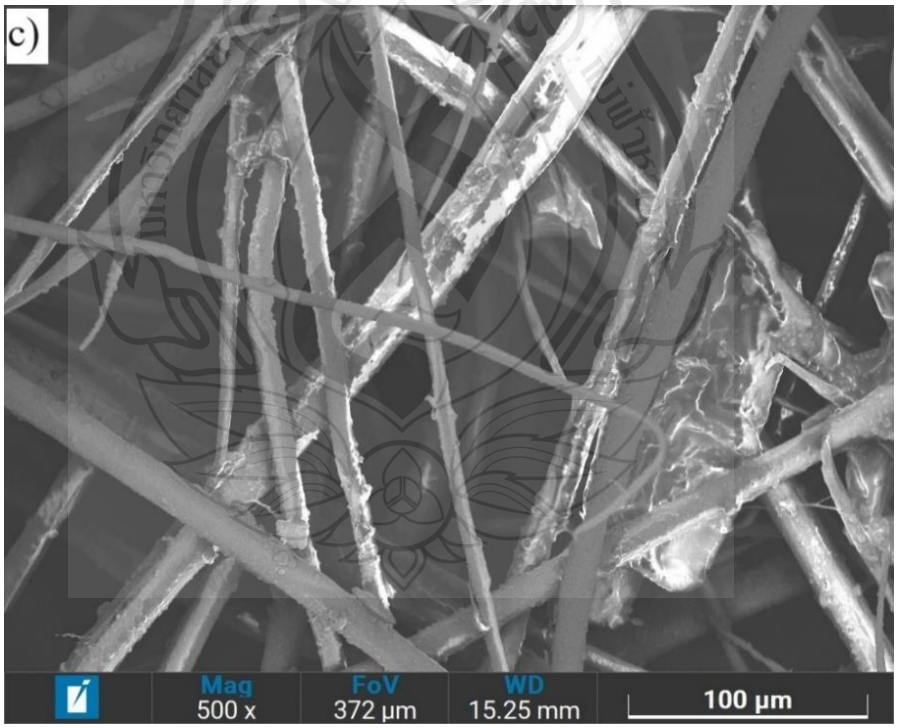

Figure 4.5 (continued)

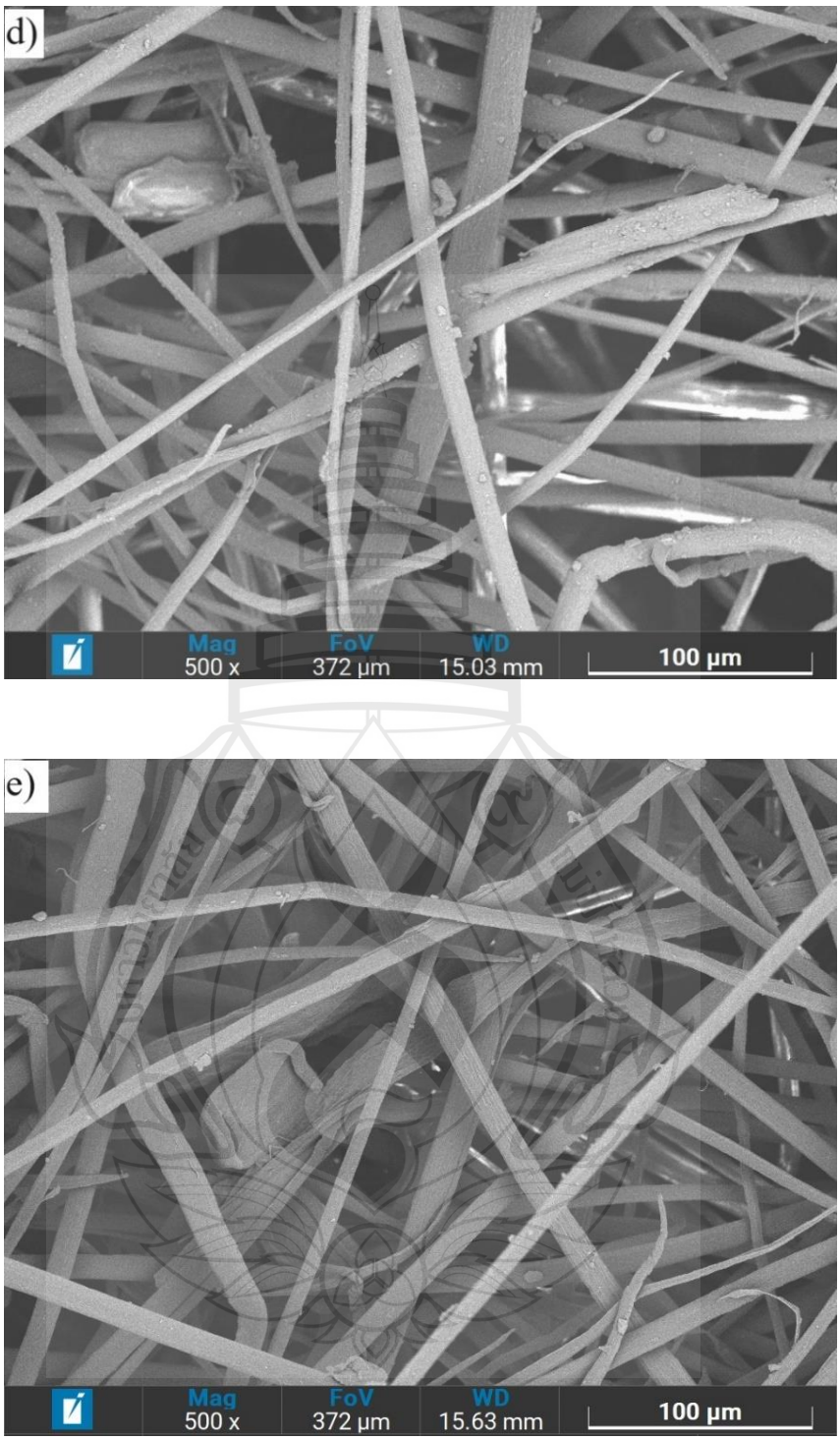

Figure 4.5 (continued)

4.3.2.5 Tensile strength index

The results of the zero-span tensile test show that the tensile strength index of extracted bamboo fiber increased with an increase in alkaline concentrations. Figure 4.6 shows the tensile strength index of bamboo fiber handsheets. The maximum tensile strength index was 19.62 Nm/g at the 10% NaOH catalyst. This result is in accordance with the previous study by Kamthai and Puthson (2005). The increase in tensile strength index is caused by an improvement in cellulose content and a better bonding network among fibers due to small diameters (larger specific surface area).

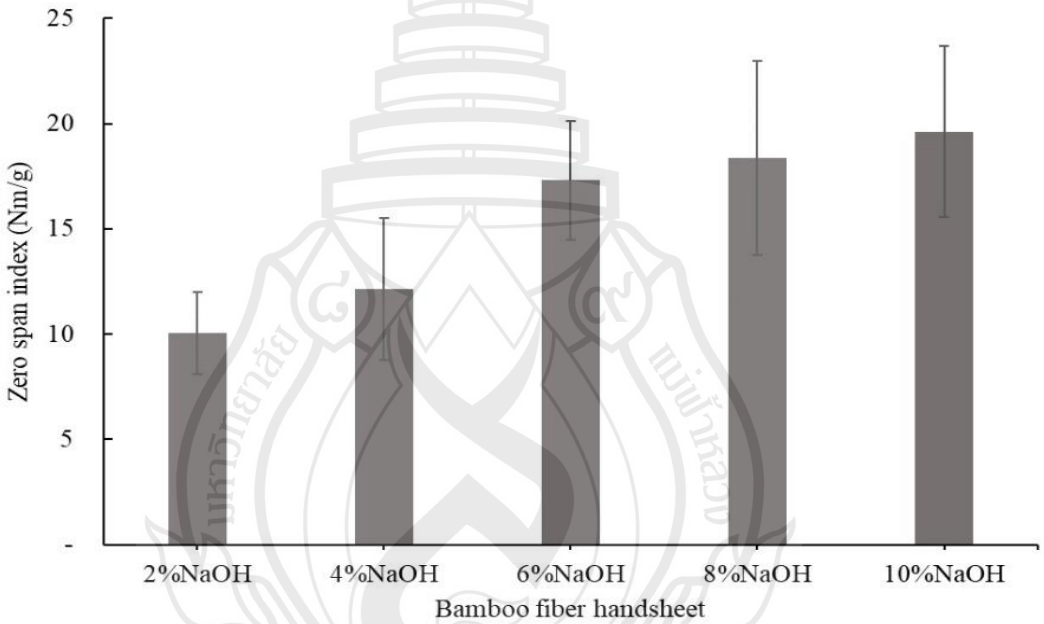

Figure 4.6 Zero-span tensile strength index of BF extracted by different concentrations of NaOH solvent

4.3.3 Commercial Virgin Eucalyptus Fiber Characteristics

4.3.3.1 Freeness

The properties of obtained virgin EF are summarized in Table 4.3. The obtained EF exhibited a freeness of 720 mL CSF due to untreated fibers.

4.3.3.2 Dimension

The length and width of eucalyptus fiber range from 0.40 to 5.30 mm and 9 to 89 μm. Appendix C shows the optical photographs for length and width measurement and the histogram of the dimensional distribution for EF. The average length and width were 2.65 mm and 41 μm, respectively. The aspect ratio was roughly 64.

4.3.3.3 Tensile strength index

Due to the ribbon-formed structure of EF, the fiber was well compacted during handsheet forming. This improved the interfacial bonding between fibers. It led to a high tensile strength index in the EF handsheet. The tensile strength index of EF was about 24 Nm/g, as shown in Table 4.3.

Table 4.3 Properties of commercial eucalyptus fiber

Properties	Eucalyptus fiber
Freeness (mL CSF)	716 ± 6.78
Minimum length (mm)	0.40
Maximum length (mm)	5.30
Average length (mm)	2.65 ± 1.13
Minimum width (μm)	9
Maximum width (μm)	89
Average width (μm)	41 ± 17
Aspect ratio	64 ± 39
Zero-span strength index (Nm/g)	24 ± 5

4.3.3.4 Surface features

Figure 4.7 shows the SEM photographs of EF. The surface of EF displays a high degree of roughness. EF has a ribbon-like shape that has a greater surface area and, therefore, bonds well together during handsheet forming. This led to good flexibility in the fiber and a good tensile strength index (see Table 4.3).

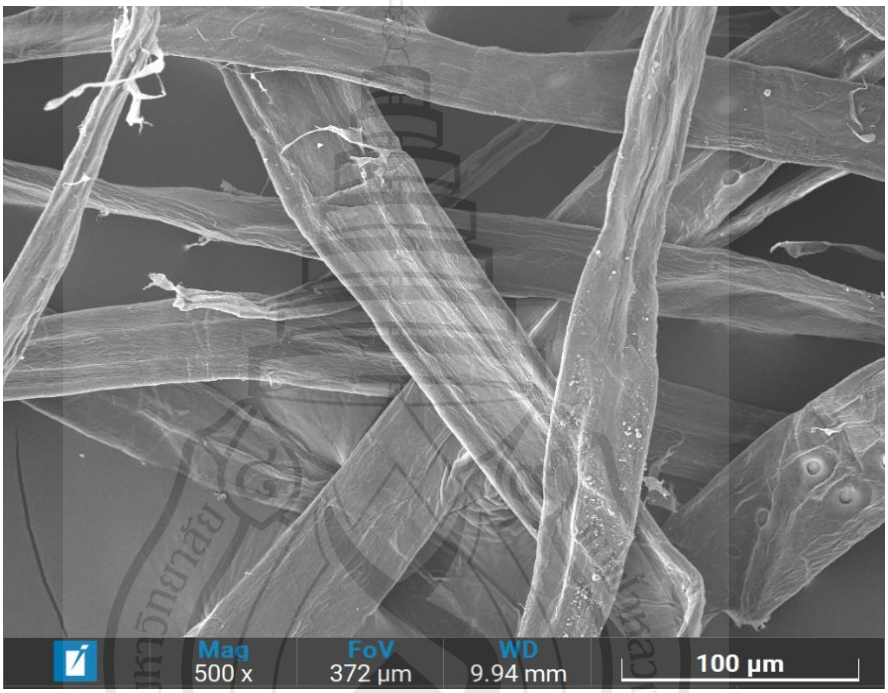

Figure 4.7 SEM photographs of the EF

4.3.4 Matrix Ingredient Characteristic

Ordinary Portland cement (OPC) Type I and ground sand were used as the ingredients for the cementitious matrix. The chemical compositions of the OPC and the ground silica sand were analyzed using an energy-dispersive X-ray fluorescence method (EDXRF) and the results are presented in Table 4.4.

Table 4.4 Chemical compositions of the OPC and the ground silica sand (by weight) based on the total sample weights

Chemical Components	Oxide equivalent weight (%)	
	OPC	Ground silica sand
Al_2O_3	2.11	0.89
SiO_2	10.70	97.14
SO_3	2.89	1.13
K_2O	0.69	-
CaO	77.72	0.58
TiO_2	0.35	-
MnO	0.24	-
Fe_2O_3	5.06	-
SrO	0.20	-
ZrO_2	-	0.22
CuO	-	0.02

The particle sizes of the OPC and the ground silica sand were analyzed using a laser scattering particle size distribution analyzer (LA-960). The particle sizes of the OPC ranged from 2.3 to 262 μm with a mean size of 25.72 μm, while those of the ground silica sand lay between 3.4 and 133 μm with a mean size of 27.9 μm. Figure 4.8 presents the distribution of particle sizes for the OPC and the ground silica sand. Figure 4.9 is an SEM photograph of the ground silica sand particles.

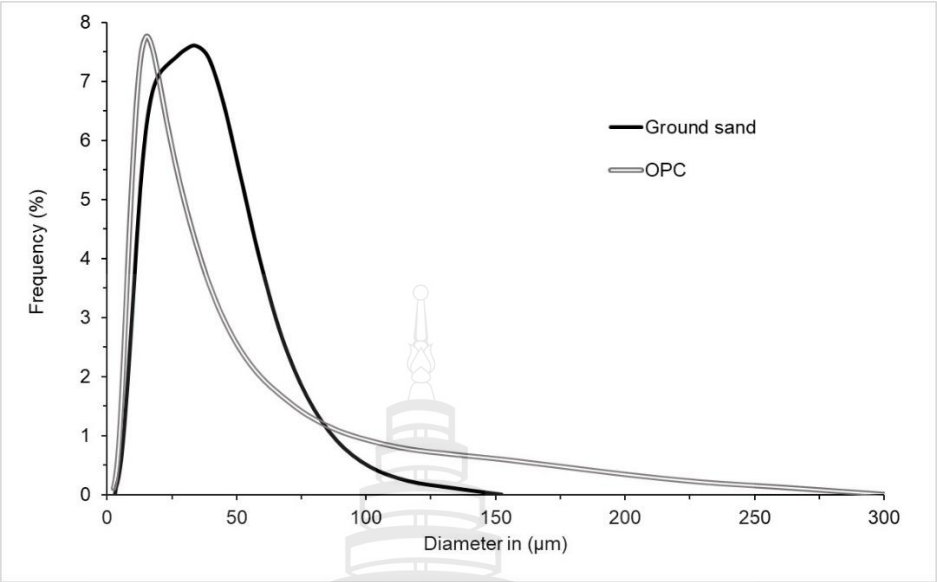

Figure 4.8 Particle size analysis results of the OPC and the ground sand

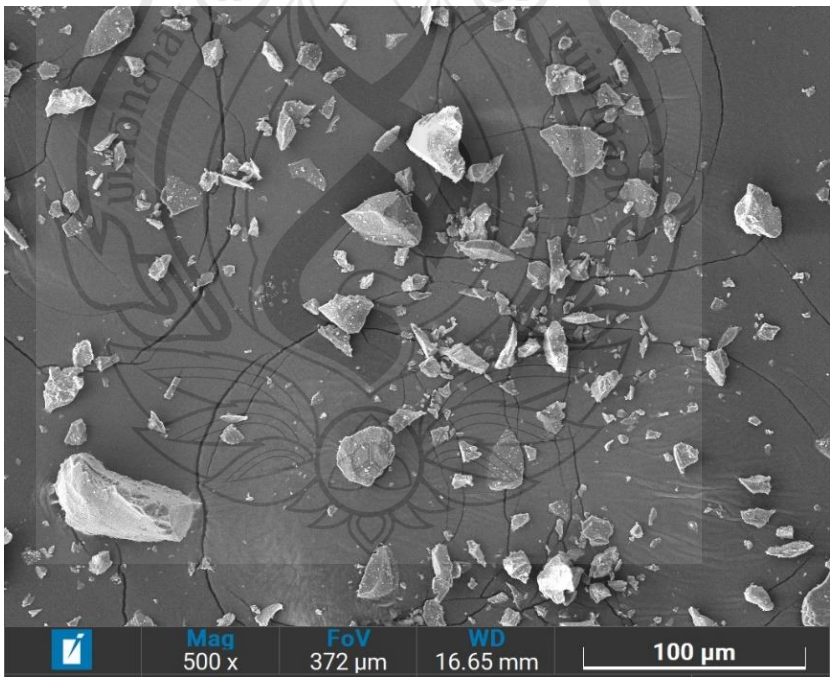

Figure 4.9 SEM photograph of sand particles

4.4 Conclusions

The important properties of RPBC, BF, and EF were investigated and reported in this Chapter. The results were primary information for the next experiment and it can be concluded as follows:

1. It was found that the shearing period affected significantly the fibrillation of the RPBC, which influenced further the properties of RPBC-reinforced cementitious composites. To know what freeness level of sheared RPBC produces acceptable properties of the RPBC cementitious composite, it is necessary to assess its contribution.

2. The BF extracted at different alkaline concentrations exhibits different properties. The BF extracted by a hydrothermal process with a 10% NaOH catalyst shows a higher tensile strength index and a suitable morphology for use as a fiber reinforcement for a cementitious composite.

3. The obtained EF exhibits the proper properties used as a reference fiber for the fiber-reinforced cementitious composites.

CHAPTER 5

PROPERTIES OF CEMENTITIOUS COMPOSITE REINFORCED WITH REFINED RPBC

5.1 Introduction

From the previous chapter, it was found that the characteristic of RPBC, such as morphologies, length-to-diameter aspect ratio, and freeness level, were changed after the repulping process due to the fibrillation of RPBC. Such fibrillation affected the properties and performance of RPBC as well as of RPBC-reinforced cementitious composites. Freeness is a measure of the fibrillated pulp's ability to allow water to drain through it. It is used to measure the level of fibrillation in recycled pulp, which is related to the surface condition and short fiber content (TAPPI T 227 om – 99, 1999). The refining treatment separated the RPBC from clumping into individual fibers, creating malleability and increasing its fibrillation, enabling it to retain water and capture mineral particles during fiber-cement production. As shown in Section 4.3.1, the shearing treatment affects the morphologies, freeness, and strength of RPBC. This influences the performance and properties of the RPBC-reinforced cementitious composite. According to Tonoli et al. (2013), the flexural strength of refined eucalyptus kraft pulp increased significantly as the refining level increased. The fibrillation improves the fiber's adherence to the cement matrix. However, if the refining of the fibers is excessive, the strengths of the composites decrease slightly due to the increased in the percentage of short fiber, which is a consequent effect of refining, as stated by Coutts et al. (1984). Therefore, to reuse the RPBC, it needs to be known that at what level the freeness of the RPBC significantly influences the properties of RPBC cement composites.

The objective of this experiment was to find out what refining level of RPBC leads to the best mechanical properties, including flexural strength and fracture toughness of RPBC-reinforced cement composites.

5.2 Materials and Methods

5.2.1 Materials

Ordinary Portland cement (OPC) Type I and ground sand were employed in this assessment. The chemical composition of OPC and ground sand is presented in Table 4.4 of Chapter 4. The particle size distribution of the OPC and the ground silica sand is presented in Figure 4.8.

The recycled pulp from beverage cartons (RPBC) obtained from the Fiber Pattana Company in Thailand was used as reinforcement fiber. The freeness levels of RPBC at 650, 600, 550, 500, and 400 mL CSF were selected for this assessment. The characteristics of RPBC at different freeness levels are presented in Table 4.1 of Chapter 4.

5.2.2 Methods

5.2.2.1 Specimen composition

The compositions of RPBC-reinforced cementitious composites as a function of freeness level are presented in Table 5.1. A cement mortar with a sand-to-cement ratio of 1:1 was employed as the cementitious matrix. The fiber content accounted for 8 wt% of the total solid mass. The total solid weight of a specimen was 90 g. The solid content in the slurry was about 20%. As a reference specimen, a mixture of cement and ground silica sand with a fraction of 1:1 was employed, and the water-to-cement ratio of 0.5 was used.

Table 5.1 Specimen compositions for the RPBC cementitious composites

Code of specimen	Shearing period (second)	Expected Freeness (mL CSF)	Cement (g)	Fine Sand (g)	Fiber content (g)
Control	-	-	45	45	-
650RPBCC	60	650	41.4	41.4	7.2
600RPBCC	140	600	41.4	41.4	7.2
550RPBCC	200	550	41.4	41.4	7.2
500RPBCC	320	500	41.4	41.4	7.2
400RPBCC	460	400	41.4	41.4	7.2

5.2.2.2 Specimen formation

All specimens were formed with the same procedure according to the description in Section 3.2.3. The specimens were pressed at 3.5 MPa for 5 minutes, according to Coutts and Warden (1990). Five samples for each freeness level were prepared for a properties assessment.

5.2.2.3 Properties of composites assessment

The properties and fracture surface analysis of RPBC-reinforced cementitious composites were conducted following the explanations in Chapter 3 (Section 3.3 and 3.4).

5.3 Results and Discussions

5.3.1 Physical Properties

Figure 5.1 shows the variations in the physical properties of RPBC-reinforced cementitious composite (RPBCC) after 7 and 28 days of curing as a function of the refining level. The graphs indicated that the bulk density increased slightly with a reduction in freeness (Figure 5.1a). Obviously, the bulk density of 400 mL CSF composite was greater than that of 650 mL CSF composite by about 2.2%. The increase in bulk density was related to the high malleability of recycled pulp, which was contributed to by the refining process (Tonoli, 2007). The external cell wall layer of refined recycled pulp was opened (see Figure 4.3), reducing of cell wall thickness and better compaction of refined recycled pulp in the cementitious composite. In contrast, the composite exhibited an opposite tendency toward porosity. After 28 days, the porosity of the composites decreased steadily with a reduction in freeness. When the freeness of recycled pulp was reduced from 650 to 400 mL CSF, the porosity of the composite decreased by 5.7% at 28 days of curing (Figure 5.1b). The composite's porosity reduction was due to the efficient packing of refined recycled pulp into the cementitious matrix (Tonoli et al., 2007). In correlation to the porosity, the water absorption has a similar tendency, it decreases with an increase in freeness levels (see Figure 5.1c). The water absorption declined by 8% when the freeness was reduced from 650 to 400 mL CSF.

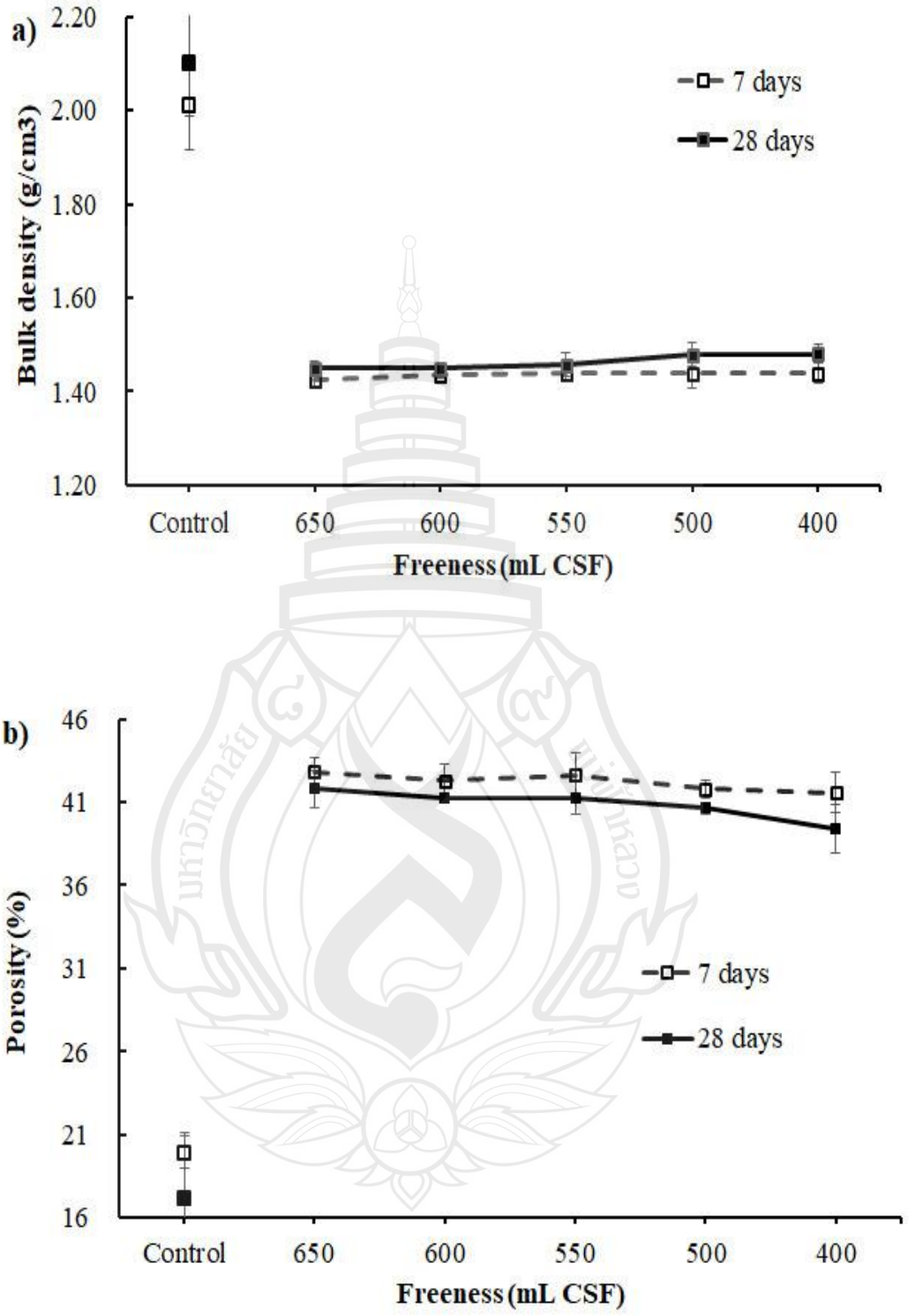

Figure 5.1 Physical properties of RPBCC with different freeness levels: a) bulk density, b) Porosity, and c) water absorption

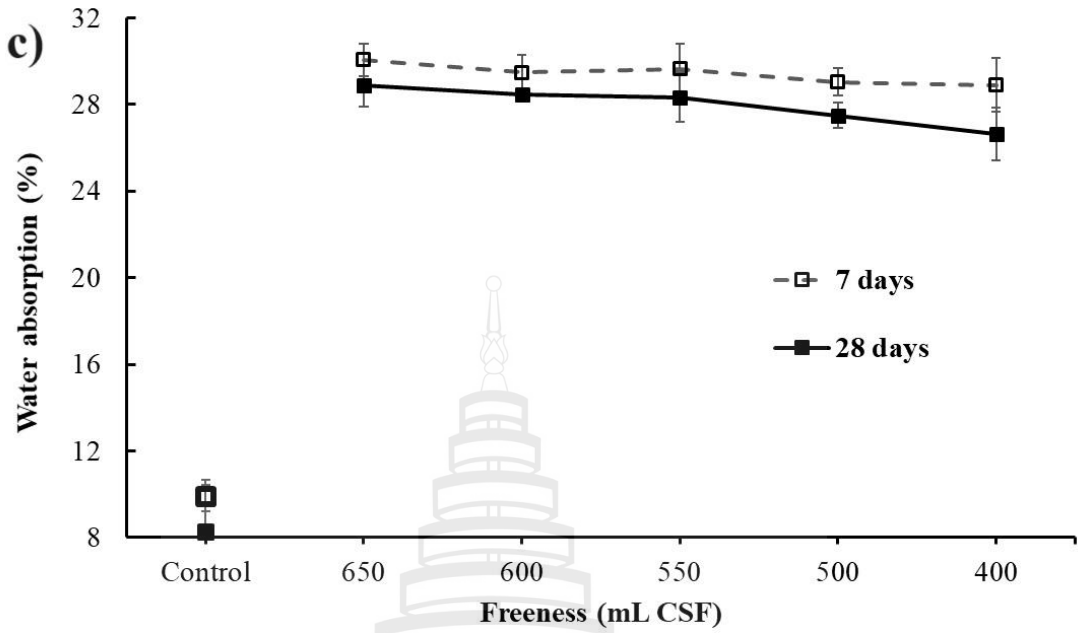

Figure 5.1 (continued)

5.3.2 Mechanical Properties

Figure 5.2 shows the mechanical properties of the RPBCC according to its freeness after 7 and 28 days of curing. The flexural strength of RPBCC tended to increase and reached its peak value as the freeness of recycled pulp reduced from 650 mL to 550 mL CSF. The strength reduced slightly with a further decrease in freeness (see Figure 5.2a). A similar trend was found in both sample sets, which were cured for 7 and 28 days. The maximum flexural strength reached 11.2 MPa at 550 mL CSF freeness after 28 days of curing. The increase in the flexural strength of RPBCC from 650 to 550 mL CSF was mainly contributed by an increase in the fibrillation of recycled pulp, which led to an improvement in the interfacial bond between the fibrillated recycled pulp and cementitious matrix (Tonoli et al., 2013). This finding indicated that the fibrillated recycled pulp improved the composite's flexural strength, although the fiber length gradually decreased. However, a prolonged shearing treatment could cause excessive damage to the refined recycled pulp, thus reducing fiber strength. As a result, the decrease in flexural strength of the composite with 500 mL CSF RPBC could either be due to the negative effect from the shorter fiber content or the reduced fiber strength

that occurred during the shearing process that could overcome the beneficial effect of fibrillation. The test result confirmed that if the refined level of the RPBC was higher than a specific value, it resulted in a decline in the flexural strength of the RPBCC.

On the other hand, the modulus of elasticity (MOE) of RPBCC was not significantly influenced by variations in freeness (see Figure 9b) after seven days of curing. Tonoli et al., (2013) also reported this behavior. However, it slightly increased after 28 days of curing. This was likely related to the increase in density and reduction in porosity of RPBCC (see Figure 5.1a,b).

The fracture toughness values of the refined RPBC composites were improved tremendously compared to those of the control specimen (~ 31 J/m^2). However, in contrast to the flexural strength, the fracture toughness of the composites showed a negative response to the refining levels of recycled pulp (Figure 5.2c). When the freeness of the RPBCC was reduced from 650 to 400 mL CSF, the fracture toughness at 7 and 28 days of curing decreased steadily by 20% and 14%, respectively. The decrease in fracture toughness could be due to increased short fiber content at higher fibrillated RPBC, resulting in less friction resistance during pullout from the matrix (Coutts, 1984). Coutts and Radikas (1982) reported that decreased fracture toughness is associated with reduced fiber length in refined fiber. As a result, the short fiber had less capacity to absorb energy. In addition, fiber damage due to excessive fibrillation, as mentioned earlier, could be another factor that reduces fracture toughness.

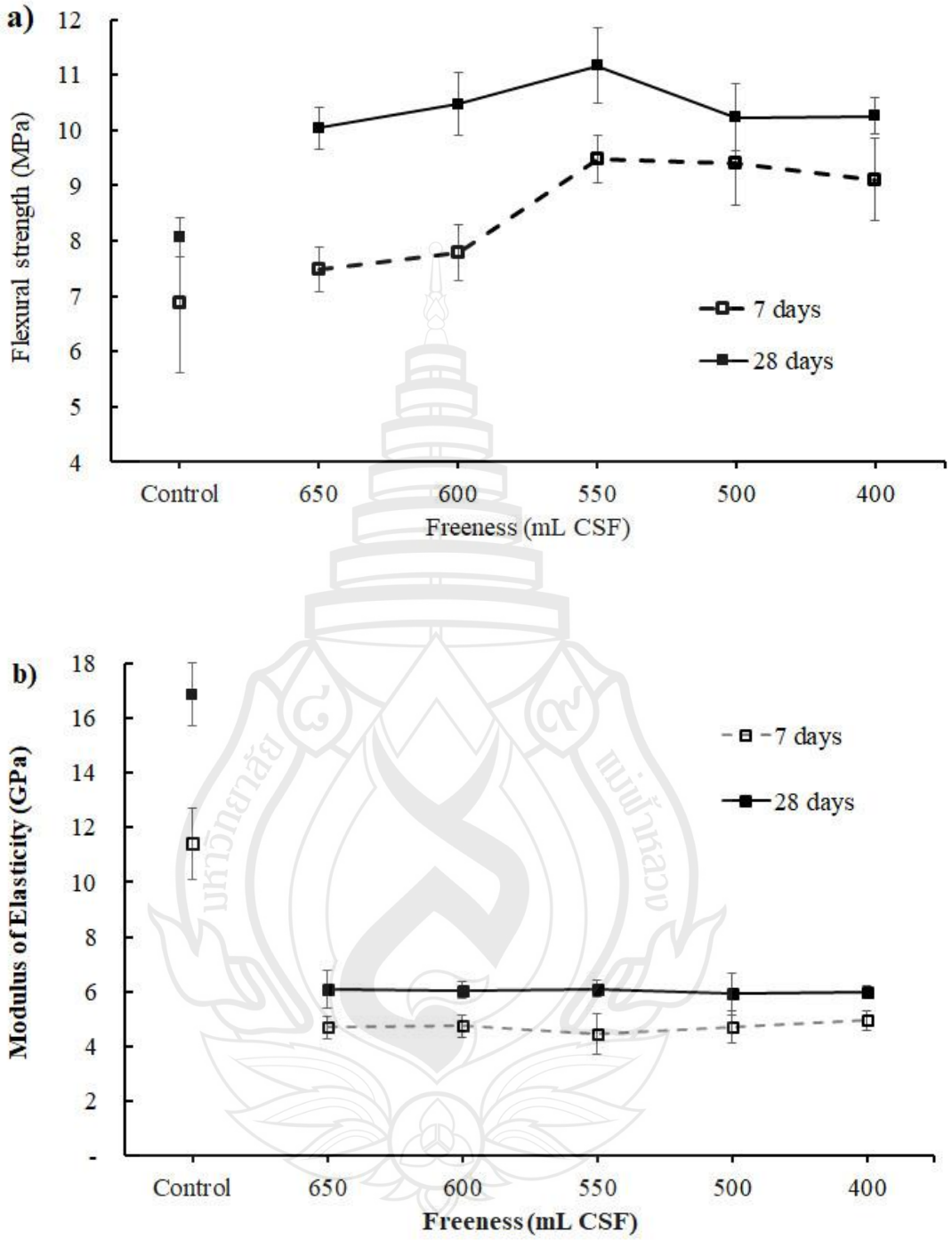

Figure 5.2 Mechanical properties of RPBCC with different freeness levels: a) flexural strength, b) modulus of elasticity, and c) fracture toughness

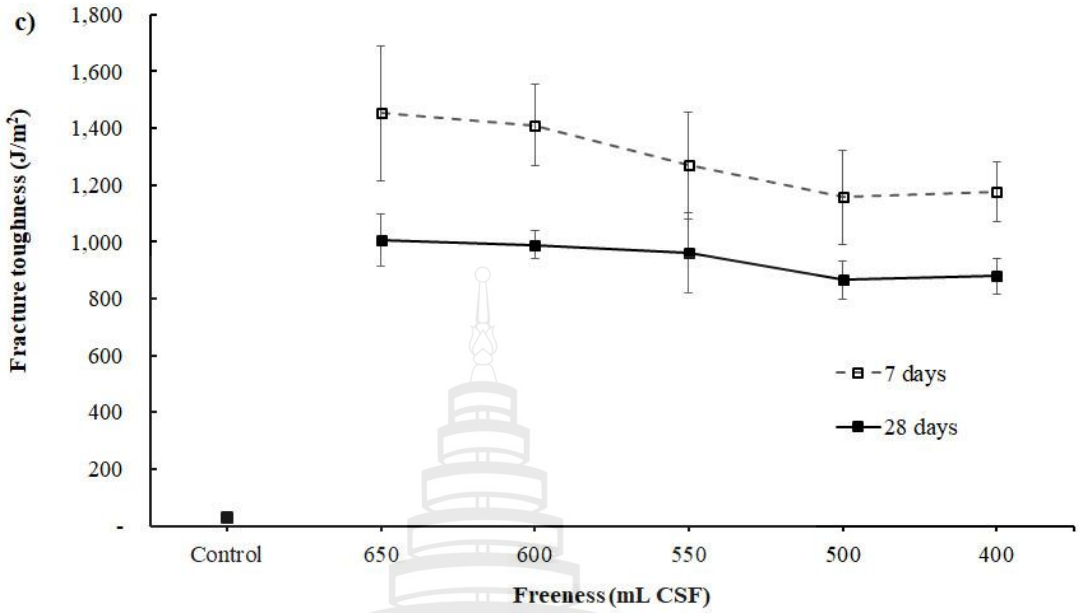

Figure 5.2 (continued)

5.3.3 Fracture Surface Analysis

Figure 5.3 shows the photographs of fracture cracks in the control and recycled pulp-reinforced cement composites. The pictures demonstrate that when reinforced with an interest fiber characteristic in the cementitious matrix, the recycled pulp inhibits crack propagation more effectively than the specimen without fiber reinforcement.

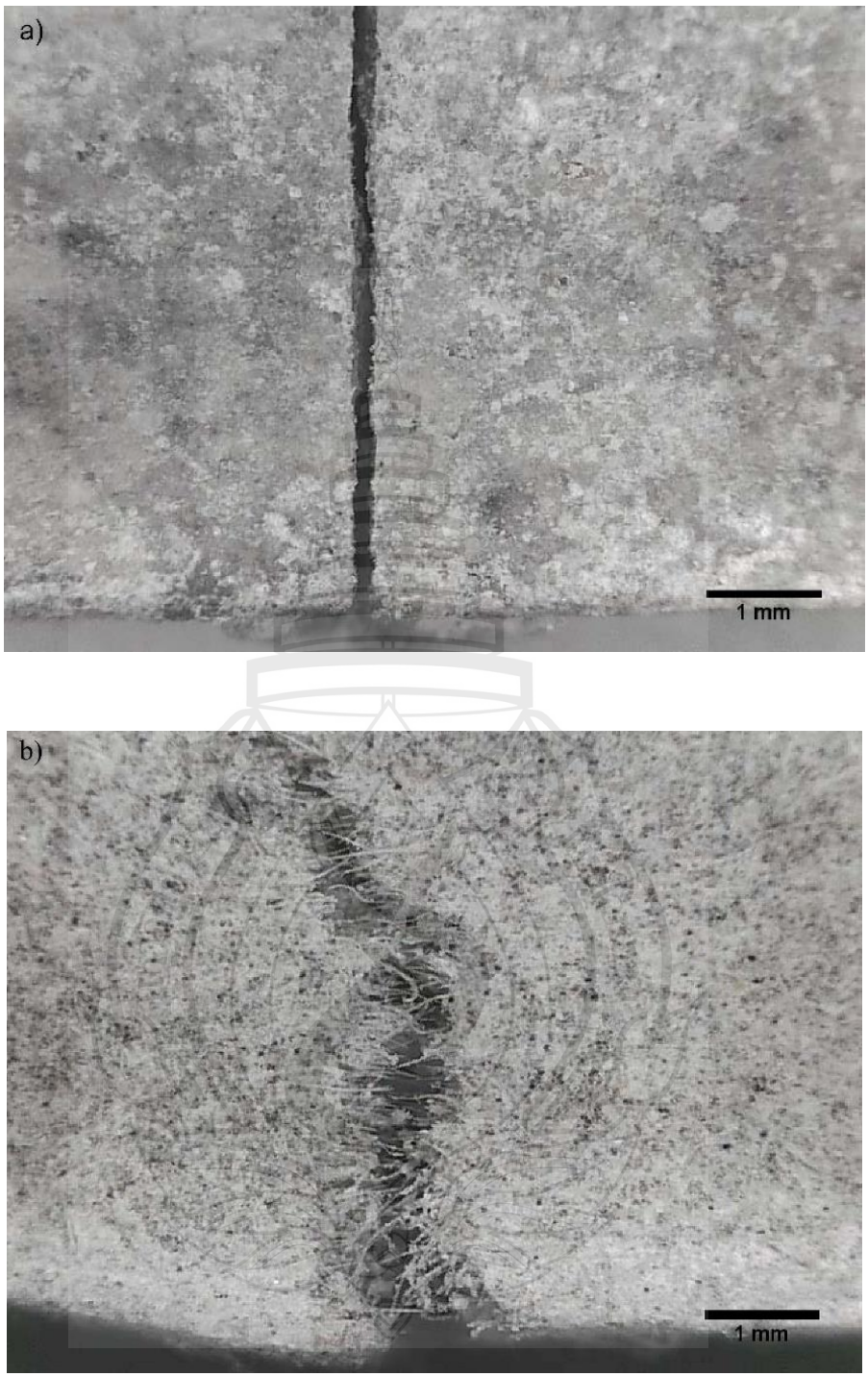

Figure 5.3 a) Fracture cracks of cement mortar and b) Recycled pulp-reinforced cement composite with 550 mL CSF freeness

The RPBC specimens were further observed under SEM analysis. Figures 5.4, 5.5, and 5.6 demonstrate the SEM photographs of the fracture surface of the composite reinforced with 650 mL, 550 mL, and 400 CSF recycled pulp. After testing, the SEM microscopy observations on the fractured surface of the hardened composites allowed us to understand better the interaction between recycled pulp with different freenesses and cementitious matrix. The SEM micrographs illustrate that the RPBC plays the role of crack bridging across the fracture surface, and the fiber pull-out was mainly observed. As a result, RPBCC fracture toughness improved significantly compared to the specimen without RPBC (Figure 5.2c). However, in the composite reinforced with 650 mL CSF recycled pulp, there was more clear fiber pull-out debris than in the composites with 550 and 400 mL CSF fibers (see Figures 5.4 –5.6). This is because the 650 mL CSF composite had less fibrillation. Figure 5.4b illustrates an apparent length of fiber pull-out, which absorbs more energy in sample breaking. Therefore, the 650 mL CSF freeness composite presents a higher fracture toughness than the other sets, as shown in Figure 5.2c.

Figure 5.4 SEM photographs of fracture surfaces of 650 mL CSF RPBCC: a) with 100x and b) 500x magnitude

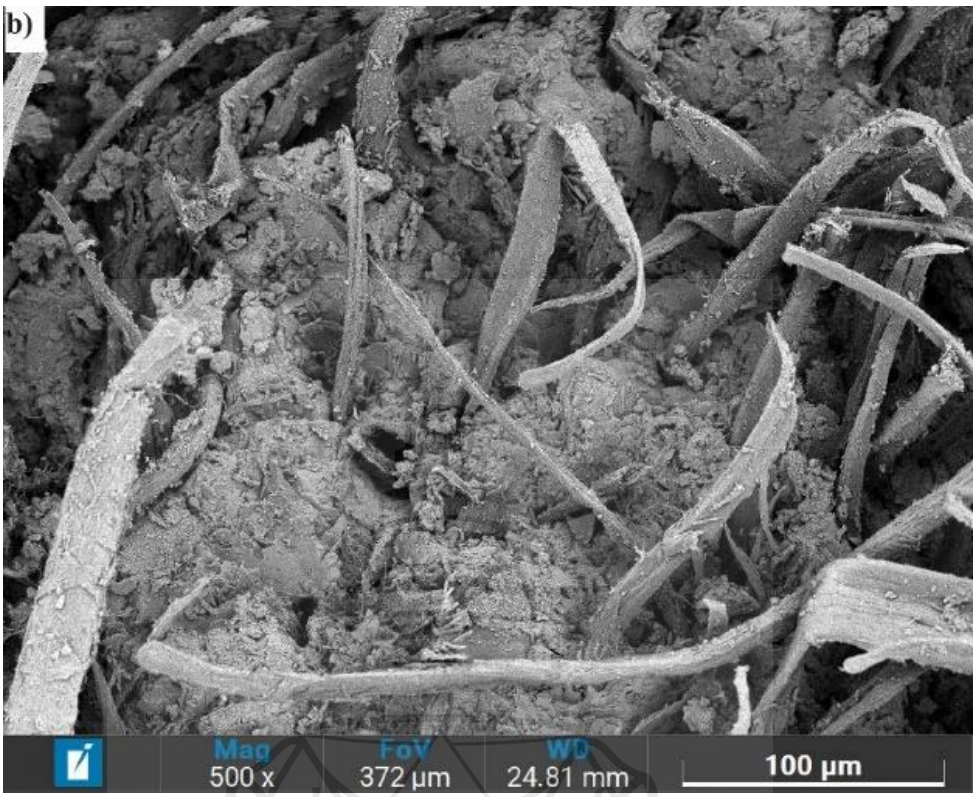

Figure 5.4 (continued)

In contrast to the composite reinforced with 650 mL CSF RPBC, Figures 5.5a and 5.6a show that more fibers were torn apart in the fracture surface of the 550 and 400 mL CSF fiber composites, although the average fiber length was decreased. As shown in Figure 5.2a, the flexural strength was highest at a freeness of 550 mL CSF. This suggests that the 550 mL CSF RPBC has the best balance of fiber length and interfacial bond. It can be seen that both failure modes are presented on the fracture surface of the specimen reinforced with 550 mL CSF (see Figure 5.5). The flexural strength and fracture toughness were reduced at a lower (400 mL CSF) freeness. This could be attributed to the excessive reduction in fiber length and the damage to sheared RPBC, which causes a decrease in fiber strength. Therefore, the sheared RPBC loses its frictional slip resistance during the pull-out process, resulting in a reduction in flexural strength and the fracture toughness of RPBCC with 400 mL CSF. In Figure 5.6b, fiber failures were clearly presented on the 400 mL CSF RPBCC surface fracture, whereas fiber pull-out was hardly observed. Arrow 1 in Figure 5.6b indicates a short

strip of fiber caused by the delamination of the fibrillated cell wall. In contrast, arrows 2 and 3 show short remnants of broken fibers protruding from the cementitious matrix.

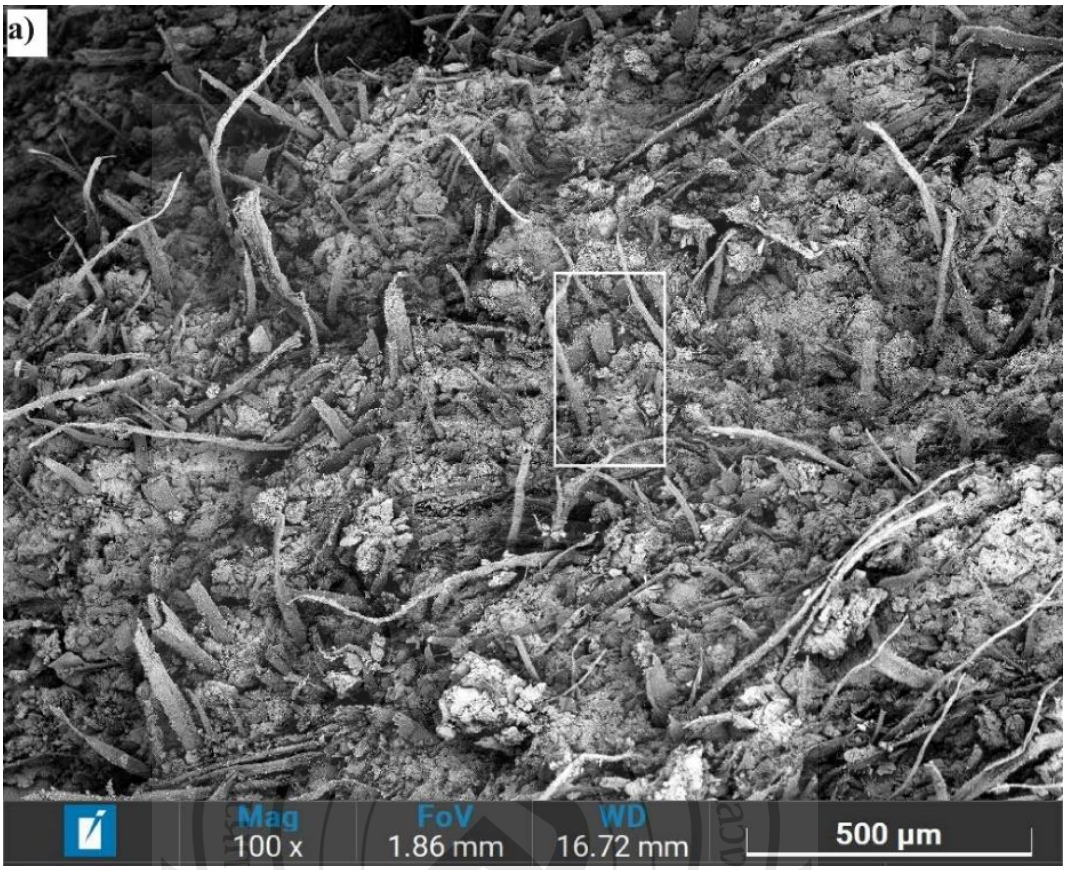

Figure 5.5 SEM photographs of surface fractures of 550 mL CSF RPBCC: a) 100x and b) 500x magnitude

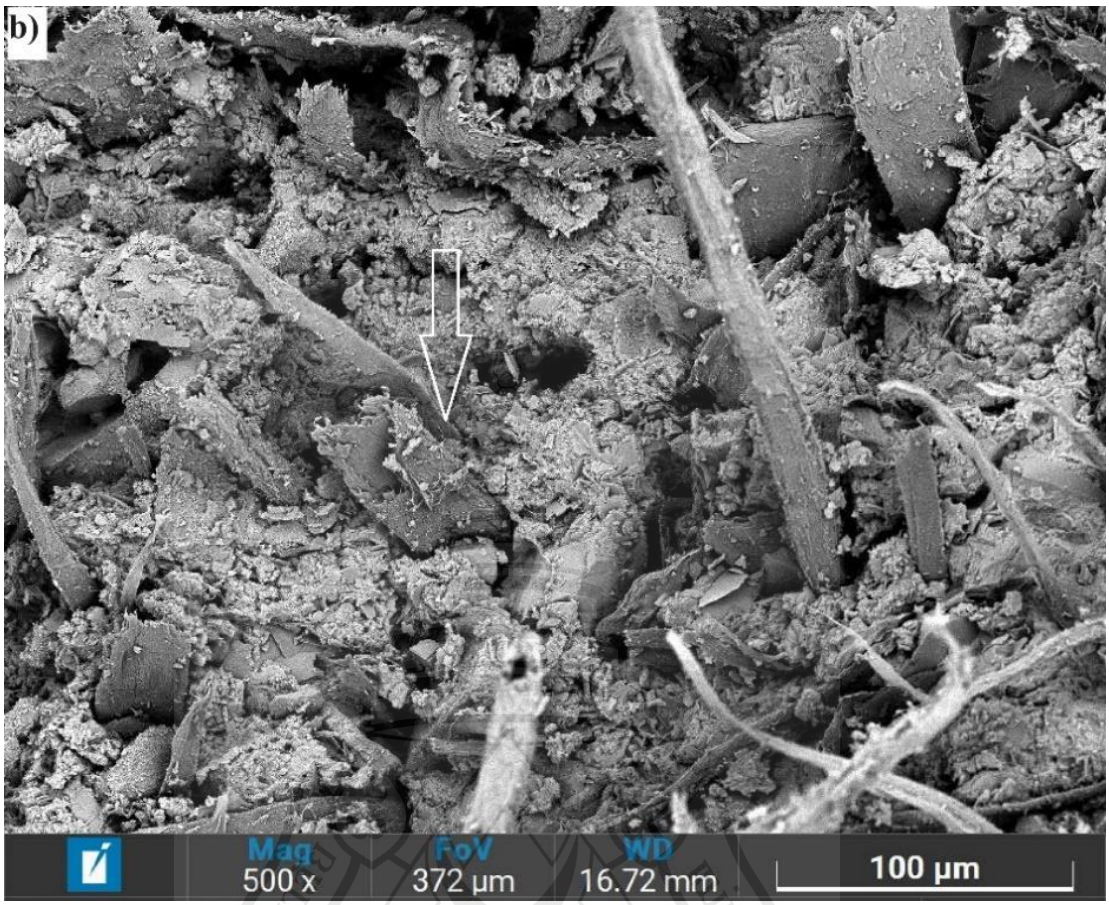

Figure 5.5 (continued)

Figure 5.6 SEM photographs of surface fractures of 400 mL CSF RPBCC: a) 100x and b) 500x magnitude

5.4 Conclusions

This chapter investigated the properties of cementitious composites reinforced with refined recycled pulp from beverage cartons having a different level of freeness. As demonstrated in Chapter 4 that the tensile strength index of RPBC increased when the freeness increase. However, it has been found in this Chapter that when the refined RPBC was used to reinforce in cementitious matrix, it illustrated a maximum value of the flexural strength of the composite at a certain level of freeness, then it declined when the freeness continues to decline.

The flexural strength of the RPBCC increased with a reduction in freeness and reached its maximum value of 11.16 MPa at the optimum freeness of 550 mL CSF. Further decreased due to the high amount of short fiber content. However, the fracture toughness decreased by about 10–13% when the freeness of RPBC was reduced from 650 to 400 mL CSF. Consequently, the bulk density increased by 2.2%, while the porosity decreased by 5.7% with a decrease in the freeness of RPBC from 650 to 400 mL CSF.

The study also demonstrated that the recycled pulp from beverage cartons is a potential source for fiber-reinforced cementitious composites. However, to gain a better understanding of the performance of RPBCC, it is subjected to comparison with other types of natural fiber-reinforced cementitious composites as presented in the following chapters.

CHAPTER 6

EFFECT OF COMPRACTION PRESSURE ON PROPERTIES OF VIRGIN EUCALYPTUS FIBER REINFORCED CEMENT COMPOSITE

6.1 Introduction

As explained in Section 2.5.3 of Chapter 2, compaction pressure is an important processing parameter that has a crucial impact on the performance and properties of cellulose fiber-reinforced cementitious composites in the slurry dewatering technique. After the de-watering treatment, the specimens were subjected to cold pressing to drain the excessive water and compact the green fiber-reinforced cement sheet. The specimens were densified and had a lower thickness. The applied pressure and holding time were different for each reinforced fiber type, fiber morphologies, and fiber content. As reported by Akers and Garrett (1986), the compaction pressure in the formation of asbestos fiber-reinforced cement composites varied from 1 to 7 MPa. The authors found that the flexural strength and fracture toughness of the composite increased as the compaction pressure increased. However, with fibers such as polypropylene, glass, carbon, and steel, the researchers suggested the proportional limit and elastic modulus of fiber-reinforced composites slightly increased, but the flexural strength and fracture toughness decreased when the applied pressure increased up to 9 MPa (Delvasto, 1986). Coutts and Warden (1990) reported that the flexural strength and the fracture toughness of wood fiber-reinforced cement composite increased with an increase in casting pressure up to 3.2 MPa at an 8 wt% fiber content.

In general agreement, the porosity of the fiber-reinforced cement composite increased as the fiber content increased. Thus, to compensate for the increased porosity, compaction pressure should be applied to the green sheet during forming to enhance the properties of the composites.

However, applying high pressure reduces the specimen's water-to-cement ratio, which impacts the hydration of the cementitious matrix and the interfacial bond, lowering the strength and toughness of the composites.

This chapter aims to investigate the influence of compaction pressure on the properties of eucalyptus fiber-reinforced cementitious composites. Due to time constraints, only eucalyptus fiber was used in this experiment as a referent fiber, and the curing period was 7 days.

6.2 Materials and Methods

6.2.1 Materials

Commercial eucalyptus fiber was employed as the reinforcement in the experiment. The used EF exhibit the properties as follow: the freeness level was around 720 mL CSF, the average fiber length and width were 2.65 mm and 41 µm, respectively. The tensile strength index was about 24 Nm/g. More details are presented in Table 4.3 of Chapter 4.

OPC and ground silica sand were used as the cementitious matrix ingredients. The chemical compositions of OPC and ground silica sand are presented in Table 4.4. The average particle size of OPC and ground silica sand were 25.72 µm and 27.9 µm, respectively. Figure 4.8 present the distribution of particle sizes of those ingredients materials

6.2.2 Methods

6.2.2.1 Specimen composition

Table 6.1 shows the composition of the EF-reinforced cementitious composites, with varying compaction pressures. The total dry solid mass was weighted at 90 g per specimen. The matrix consisted of 41.4 g (46 wt%) of ordinary Portland cement and 41.4 g (46 wt%) of ground silica sand. The slurry contained 400 ml of water (about 22.5% solid content). The EF content was selected at 7.2 g, which is equivalent to 8 wt% of the total solid weight as suggestion by the early study (Coutts & Warden, 1990).

Table 6.1 Composition of the EF cementitious composites

Code of specimen	Compression pressure (MPa)	Eucalyptus fiber (g)	Cement (g)	Fine sand (g)
P1EFC	1	7.2	41.4	41.4
P2EFC	2	7.2	41.4	41.4
P3EFC	3	7.2	41.4	41.4
P4EFC	4	7.2	41.4	41.4
P5EFC	5	7.2	41.4	41.4
P6EFC	6	7.2	41.4	41.4
P7EFC	7	7.2	41.4	41.4

6.2.2.2 Specimen formation

Generally, the specimen was prepared following the procedure described in 3.2.3. After draining the excessive water using a vacuum pumping, the green specimens were pressed to drain out the excessive water. The pressure ranges from 1 to 7 MPa, with a holding time of 5 minutes. The pressed specimen was cured at 99% humanity at room temperature for 7 days. As a reference specimen, a mixture of cement and ground silica sand with a fraction of 1:1 was employed, and the water-to-cement ratio of 0.5 was used. The control specimen was pressed at 3.5 MPa (a similar condition used in the previous experiment described in section 5.2.2) and cured under the same conditions as the EFC.

6.2.2.3 Properties assessments

The properties of EF-reinforced cementitious composites were evaluated according to the description in 3.3. The density of the fiber cement composite was expected to increase and the porosity and water absorption to decrease with an increase in compaction pressure. Correlated to this, the flexural strength was also expected to increase, and the fracture toughness was expected to reduce for some distance.

6.2.2.4 Fracture surface analysis

The fracture surfaces of the EF-reinforced cementitious composites were analyzed by following the method in 3.4. The observations in the SEM photographs could help us analyze the behavior of the fiber reinforcement and the toughening mechanism of the composites. It was expected to see the effect of the compaction pressure on the morphologies of reinforced fiber and the interaction between fiber and cementitious matrix at different compaction pressure levels.

6.3 Results and Discussions

6.3.1 Physical Properties

The physical behaviors of the EF-reinforced cementitious composite in dependence on the compaction pressure are shown in Figure 6.1. The graph illustrated that the specimen was denser by about 2.5% as the compaction pressure increased from 1 to 7 MPa (see Figure 6.1a). At the same time, the porosity and water absorption of the composite indicated a decrease by 2.73 and 56%, respectively (see Figures 6.1b and c).

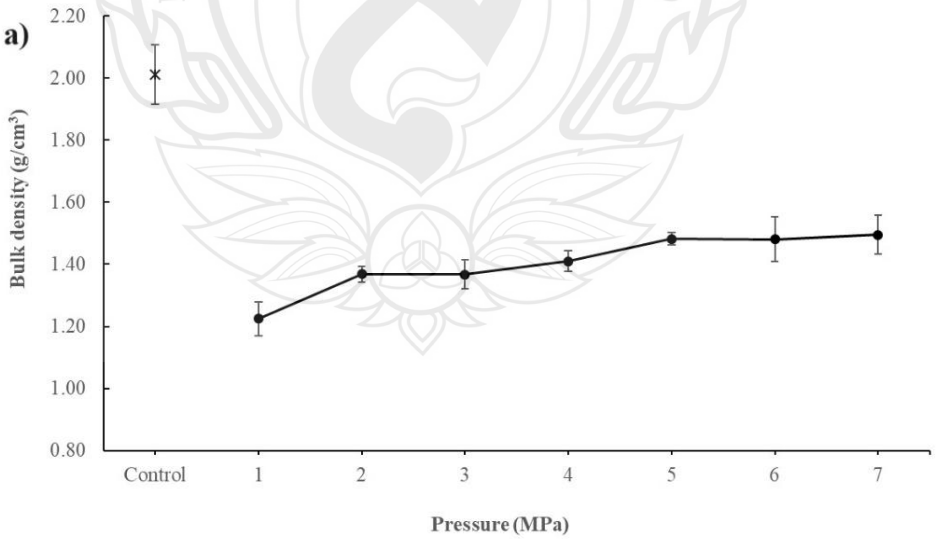

Figure 6.1 Physical properties of EF reinforced cement composite: a) bulk density, b) porosity, and c) water absorption

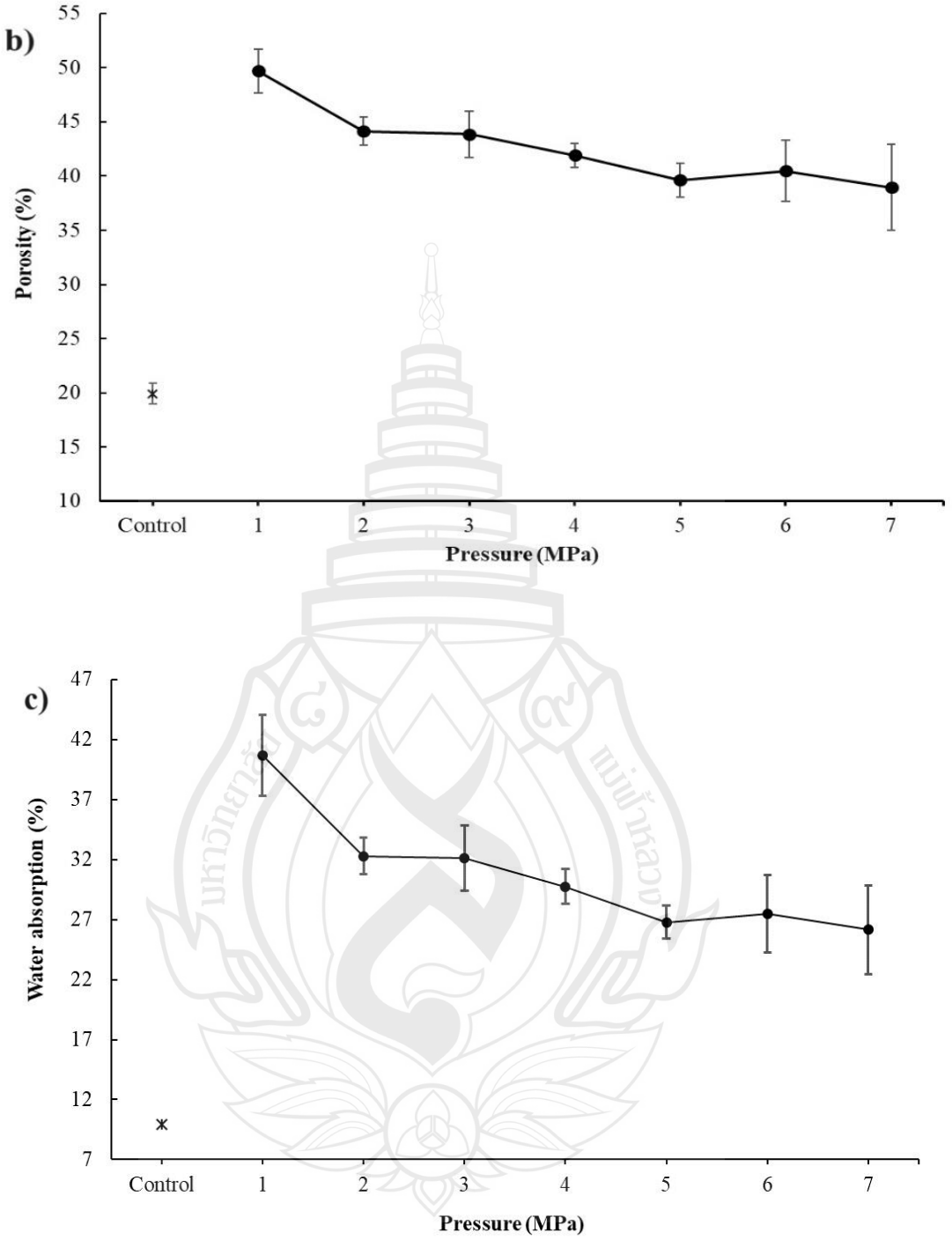

Figure 6.1 (continued)

The increase in density and the reduction in porosity and water absorption of the composites at a higher compaction pressure lead to the densification of the matrix.

A denser and more compacted matrix at high compaction pressure was observed to also close the fiber (see Figure 6.3 d-g). The high compaction pressure provides a stronger bond strength between the fiber and the matrix than the lower one.

6.3.2 Mechanical Properties

The effect of compaction pressure on the mechanical properties of EF-reinforced cementitious composites is demonstrated in Figure 6.2. At a fiber content of 8 wt%, the composite's flexural strength continuously increased as the compaction pressure increased up to 5 MPa, reaching its maximum value of 8.44 MPa at 5 MPa. The increase in strength was about 90% compared with the 1 MPa pressure. In comparison to the control specimen, the flexural strength increased by about 22%. It had been observed that over the range of compaction pressures (1 to 5 MPa), there was a linear improvement in flexural strength with increasing compaction. When the compaction pressure goes from 1 MPa to 5 MPa, the bond between the EF and the cementitious matrix gets stronger, which makes the flexural strength go up (see Figure 6.2a).

As the compaction pressure increased above 5 MPa, the flexural strength gradually declined. Too high compaction during specimen formation likely led to excessive densification and brittle behavior in the matrix, influencing the hydration reaction of the cementitious matrix and the interfacial bonding (Akers & Garrett, 1986). The high compaction pressure leads to the appearance of microcracks in the matrix and damage to the fiber, resulting in a reduction in the reinforcement efficiency of the fiber and finally a decrease in strength (Coutts & Warden, 1990).

The modulus of elasticity of the composite increased with a growth in compaction pressure (see Figure 6.2b). This is related to an increase in density and a reduction in the porosity of the composite (see Figure 6.1).

Furthermore, the fracture toughness of the composite shows a similar tendency to the flexural strength as the compaction pressure increases up to 5 MPa (see Figures 6.2c). The fracture toughness increased by 64% compared to 1 MPa compaction pressure. The growth in fracture toughness was contributed by the significant improvement of interfacial bonding, and simultaneously, the unique characteristic of EF, which has a long length and large width with a ribbon-like cross-section form,

contributed significantly to the increase in fracture toughness of the composite. The EF can absorb a higher amount of de-bonding energy during the pull-out process. As the compaction was greater than 5 MPa, the fracture toughness decreased slightly. This could be caused by damage to the EF, leading to a failure of the fiber.

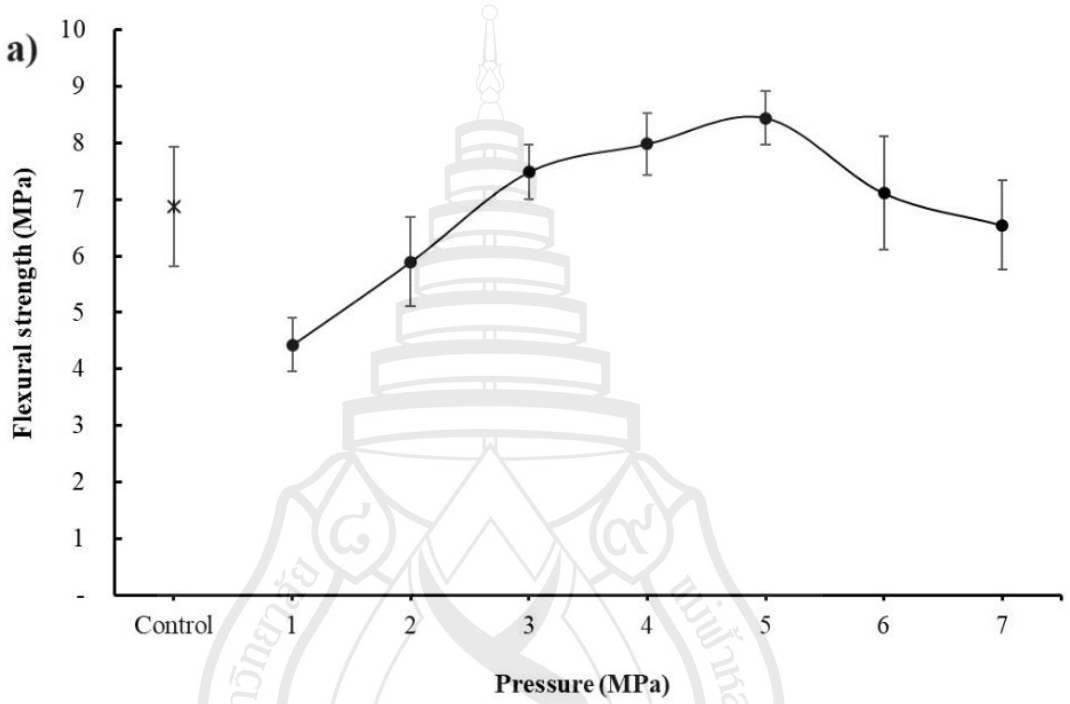

Figure 6.2 Mechanical properties of EF reinforced cement depending on pressure: a) flexural strength, b) modulus of elasticity, and c) fracture toughness

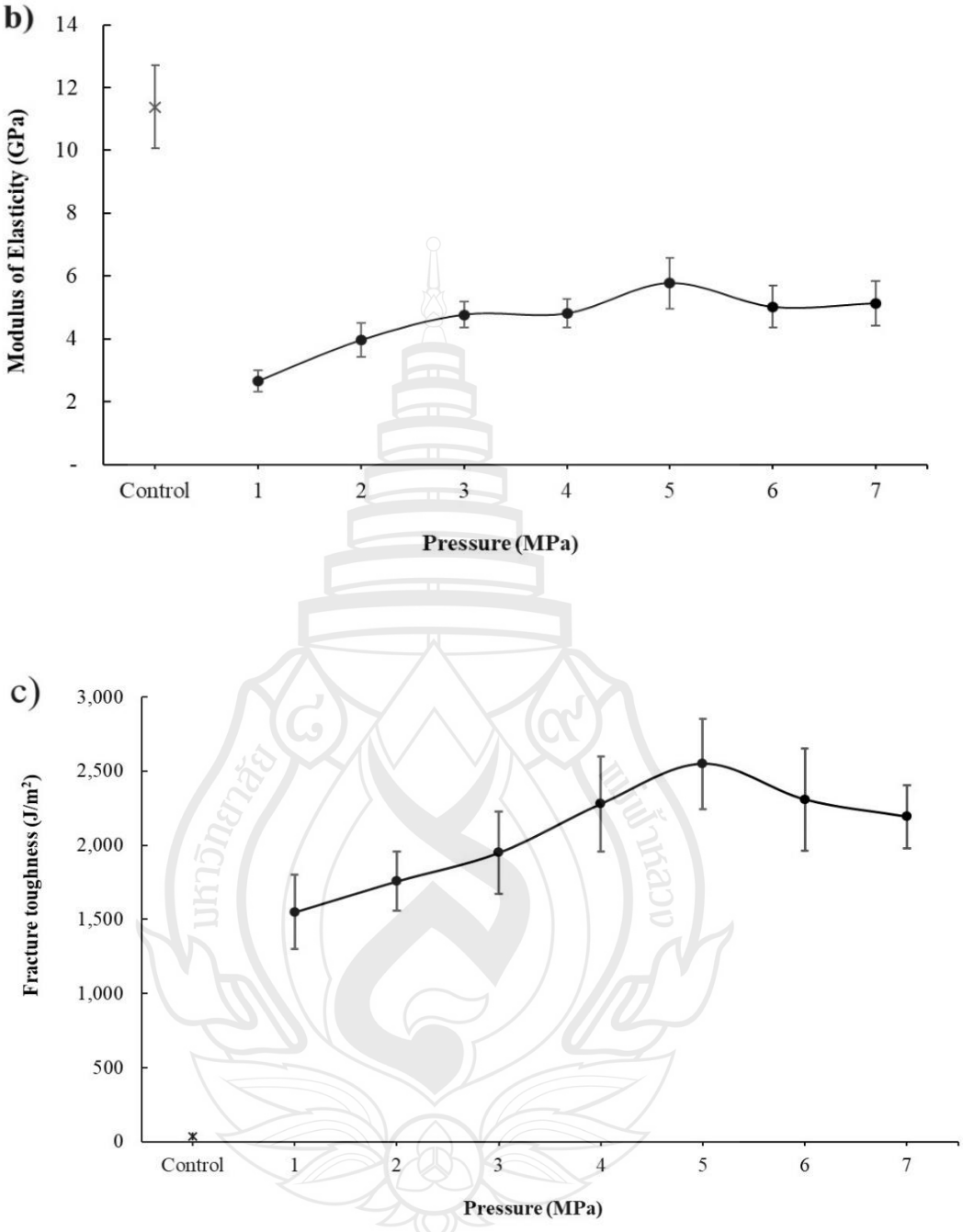

Figure 6.2 (continued)

6.3.3 Fracture Surface Analysis

Figure 6.3 presents SEM micrographs of the EF-reinforced cementitious composites with different compaction pressures.

It can be noted that the high compaction pressure provides a stronger bonding between the EF and the cementitious matrix. Based on SEM photographs and observation, fiber fracture was the primary mode of failure for the composites with a compaction pressure greater than 5 MPa (see Figures 6.3 e to g). On the other hand, Figures 6.3a to d show a weaker interfacial bond between fiber and matrix, and the primary mode of fiber failure was fiber pullout. In addition to that, the composites with lower compaction pressure presented also a large gap between the fiber and the matrix, resulting in higher porosity of the composite (see Figure 6.2d). Figure 6.3a shows a large number of fiber pull-out, while Figure 6.3e to g present mostly fiber failure.

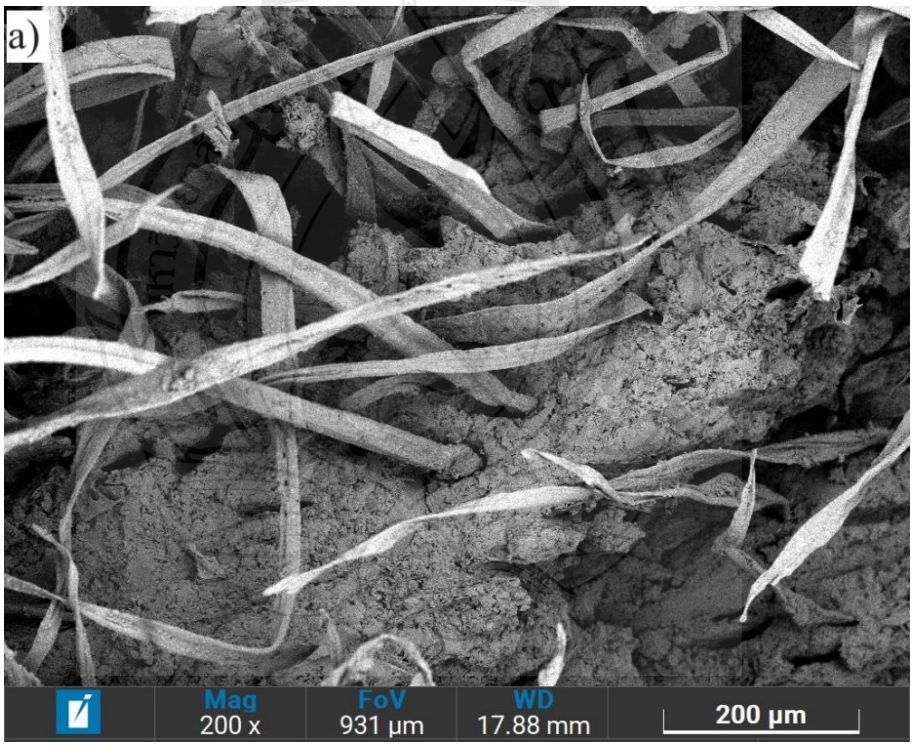

Figure 6.3 SEM photographs of EFC with different pressures: a) 1 MPa, b) 2 MPa, c) 3 MPa, d) 4 MPa, e) 5 MPa, f) 6 MPa, and g) 7 MPa

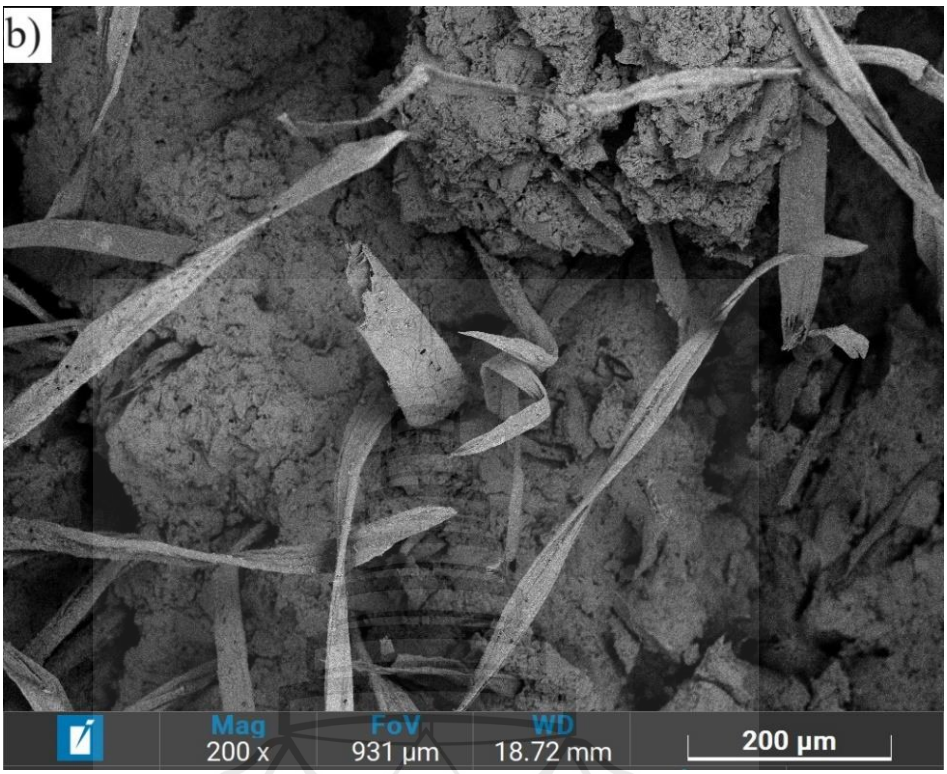

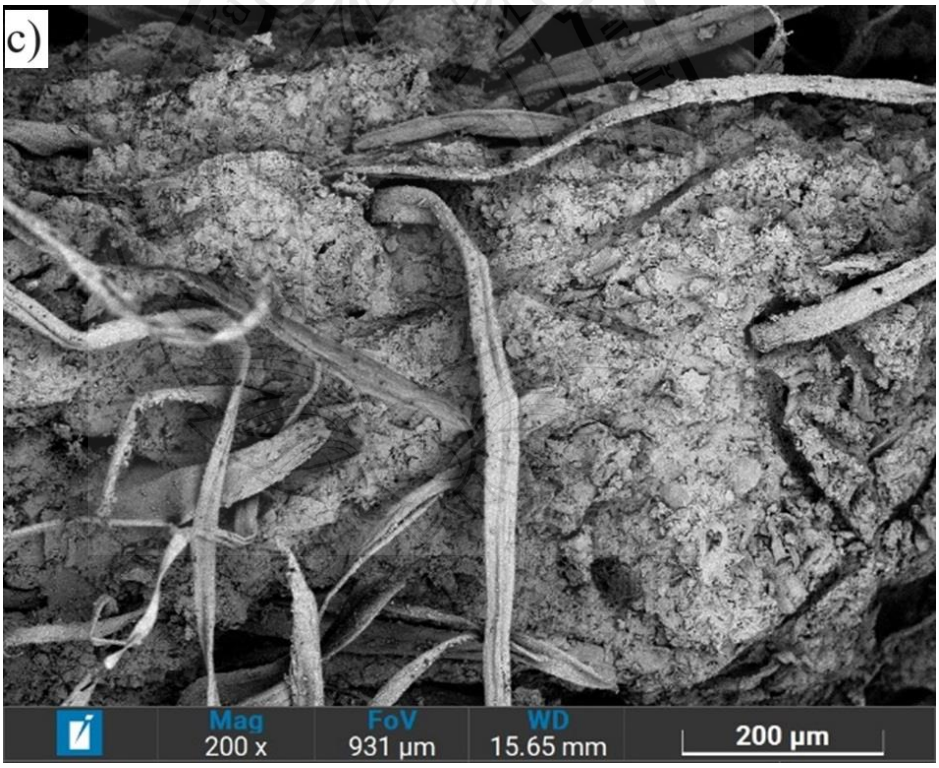

Figure 6.3 (continued)

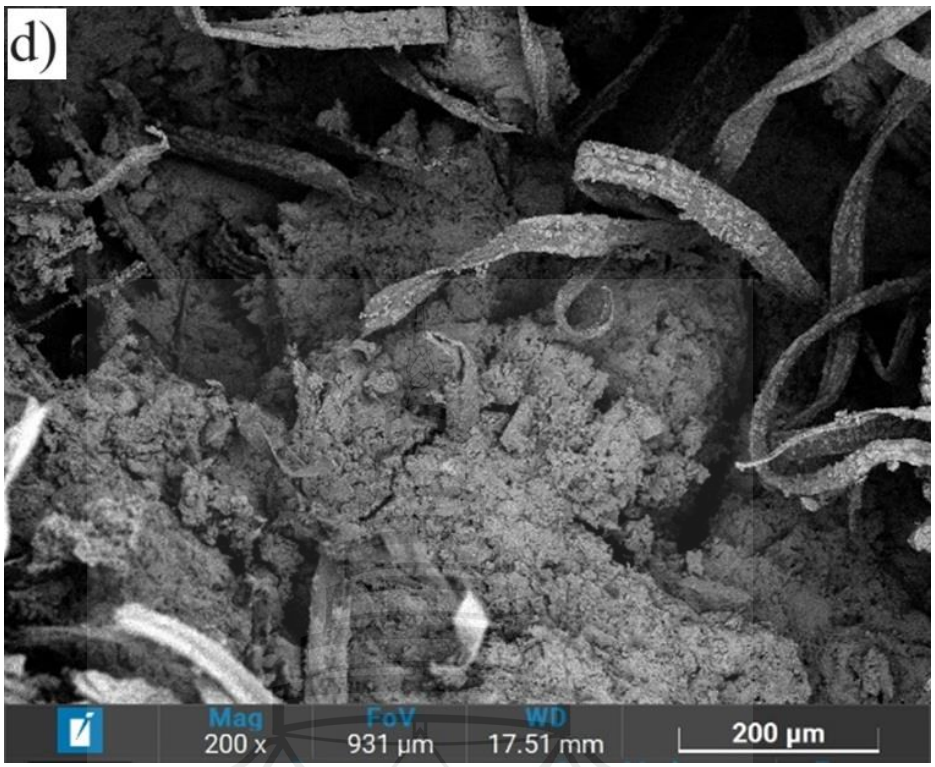

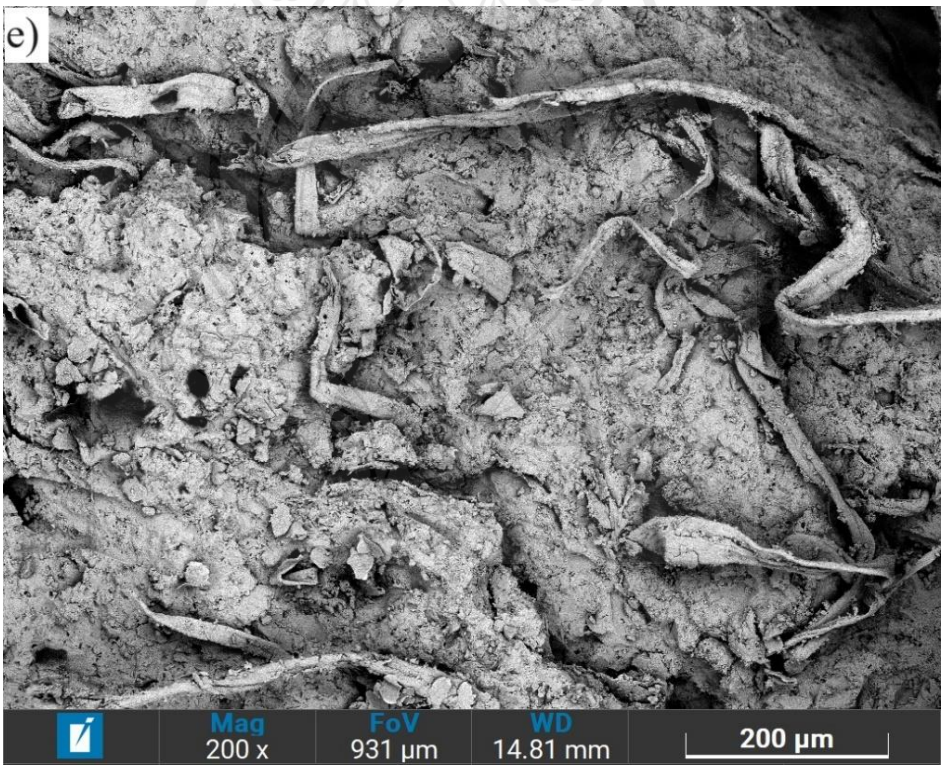

Figure 6.3 (continued)

Figure 6.3 (continued)

6.4 Conclusions

This study showed how the processing parameter (compaction pressure) changes the way EF-reinforced cementitious composites behave physically and mechanically. The study revealed a 2.5% increase in density. When the compaction pressure increased, the composites' porosity and water absorption decreased steadily by 2.75% and 65%, respectively. The flexural strength and fracture toughness of the composites rose by 22% and 65% as the compaction pressure increased because the interfacial bond between eucalyptus fiber and cementitious matrix was dramatically improved.

In Chapter 5, the experiment demonstrated that the RPBC fibrillation improved the flexural strength and fracture toughness of the RPBC-reinforced cementitious composite. This study reveals that the compaction pressure can also contribute to improving the flexural strength and fracture toughness of the eucalyptus fiber-reinforced cementitious composite. The next chapter will focus on how fiber characteristics influence the properties of fiber-reinforced cementitious composites.

CHAPTER 7

EFFECT OF NATURAL FIBER CHARACTERISTICS ON PROPERTIES OF CEMENTITIOUS COMPOSITES: A COMPARATIVE ANALYSIS BETWEEN RPBC, BF, AND EF

7.1 Introduction

In previous chapters, the influences of fibrillation and compaction pressure on the properties of RPBC and EF-reinforced cementitious composites were investigated. The flexural strength and the fracture toughness of the composites increased with an increase in the fibrillation level of RPBC and in compaction pressure, but when the fibrillation level or compaction pressure were excessive, the strength and fracture toughness decreased accordingly. It was found that the suitable fibrillation for wood pulp used to reinforce the cementitious composites was about 550 mL CSF, and the appropriate compaction pressure for the EF-reinforced cementitious composite was 5 MPa for a maximum flexural strength and a considerable fracture toughness.

This chapter evaluated the influence of fiber characteristics on the physical and mechanical properties of cementitious composites using recycled pulp from beverage cartons (RPBC), virgin bamboo fiber (BF), and virgin eucalyptus fiber (EF) as reinforcement fibers as a function of fiber contents. The performance of cementitious composites reinforced with natural cellulosic fiber depends on various factors, such as the type of fiber, fiber morphologies, fiber content, fiber aspect ratio, fiber distribution, the structure of the fiber-matrix interface, processing parameters, and the properties of the matrix (Bentur & Mindess, 2005). Among those influent factors, fiber content is a crucial parameter affecting the composites' strength, density, porosity, and water absorption (Coutts & Ni, 1995). The flexural strength increased with an increase in fiber

fraction; however, it decreased when the fiber content was too high due to the non-uniform distribution of fiber and the fibers not evenly embedded by the cementitious matrix. This leads to a reduction in the strength of the fiber-reinforced cement composite.

With a careful experimental design, this study aimed to examine the influence of the fiber content of each fiber type (RPBC, EF, and BF) on the physical and mechanical properties of the composite. The fiber content, ranging from 2% to 14% by mass, was carefully selected to ensure a comprehensive analysis of the properties, including flexural strength, modulus of elasticity, fracture toughness, bulk density, and porosity, of each fiber-reinforced composite. This approach enhances the reliability and validity of the research findings.

7.2 Materials and Methods

7.2.1 Materials

The reinforcement fibers (RPBC, BF, and EF) were used in the experiment. Their characteristics were presented in Chapters 3 and 4. The RPBC with a freeness of 550 mL CSF was employed because the previous experiment showed that the cementitious composite reinforced with 550 mL CSF RPBC performed the best (see Chapter 5 for detailed results).

Ordinal Portland cement (OPC) Type I and ground silica sand (fine sand) were employed as the ingredients of the cementitious matrix. Their chemical compositions are presented in Table 4.4. OPC and ground silica sand have an average particle size of 25.72 μm and 27.9 μm, respectively. The distribution of particle sizes for the OPC and the ground silica sand is presented in Figure 4.8 of Chapter 4.

7.2.2 Methods

7.2.2.1 Specimen composition

The compositions of the specimen for each fiber type are presented in Tables 7.1, 7.2, and 7.3.

Table 7.1 Specimen composition for the RPBC cementitious composites

Sample codes	RPBC		Cement	Fine Sand
	(%)	(g)	(g)	(g)
Control	0	-	45	45
2RRBCC	2	1.8	44.1	44.1
4RPBCC	4	3.6	43.2	43.2
6RPBCC	6	5.4	42.3	42.3
8RPBCC	8	7.2	41.4	41.4
10RPBCC	10	9	40.5	40.5
12RPBCC	12	10.8	39.6	39.6
14RPBCC	14	12.6	38.7	38.7

Table 7.2 Specimen composition for BF cementitious composites

Sample codes	BF content		Cement	Fine Sand
	(%)	(g)	(g)	(g)
2BFC	2	1.8	44.1	44.1
4BFC	4	3.6	43.2	43.2
6BFC	6	5.4	42.3	42.3
8BFC	8	7.2	41.4	41.4
10BFC	10	9	40.5	40.5
12BFC	12	10.8	39.6	39.6
14BFC	14	12.6	38.7	38.7

The fiber mass fraction varied from 2 to 14 wt% by the dry weight of the total solid mass. The total solid weight was 90 g and consisted of OPC and ground silica sand (sand-to-cement ratio = 1:1). The water in the slurry was 400 ml. The control specimen was formed with a water-to-cement ratio of 0.5 and compacted at the same pressure (5 MPa).

Table 7.3 Specimen composition for EF cementitious composites

Sample codes	EF content		Cement	Fine sand
	(%)	(g)	(g)	(g)
2EFC	2	1.8	44.1	44.1
4EFC	4	3.6	43.2	43.2
6EFC	6	5.4	42.3	42.3
8EFC	8	7.2	41.4	41.4
10FEC	10	9	40.5	40.5
12FEC	12	10.8	39.6	39.6
14FEC	14	12.6	38.7	38.7

7.2.2.2 Specimen forming

All specimens were formed according to the procedure in Section 3.2.3. The specimens were pressed at 5 MPa and maintained for 5 minutes. This pressure value was obtained from the previous experiment, which lead to a maximum flexural strength of the composites.

7.2.2.3 Assessment of composite properties

The physical and mechanical properties and fracture surface analysis of the composites were assessed in accordance with the description in Sections 3.3 and 3.4.

7.3 Results and Discussions

7.3.1 Physical Properties

The physical properties of RPBC, BF, and EF cementitious composites are presented in Figure 7.1 as a function of fiber contents. The bulk density of composites decreased steadily as the percentage of fiber content increased. The reduction in density of the fiber-reinforced composites depends on the increase in void volume caused by the fibers incorporated (Achour, 2017). This result is due to the composite's poor compactness of the reinforced fibers, which increases the porosity of the composite in its hardened state, decreasing its density (see Figures 7.1a and b). It can be observed

that the bulk density of RPBCC, BFC, and EFC has a similar level of value as the fiber content below 4 wt%; however, the bulk density of RPBCC was higher than that of BFC and EFC when the fiber content was above 4 wt%, as shown in Figure 7.1a. In addition, it should be noted for BF and EF that the decrease in density is linear; however, for the RPBC, the reduction in density is more pronounced at a low slope as the fiber content increases. This can be linked to the length and morphologies of the fibers. The short fiber of RPBC with a ribbon-formed shape can be better compacted than that of long BF and EF in the cementitious matrix; therefore, it results in a higher density of RPBCC with a higher fiber content than that of BFC and EFC.

Figure 7.1b shows the variation of the porosity value of RPBC, BF, and EF composites as a function of fiber content. The graphs show that the increase in fiber content contributes to increasing the porosity of composites, which is interrelated to the density. The porosity of the RPBC specimen rises by 17%, while the porosity of the BF and EF specimens increases by 33% and 25% as the fiber content increases from 2 to 14 wt%, respectively. At a fiber content below 8 wt%, the porosity of BF composites illustrates a lower value than that of RPBC and EF composites due to the small diameter of BF. As the fiber content exceeds 8 wt%, the porosity of BF and EF specimens increases linearly, while the porosity of RPBC specimens rises at a reduced slope. The steady increase in porosity of BF and EF composites with an increase in fiber content is related to the porosity of the composite and the interaction grape between fibers and the matrix. The grape would occur after hardening of the composite due to the high water absorption of natural fibers. When the composite is in dry state, water drains out from the fiber leading to a shrinkage of natural fibers (Savastano & Agopyan, 1999).

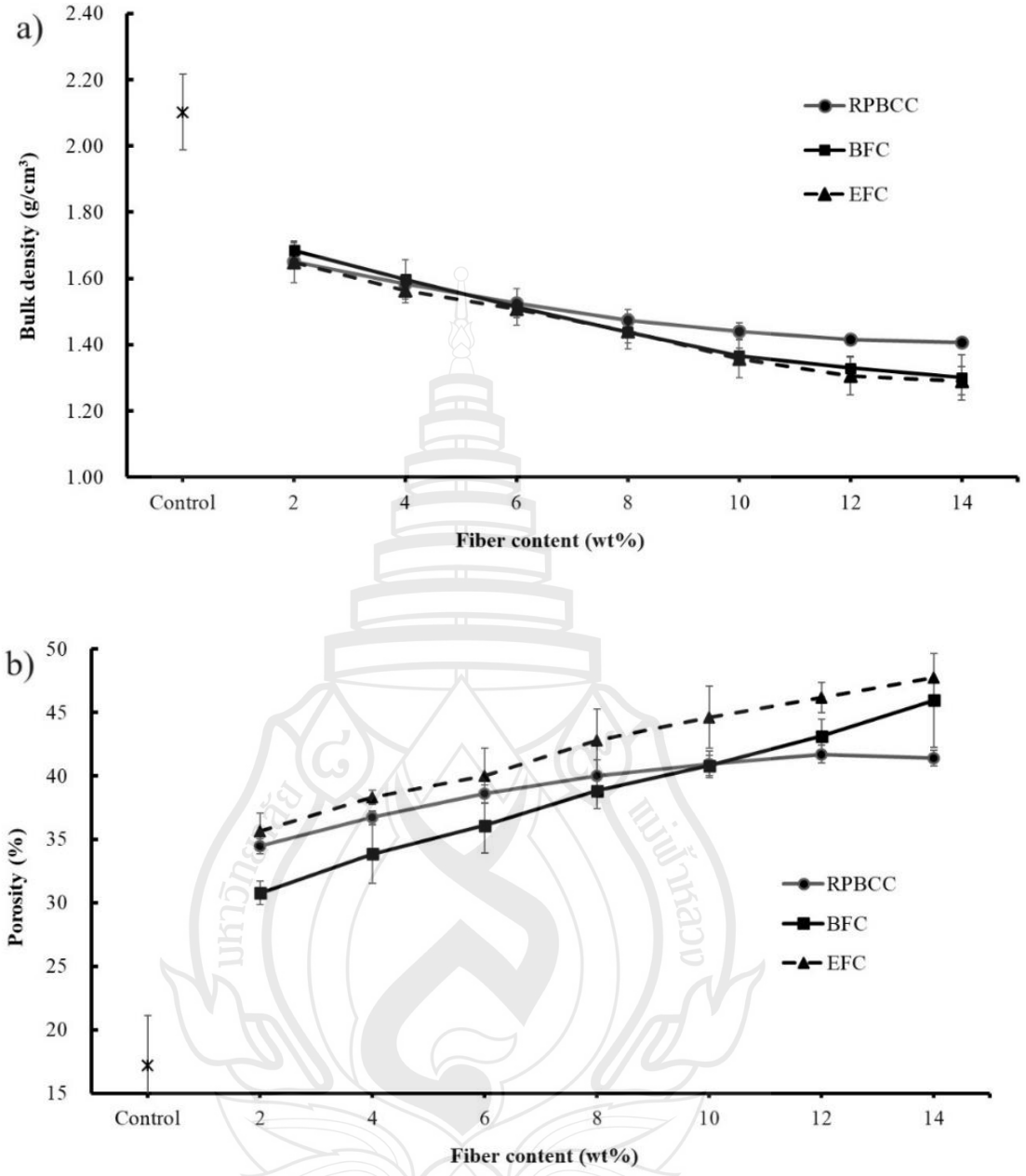

Figure 7.1 Physical properties of RPBCC, BFC, and EFC: a) bulk density, b) porosity, and c) water absorption

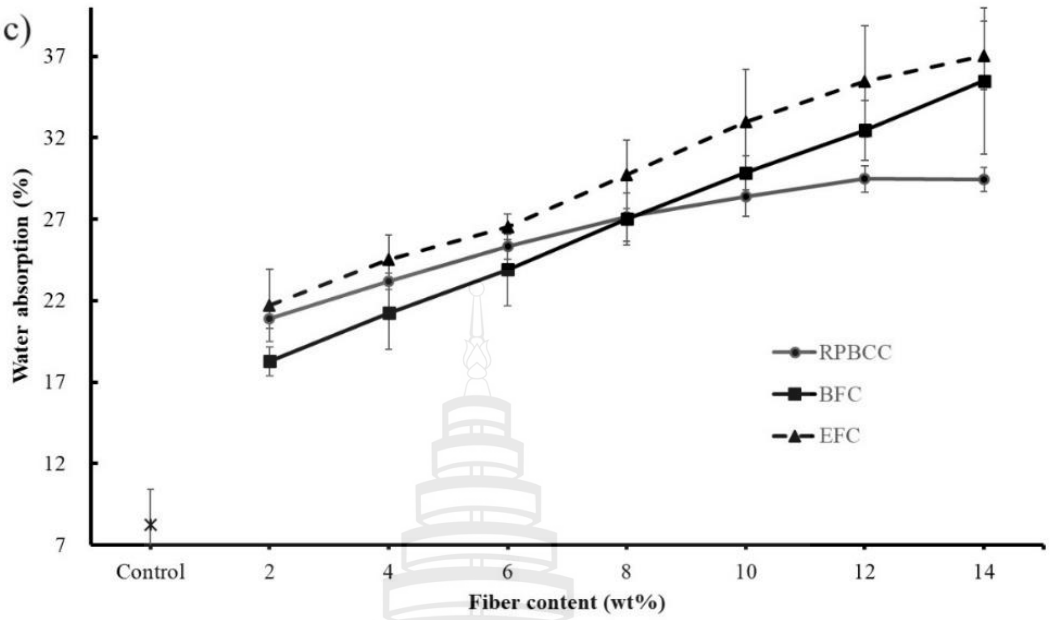

Figure 7.1 (continued)

7.3.2 Mechanical Properties

The mechanical properties of cementitious composites reinforced with RPBC, BF, and EF are presented as a function of fiber contents in Figure 7.2. The flexural strength development of RPBC composite (RPBCC), BF composite (BFC), and EF composite (EFC) is shown in Figure 7.2a. As can be seen, the flexural strength of composites tends to increase as the fiber content increases. In the case of RPBCC and BFC, the flexural strengths at 2 and 4 wt% fiber content were lower than those of the control specimen. The reduction in flexural strength of RPBCC and BFC between 2 and 4 wt% was caused by a non-uniform distribution of fiber in the cementitious matrix, as suggested by previous studies (Oriyomi et al., 2015). Microcrashes could occur where no fiber was present, resulting in a reduction in strength. This was also seen on the EF specimen at 2 wt%. Adding more than 4 wt% of fibers led to a continuous increase in the flexural strength of RPBCC, reaching a maximum strength value of 11.91 MPa at 14 wt% fiber content. The constant increase in the strength of RPBCC could be caused by homogenous dispersion and a high degree of bonding between the fibers and cementitious matrix due to the highly fibrillated RPBC. However, the high fibrillation leads to lower fracture toughness compared to that of EFC and BFC (see Figure 7.2c).

Figure 7.3 presents the stress-strain relationship of the composites reinforced with 8 wt% and 14 wt% fiber content. The RPBC composite showed a lower strain with increased fiber content than the EFC and BFC.

BFCC and EFC, on the other hand, had a maximum flexural strength of 9.08 MPa and 9.94 MPa, respectively, at 8 wt% fiber content. After that, it gradually decreased. The increase in flexural strength of EFC and BFC from 4 wt% to 8 wt% was caused by sufficient reinforcement of fibers in the cementitious matrix, and the composite had good interfacial bonding. The observed reduction in flexural strength values of BFC and EFC when the fiber content is higher than 8 wt% is probably caused by poor distribution of long fiber within the matrix and inefficient compaction, which led to a reduction in bulk density, an increase in porosity (see Figure 7.1), and a lower interfacial bonding between the reinforcement fiber and the matrix (Savastano et al., 2000; da Correia et al., 2014). It is shown that the strength of BFC was lower than that of EFC, although the aspect ratios of BF were higher than those of EF.

The modulus of elasticity (MOE) values decreased steadily for all types of fiber-reinforced composites, as shown in Figure 7.2b. The decrease in MOE of the composites with an increase in fiber content is due to the natural cellulose fiber having a lower modulus of elasticity than the cementitious matrix. That can be explained by the rule of mixture (Coutts & Ni, 1994).

Figure 7.2c shows the variations in fracture toughness values of composites reinforced with RPBC, BF, and EF depending on fiber content. The fracture toughness increased with an increase in fiber content for all samples. It was observed that the composite containing RPBC presented a lower fracture toughness than the composite reinforced with BF and EF. The reasons could be due to the low freeness level of RPBC and fiber length compared to EF and BF. The high degree of fibrillation of RPBC leads to good bonding between RPBC and the cementitious matrix. This contributed to enhancing the strength of the RPBC composite (Figure 7.2a) and its low fracture toughness (Figure 7.2c). It can be observed that the fiber pulls out on the fracture surface of RPBC, which is caused by the short fiber of RPBC and leads to a short-embedded length of the fiber. The short-embedded length generated insufficient friction stress equal to the fiber strength, resulting in low fracture energy. As a consequence, the fiber slipped and was pulled out.

The BF-reinforced cementitious composite presents a middle fracture toughness value compared to EFC and RPBCC because BF exhibits a circle-forming cross-section with a small diameter, leading to lower interfacial adhesion compared to EFC, which leads to fiber pullout mainly with low debonding energy (see Figures 7.2c and 7.3). On the other hand, the EF-reinforced composite shows significant de-bonding energy because the pull-out of long fiber consumes more energy than that of short fiber due to higher frictional stress during fiber pull-out. It can be seen that the fracture toughness of RPBC and BF composites has similar values at high fiber content.

An important observation regarding the mechanical performance of RPBC composites compared to BF and EF composites is that RPBC produced better flexural strengths when the fiber content was above 8 wt%. However, the fracture toughness of samples reinforced with RPBC presented a lower value than the BF and EF composites, except at 14 wt% fiber content (Figures 7.2a and c). The fibrillation of RPBC, which is well known to have significantly reduced the composite's fracture toughness, may be the reason.

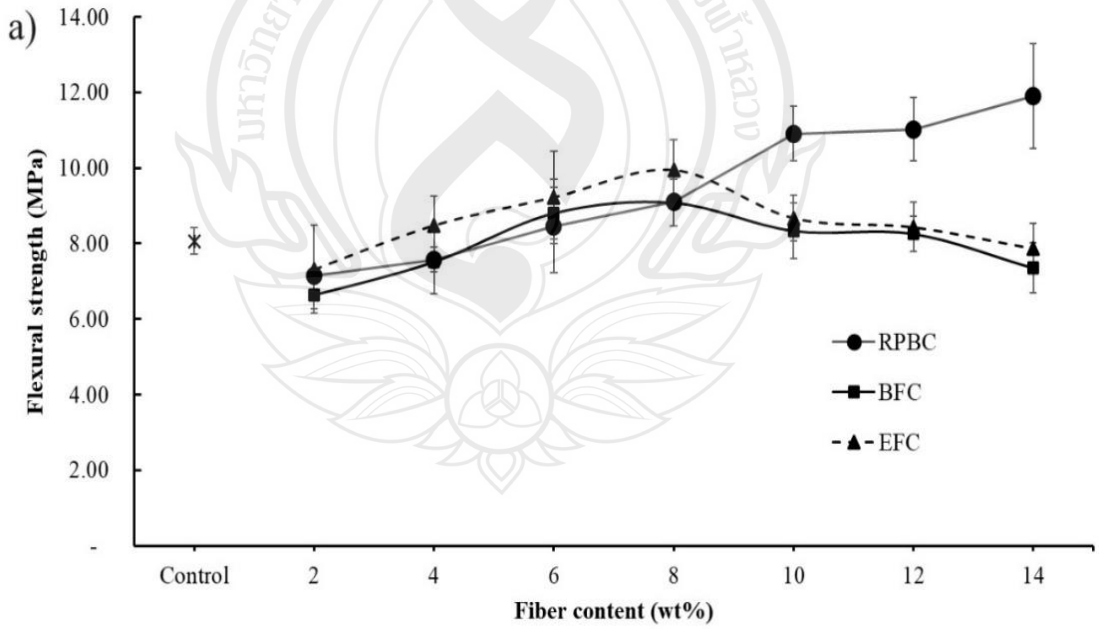

Figure 7.2 Mechanical properties of cementitious composites reinforced with RPBC, BF, and EF: a) flexural strength, b) modulus of elasticity, and c) fracture toughness

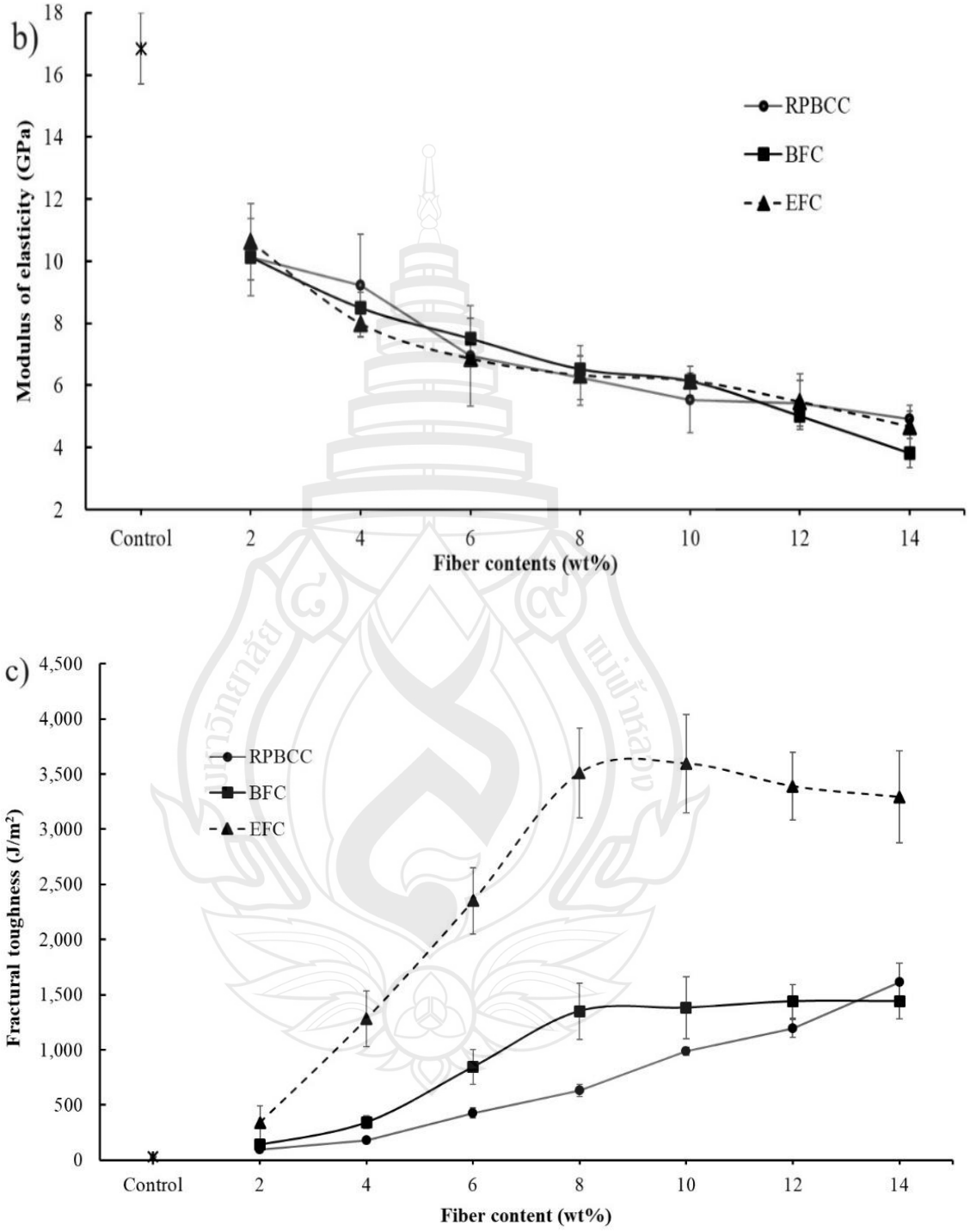

Figure 7.2 (continued)

Figure 7.3 presents the stress-strain curves of RPBCC, BFC, and EFC. The graphs show that the EFC exhibits a large elongation compared to BFC and RPBCC, both at 8 wt% and 14 wt% fiber content. However, RPBCC shows a higher stress with a small elongation of 14 wt% (see Figure 7.3b).

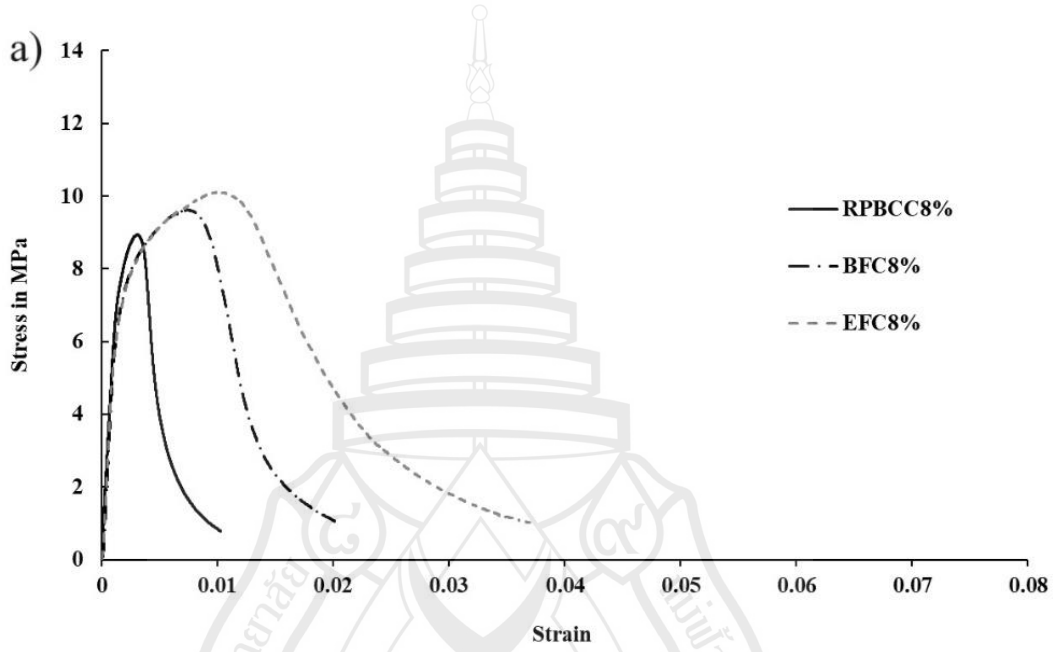

Figure 7.3 Stress-strain curves of RPBC, BF, and EF reinforced cementitious composite: a) 8 wt% and b) 14 wt% fiber content

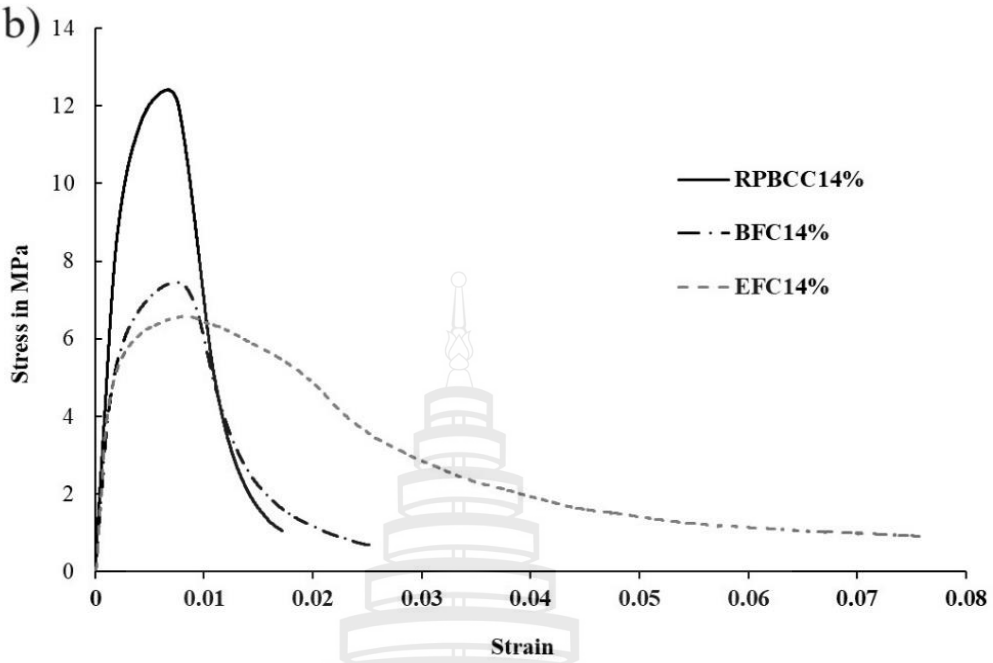

Figure 7.3 (continued)

7.3.3 Fracture Surface Analysis

The microstructural features of the fracture surface of the RPBC, BF, and EF composites at 8 wt% fiber content are presented in Figures 7.4, 7.5, and 7.6, respectively. The fracture surface characteristics in SEM micrographs, such as bonding between fiber and matrix, fiber failure, fiber pullout, and porosity appearance, can indicate the mechanical behaviors of composites of different fiber types. Every picture shows a clear fiber pullout mode. In the case of RPBCC, broken and unbroken fibers were found on the fracture surfaces (see Figure 7.4). This is also observed in the BF and EF composites (see Figures 7.5 and 7.6). However, it is seen that the length of the pullout fiber in the RPBC specimen was shorter than that in the BF and EF specimens. This behavior can be influenced by the high degree of fibrillation of RPBC fibers, resulting in good adhesion between RPBC and the cement matrix. Thus, the fiber failure occurred more than fiber pulled out from the matrix, leading to a relatively low fracture toughness of RPBCC.

In contrast to RPBCC, most of the BF and EF were slipped and pulled out rather than breaking on the fracture surface of the BFC and EFC (see Figures 7.5 and 7.6). The BF and EF were mainly pulled out with considerable length and integrity, resulting in the higher toughness of the composites. Figure 7.6b shows some grapes on the interaction between the EF and the cementitious matrix, which helps explain why the composites are more porous.

The SEM revealed that the failure modes for each fiber type were obviously different. RPBC and EF are wood fibers that exhibit a similar morphology but show a distinct failure mode. Most fiber fractures occurred in RPBCC, while most fiber pullouts occurred in EFC. BF, on the other hand, is a plant fiber with a circular-shaped cross-section and long fiber. It shows both modes of failure in BFC.

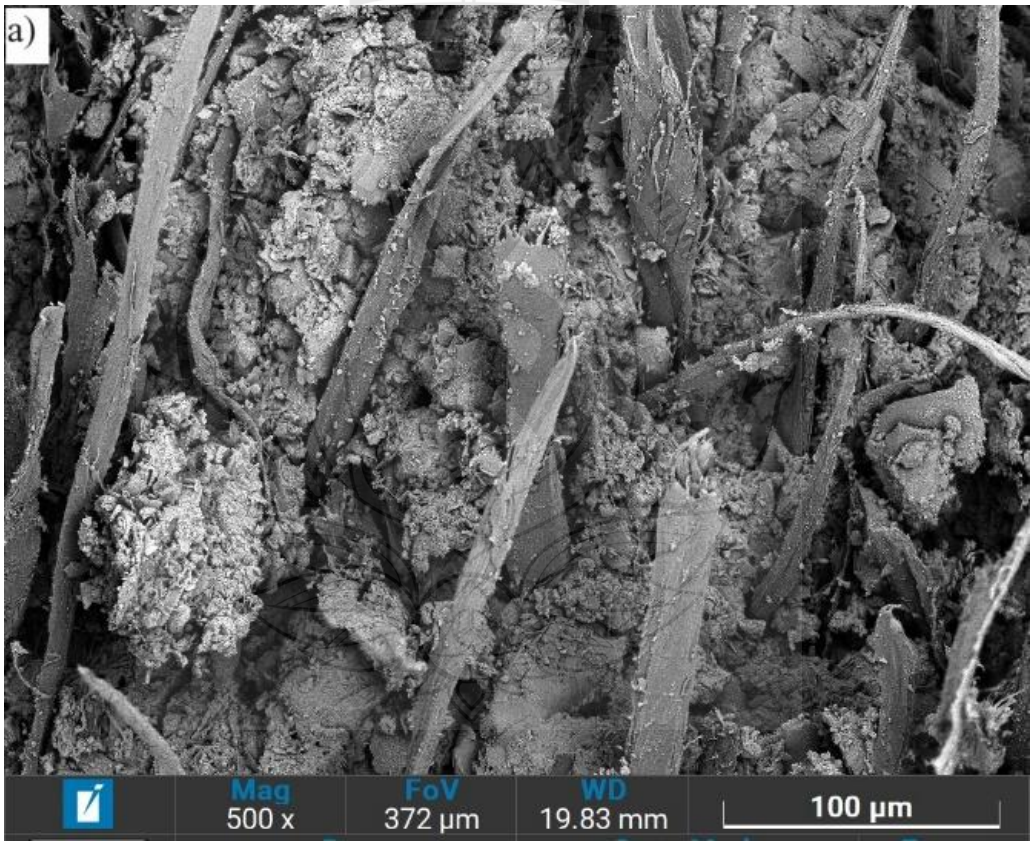

Figure 7.4 SEM graphs of fracture surfaces of RPBCC: a) fiber pull out mode and b) fiber fracture mode

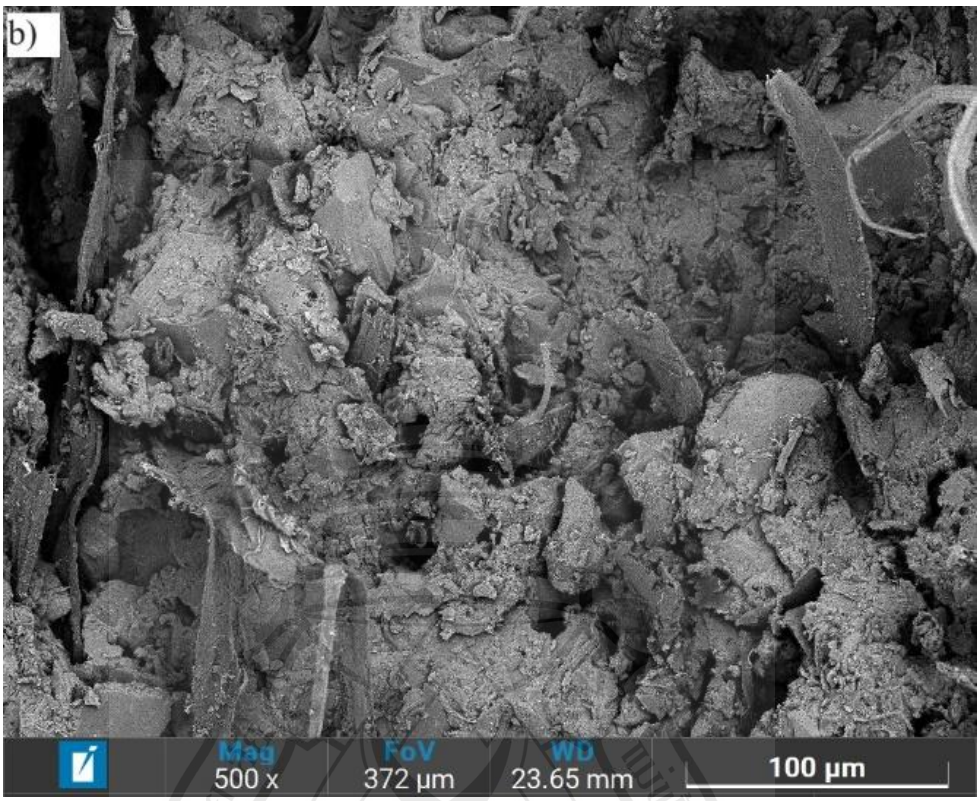

Figure 7.4 (continued)

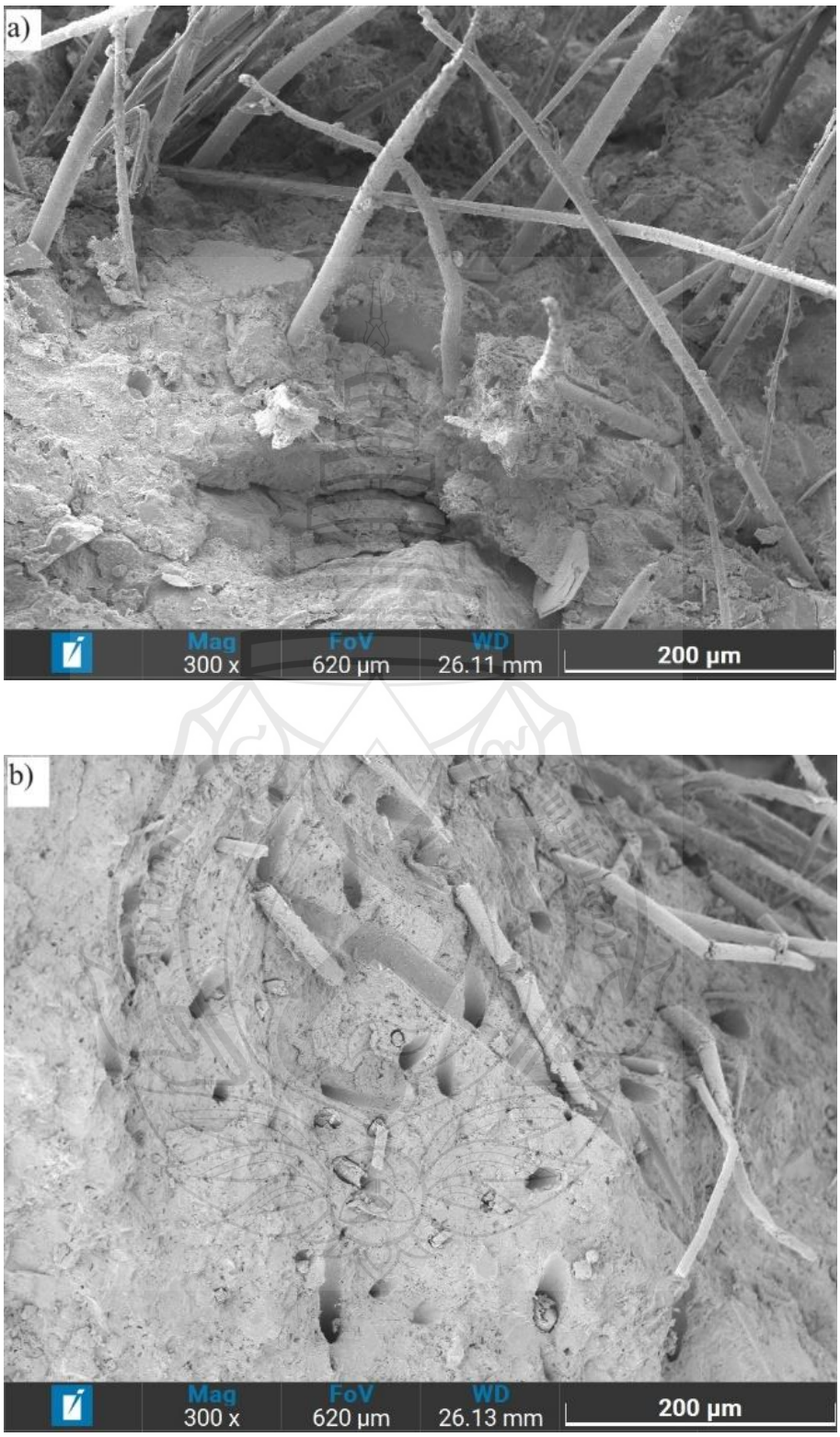

Figure 7.5 Micrographs of fracture surfaces of bamboo fiber reinforced cement composite: a) fiber pull out mode and b) fiber failure mode

Figure 7.6 Micrographs of fracture surfaces of EFC: a) fiber pull out mode and b) fiber failure mode

7.4 Conclusions

The effects of the fiber characteristics of RPBC, BF, and EF on the properties of fiber-reinforced cementitious composites were examined as a function of fiber content, which ranged from 2 to 14 wt% after 28 days of curing.

The results demonstrated that the optimal flexural strength of RPBC composites was achieved by adding 14 wt% RPBC. The flexural strength of RPBCC was improved by 47.61% compared to the control specimen. In contrast, the optimal fiber content for BF and EF composites was found at 8 wt%, of which the flexural strength was enhanced by only 12.58% and 23.19%, respectively. The RPBC shows better reinforcement in cementitious composites due to the high fibrillation of the fiber, which enhances the interfacial bond between the fiber and the matrix and increases the strength of the composite.

In addition, the fracture toughness of composites improves steadily with an increase in fiber content. The EFC exhibited the highest fracture toughness value of 3,600 J/m^2 compared to the BFC and RPBCC, with 1,400 J/m^2 and 1,600 J/m^2, respectively, because EF has a high amount of long and strong fiber, which contributed significantly to the absorption of energy during the pull-out process. The bulk density decreased gradually, while the porosity of the composites increased steadily as the fiber content increased. The porosity of EFC depicted a higher value than that of RPBCC and BF due to the large dimension of EF.

From this study, it was found that RPBC with a fibrillation level of 550 mL CSF performed the best, while EF provided high fracture toughness due to its unique fiber morphology and long fiber length.

The next study will assess how to improve the fracture toughness of RPBC-reinforced cementitious composites by mixing this fiber with other virgin cellulose fibers.

CHAPTER 8

OPTIMIZATION OF HYBRID FIBER FRACTION

8.1 Introduction

In the earlier chapters, it was shown that the cementitious composite reinforced with RPBC had a maximum flexural strength of 12 MPa at a fiber content of 14 wt%. However, its fracture toughness was only 1.6 kJ/m^2, which was 55% less than that of the virgin EF-reinforced composite. In the practical application of fiber-reinforced cement composites, fracture toughness is also an important property that indicates the composite's ability to absorb energy under stress, in addition to strength. The composite's high impact resistance can reduce cracking and crack propagation in the brittle matrix. The preliminary experiment revealed that a commercial wood fiber-reinforced cement composite has a fracture toughness of 2 kJ/m^2.

The use of RPBC fiber alone as reinforcement in the cementitious composite has shown low fracture toughness, as demonstrated in the previous chapters. Therefore, this experiment is crucial as it aims to enhance the reinforcement efficiency of recycled pulp from beverage cartons (RPBC) in the cementitious composite. This is achieved by mixing it with virgin cellulose fibers. Due to the re-pulping process of used drink cartons, the RPBC is known to contain a high fraction of relatively short fiber. This has been a drawback in producing fiber-reinforced cementitious products. Soroushian *et al.* (1995) proposed substituting virgin cellulose fibers for recycled pulp to enhance its reinforcement. However, we need to investigate the level of virgin fiber substitution.

The primary objective of this experiment was to identify a suitable mass proportion between RPBC and virgin cellulose fiber. The initial work determined a suitable fiber content of 8 wt% for wood fiber. For this study, RPBC with 550 mL CSF was used because the composite showed better flexural strength at this fibrillation level.

8.2 Materials and Methods

8.2.1 Materials

The materials used in this experiment were RPBC with 550 mL CSF as the recycled pulp and commercial eucalyptus fiber (EF) as the virgin cellulose fiber. The RPBC was mixed with EF in the proportions described in Section 8.2.2. Chapters 3 and 4 provide the detailed properties of RPBC and EF, including a comprehensive understanding of their characteristics and roles in the experiment.

OPC and ground silica sand were employed for the cementitious matrix mixture. The chemical compositions and particle sizes of the matrix ingredients were presented in Section 4.3.4.

8.2.2 Methods

8.2.2.1 Specimen compositions

Table 8.1 presents the specimen's sample codes and corresponding compositions reinforced with various fiber mixtures between RPBC and EF. The total dry fiber content was fixed at 8 wt%. The fiber mixture between RPBC and virgin fiber ranges from 8:0 to 6:2, 4:4 to 2:6, and 0:8. The number in the sample code following the fiber type abbreviation indicates the fiber's dry mass percentage. The total dry mass of ingredient materials was 90 g per specimen. The cementitious matrix consisted of a mixture of OPC and ground silica sand, with a sand-to-cement ratio of 1:1.

Table 8.1 Specimen composition for the RPBC-EF reinforced cementitious composites

Sample codes	RPBC		EF	
	(%)	(g)	(%)	(g)
RPBC8EF0C	8	7.2	0	0
RPBC6EF2C	6	5.4	2	1.8
RPBC4EF4C	4	3.6	4	3.6
RPBC2EF6C	2	1.8	6	5.4
RPBC0EF8C	0	0	8	7.2

All specimens were produced according to the procedure in Section 3.2.3. After immersion in water for 24 hours, 7.2 g RPBC was sheared using a fruit blender for 200 seconds to produce RPBC with a freeness of 550 mL CSF. Afterward, the wet EF was mixed with RPBC and stirred using a homogenizer for 5 minutes. The mixture of cementitious matrix was added. All specimens were formed utilizing the slurry vacuum dewatering method. The amount of water in the slurry was 400 ml. The pressure of 5 MPa was employed, and the pressing was held for 5 minutes.

8.2.2.2 Properties assessment

The physical and mechanical properties of the composites were assessed following the methods described in Sections 3.3.1 and 3.3.2.

8.2.2.3 Fracture surface analysis

The fracture surface analysis of the composites was conducted in accordance with the description in 3.4.

8.3 Results and Discussions

8.3.1 Physical Properties

The physical properties of mixed fiber-reinforced cementitious composites are displayed in Figure 8.1. It can be noted that the bulk density of the composites decreased with a decrease in the RPBC fraction. The variation the mixtures was not significantly different, except for the fraction of 6:2 specimens. This could be an error caused by the inhomogeneous mixing of fibers. As described in Section 7.3.1 of chapter 7, the bulk density of RPBCC was greater than that of EFC by about 2%.

The porosity of the specimens was remarkably changed with the fiber mixture proportion. Generally, the porosity of the hybrid fiber-reinforced composites increased with a decrease in the mass fraction of RPBC. This could be caused by the morphology of EF, which has a large diameter and long fiber length. It led to non-well compaction, resulting in high porosity. A similar tendency was also seen in the water absorption ability of the composites (see Figure 8.1c).

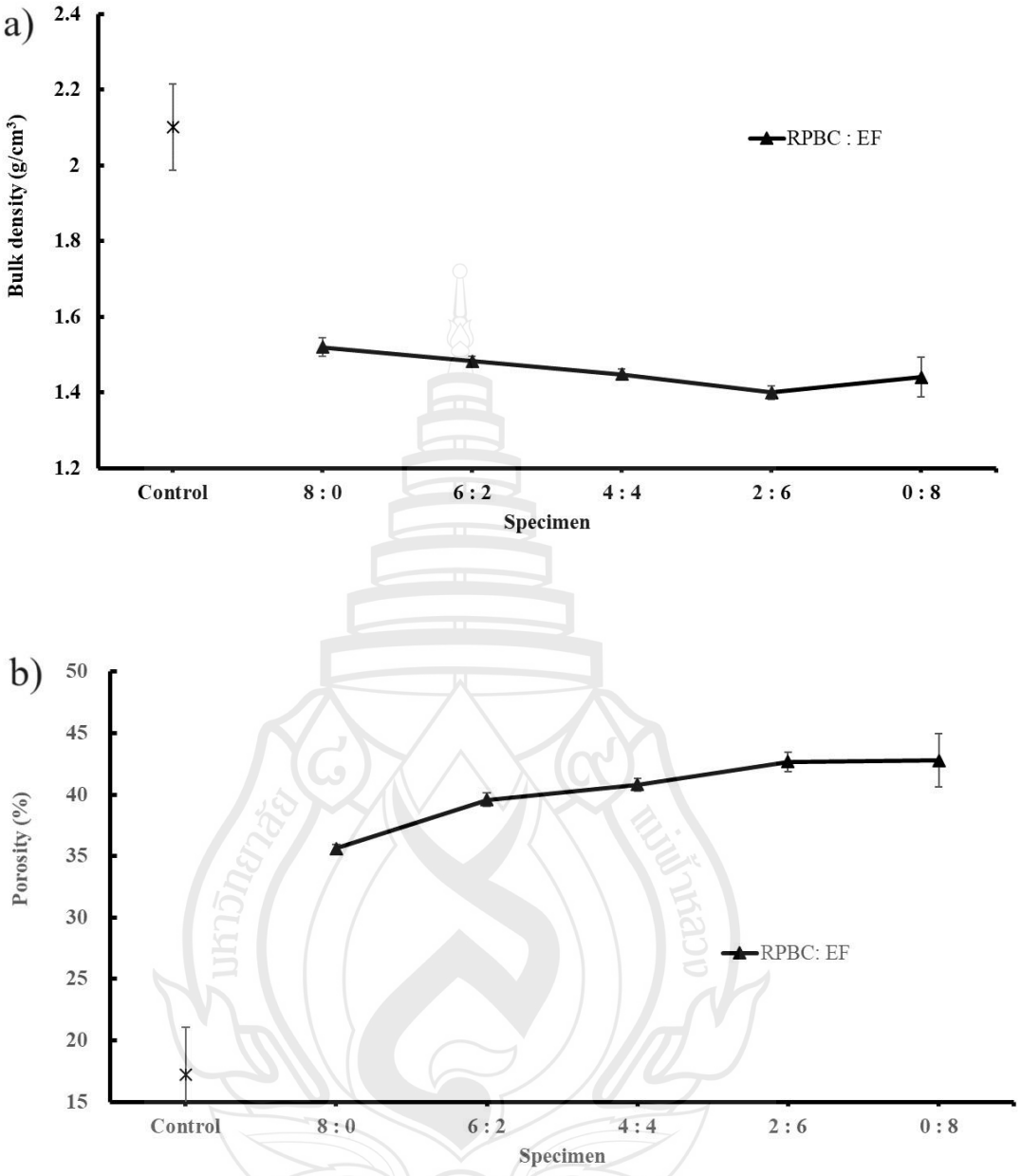

Figure 8.1 Physical properties of hybrid fiber cement composites: a) bulk density, b) porosity, and c) water absorption

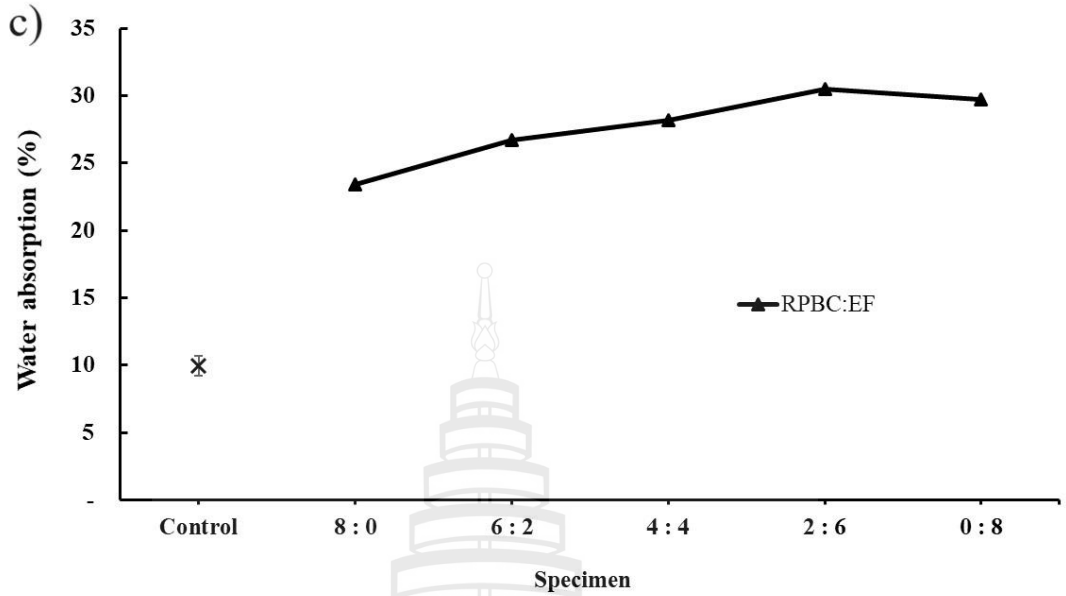

Figure 8.1 (continued)

8.3.2 Mechanical Properties

Figure 8.2 displays the mechanical behavior of the hybrid fiber-reinforced cementitious composites. Generally, the flexural strength increased with a decrease in the mass fraction of RPBC. However, it can be observed that the increase in the flexural strength of RPBC and EF-reinforced composites reached a maximum value of 11 MPa at an equal fraction (4:4). After that, it decreased gradually (see Figure 8.2a). This value exceeds the flexural strength of pure RPBCC by 72% and EFC by 10%, respectively. This figure shows that by mixing the RPBC and EF with an equal mass fraction, the flexural strength of the composites was enhanced significantly because the RPBC and EF are well corporate, which could contribute to the improvement of the reinforcement efficiency. On the other hand, RPBC also contributed to the improvement with a high fibrillation level, which enhanced the interfacial bonding between fiber and the cementitious matrix. Additionally, with a long EF with a wide diameter, the composite shows ductile behavior rather than brittle behavior. The fracture toughness increased with an increase in EF content (see Figure 8.2c). At the fraction of 4:4, the fracture toughness of the hybrid fiber composite rose by 370% compared to the pure RPBC

composite at the fiber content of 8 wt%. The increase in fracture toughness of the hybrid fiber reinforced cement caused by EF with long and strong fiber characteristic.

Figure 8.2b presents the variation of the modulus of elasticity of both hybrid fiber-reinforced cementitious composites. The variation in hybrid fiber proportion does not significantly affect the MOE (see Figure 8.2b).

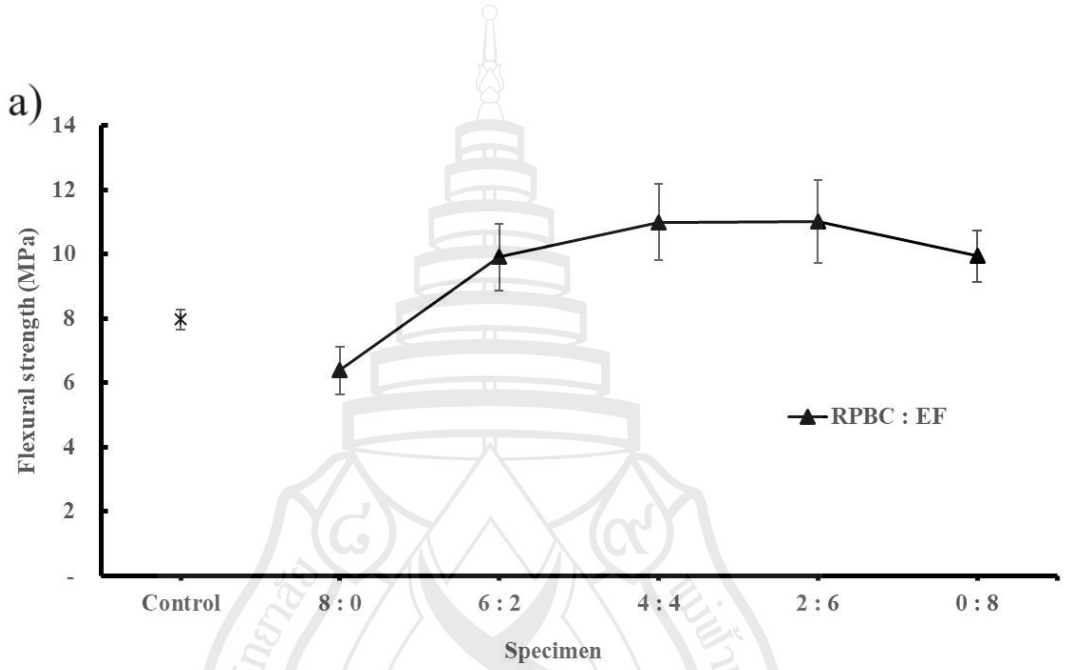

Figure 8.2 Mechanical properties of hybrid fiber cementitious composites: a) flexural strength, b) modulus of elasticity, and c) fracture toughness

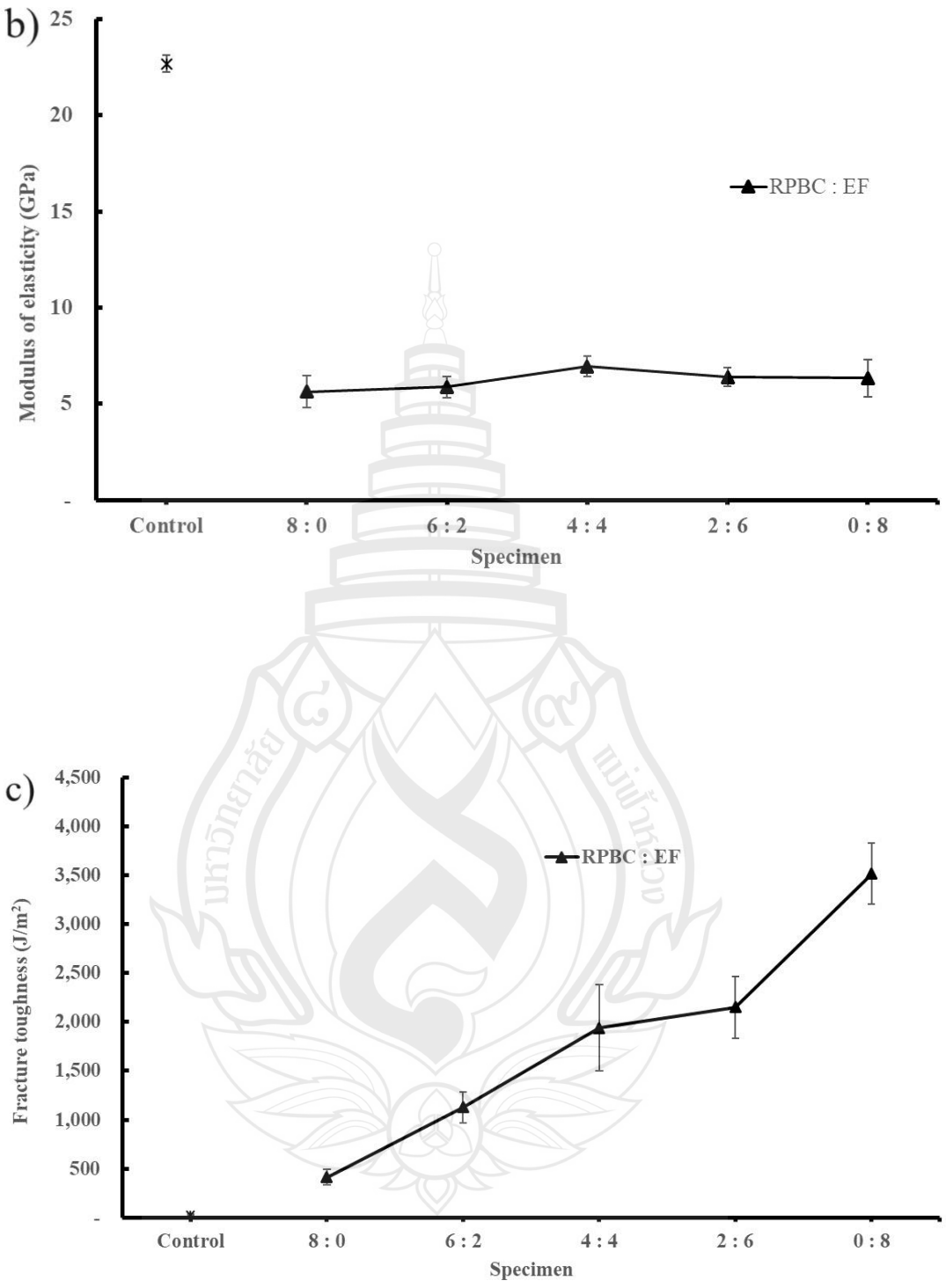

Figure 8.2 (continued)

8.3.3 Fracture Surface Analysis

Figures 8.3 and 8.4 demonstrate the microstructure behavior on the fracture surface of pure and hybrid fiber-reinforced cementitious composites. The fracture surface of the composite was reinforced only with the RPBC and EF displayed in Figure 8.3a and b. Figures 8.4a to c show the SEM photographs of the combination of RPBC and EF.

The fiber distribution in the RPBC-EF composite was uniform because RPBC and EF exhibit a similar morphology, resulting in homogeneous fiber dispersion in the composites. The SEM photographs of RPBC-EF composites showed excellent bonding between the hybrid fiber and the cementitious matrix, which enhanced the composite's mechanical properties (see Figure 8.4b). The short and highly fibrillated RPBC could fill the space between EFs and improve the bonding between the fiber and the matrix, reducing the composite's porosity reinforced with only EF (see Figures 8.1a and 8.1b). Subsequently, the flexural strength of hybrid fiber-reinforced cement composites was higher than that of composites reinforced with individual fibers (see Figure 8.2a). The EF was mostly pulled out, while the RPBC was broken and stuck in the matrix (see Figure 8.4b). Therefore, EF could absorb energy better than RPBC, resulting in an increase in the fracture toughness of the hybrid fiber composite compared to the only RPBC-reinforced composite.

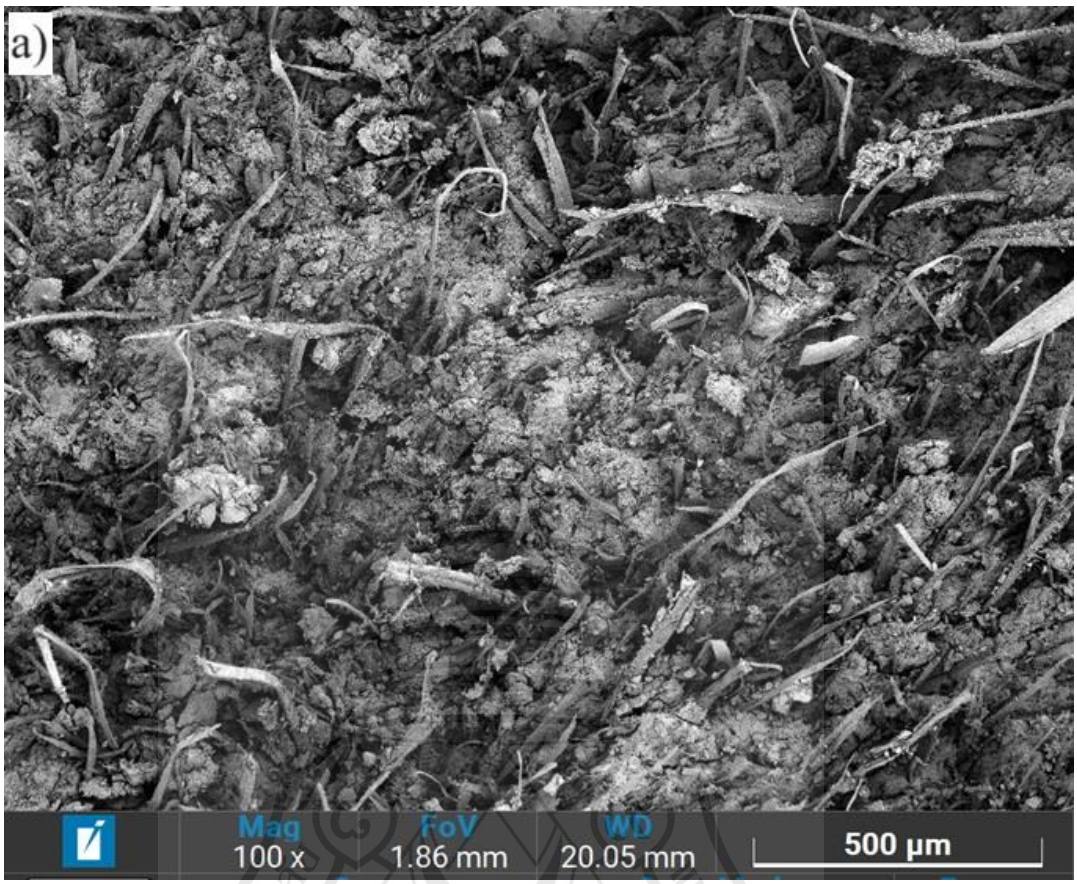

Figure 8.3 SEM photographs of pure fiber reinforced cement composite: a) RPBC8% and EF0% and b) RPBC0% and EF8%

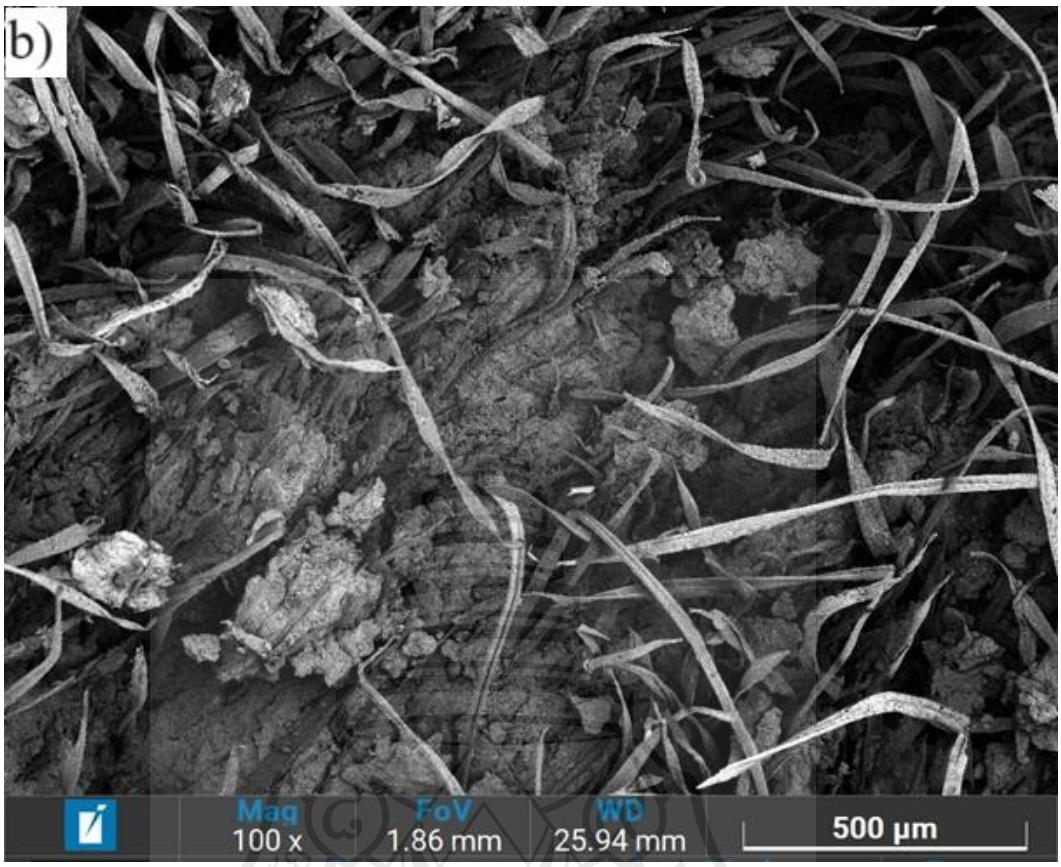

Figure 8.3 (continued)

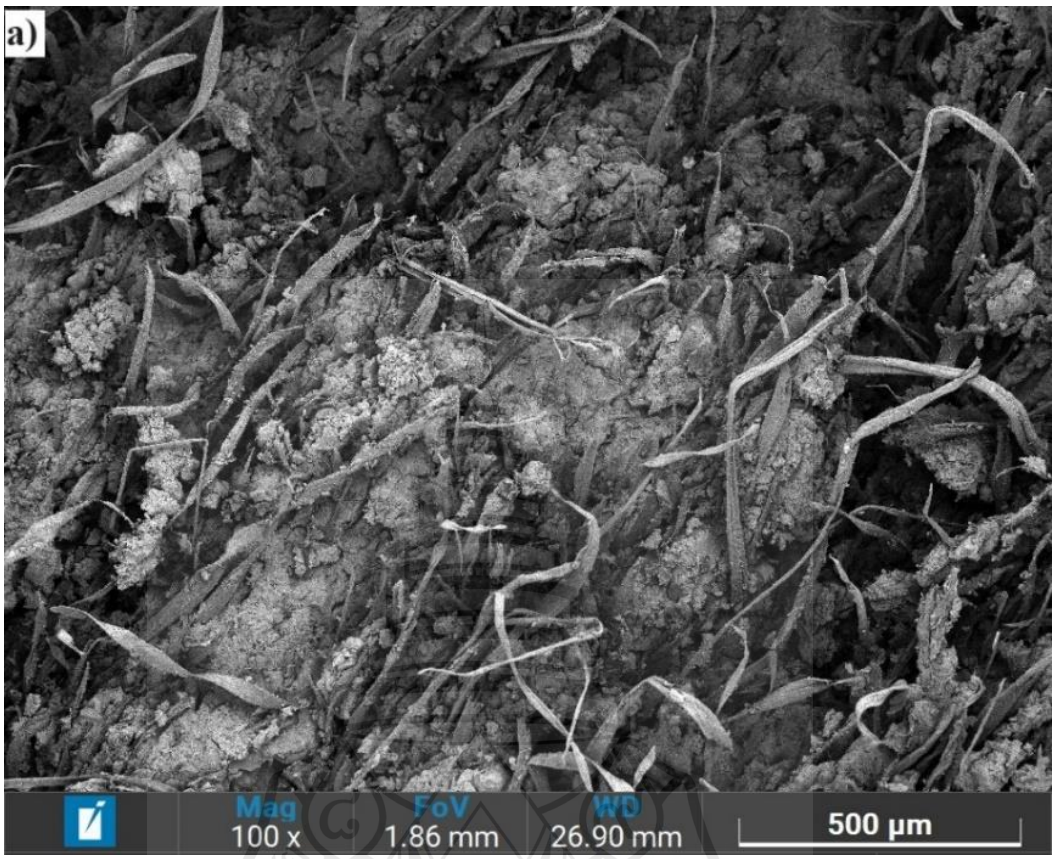

Figure 8.4 SEM photographs of hybrid fiber cement composites: a) RPBC6EF2C, b) RPBC4EF4C, and c) RPBC2EF6C

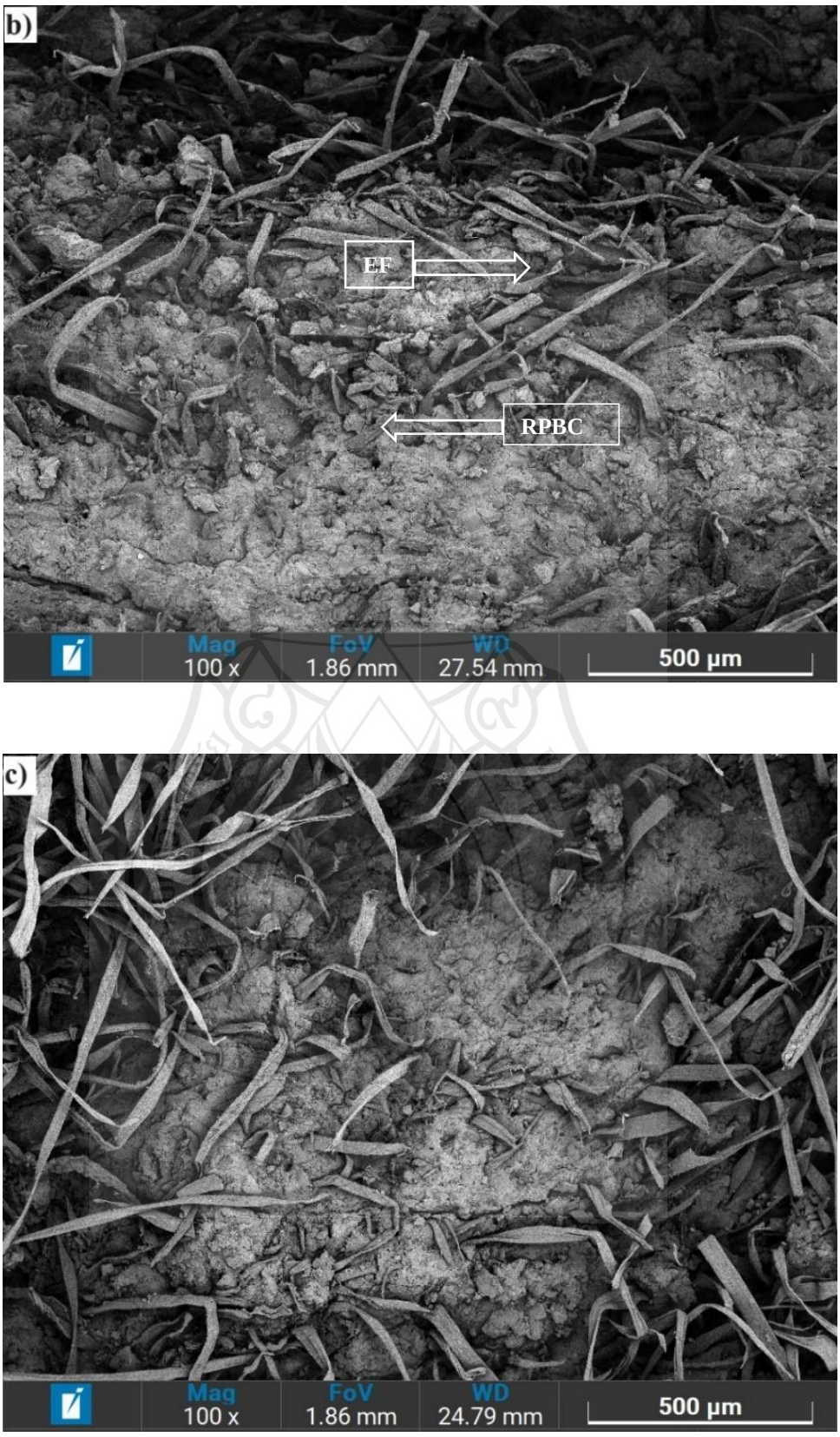

Figure 8.4 (continued)

8.4 Conclusions

This chapter demonstrated the difference in properties of cementitious composites reinforced with recycled pulp mixed with virgin cellulose fiber. The obtained experiment results allow for the following conclusions:

1. The composite reinforced with mixed RPBC and EF significantly improved the properties, particularly flexural strength and fracture toughness, compared to the individual fiber composite.

2. With the fraction 1:1 of RPBC and EF, the composite's flexural strength and fracture toughness increased by 72% and 370%, respectively, compared to only the RPBC-reinforced composite.

CHAPTER 9

ECONOMIC AND SUSTAINABLILTY ASSESSMENT OF THE PRODUCT

9.1 Introduction

Previous chapters have established the technological feasibility of utilizing RPBC as a reinforcement in cementitious composites. The findings indicate that the composite reinforced with 14 wt% RPBC achieved a flexural strength of 12 MPa and a fracture toughness of 1.6 kJ/m^2. When RPBC and virgin cellulose pulp (EF) were mixed in a 1:1 ratio, with a fiber content of 8 wt%, the resulting flexural strength was around 11 MPa and the fracture toughness was 1.93 kJ/m^2. These values meet the grade II standards specified in ASTM C 1186-02 (2002).

A cost-benefit analysis was undertaken to elucidate the economic viability. This chapter primarily examined the economic analysis of producing cementitious composites reinforced with RPBC, comparing it to the use of virgin cellulose pulp and hybrid fiber. The cost-benefit analysis of a product typically encompasses several factors such as material cost, equipment and tool cost, labor cost, overhead and utility cost, quality control, testing, and so on (Nas, 1996). Assuming that the cellulose fiber-reinforced cementitious composites were made using the same method, it was presumed that the cost of each manufacturing stage would be similar, except for the cost of materials. Hence, this analysis specifically examined the cost of materials for RPBC, virgin cellulose pulp, and the combination of both fibers.

Furthermore, the sustainability of utilizing RPBC was assessed by considering environmental effect indicators like as carton footprint and energy conservation.

9.2 Cost-Benefit Analysist

Cost-benefit analysis is a thorough approach for assessing the economic feasibility of a project or decision. It offers crucial information that aids in making efficient choices (Nas, 1996). The analysis is conducted based on the capital cost and operational cost. The cost encompasses the expenses for supplies, equipment, labor, overhead, and quality control. This study primarily assessed the materials expenditure for fiber cement products, given they were manufactured using the same procedure and incurred similar costs.

Table 9.1 displays the current costs of materials ingredients and significant information for fiber cement composite products based on prior studies. The fiber cement board has dimensions of 2.4 m x 1.2 m x 0.01 m. Based on the previous experiment, the bulk density of the board was approximately 1.45 g/cm^3 (1,450 kg/m^3). Consequently, we have achieved a fiber cement board that weighs about 42 kg per sheet. The estimation of materials cost was based on the weight of a fiber cement sheet and the weight fraction of ingredients and fiber contents.

Table 9.2, 9.3, 9.4, and 9.5 show the calculated cost for cementitious composites reinforced with 8 wt% RPBC, 14 wt% RPBC, 8 wt% EF, and mixed of 4 wt% RPBC and 4 wt% EF. The cementitious matrix consisted of OPC and ground silica sand with a ratio of 1:1. The total cost for 8 and 14 wt% RPBCC was 165.69 and 206.11 THB per sheet, respectively. On other hand, the materials cost for hybrid fiber and virgin pulp contained composites was about 186.63 and 207.02 THB per sheet, respectively. Figure 9.1 presents a comparison of the materials cost for 4 types of fiber-reinforced cement composites. The graph shows that the cost of 8wt% RPBC-reinforced composites was lower than that of virgin pulp reinforced product by 20%. When RPBC was mixed with virgin cellulose fiber in a ratio of 1:1, the materials cost was lower than that of pure virgin cellulose fiber by about 10 %. The result shows that considering to the economic calculation, the utilization of recycled pulp for the fiber-reinforced cement product economically feasible.

Table 9.1 Current prices of some materials and information for fiber cement board production

Item	Descriptions	Units	Current price (THB) per unit	References
1	Ordinal Portland cement	1 bag (50kg)	175	SCG Home (2024)
2	Ground silica sand (#200)	1 bag (25 kg)	45	Thaiwatsadu (2024)
3	Recycled pulp from beverage cartons	1 tonne	18,700	Fiber Pattana (2024)
4	Virgin cellulose pulp (EF)	1 tonne	31,000	Morris (2024)
5	Water tape	1 m^3	36	
6	Fiber cement board dimension	m	2.4 x 1.2 x 0.01	-
7	Density of fiber cement board	kg/m^3	1,450	-
8	Water-to-cement ratio		0.6	-

Table 9.2 Materials cost of RPBC cement board with 8 wt% fiber content (8RPBCC)

Item description	Unit	Mass fraction (wt%)	Quantity (per Sheet)	Unit Cost (THB)	Total Cost (THB)
Cement	kg	46	19.32	3.50	67.62
Ground silica sand	kg	46	19.32	1.80	34.78
RPBC	kg	8	3.36	18.70	62.83
Water	litters		11.60	0.04	0.46
			Total of materials cost per sheet:		**165.69**

Table 9.3 Materials cost of RPBC-reinforced cement composite with 14 wt% fiber content (14RPBCC)

Item description	Unit	Mass fraction (wt%)	Quantity (per Sheet)	Unit Cost (THB)	Total Cost (THB)
Cement	kg	43	18.06	3.50	63.21
Ground silica sand	kg	43	18.06	1.80	32.51
RPBC	kg	14	5.88	18.70	109.96
Water	litters		10.836	0.04	0.34
			Total of materials cost:		**206.11**

Table 9.4 Materials cost of EF-reinforced cement composite with 8 wt% fiber content (8EFC)

Item description	Unit	Mass fraction (wt%)	Quantity (per Sheet)	Unit Cost (THB)	Total Cost (THB)
Cement	kg	46	19.32	3.50	67.62
Ground silica sand	kg	46	19.32	1.80	34.81
Eucalyptus fiber	kg	8	3.36	31.00	104.16
Water	litters		11.6	0.04	0.46
			Total of materials cost:		**207.02**

Table 9.5 Materials cost of hybrid fiber-reinforced cement composite with 4 wt% of RPBC and 4 wt% of EF fiber content (RPBC4EF4C)

Item description	Unit	Mass fraction (wt%)	Quantity (per Sheet)	Unit Cost (THB)	Total Cost (THB)
Cement	kg	46	19.32	3.50	67.62
Ground silica sand	kg	46	19.32	1.80	34.84
RPBC	kg	4	1.68	18.70	31.42
Eucalyptus fiber	kg	4	1.68	31.00	52.08
Water	litters		11.60	0.04	0.46
			Total of materials cost:		**186.63**

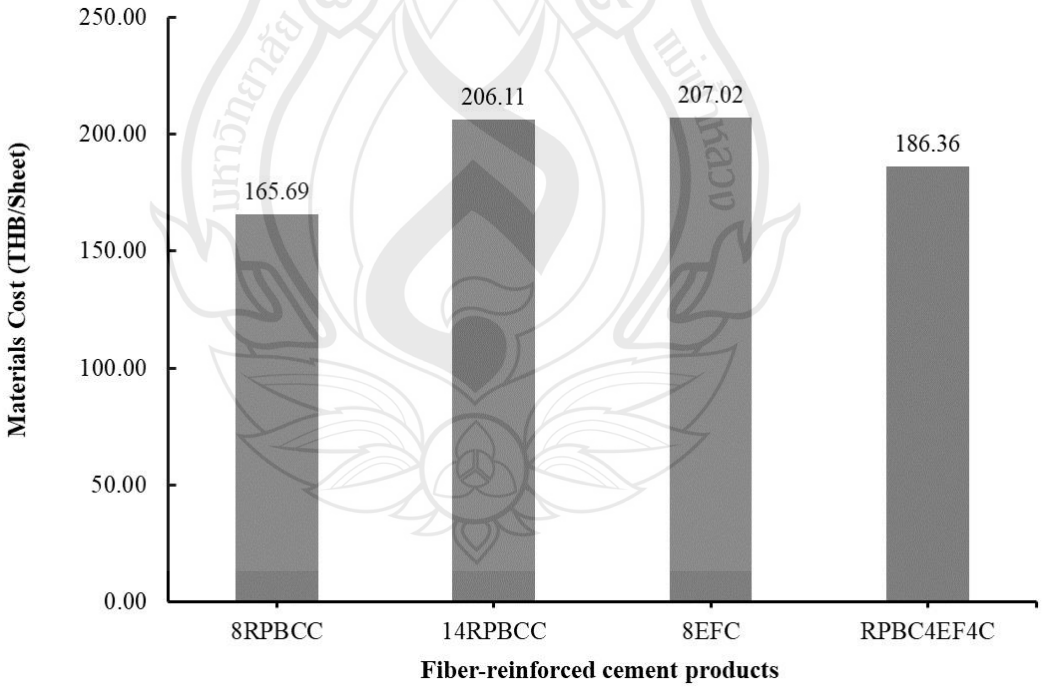

Figure 9.1 Comparison of materials cost for RPBC, virgin pulp and hybrid fiber reinforced cementitious composites

9.3 Sustainability

Sustainable development refers to a form of development that fulfills the requirements of the current generation while also safeguarding the capacity of future generations to fulfill their own demands (WCED, 1987). Presently, 50% of carton trash is either deposited in landfills or subjected to incineration, as reported by the European Paper Recycling Council in 2020. Due to increasing worries regarding the environmental consequences of traditional landfilling or incineration, several recycling techniques have been devised to repurpose recycled pulp derived from beverage cartons. Utilizing RPBC in cementitious composites is an effort to mitigate environmental effect and promote a circular economic strategy.

The utilization of recycled pulp from beverage cartons in cement composite as a repurposing method not only employs waste resources for the creation of new products, but also conserves energy and minimizes the environmental consequences of deforestation. According to Gorte and Sheikh (2010), deforestation results in the annual release of around 5.9 gigatons of CO_2 (carbon dioxide) throughout the 1990s. This accounted for around 17% of the total global greenhouse gas emissions. Furthermore, in the process of producing wood pulp, the yield of pulp typically falls within the range of 40-45% of the weight of dry wood when using the kraft pulping method (Bajpai, 2018). The energy consumption for the kraft pulping process is estimated to be between 500 and 700 kilowatt-hours per tonnes of pulp, according to Bajpai (2018). The authors also proposed that mechanical recycling is a cost-effective recycling technology that requires much less energy compared to alternative methods such as chemical recycling and pyrolysis.

However, in contrast, if the forest is preserved, just one hectare of tropical forest has the capacity to sequester approximately 25-30 metric tons of CO_2 annually. According to Raihan (2019), a temperate forest has the capacity to absorb and store approximately 10-20 tons of carbon dioxide per year per hectare.

9.4 Conclusions and Recommendations

The objective of this research was to identify suitable materials and methods for creating an environmentally friendly building material by utilizing recycled pulp from beverage containers. The experimental programs involved conducting a series of research studies by creating fiber-reinforced cement specimens simultaneously varying important parameters. An assessment was conducted on the characteristics of the specimens. Based on the acquired findings, the following conclusions can be drawn:

1. The dry RPBC, intended for use as a reinforcing fiber in cementitious composites, needed to be mechanically treated in order to disintegrate and fibrillate. The fibrillation process is contingent upon the duration of treatment. Using a fruit blender, the fibrillation of RPBC was due in 60, 140, 200, 320, and 460 seconds, yielding freeness of 650, 600, 550, 500, and 400 mL CSF, respectively.

2. The level of fibrillation of RPBC has a significant impact on the characteristics of the composites. The bulk density of RPBC composites had a modest rise of 2.2% as the freeness fell from 650 mL CSF to 400 mL CSF. Additionally, the porosity and water absorption of the composites reduced by 5.7% and 8% respectively. The flexural strength of RPBC composites rose up to a freeness level of 550 mL CSF, after which it steadily decreased. The composites reinforced with 550 mL CSF RPBC exhibited the highest flexural strength (11.2 MPa) among the different freeness levels. This can be attributed to the optimal balance between fiber strength and fibrillation achieved at this particular freeness level. Nevertheless, the fracture toughness was average.

3. The findings in Chapter 6 demonstrated that the application of compaction pressure had an impact on the characteristics of EF-reinforced cementitious composites. When the compaction pressure increased from 1 to 7 MPa, the bulk density of the specimen increased by 2.5%. Additionally, the porosity reduced by 2.73% and the water absorption decreased by 56%. These changes were attributed to the effective compaction of both the fiber and the matrix. The flexural strength and fracture toughness of the material achieved their highest values, 8.44 MPa and 2.5 kJ/m^2 respectively, when the pressure was 5 MPa. The flexural strength decreased as the

compaction pressure increased due to fiber failure and a lower water-to-cement ratio. The impact of compaction pressure on the characteristics of fiber-reinforced cement composite in this study was not comprehensively assessed due to the use of only one type of fiber (EF).

4. The properties of fiber-reinforced cementitious composites are significantly influenced by the characteristics of the fibers. The composites reinforced with RPBC exhibited a greater bulk density compared to those reinforced with EF and BF, particularly at increasing fiber content. Concurrently, the RPBC composites demonstrated reduced porosity and water absorption compared to the EF and BF composites. The explanation for this was the effective compaction of the RPBC, which had a significant amount of short fibers and a higher degree of fibrillation compared to EF and BF. Unlike the physical properties, the composites exhibited distinct variations in mechanical properties. The flexural strength of the RPBC composite exhibited a consistent increase as the fiber content rose. However, the flexural strength of the EF and BF achieved its highest value at the 8wt% fiber content. The inclusion is related to the fibrillated RPBC, which leads to enhanced bonding between the fiber and matrix. However, the fracture toughness of composites reinforced with EF exhibited a higher value compared to those reinforced with BF and RPBC. This was caused by fiber characteristic such as fiber length, fiber cross-section form, aspect ratio, fiber strength of RPBC, BF, and EF.

5. By mixing RPBC with virgin cellulose fiber, the fracture toughness of the composites was improved significantly. The optimal ratio was 1:1. The fracture toughness of the hybrid fiber composite exhibited a significant increase of 370% when compared to the pure RPBC specimen, while the flexural strength was increased by 72%.

6. The materials cost analysis showed that using 14wt% RPBC was 8% more cost-effective than using 8wt% virgin cellulose pulp. By incorporating the RPBC with virgin cellulose fiber, the cost of materials decreased by 10% in comparison to using pure virgin cellulose fiber alone.

7. The RPBC has the potential to partially replace virgin cellulose pulp in the manufacturing of fiber-reinforced cementitious composites. The RPBC has the potential to generate cost-effective and eco-friendly construction materials.

8. It is advised that the subsequent research investigation should ascertain the appropriate correlation between fiber content and compaction pressure. The optimal compaction pressure is influenced by both the fiber content and the kind of fiber. The investigation should also determine the approach to enhancing the flexural strength by altering the matrix components or using other elements like wollastonite. Thoroughly examining the durability of the composite is necessary to verify that the product meets the basic standards for its actual application.

REFERENCES

REFERENCES

Abreu, M. (2000). *Recycling the Fibres on Tetra Pak Cartons*. Tetra Pak Cananda Inc.

Achour, A., Ghomar, F., & Belayachi, N. (2017). Properties of cementitious mortars reinforced with natural fibers. *Journal of Adhesion Science and Technology*, 1-25. https://doi.org/10.1080/01694243.2017.1290572.

Akers, S. A. S. , & Garrett, G. G. (1986). The influence of processing parameters on the strength and toughness of asbestos cement composites. *The International Journal of Cement Composites and Lightweight Concrete*, *8*(2), 93-100.

Almeida, A. E. F. S., Tonoli, G. H. D., Santos, S. F., & Savastano, Jr. H. (2013). Improved durability of vegetable fiber reinforced cement composite subject to accelerated carbonation at early age. *Cement & Concrete Composites*, *42*, 49-58. https://doi.org/10.1016/j.cemconcomp.2013.05.001.

Amenu, B. T. (2017). Review on impact of eucalyptus plantation on the soil. *International Journal of Scientific Research in Civil Engineering*, *2*(2).

Amiandamhen, S. O., & Osadolor, S. O. (2020). Recycled waste paper–cement composite panels reinforced with kenaf fibres: Durability and mechanical properties. *Journal of Material Cycles and Waste Management*, *22*, 1492-1500. https://doi.org/10.1007/s10163-020-01041-2.

Ardanuy, M., Claramunt, J., & Filho, R. D. T. (2015). Cellulosic fiber reinforced cement-based composites: A review of recent research. *Construction and Building Materials*, *79*, 115-128. https://doi.org/10.1016/j.conbuildmat.2015.01.035.

Ashaari, Z., Salim, S., Halis, R., Yusof, M. N. M., & Sahri, M. H. (2010). Characteristics of pulp produced from refiner mechanical pulping of tropical bamboo (*Gigantochloa scortechinii*). *Pertanika Journal of Tropical Agriculture Science*, *33*(2), 251-258.

ASTM C 1185–08. (1999). *Standard test methods for sampling and testing non-asbestos fiber-cement flat sheet, roofing and siding shingles, and clapboards*. American Society for Testing and Materials.

ASTM C 20–00. (2000). *Standard test methods for apparent porosity, water absorption, apparent specific gravity, and bulk density of burned refractory brick and shapes by boiling water*. American Society for Testing and Materials.

ASTM C1186-08. (2002). *Standard specification for flat non-asbestos fiber-cement sheets*. American Society for Testing and Materials.

ASTM D 2320-98. (2003). *Standard test method for density (relative density) of solid pitch (pycnometer method)*. American Society for Testing and Materials.

ASTM D 4442-92. (2003). *Standard test methods for direct moisture content measurement of wood and wood-base materials.* American Society for Test and Materials.

Badogiannis, E., Kakali, G., Dimopoulou, G., Chaniotakis, E., & Tsivilis, S. (2005). Metakaolin as a main cement constituent: Exploitation of poor Greek kaolins. *Cement & Concrete Composites*, *27*, 197-203.

Bajpai, P. (2018). Pulping fundamentals. *Biermann's handbook of pulp and paper* (3rd ed.). Elesevier. https://doi.org/10.1016/C2017-0-00530-X.

Ban, Y., Zhi, W., Fei, M., Liu, W., Yu, D., Fu, T., . . . (2020). Preparation and performance of cement mortar reinforced by modified bamboo fibers, *Polymers, 12*(11), 2650. https://doi.org/10.3390/polum12112650.

Bassani, C., Cavalli, R. M., Cavalcante, F., Cuamo, V., Palombo, A., Pascucci, S., . . . (2007). Deterioration status of asbestos-cements roofing sheets assessed by analyzing hyperspectral data. *Remote Sensing of Environment*, *109*, 361-378.

Basu, P. (2018). *Analytical techniques in biomass gasification, pyrolysis and torrefaction* (pp. 479-495). Academic Press.

Bentchikou, M., Guidoum, A., Scrivener, K., Silhadi, K., & Hanini, S. (2012). Effect of recycled cellulose fibres on the properties of lightweight cement composite matrix. *Construction and Building Materials*, *34*, 451-456. http://dx.doi.org/10.1016/j.conbuildmat.2012.02.097.

Bentur, A. & Mindess, S. (2005). *Fiber reinforced cementitious composites*. Elsevier.

Biagiotti, J., Puglia, D., & Kenny, J. M. (2004). A review on natural fibre-based composites - Part I. *Journal of Natural Fibers*, 37-68. https://doi,org/ 10.1300/J395v01n02_04.

Blazey, M. A., Chen, G. C., Edmonds, C. B., & Grimsley, S. A. (n.d.), *Eliminating a common OCC Stickies problem*. Ciba Specialty Chemicals.

Bredy, P., Chabannet, M., & Pera, J. (1988). Microstructure and Porosity of metakaolin blended cements. *MRS Online Proceedings Library*, *136*, 275–280.

Campbell, M. D., & Coutts, R. S. P. (1980). Wood fiber-reinforced cement composites, *Journal of Materials Science*, *15*, 1962-1970.

Chaowana, P. (2013). Bamboo: An alternative raw material for wood and wood-based composites. *Journal of Materials Science Research*, *2*(2), 90-102.

Chen, Y., Wan, J., Zhanga, X., Maa, Y., & Wang, Y. (2012). Effect of beating on recycled properties of unbleached eucalyptus cellulose fiber. *Carbohydrate Polymers*, *87*, 730-736.

Courard, L., Darimont, A., Schouterden, M., Ferauche, F., Willem, X., & Degeimbre, R. (2003). Durability of mortars modified with metakaolin. *Cement and Concrete Research*, *33*, 1473–1479.

Coutts, R. S. P., & Campbell, M. D. (1979). Coupling agents in wood fiber reinforced cement composites. *Composite*, 228-232.

Coutts, R. S. P. & Warden, P. G. (1985). Air-cured, wood pulp, fibre cement composites. *Journal of Materials Science Letters*, *4*, 117-119.

Coutts, R. S. P., & Warden, P. G. (1990). Effect of compaction on the properties of air-cured wood fibre reinforced cement. *Cement & Concrete Composites, 12*, 151-165.

Coutts, R. S. P. (1987). Eucalyptus wood fibre-reinforced cement. *Journal of Materials Science Letters*, *5*, 955-957.

Coutts, R. S. P., & Kightly, P. (1982). Microstructure of autoclaved refined wood-fiber cement mortars. *Journal of Material Science*, *17*, 1801-1806.

Coutts, R. S. P., & Michell, A. J. (1983). Wood pulp fiber-cement composites. *Journal of Applied Polymer Science*, *37*, 829-844.

Coutts, R. S. P., & Ni, Y. (1995). Autoclaved bamboo pulp fiber reinforced cement. *Cement and Concrete Composite*, *17*, 99-106.

Coutts, R. S. P., & Ridikas, V. (1982). Refined wood fiber-cement product, *J. Appita*, *35*(5), 395-400.

Coutts, R. S. P. (1983). Flax fiber as reinforcement in cement mortars. *The International Journal of Cement Composites and Lightweight Concrete*, *5*(4).

Coutts, R. S. P. (1984). Autoclaved beaten wood fiber-reinforced cement composites. *Composites*, *15*, 139-143.

Coutts, R. S. P. (1984). Autoclaved beaten wood fibre - reinforced cement composites. *Composites, 15*, 139-143.

Coutts, R. S. P. (1987). Air-cured wood pulp fiber cement mortars. *Composites, 18*(4), 325-328.

Coutts, R. S. P. (1989). Wastepaper fibres in cement products. *The International Journal of Cement Composites and Lightweight Concrete, 11*(3).

Coutts, R. S. P. (2005). A review of Australian research into natural fiber cement composites. *Cement and Concrete Composites, 27*, 518-526.

Coutts, R. S. P., Ni, Y., & Tobias, B. C. (1994). Air-cured bamboo pulp reinforced cement. *Journal of Materials Science Letters, 13*, 283-285.

de Correia, C. V., Santos, S. F., Marmol, G., Aprigio, A., Curvelo, S., & Savastano, Jr. H. (2014). Potential of Bamboo organosoly pulp as a reinforcing element in fiber-cement materials. *Construction and Building Materials, 72*, 65-71.

de Gutirrez, R. M., Dıaz, L. N., & Delvasto, S. (2005). Effect of pozzolans on the performance of fiber-reinforced mortars. *Cement & Concrete Composites, 27*, 593–598.

Delvasto, S., Naaman, A. E., & Throne, J. L. (1986). Effect of pressure after casting on high strength fiber reinforced mortar. *International Journal of Cement Composites and Lightweight Concrete, 8*(3), 181- 190.

Deshpande, A. P., Rao, M. B., & Rao, C. L. (2000). Extraction of bamboo fibers and their use as reinforcement in polymeric composites. *Journal of Applied Polymer Science, 76*(6), 83-92.

Eunomia Research & Consulting Ltd. (2020). *Recycling of multilayer composite packaging: the beverage carton*. Zero Waste Europe. https://zerowasteeurope.eu/wp-content/uploads/2020/12/zero_waste_europe_report_-beverage-carton_en.pdf

European Paper Recycling Council (EPRC). (2020). *Monitoring Report 2020, Brussels*. https://www.paperforrecycling.eu

Fardim, P., & Durán, N. (2003). Modification of fibre surfaces during pulping and refining as analysed by SEM, XPS and ToF-SIMS. *Colloids and Surfaces A, 223*, 263-276. https://doi.org/10.1016/S0927-7757(03)00149-3.

Faruk, O., Bledzki, A. K., Fink, H. P., & Sain, M. (2012). Biocomposites reinforced with natural fibers: 2000-2010. *Progress in Polymer Science, 37*, 1552-1596.

Fiber Pattana. (2024). *Fiber pattana Co. ltd*. https://www.fiberpattana.com

Filho, R. D. T., Ghavami, K., England, G. L., & Scrivener, K. (2003). Development of vegetable fibre–mortar composites of improved durability. *Cement & Concrete Composites, 25*, 185-196.

Gharehkhani, S., Sadeghinezhad, E., Kazi, S. N., Yarmanda, H., Badarudin, A., Safaeib, M.R., . . . (2015). Basic effects of pulp refining on fiber properties - A review. *Carbohydrate Polymers, 115*, 785-803.

Gorte, R. W., & Sheikh, P. A. (2010). Deforestation and Climate Change. *Congressional Research Service*. https://www.crs.gov

Habibi, M., Ruiz, E., Lebrun, G., & Laperriere, L. (2017). Effect of surface density and fiber length on the porosity and permeability of nonwoven flax reinforcement. *Textile Research Journal, 0*(00), 1-12. https://doi.org/ 10.1177/0040517517708542

He, Z., Shen, A. A., Lyu, Z., Li, Y., Wu, H., & Wang, W. (2020). Effect of wollastonite microfibers as cement replacement on the properties of cementitious composites: A review. *Construction and Building Materials, 261*, 1-13.

Hospodarova, V., Stevulova, N., Briancin, J., & Kostelanska, K. (2018). Investigation of waste paper cellulosic fibers utilization into cement based building materials. *Buildings, 8*(43), 1-12.

Huang, J. K., & Young, W. B. (2019). The mechanical, hygral, and interfacial strength of continuous bamboo fiber reinforced epoxy composites. *Composites Part B, 166*(6), 272-283. https://doi.org/10.1016/j.compositesb.2018.12.013

Illston, J. M., & Domone, P. L. J. (2001). *Construction materials, their nature and behaviors* (pp. 409-410). SPON Press.

ISO 8336:2017(E). (2017). *Fiber-cement flat sheets - Product specification and test methods.* International Standard Organization.

Jacob, P., Kashyap, P., Suwannapan, T., & Visvanathan, C. (2021). Status of beverage carton wastemanagement in Thailand: Challenges and opportunities. *Environment Quel Management*, 1-12.

Jawaid, M., & Khali, H. P. S. A. (2011). Cellulosic/synthetic fiber reinforced polymer hybrid composites: A review. *Carbohydrate Polymers*, *86*, 1-18.

Kamthai, S., & Puthson, P. (2005). Effect of beating revolution on sweet bamboo (*Dendrocalamus asper* Backer) kraft pulp properties. *CMU Journal*, *4*(2), 137.

Khorami, M., & Ganjian, E. (2011). Comparing flexural behaviour of fiber-cement composites reinforced bagasse: Wheat and Eucalyptus. *Construction and Building Materials*, *25*, 3661-3667.

Khorami, M., Ganjian, E. & Srivastav, A. (2016), Feasibility study on production of fiber cement board using waste kraft pulp in corporation with polypropylene and acrylic fibers. *Materials Today: Proceedings*, *3*, 376-380. https://doi.org/10.1016/j.matpr.2016.01.023

Kim, H., Okubo, K., Fujii, T., & Takemura, K. (2013). Influence of fiber extraction and surface modification on mechanical properties of green composites with bamboo fiber. *Journal of Adhesion Science and Technology*, *27*(12), 1348-1358. https://doi.org/10.1080/01694243.2012.697363

Liese, W., & Koehl, M. (2015). *Bamboo: The plant and its uses*. Springer.

Lu, Z., Su, Z., Song, S. Zhao, Y., Ma, S., & Zhang, M. (2018). Toward high-performance fibrillated cellulose-based air filter via constructing spider-web-like structure with the aid of TBA during freeze-drying process. *Cellulose, 25*(11), 619-629. https://doi.org/10.1007/s10570-017-1561-x

Ma, X. J., Cao, S. L., Lin, L., Luo, X. L., Hu, H. C., . . . (2013). Hydrothermal pretreatment of bamboo and cellulose degradation. *Bioresource Technology, 148*, 408-413.

Marikunte, S., Aldea, C., & Shah, S. P. (1997). Durability of glass fiber reinforced cement composites: Effect of silica fume and metakaolin. *Glass Fiber Reinforced Cement Composites, 5*, 100-108.

Market Research Future. (2021). *Fiber cement market overview.* Want Stats Research and Media Pvt. Ltd.

Mohr, B. J., Biernacki, J. J., & Kurtis, K. E. (2007). Supplementary cementitious materials for mitigating degradation of kraft pulp fiber-cement composites. *Cement and Concrete Research, 37*, 1531-1543.

Morris, H. (2024). *Range of pulp price increases announced by world's producers*. Tissure World Magazine. https://www.tissueworldmagazine.com/world-news/raft-of-pulp-price-increases-announced-by-worlds-pulp-producers/

Mwaikambo, L. Y. (2006). Review of the history, properties, and application of plant fibers. *African Journal of Science and Technology, 7*(2), 120-133.

Nas, T. F. (1996). *Cost-benefit analysis, theory and application*. SEGE Publications.

Nelson, E. B. (2006). *Well cementing*, (pp. 25-235). Elservier.

Nicole, M., & Cai, S. Z. (2021). *Wood handbook: Wood as an engineering material*. Forest Products Laboratory.

Okubo, K., Fujii, T., & Yamamoto, Y. (2004). Development of bamboo-based polymer composites and their mechanical properties. *Composites Part A*: *Applied Science and manufacturing*, *35*, 377-383. https://doi.org/10.1016/j.compositesa.2003.09.017

Oriyomi, M. O., David, A. O., & Khatib, J. (2015). *A review of recycled use of post-consumer waste paper in construction*. *Proceedings of the First International Conference on Bio-based Building Materials, France*, *33*(2), 711-717.

Osorio, L., Trujillo, E., van de Vuure, A. W., & Verpoest, I. (2011). Morphological aspect and mechanical properties of single bamboo fiber and flexural characterization of baboo/expoxy composites. *Journal of Reinforced Plastics and Composites*, *30*(5), 396-408.

Phong, N. T., Fujii, T., Chuong, B., & Okubo, K. (2012). Study on how to effectively extract bamboo fibers from raw bamboo and wastewater treatment. *Journal of Materials Science Research*, *1*(1), 144-155.

Qien S., Wang, H., Zarei, E., & Sheng K. (2015). Effect of hydrothermal pretreatment on the properties of Moso bamboo particles reinforced polyvinyl chloride composite. *Composites Part B*, *82*, 23-29.

Raihan, A., Begum, R. A., Said, M. N. M., & Abdullah, S. M. S. (2019). A review of emission reduction potential and cost saving through forest carbon sequestration. *Asian Journal of Water, Environment and Pollution*, *16*(3), 1-7. https://doi.org/10.3233/AJW190027

Ranachowski, Z., & Schabowicz, K. (2018). *The fabrication, testing and application of fiber cement board*, (pp. 20-25). Cambridge Scholars Publishing.

Rao, K. M. M., & Rao, K. M. (2007). Extraction and tensile properties of natural fibers: Vakka, date and bamboo. *Composite Structure*, *77*, 288-295.

Rashad, A. M. (2013). Metakaolin as cementitious material: History, scours, production and composition –A comprehensive overview. *Construction and Building Materials*, *41*, 303-318.

Robertson, G. L. (2021). Recycling of aseptic beverage cartons: A review. *Recycling*, *6*(20), 1-20. https://doi.org/10.3390/recycling6010020

Sanchez-Echeverri, L. A., Ganjian, E., Medina-Perilla, J. A., Quintana, G. C., Sanchez-Toro, J. H., & Tyrer, M. (2021). Mechanical refining combined with chemical treatment for the processing of Bamboo fibres to produce efficient cement composites. *Construction and Building Materials*, *269*(10), 121-232. https://doi.org/10.1016/j.conbuildmat.2020.121232.

Savastano, Jr. H., & Agopyan, V. (1999). Transition zone studies of vegetable fiber cement paste composites. *Cement and Concrete Composites*, *21*, 49-57.

Savastano, Jr. H., Warden, P. G., & Coutts, R. S. P. (2000). Brazilian waste fibers as reinforcement for cement-based composites. *Cement and Concrete Composites*, *22*, 379-384.

Savastano, Jr. H., Warden, P. G., & Coutts, R. S. P. (2005). Microstructure and mechanical properties of waste. *Cement & Concrete Composites*, *27*, 583-592.

SCG Home. (2024). *Products and services*. https://www.scghome.com/products/

Seethalakshmi, K. K., Jijeesh, C. M., & Balagopalan, M. (2009). Bamboo plantations: An approach to carbon sequestration. *Proceedings of the National Workshop on Global Warming and its Implication for Kerala, Kerala,* (pp 127-133). ResearchGate.

Silva, F. A., Mobasher, B., Soranakom, C., & Filho, R. D. T. (2011). Effect of fiber shape and morphology on interfacial bond and cracking behaviors. *Cement and Concrete Composites*, *33*, 814 - 823.

Smalley, M. (2021). *Recycled pulp prospects - Recycling Today*. https://www.recyclingtoday.com/news/recycled-pulp-projects-pipeline/

Soroushian, P., Shah, Z., & Won, J. P. (1995). Optimization of wastepaper fiber-cement composites. *ACI Materials Journal*, *92*(1), 82-89.

Soroushian, P., Shah, Z., Won, J. P., & Hsu, J. W. (1994). Durability and moisture sensitivity of recycled wastepaper-fiber-cement composites. *Cement & Concrete Composites*, *16*, 115-128.

Sudin, R., & Swamy, N. (2006). Bamboo and wood fibre cement composites for sustainable infrastructure regeneration. *Journal of Materials Science*, *41* (9), 6917–6924. https://doi.org/10.1007/s10853-006-0224-3

TAPPI 494 om-01. (2006). *Tensile properties of paper and paperboard*. Technical Association of the Pulp and Paper Industry.

TAPPI T 205 sp-02. (2006). *Forming handsheets for physical tests of pulp*. Technical Association of the Pulp and Paper Industry.

TAPPI T 227 om-99. (1999). *Freeness of pulp (Canadian standard method)*. Technical Association of the Pulp and Paper Industry.

TAPPI T 231 cm-96. (1996). *Zero-span breaking strength of pulp (dry zero-span tensile)*. Technical Association of the Pulp and Paper Industry.

TAPPI T222 om-02. (2002). *Acid-insoluble lignin in wood and pulp*. Technical Association of the Pulp and Paper Industry.

Teixeira, D. E. (2018). Asbestos-free autoclaved wood fiber-cement sheet from recycled old corrugated containers and kraft pulp of douglas fir: Properties and scanning electron microscopy. *Maderas Ciencia y Tecnologia*, *20*(4), 747-756.

Teixeira, D. E., Castedo-Dorado, F., & Yildiz, S. (2012). Recycled Old Corrugated Container Fibers for Wood-Fiber Cement Sheets. *International Scholarly Research Network*, 1-8. https://doi.org/10.5402/2012/923413

Thaiwatsadu. (2024). *Center for home products and construction materials for Thais*. https://www.thaiwatsadu.com/th/category/

Tichi, A. H., Bazyar, B., Khademieslam, H., Rangavar, H., & Talaeipour, M. (2016). The effect of nano-wollastonite on biological, mechanical, physical, and microstructural properties of the composite made of wood-cement fiber. *Journal of Fundamental and Applied Sciences*, *8*(3S), 1466-1479.

Tiseo, I. (2021). *Statista*. https://www.statista.com/ statistics/1089078/demand-paper-globally-until-2030/

Tonoli, G. H. D., Filho, U. P. R., Savastano, Jr. H., Bras, J., Belgacem, M. N., & Lahr, F. A. R. (2009). Cellulose modified fibres in cement based composites. *Composites: Part A, 40*, 2046–2053.

Tonoli, G. H. D., Fuente, E., Monte, C., Savastano, Jr. H., Lahr, F. A. R., & Blanco, A. (2009). Effect of fibre morphology on flocculation of fibre–cement suspensions. *Cement and Concrete Research*, *39*, 1017-1022.

Tonoli, G. H. D., Joaquin, A. P., Arsene, M. A., Balba, K., & Savastano, Jr. H. (2007). Performance and durability of cement based composites reinforced with refined sisal pulp. *Materials and Manufacturing Processes*, *22*, 149-156.

Tonoli, G. H. D., Santos, S. F., Savastano, Jr. H., Delvasto, S., de Gutierrez, R. M., de Gutiérrez, R. M. and . . . (2011). Effects of natural weathering on microstructure and mineral composition of cementitious roofing tiles reinforced with fique fiber. *Cement & Concrete Composites*, *33*, 225-232.

Tonoli, G. H. D., Santos, S. F., Teixeira, R. S., da-Silva, M. A., Lahr, F. A. R., Silva, F. H. P. & . . . (2013). Effects of eucalyptus pulp refining on the performance and durability of fiber-cement composites. *Journal of Tropical Forest Science*, *25*(3), 400-409.

Uetani, K., & Yano, H. (2011). Nanofibrillation of wood pulp using a high-speed blender. *Biomacromolecules*, *12*, 348–353.

van den Oever, M. J. A., & Bos, H. L. (1998). Critical fiber length and apparent interfacial shear strength of single flax fiber polypropylene composites. *Advanced Composite Letters*, *7*(3), 81-85.

Wai, N. N., Nanko, H., & Murakami, K. (1985). A morphological study on the behavior of bamboo pulp fibers in the beatign process. *Wood Science and Technology*, *19*, 211-222.

Weng, T. L., Lin, W. T., & Cheng, A. (2013). Effect of metakaolin on strength and efflorescence quantity of cement-based composites. *The Scientific World Journal*, 1-11.

World Commission on Environment and Development (WCED). (1987). *Report of the World Commission on Environment and Development: Our Common Future*. https://www.are.admin.ch/are/en/home/media/publications/sustainable-development/brundtland-report.html

Xie, X. L., Zhou, Z., & Yan, Y. (2019). Flexural properties and impact behaviour analysis of bamboo cellulosic fiber filled cement based composites. *Construction and Building Materials*, *220*, 403-414.

Xie, X., Zhou, Z., Jiang, M., Xu, X., Wang, Z., & Hui, D. (2015). Cellulosic fibers from rice straw and bamboo used as reinforcement of cement-based composites for remarkably improving mechanical properties. *Composites Part B*, *78*, 153-161.

APPENDICES

APPENDIX A

DIMENSIONAL MEASUREMENT OF RPBC

1. RPBC with 650 ml CSF freeness

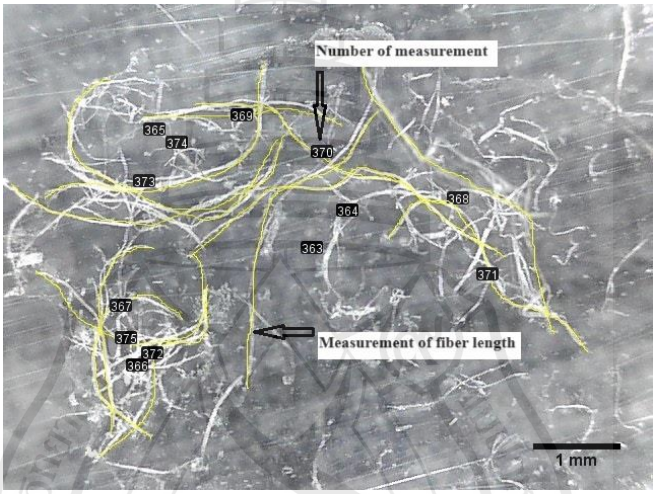

Figure A1 Photograph for length measurement of 650 ml CSF RPBC

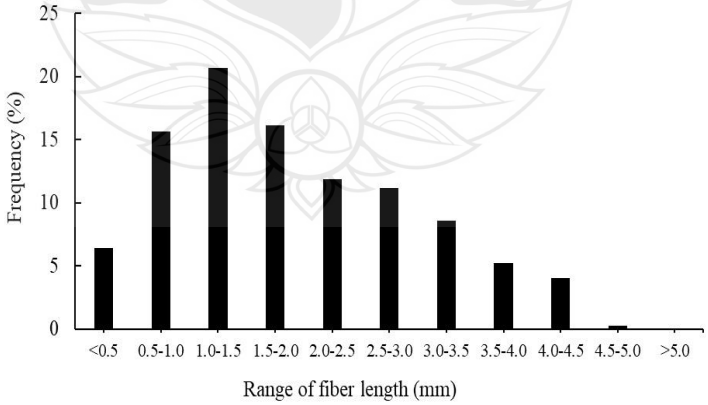

Figure A2 Histogram of length distribution for 650 mL CSF RPBC

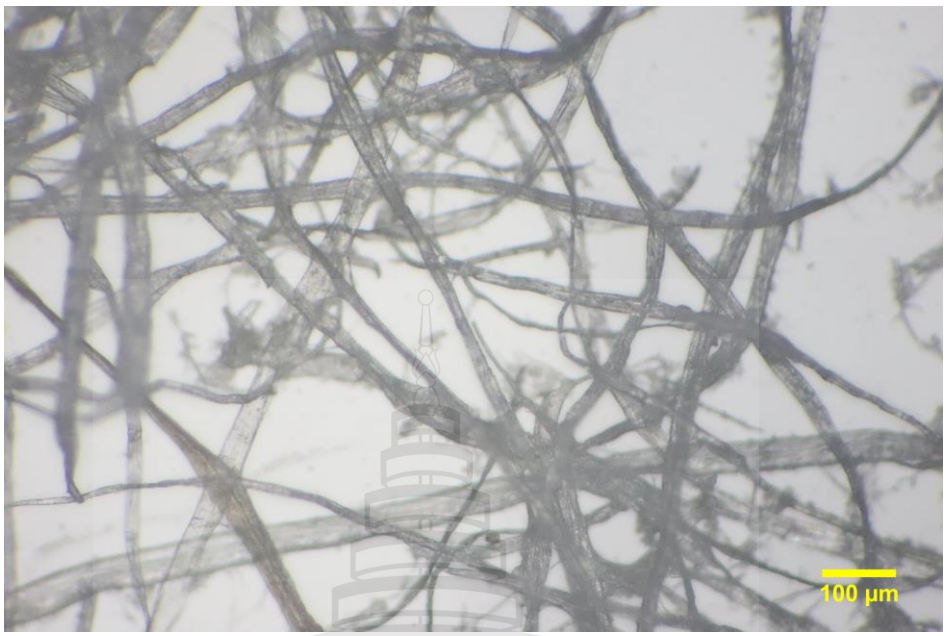

Figure A3 Photograph for width measurement of 650 ml CSF RPBC

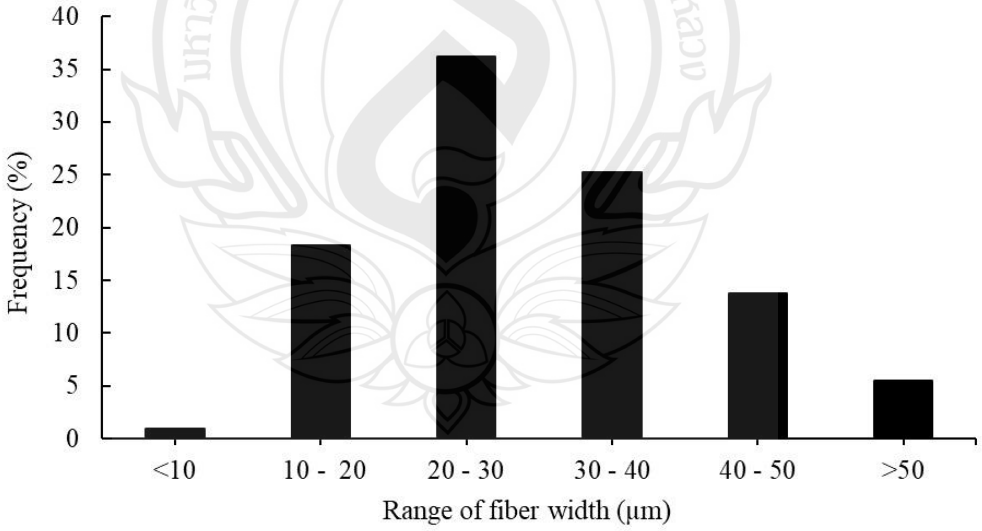

Figure A4 Histogram of width distribution for 650 mL CSF RPBC

2. RPBC with 600 ml CSF freeness

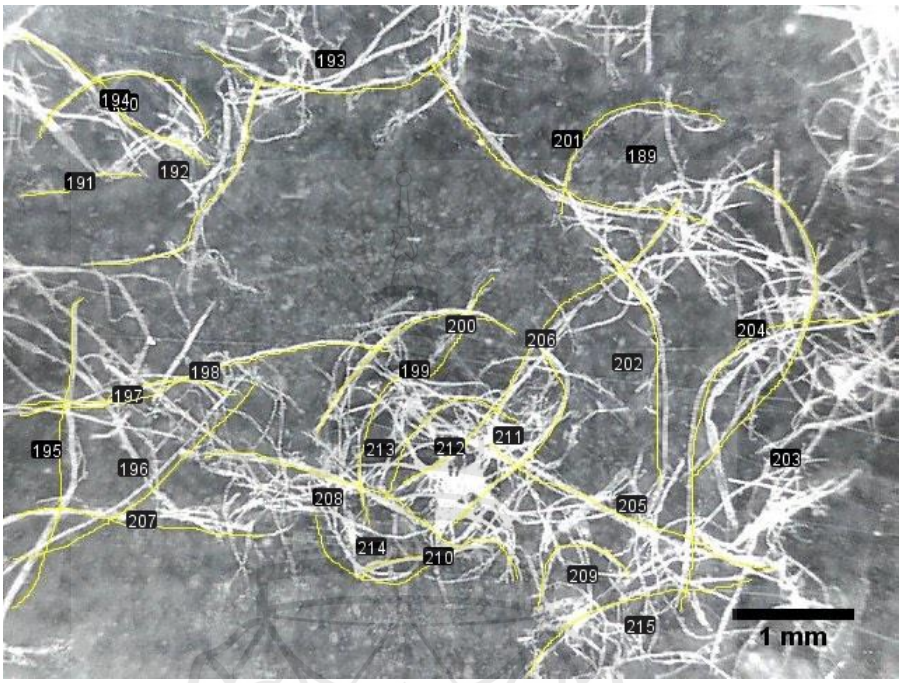

Figure A5 Photograph for length measurement of 600 ml CSF RPBC

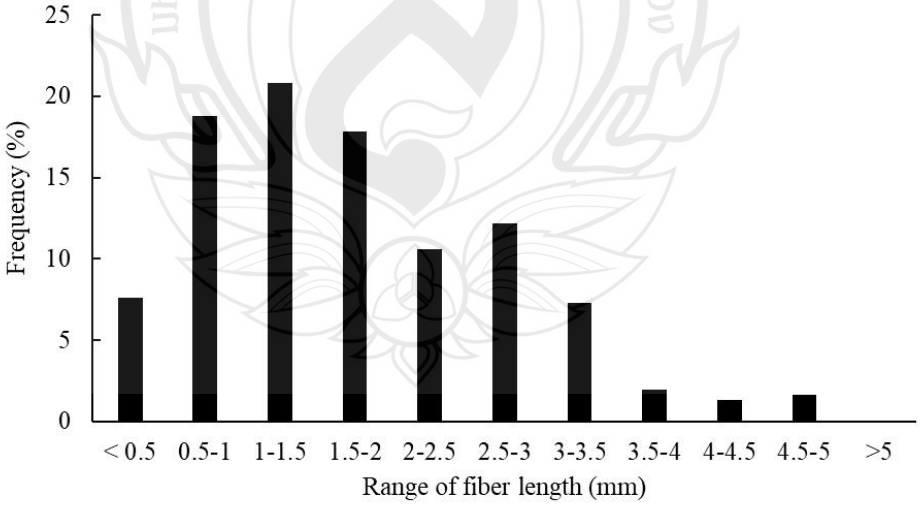

Figure A6 Histogram of length distribution for 650 mL CSF RPBC

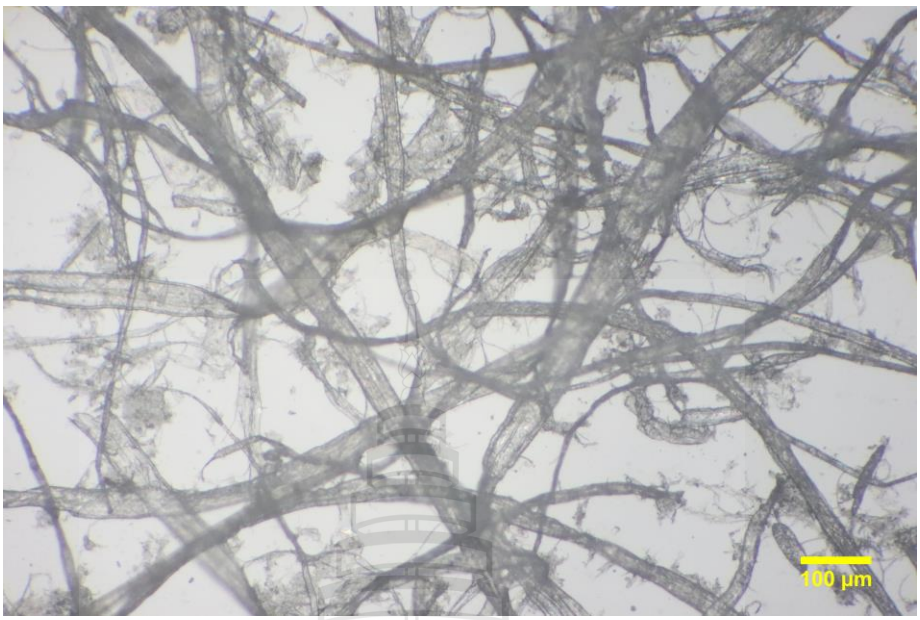

Figure A7 Photograph for width measurement of 600 ml CSF RPBC

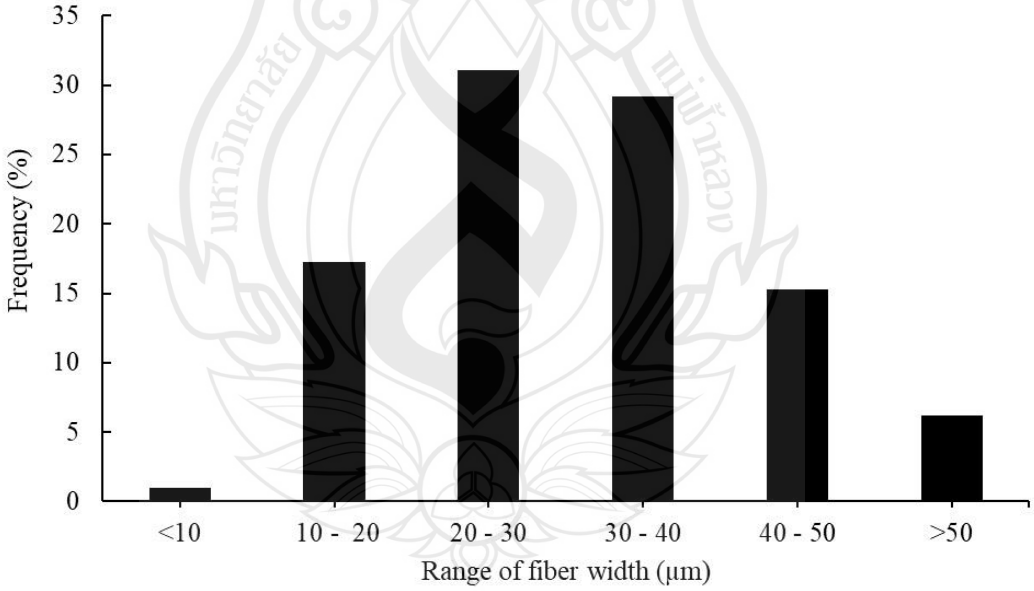

Figure A8 Histogram of width distribution for 600 mL CSF RPBC

3. RPBC with 550 ml CSF freeness

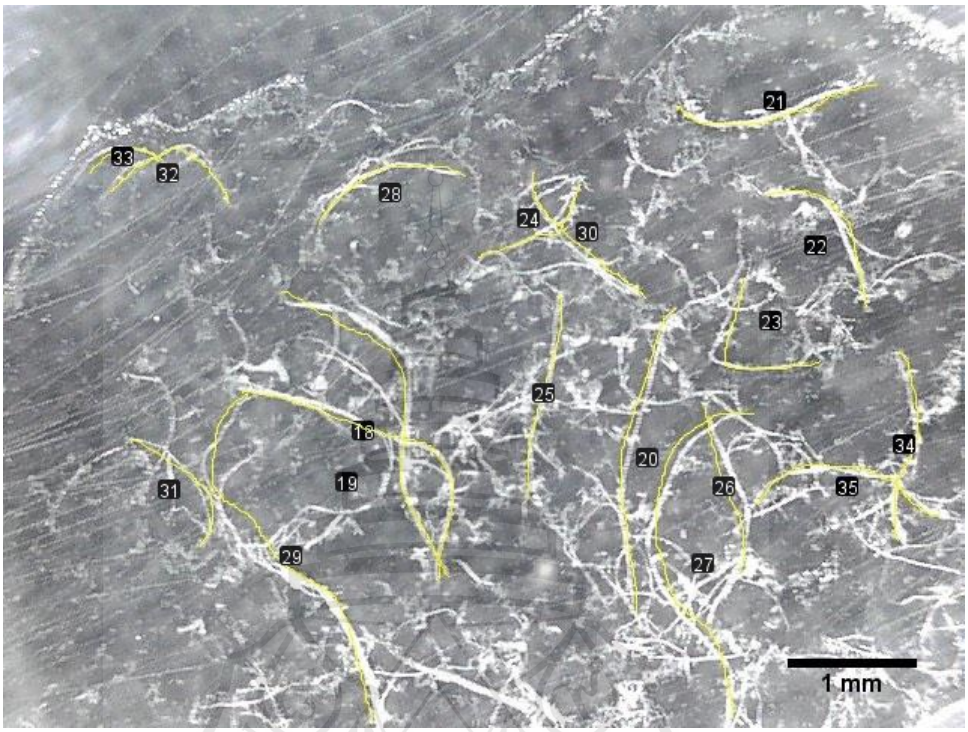

Figure A9 Photograph for length measurement of 550 ml CSF RPBC

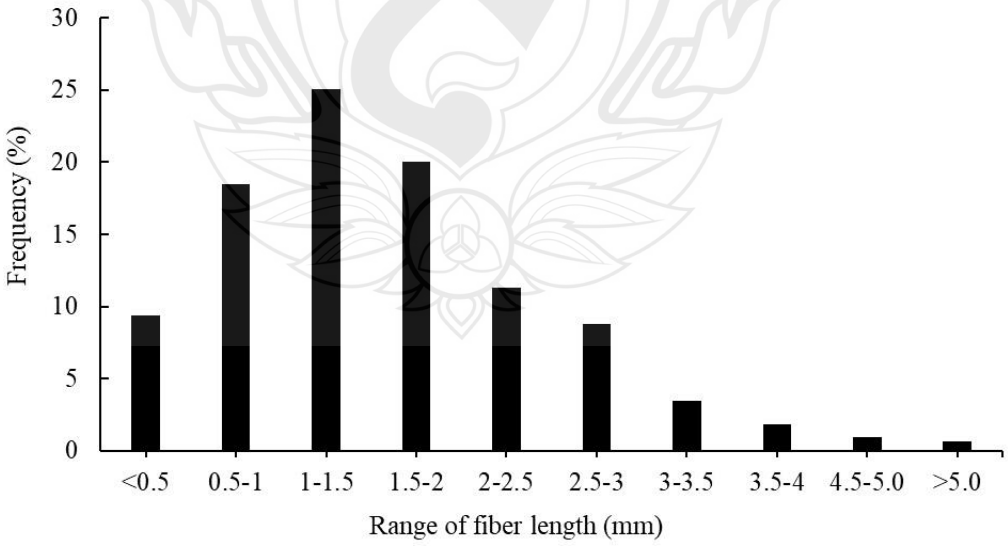

Figure A10 Histogram of length distribution for 550 mL CSF RPBC

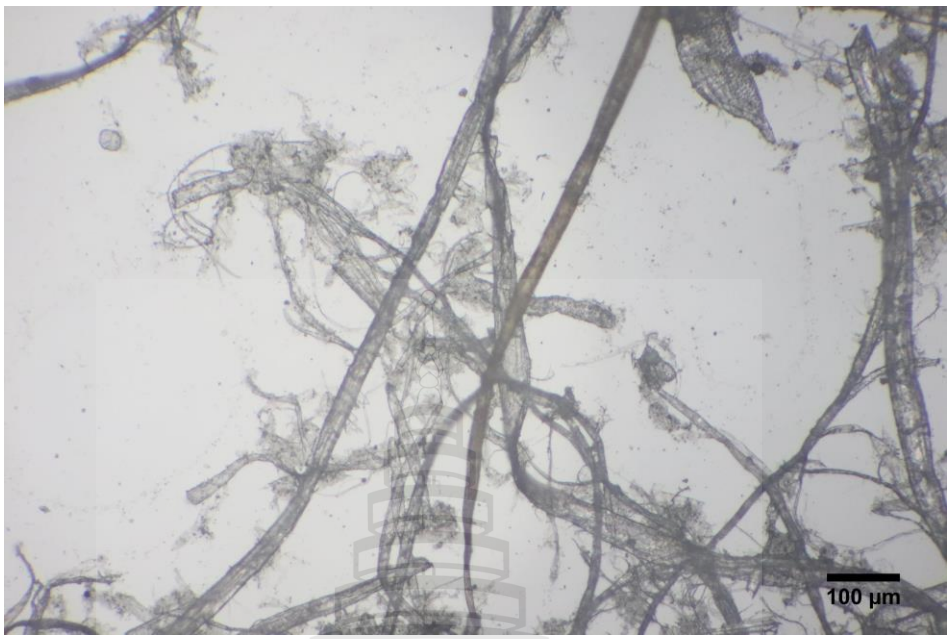

Figure A11 Photograph for width measurement of 550 ml CSF RPBC

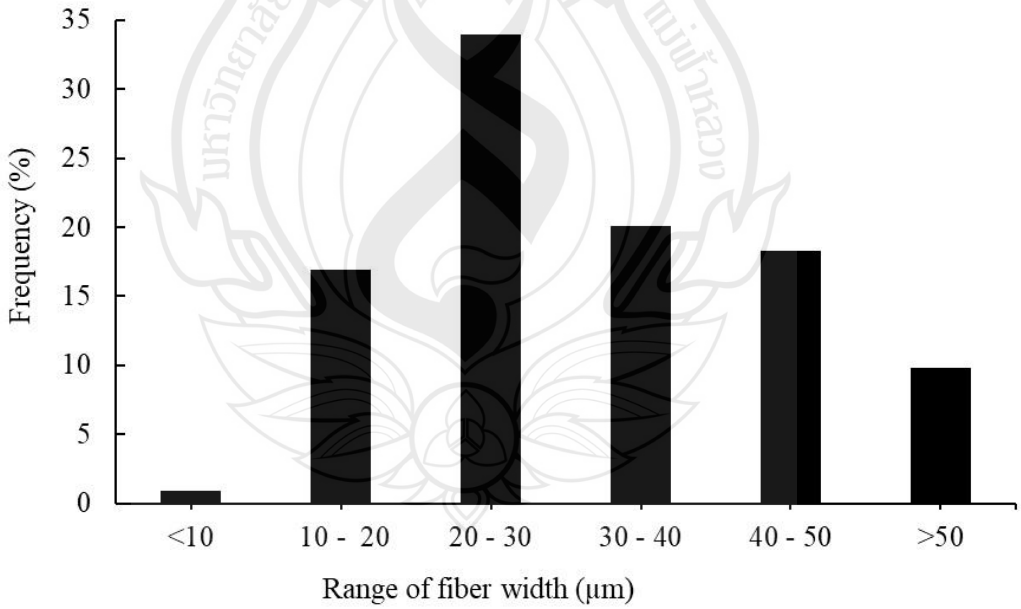

Figure A12 Histogram of width distribution for 550 mL CSF RPBC

4. RPBC with 500 ml CSF freeness

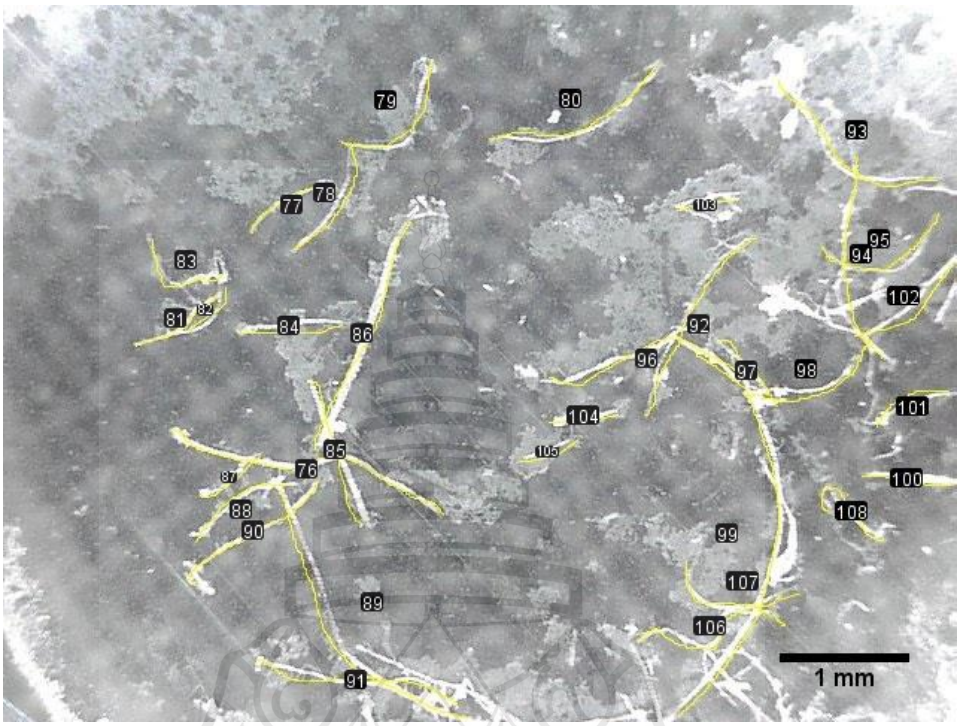

Figure A13 Photograph for length measurement of 500 ml CSF RPBC

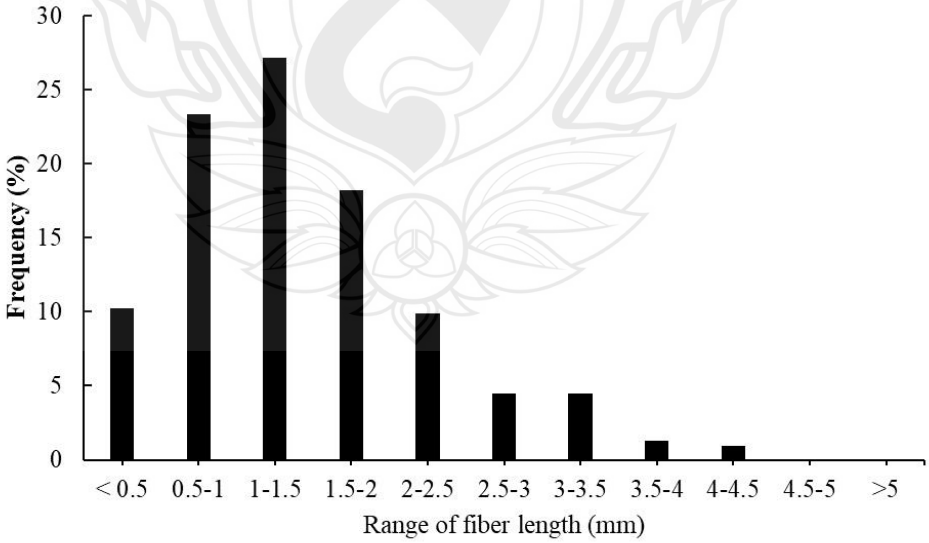

Figure A14 Histogram of length distribution for 500 mL CSF RPBC

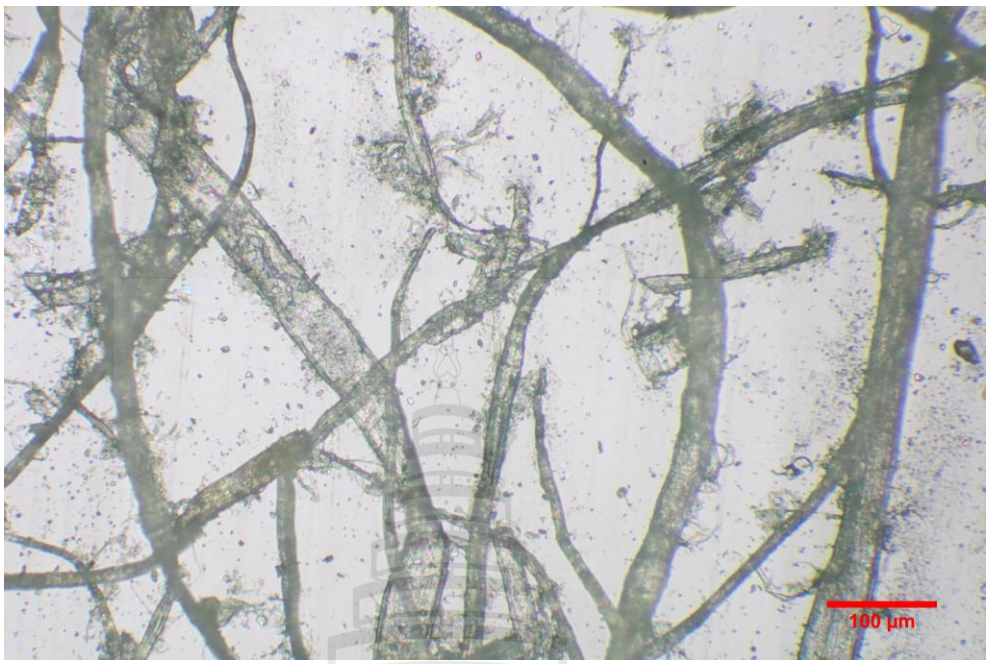

Figure A15 Photograph for width measurement of 500 ml CSF RPBC

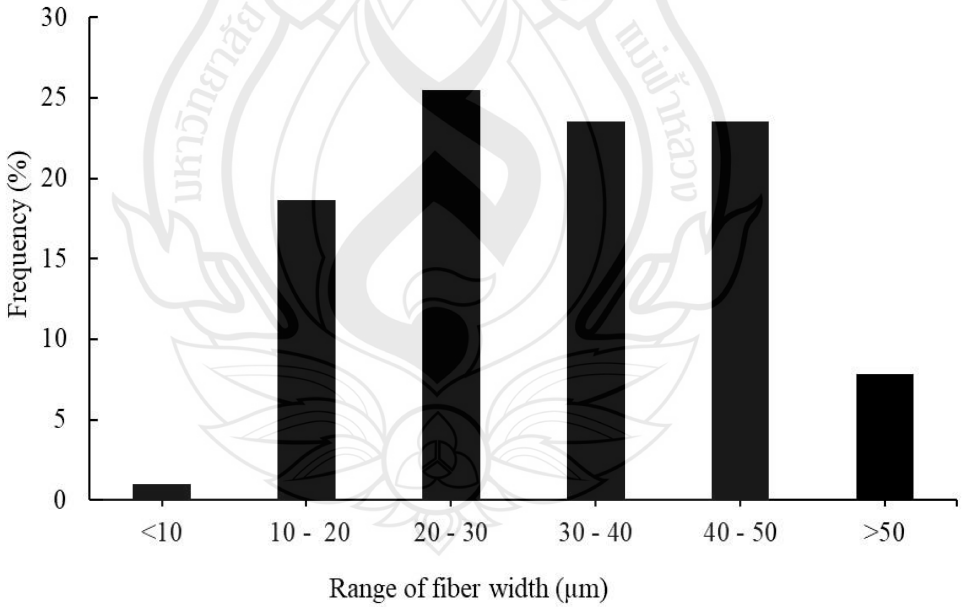

Figure A16 Histogram of width distribution for 500 mL CSF RPBC

5. RPBC with 400 ml CSF freeness

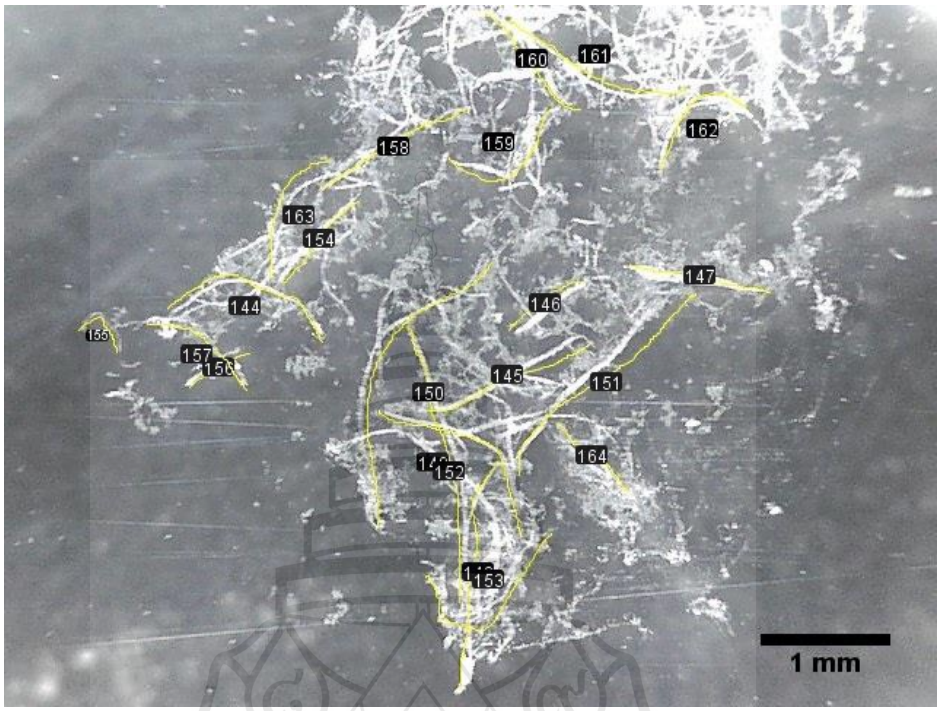

Figure A17 Photograph for length measurement of 400 ml CSF RPBC

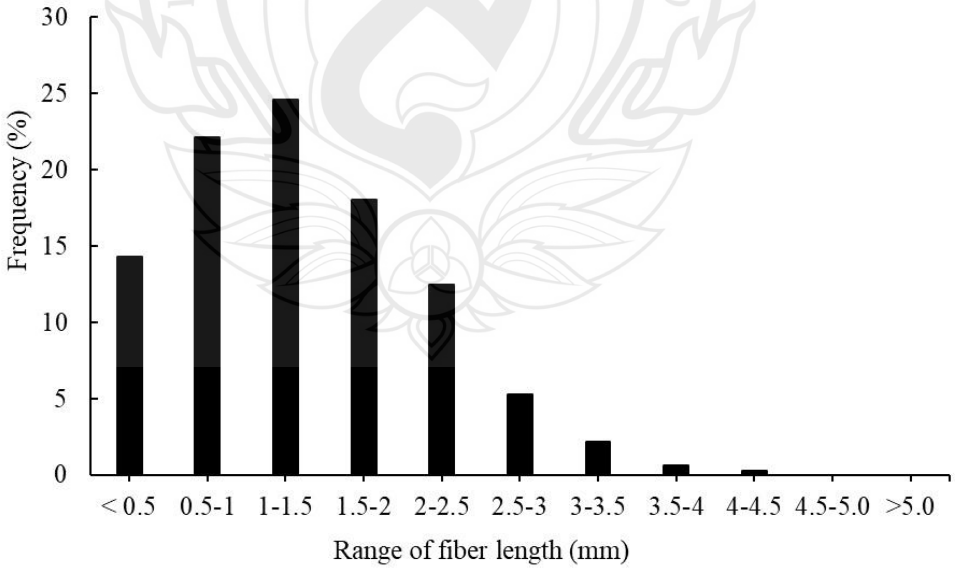

Figure A18 Histogram of length distribution for 400 mL CSF RPBC

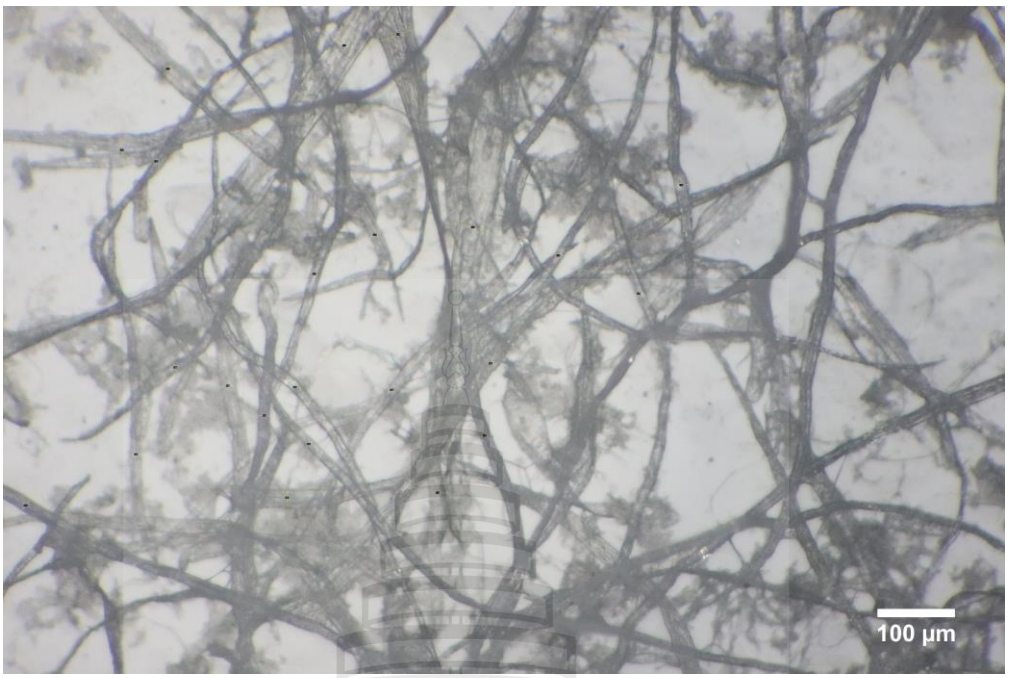

Figure A19 Photograph for width measurement of 400 ml CSF RPBC

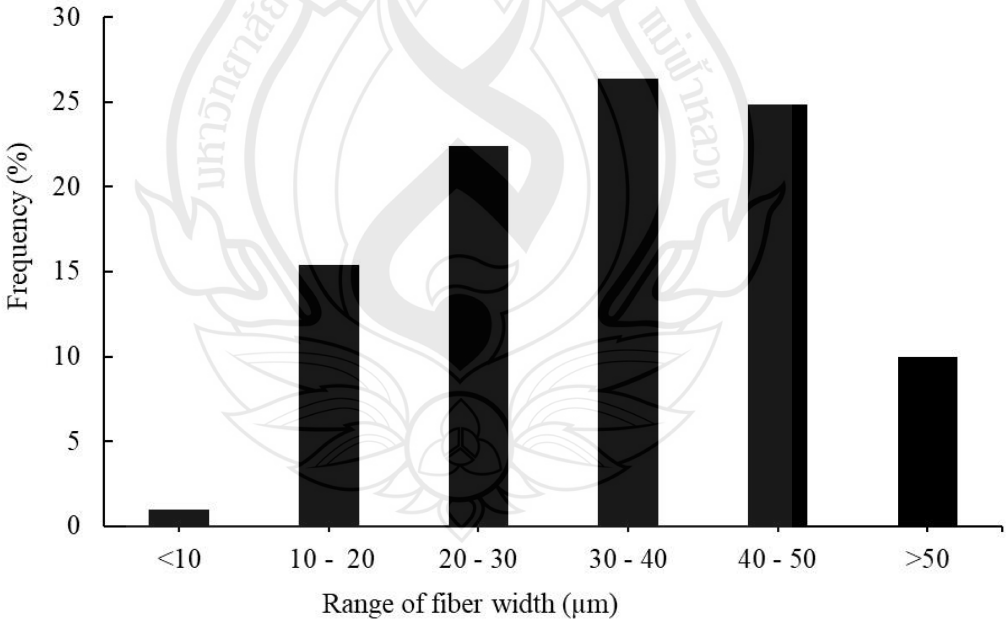

Figure A20 Histogram of width distribution for 400 mL CSF RPBC

APPENDIX B

DIMENSIONAL MEASUREMENT OF VIRGIN BAMBOO FIBER

1. Bamboo fiber extracted by 2%NaOH

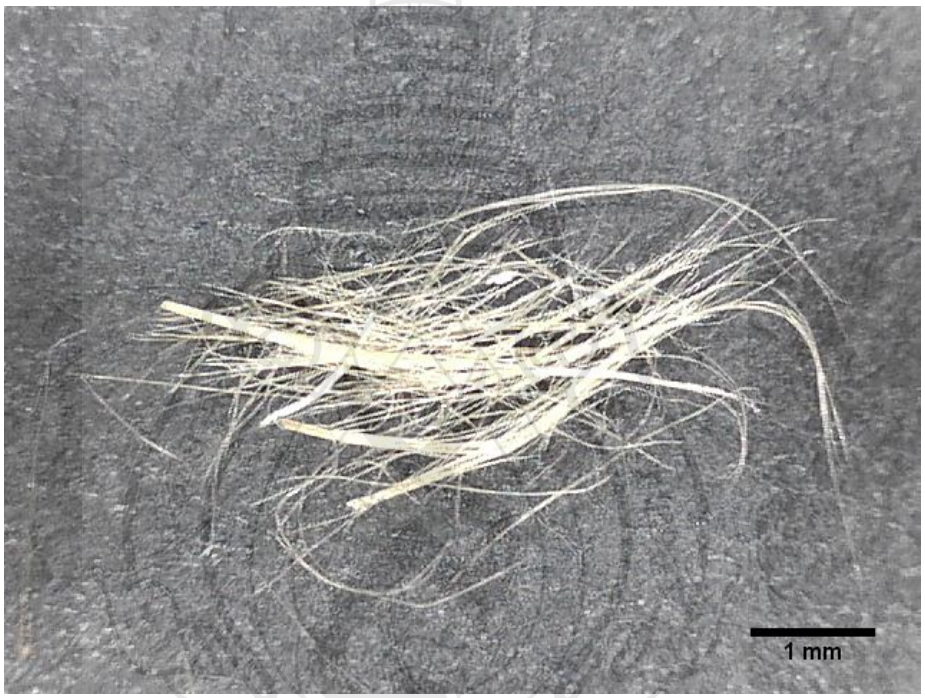

Figure B1 Photograph of 2%NaOH BF for length measurement

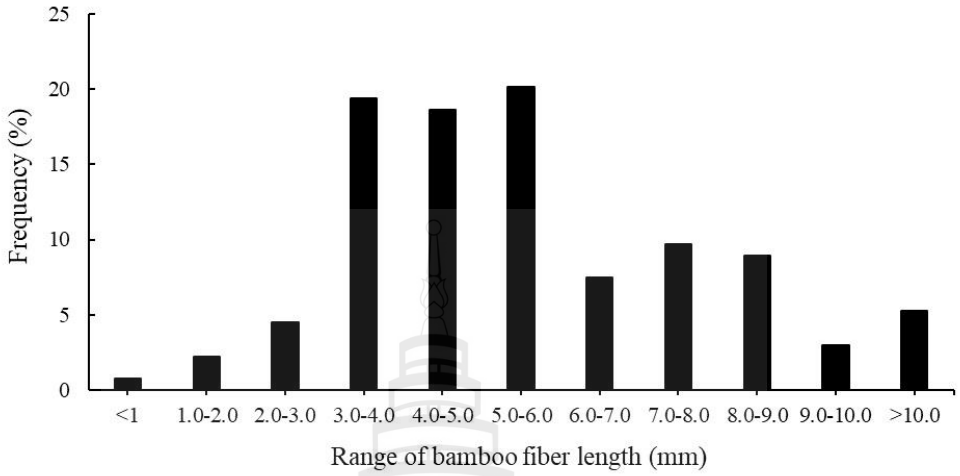

Figure B2 Histogram of length distribution for 2%NaOH BF

Figure B3 Photograph of 2%NaOH BF for width measurement

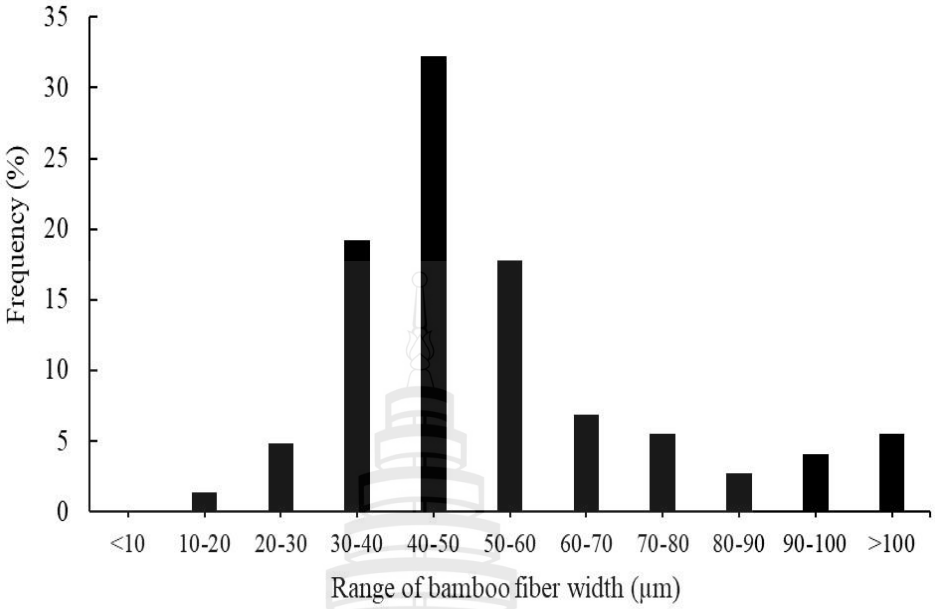

Figure B4 Histogram of width distribution for 2%NaOH BF

2. Bamboo fiber extracted by 4%NaOH

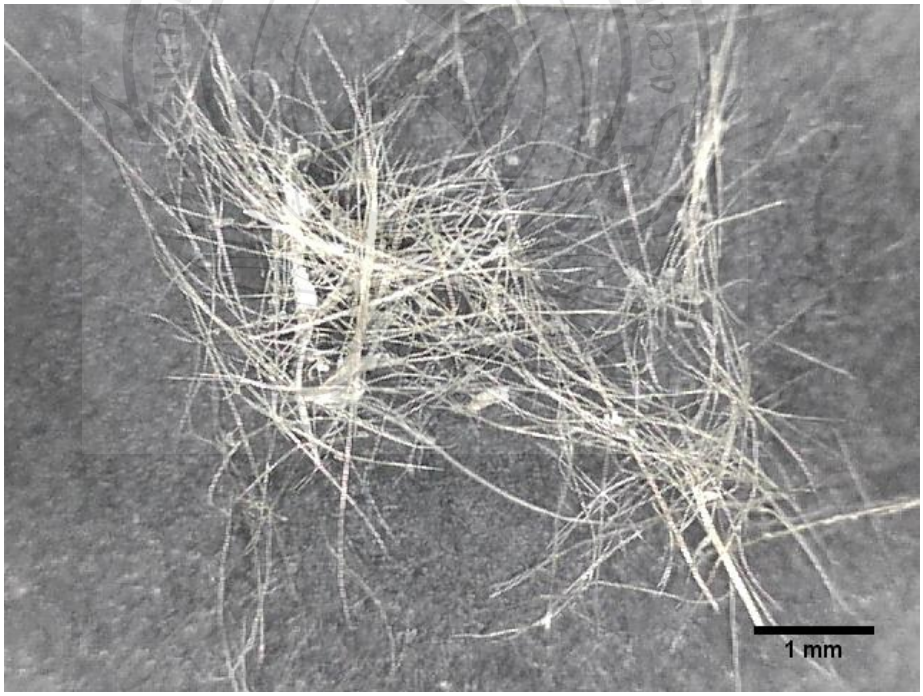

Figure B5 Photograph of 4%NaOH BF for length measurement

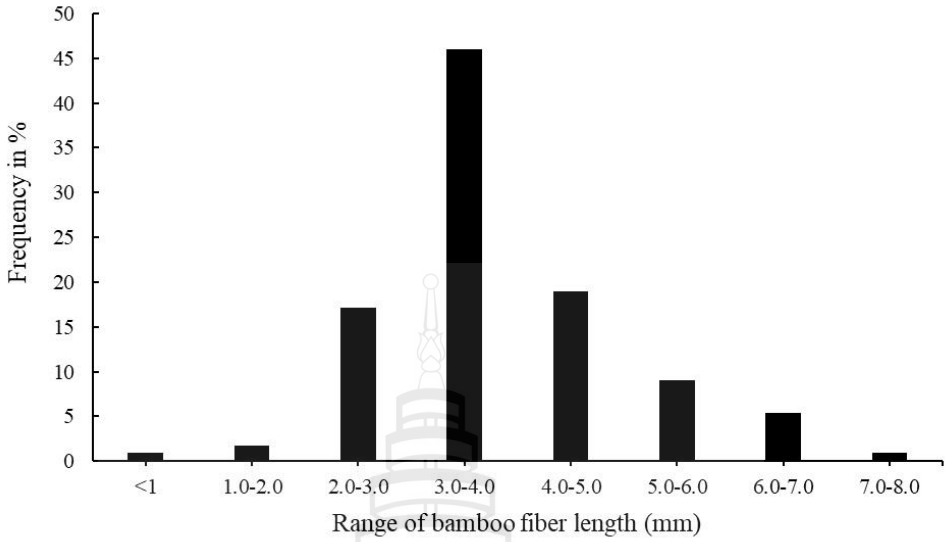

Figure B6 Histogram of length distribution for 4%NaOH BF

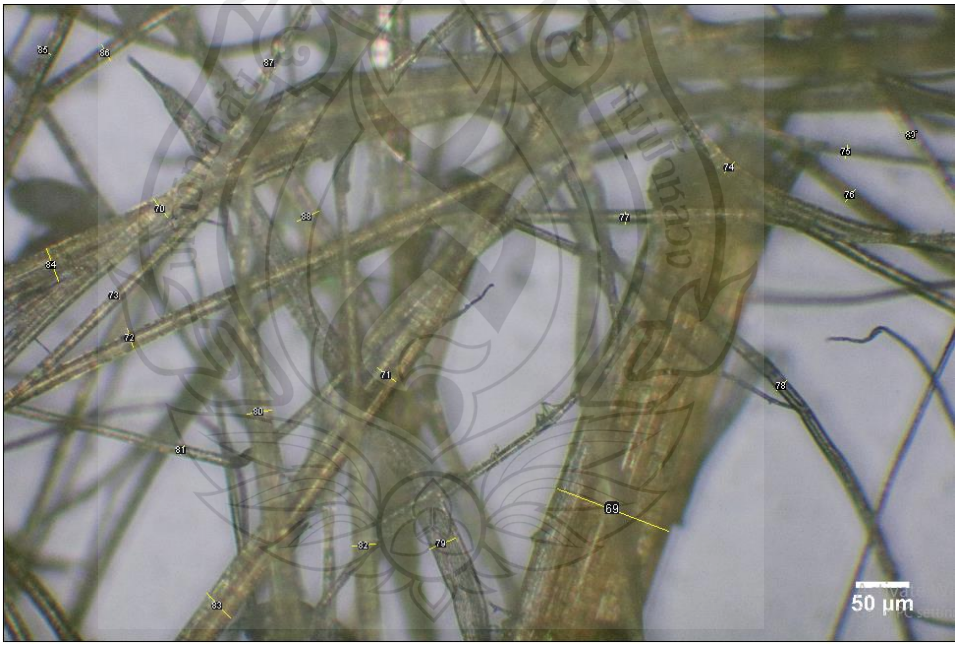

Figure B7 Photograph of 4%NaOH BF for width measurement

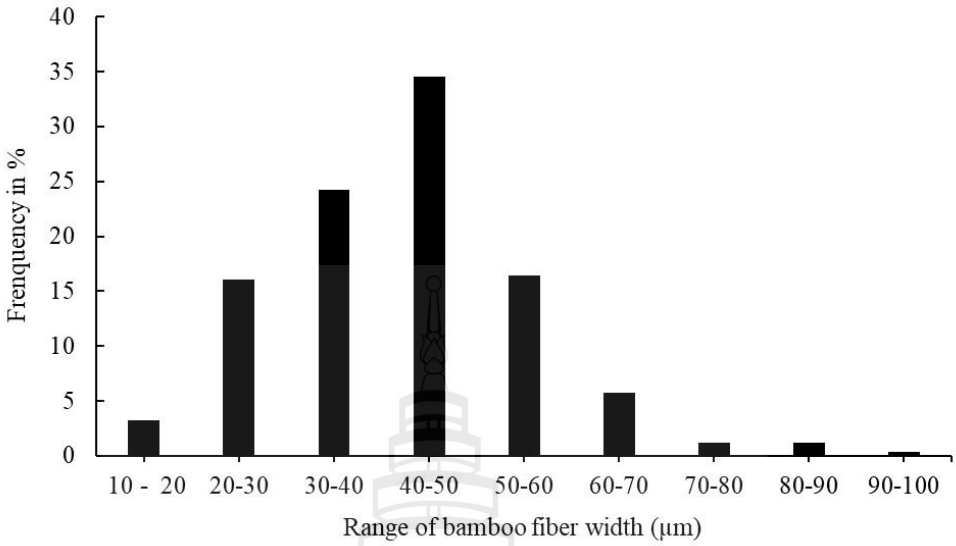

Figure B8 Histogram of width distribution for 4%NaOH BF

3. Bamboo fiber extracted by 6%NaOH

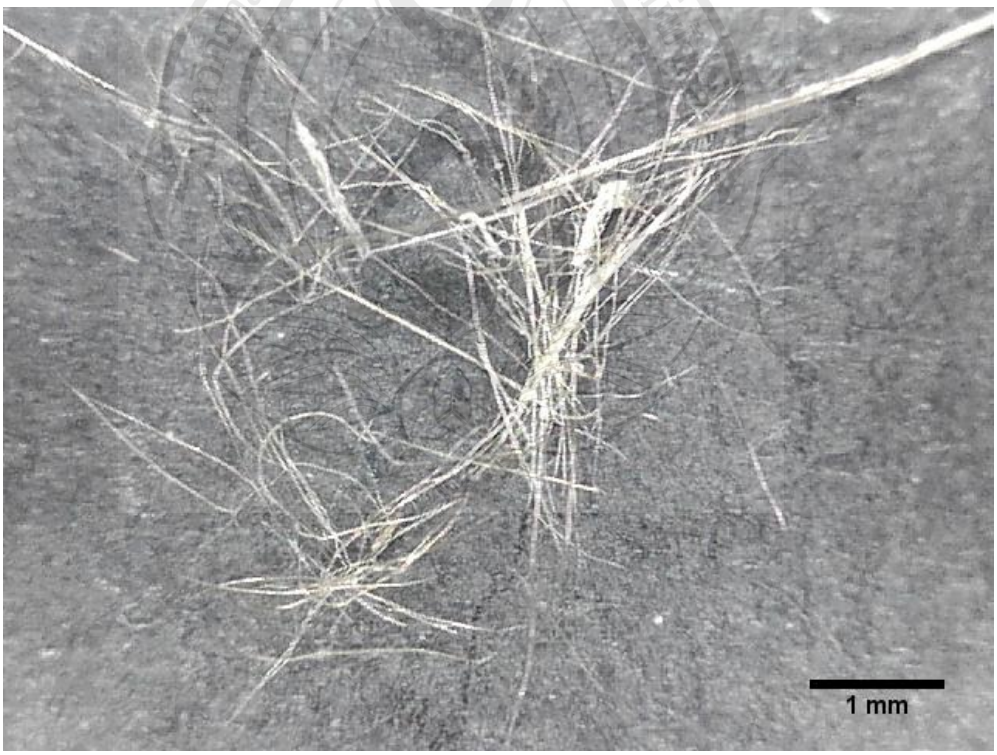

Figure B9 Photograph of 6%NaOH BF for length measurement

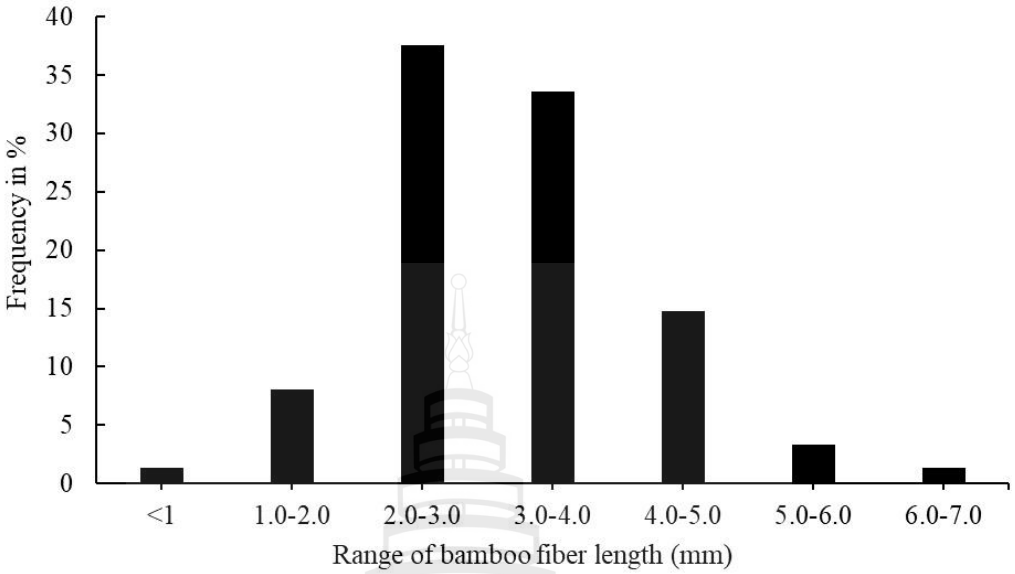

Figure B10 Histogram of length distribution for 6%NaOH BF

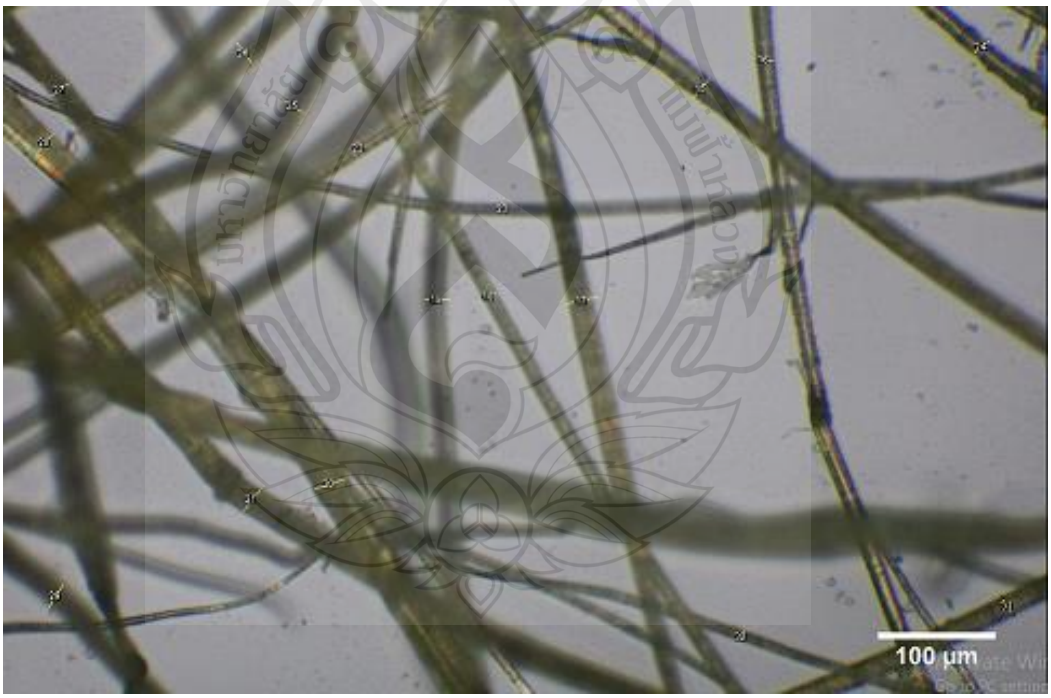

Figure B11 Photograph of 6%NaOH BF for width measurement

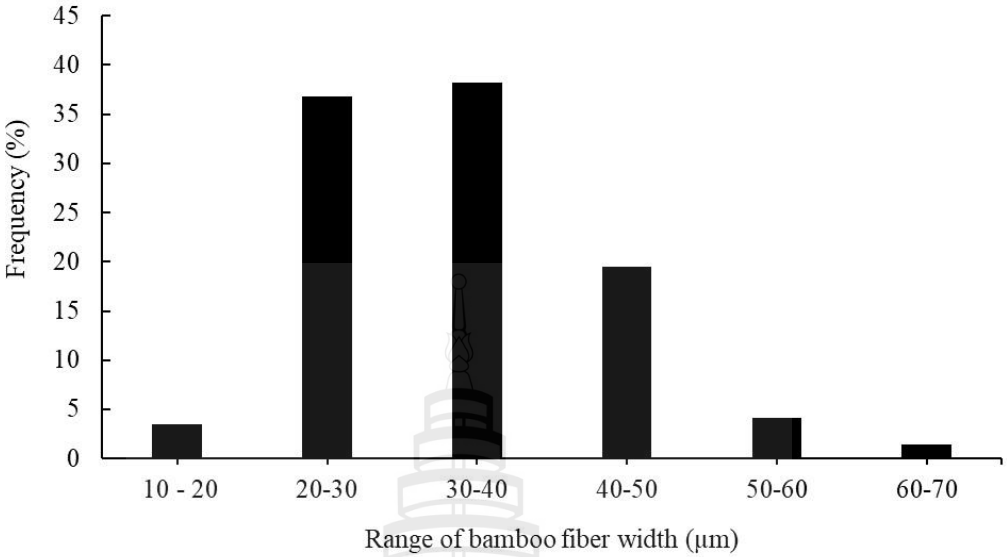

Figure B12 Histogram of width distribution for 6%NaOH BF

4. Bamboo fiber extracted by 8%NaOH

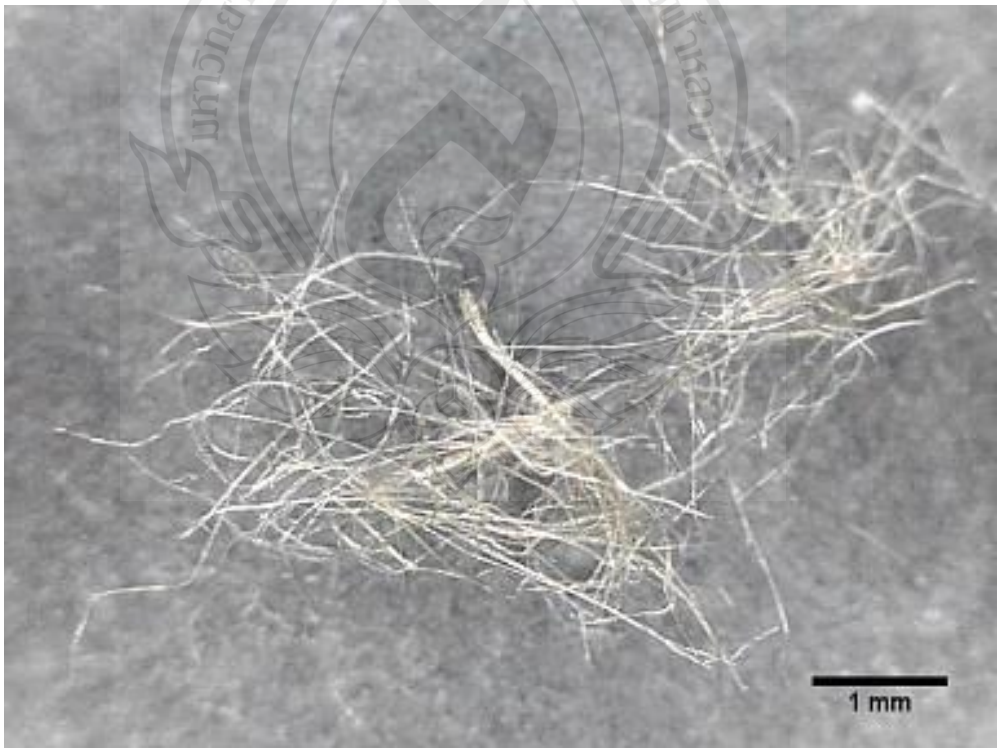

Figure B13 Photograph of 8%NaOH BF for length measurement

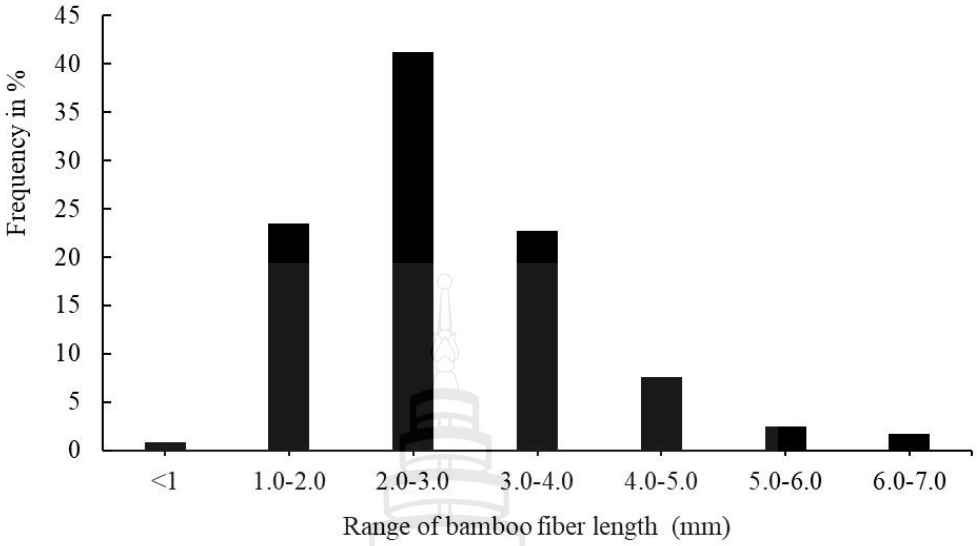

Figure B14 Histogram of length distribution for 8%NaOH BF

Figure B15 Photograph of 8%NaOH BF for width measurement

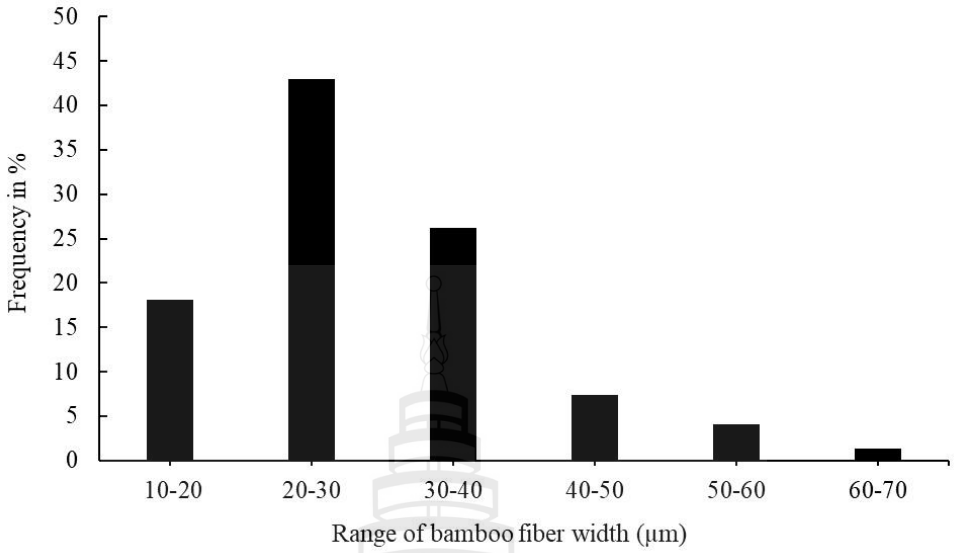

Figure B16 Histogram of width distribution for 8%NaOH BF

5. Bamboo fiber extracted by 10%NaOH

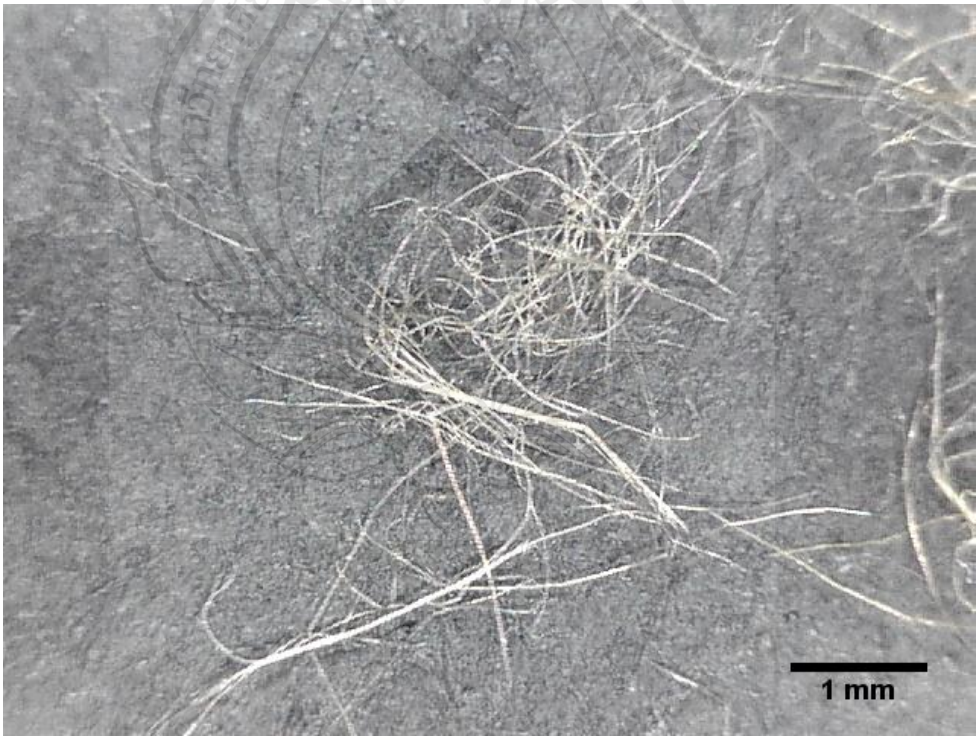

Figure B17 Photograph of 10%NaOH BF for length measurement

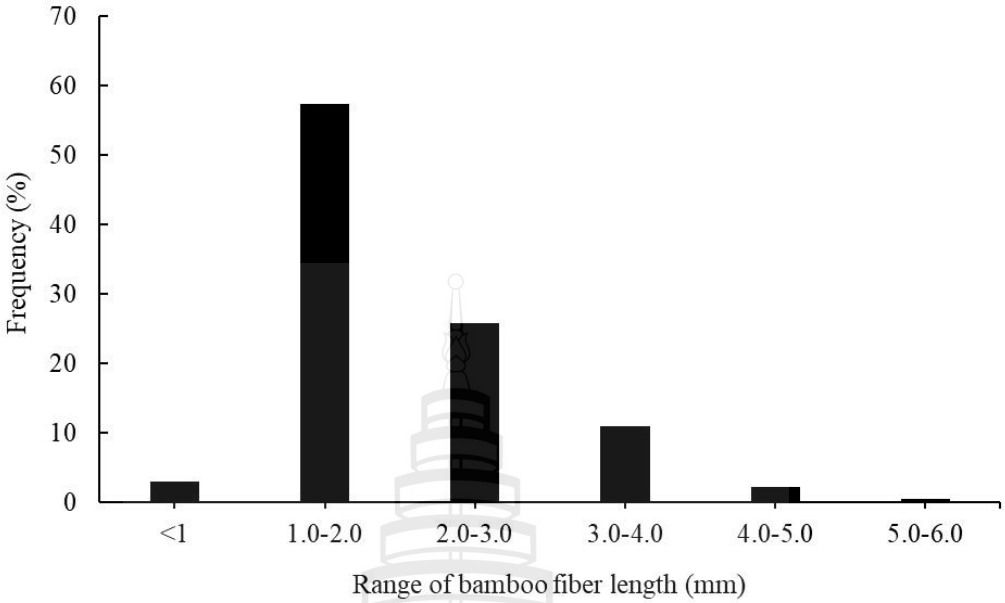

Figure B18 Histogram of length distribution for 10%NaOH BF

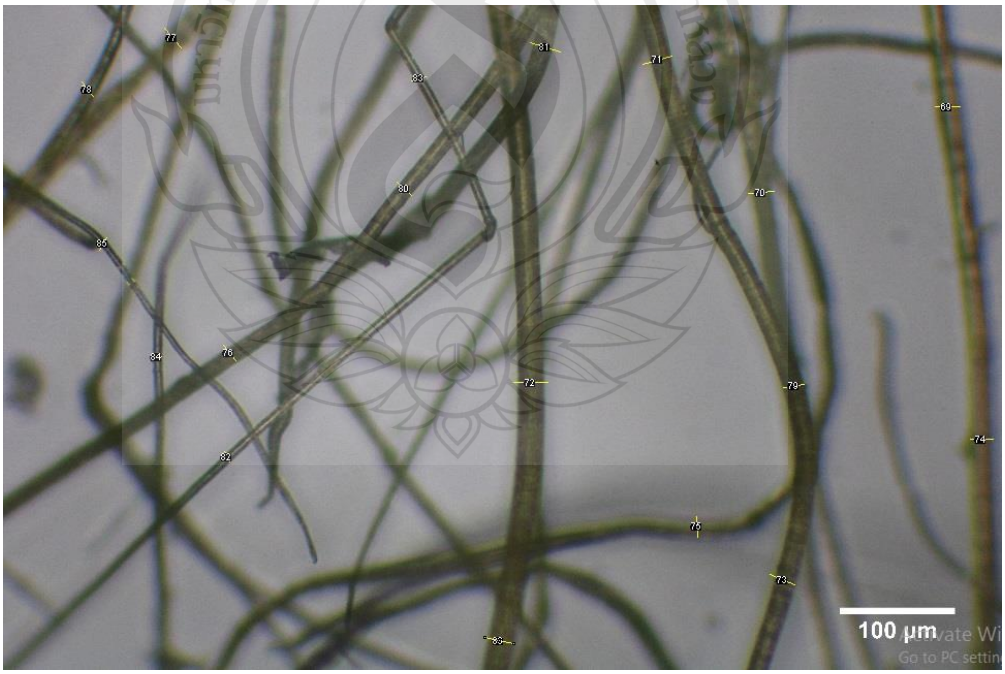

Figure B19 Photograph of 8%NaOH BF for width measurement

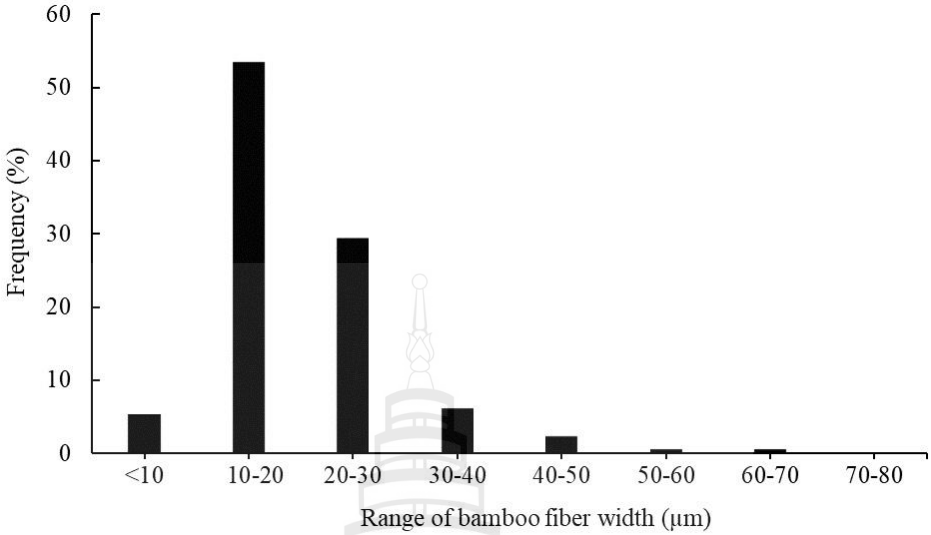

Figure B20 Histogram of width distribution for 10%NaOH BF

APPENDIX C

DIMENSIONAL MEASUREMENT OF VIRGIN EUCALYPTUS FIBER

1. Fiber length measurement

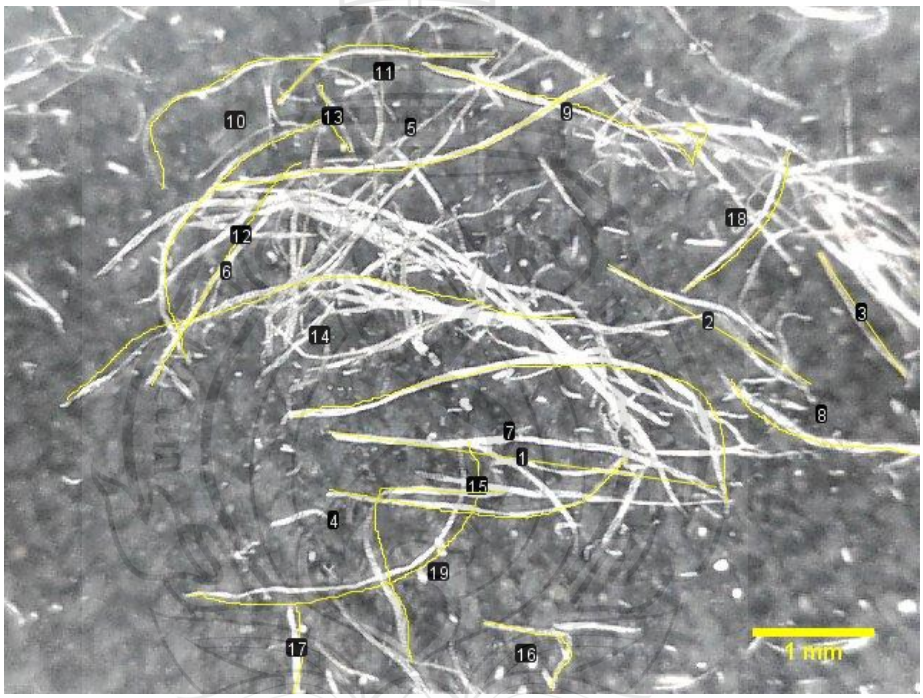

Figure C.1 Photograph of EF for length measurement

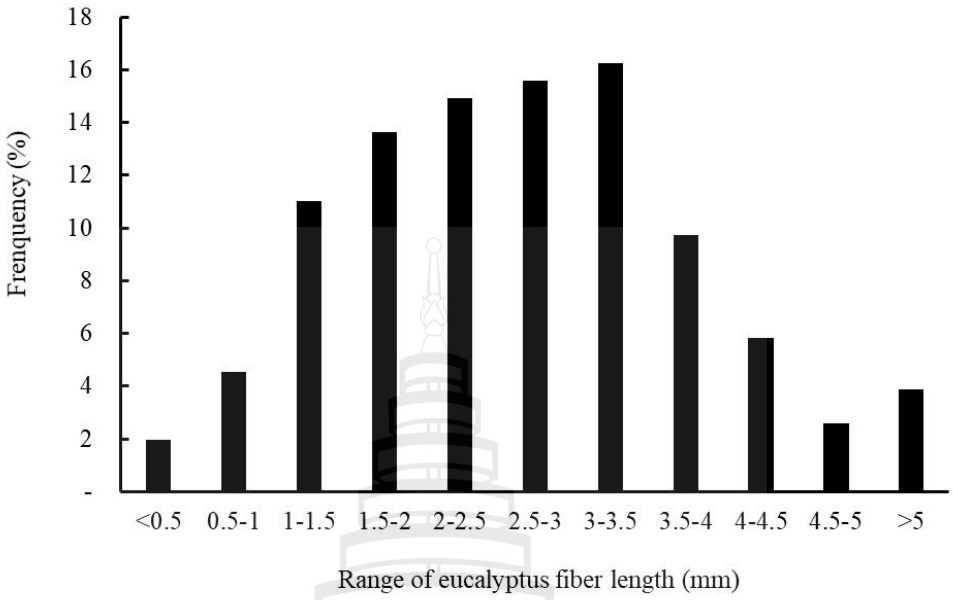

Figure C2 Histogram of length distribution for eucalyptus fiber

2. Fiber width measurement

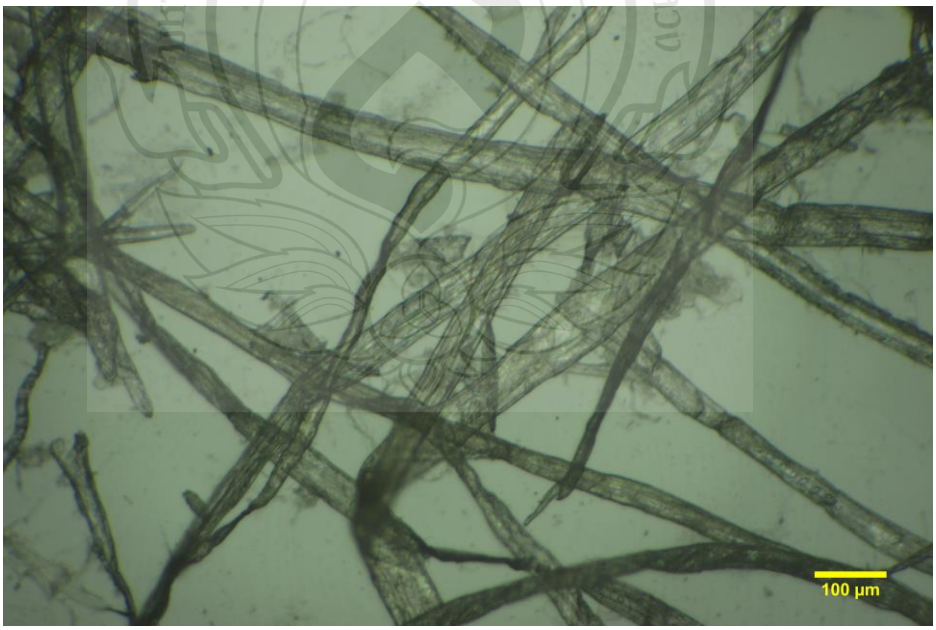

Figure C3 Photograph of EF for width measurement

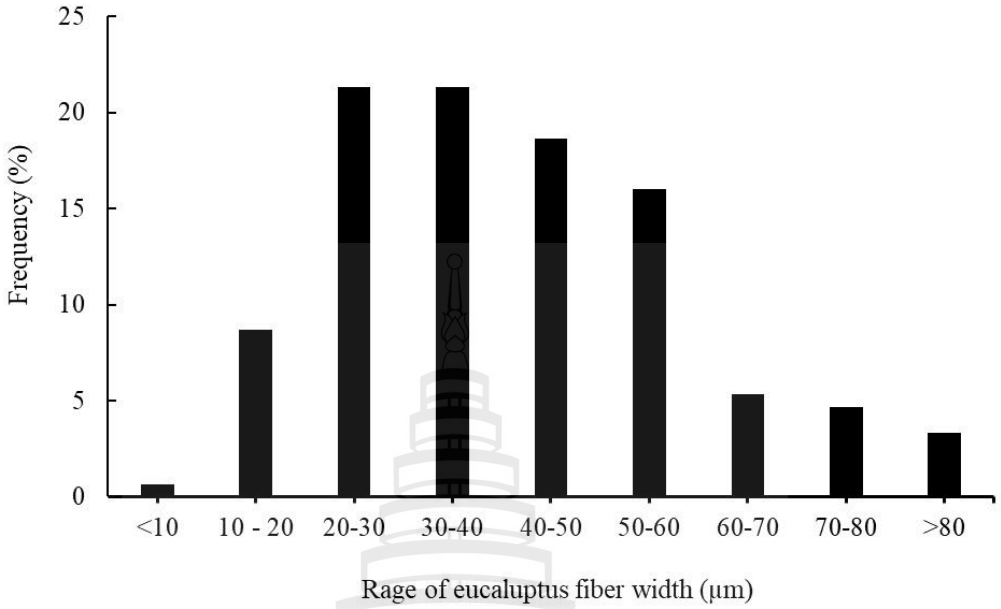

Figure C4 Histogram of width distribution for EF

APPENDIX D

PICTURES OF SPECIMENS

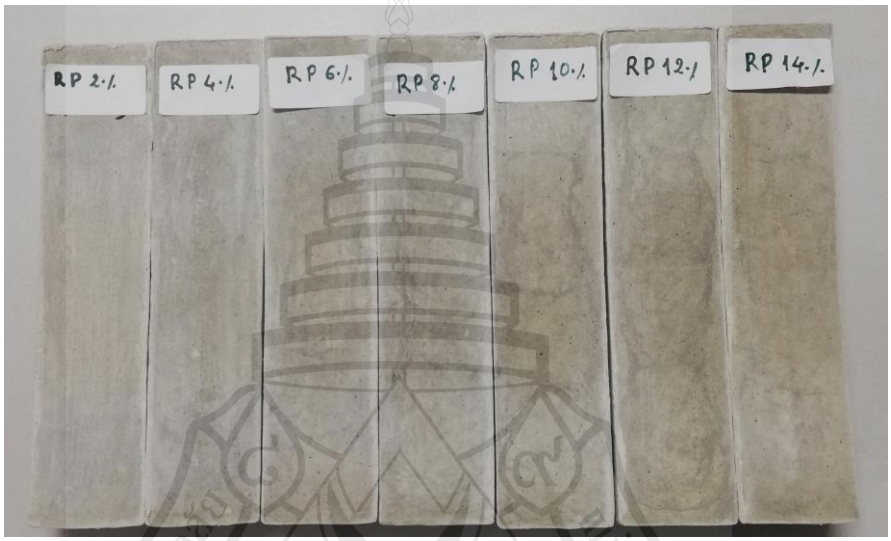

Figure D1 Specimens of RPBC reinforced cement composites

Figure D2 Specimens of BF reinforced cement composites

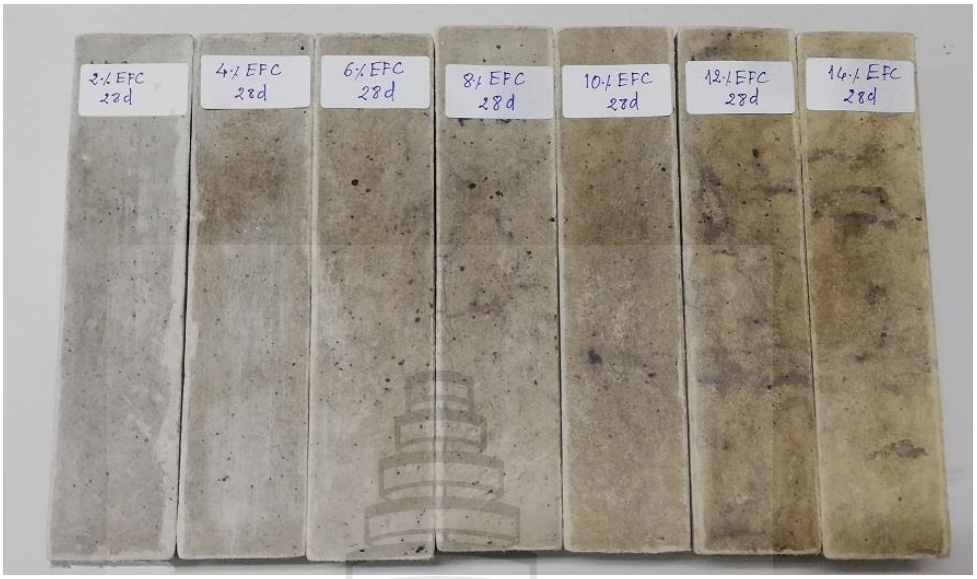

Figure D3 Specimens of EF reinforced cement composites

APPENDIX E

BENDING TEST

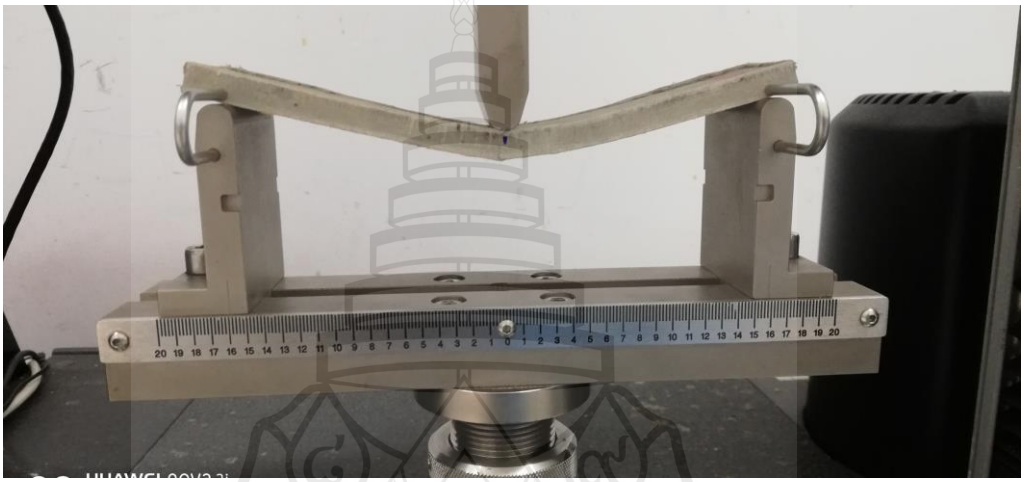

Figure E1 Bending test of 14%RPBC reinforced cementitious composites

Figure E2 Bending test of 14%BF reinforced cementitious composites

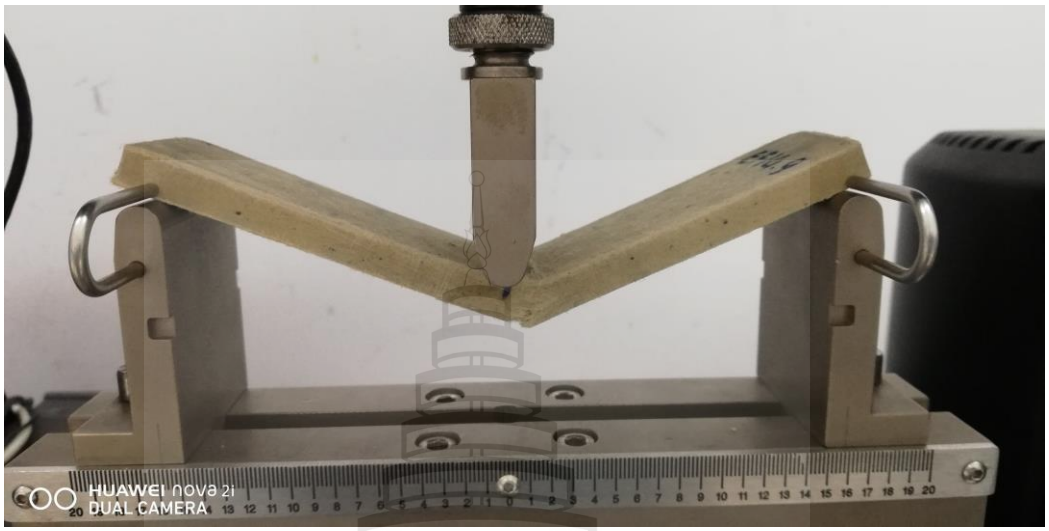

Figure E3 Bending test of 14%EF reinforced cementitious composites

APPENDIX F

ABSTRACT OF PUBLICATIONS

Publications in International Journals

Chiang Mai J. Sci. 2024; 51(4): e2024063
https://doi.org/10.12982/CMJS.2024.063
Journal homepage : http://epg.science.cmu.ac.th/ejournal/

Research Article

Properties of Cementitious Composite Reinforced with Recycled Pulp from Beverage Cartons

Phouthanouthong Xaysombath [a], Nattakan Soykeabkaew [b], Darunee Wattanasiriwech [a] and Suthee Wattanasiriwech [a]*

[a] Materials Innovation Graduate Program, School of Science, Mae Fah Luang University, Chiang Rai 57100, Thailand.
[b] Center of Innovative Materials for Sustainability, Mae Fah Luang University, Chiang Rai 57100, Thailand.

*Author for correspondence; e-mail: suthee@mfu.ac.th

Received: 5 March 2023
Revised: 26 May 2024
Accepted: 5 June 2024

ABSTRACT

This study presents a comprehensive evaluation of the effects of the refining level of recycled pulp from beverage cartons (RPBC) on the properties of its cementitious composite. The RPBC with various freeness levels, ranging from 400 to 650 mL of the Canadian Standard Freeness test method (CSF), was prepared using a high-speed fruit blender. The specimens were formed by the slurry de-watering method with 8wt% fiber content and mortar matrix with a sand-to-cement ratio of 1:1. The key findings reveal that the cementitious composites reinforced with the RPBC exhibited a maximum value of flexural strength of 11.17 MPa and the freeness of 550 mL CSF. The fracture toughness values of the RPBC composites were significantly improved compared to that of the control specimen. However, the values decreased by about 14% to 20 % as the freeness reduced from 650 to 400 mL CSF. The bulk density and porosity of the RPBCC were not significantly affected by the freeness of RPBC.

Keywords: recycled pulp, beverage carton, refining, fiber cement composite, freeness.

1. INTRODUCTION

The beverage carton, a common packaging material for long-life liquid products, is a significant contributor to waste. The beverage carton comprises 75% paperboard, 20% low-density polyethylene, and 5% aluminum foil compacted in multilayer-coated phases [1, 2]. The paperboard used for the beverage carton production was produced from various pulp types, such as bleached and unbleached sulfate pulp and chemo-thermomechanical pulp, which depend on the type of drinking product [3]. The pulp from the beverage carton could be recovered by the conventional pulping process using a hydra-pulper to separate the pulp fiber from polyethylene and aluminum [1]. According to the Alliance for Beverage Cartons and the Environment (ACE), only half of 900,000 tons of beverage cartons placed on the EU market in 2019 were recycled [4]. However, the findings from this study, which explored the potential of recycling the pulp from beverage cartons for use in cementitious composites, indicate a positive direction. This approach offers a sustainable solution to waste management, potentially reducing the environmental impact of beverage cartons.

The bio-circular-green (BCG) economy model has been implemented in many sectors, especially the construction and building industry, to promote a more sustainable globe. The recycled

CURRICULUM VITAE

CURRICULUM VITAE

NAME Phouthanouthong Xaysombath

EDUCATION BACKGROUND

1997 Diplomingenieur Degree on Wood and Fibrous Materials Process Engineering, Faculty of Mechanical Engineering, Dresden University of Technology, Germany

WORK EXPERIRNCES

2018-2020 Deputy Director General
Department of Planning and Cooperation (DPC), Ministry of Science and Technology (MOST) of Lao PDR.

2015-2017 Director
Domestic Cooperation Division, Planning and Cooperation (DPC), Ministry of Science and Technology (MOST) of Lao PDR.

2011-2015 Director
Administration Division, BEI, MOST of Lao PDR.

2008-2010 Deputy Director
Administration Division, Biotechnology and Ecology Institute (BEI), Ministry of Science and Technology (MOST) of Lao PDR.

2005-2008	Researcher Technology Research Institute (TRI) of the Science, Technology, and Environment Agency (STEA), Lao PDR.
2000-2005	Technician Technology Research Institute (TRI) of the Science, Technology, and Environment Agency (STEA), Lao PDR.

PUBLICATIONS

Xaysombath, P., Wattanasiriwech, S., Soykeabkaew, N., & Wattanasiriwech, S. (2024). Properties of cementitious composite reinforced with recycled pulp from beverage cartons. *Chiang Mai Journal of Science, 51*(4), e2024000. https://doi.org/10.12982/CMJS.2024.063